


2015

# Bridging In Vi Tro & In S Il Ico Techniques: Uncovering the Structural Characteristics and Light-Dependent Modifications of the Light- Response Btb Proteins in Arabidopsis Thaliana

Nicholas Reitz  
*Grand Valley State University*

Follow this and additional works at: <http://scholarworks.gvsu.edu/theses>

 Part of the [Biology Commons](#), and the [Cell and Developmental Biology Commons](#)

---

## Recommended Citation

Reitz, Nicholas, "Bridging In Vi Tro & In S Il Ico Techniques: Uncovering the Structural Characteristics and Light-Dependent Modifications of the Light-Response Btb Proteins in Arabidopsis Thaliana" (2015). *Masters Theses*. 795.  
<http://scholarworks.gvsu.edu/theses/795>

This Thesis is brought to you for free and open access by the Graduate Research and Creative Practice at ScholarWorks@GVSU. It has been accepted for inclusion in Masters Theses by an authorized administrator of ScholarWorks@GVSU. For more information, please contact [scholarworks@gvsu.edu](mailto:scholarworks@gvsu.edu).

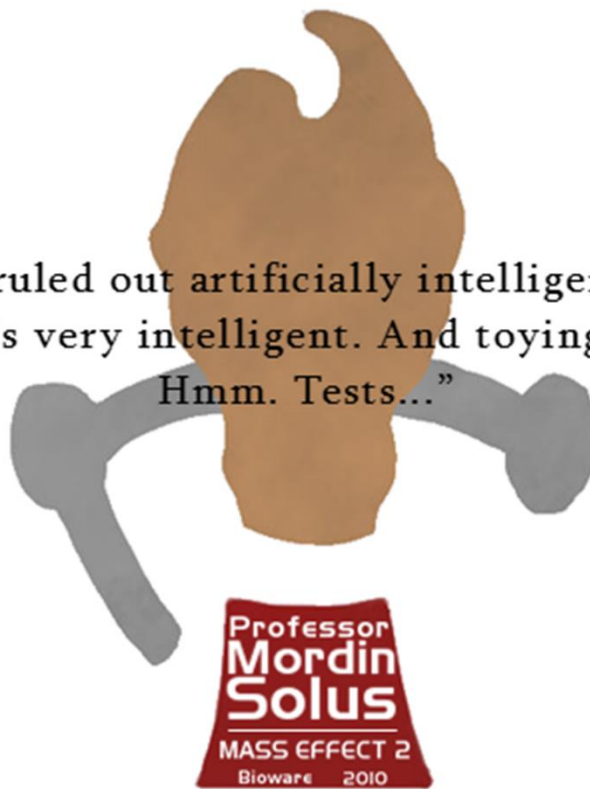
BRIDGING *IN VITRO* & *IN SILICO* TECHNIQUES: UNCOVERING  
THE STRUCTURAL CHARACTERISTICS AND LIGHT-DEPENDENT  
MODIFICATIONS OF THE LIGHT-RESPONSE BTB PROTEINS IN  
*ARABIDOPSIS THALIANA*

Nicholas Reitz

A Thesis Submitted to the Graduate Faculty of  
GRAND VALLEY STATE UNIVERSITY  
In Partial Fulfillment of the Requirements  
For the Degree of  
MASTER OF SCIENCE  
in  
CELL & MOLECULAR BIOLOGY


December 2015

“Have ruled out artificially intelligent virus.  
Unless it’s very intelligent. And toying with me.  
Hmm. Tests...”



Copyright by  
Nicholas Adam Reitz  
2015

# DEDICATION

This thesis is dedicated to my Grandma,   
because I know I haven't been coming to the garden alone.

## ACKNOWLEDGEMENTS

I want to first express my sincere gratitude for the overwhelming amount of guidance and support I have received from Dr. Christians while working in his lab. I'm grateful for the opportunity to learn from you over these last two years. You have consistently allowed me to branch out with my ideas and grow as a scientist, and I am confident in saying that I have acquired valuable skills from your expertise.

I would also like to acknowledge the vast amount of influence that Dr. Szarecka has had on my graduate education at Grand Valley. The effort that you put into educating your students and making sure that everyone has the necessary tools to succeed is inspirational, and I am truly lucky to have received your guidance and wisdom.

Dr. Blackman, who very kindly agreed to also be on my committee, has been an invaluable part of my thesis project. I am very thankful that you have been a part of my thesis journey, and I appreciate the effort you have put forth to help improve my project.

The help and support that is consistently present in all the CMB department faculty should also be acknowledged, and I am very grateful to have been part of a community that cares very deeply about advancing scientific education.

Of course, I must express my appreciation and overwhelming gratitude for my loving and patient partner, Timothy Schiller, who has consistently given me support and encouragement throughout my graduate career. Thank you for always pushing me to be my very best.

I must also acknowledge my friends, Jim LaFleur, Christopher Howard, Sarah Dawson, and Danielle Womeldorf, who were consistently ready to join me in doing labwork until 5am on a Friday night or keeping me motivated during late night thesis editing at my house. Thank you for providing me with the tools I needed to succeed in my academic pursuits. I couldn't have retained my sanity without you, and I owe a small part of my degree to each one of you. I also need to express my appreciation for Garrus Vakarian, who taught me how to improve calibration accuracy by a margin of 0.43 percent.

## ABSTRACT

The conjugation of the **NEDD8** protein has been found to cause a wide range of changes to the overall function of a protein. The addition of NEDD8 to a conserved lysine on Cul proteins has been found to provide Cul with increased flexibility, while the transcription factor protein p53 was prevented from binding to DNA after NEDD8 conjugation. Using *Arabidopsis thaliana*, we investigated the potential conjugation of NEDD8 to the **AtLRB1** and **AtLRB2** proteins, which are both members of Cul3-RING E3 Ubiquitin Ligase complexes, using both *in vitro* and *in silico* techniques. The *AtLRBs* are negative regulators of the red light response pathway, interacting preferentially with Cul3 in red light conditions by an unknown mechanism.

Our investigation into the amino-terminal portion of *AtLRB2* (residues 1-144) found two conserved regions which contained high sequence identity with Cul1 and Rbx1, two members of Cullin-RING ligase complexes. These two conserved regions were also found to share a similar distribution and placement on both the native crystal structure of Cullin proteins in complex with Rbx1 and on the predicted *AtLRB2* structural protein model. Furthermore, the region of Rbx1 sharing sequence similarity to the LRBs directly interacts with NEDD8. Preliminary *in vitro* results also suggest that purified *AtLRB2* is modified by NEDD8, but the significance of this modification on the function of the LRB proteins is not yet known.

# TABLE OF CONTENTS

|   |     |
|---|-----|
| <b>I. BACKGROUND</b>  | 14  |
| PHYTOCHROMES & RED LIGHT RESPONSE   | 14  |
| UBIQUITIN / 26S PROTEASOME SYSTEM   | 22  |
| CULLIN-RING LIGASE COMPLEXES  | 25  |
| CUL3 & THE BTB DOMAIN   | 30  |
| NEDD8 & NEDDYLYATION  | 33  |
| LIGHT-RESPONSE BTB PROTEINS   | 37  |
| <b>II. RESEARCH SIGNIFICANCE</b>  | 45  |
| <b>III. PROJECT AIMS &amp; OVERVIEW</b>   | 48  |
| <b>IV. RESULTS &amp; DISCUSSION</b>   | 55  |
| <i>IN SILICO</i> INVESTIGATIONS OF THE LRB PROTEINS   | 55  |
| DETERMINING THE ROLE OF PHOSPHORYLATION ON<br>LRB FUNCTION  | 90  |
| NEDD8 CONJUGATION PREDICTED ON <i>At</i> LRB2   | 96  |
| <b>V. CONCLUSIONS</b>   | 102 |
| TWO AMINO-TERMINAL REGIONS FOUND TO BE<br>CONSERVED IN ALL LRB PROTEIN HOMOLOGS                                     | 102 |
| CONSERVED AMINO-TERMINAL LRB REGIONS SHOW<br>SEQUENCE SIMILARITY TO OTHER CRL<br>PROTEIN MEMBERS                    | 103 |
| LRB HOMOLOGY MODELS REPRESENT THE OVERALL<br>FOLD OF THE BTB/3BOX/BACK DOMAINS                                      | 104 |
| NEDD8 MAY HAVE A ROLE IN THE FUNCTION OR<br>REGULATION OF THE LRB PROTEINS  | 109 |
| <i>At</i> LRB PHOSPHORYLATION COULD NOT BE DETECTED<br>DESPITE <i>IN SILICO</i> PHOSPHORYLATION SITE<br>PREDICTIONS | 113 |
| THE INTERACTION BETWEEN LRB1 AND HISTONE-LYSINE<br>N-METHYLTRANSFERASE EZA1 SHOULD BE<br>INVESTIGATED FURTHER       | 115 |
| <b>VI. MATERIALS &amp; METHODS</b>  | 117 |
| <b>VII. SUPPLEMENTAL INFORMATION</b>  | 127 |
| <b>VIII. REFERENCES</b>   | 150 |



## LIST OF FIGURES

|  |    |
|--|----|
| 1. PHYTOCHROME RESPONSE TO RED LIGHT   | 16 |
| 2. PHYB-PIF3 INTERACTION AND TRANSPHOSPHORYLATION  | 19 |
| 3. SIMPLE MECHANISM FOR THE UBIQUITIN CONJUGATION<br>CASCADE                                   | 23 |
| 4. STRUCTURE OF CULLIN-RING LIGASE COMPLEXES   | 27 |
| 5. CONSERVED BTB FOLD TOPOLOGY AND INTERACTION<br>WITH CUL3                                    | 32 |
| 6. NEDD8 CONJUGATION CASCADE   | 35 |
| 7. PHOTOMORPHOGENIC DIFFERENCES OF <i>lrb1 lrb2</i> KNOCK<br>OUTS IN <i>ARABIDOPSIS</i>        | 38 |
| 8. THE LRBS ARE THE ADAPTOR PROTEINS IN CRL3<br>COMPLEXES                                      | 40 |
| 9. POTENTIAL MECHANISM FOR LRB ACTIVATION IN<br>RED LIGHT                                      | 52 |
| 10. MULTIPLE SEQUENCE ALIGNMENT OF THE AMINO-<br>TERMINAL REGION IN HOMOLOGOUS LRB<br>PROTEINS | 58 |
| 11. PHYLOGENETIC ANALYSIS AND DIVISION OF LRB<br>PROTEIN HOMOLOGS                              | 59 |
| 12. PROXIMITY OF THE NEDD8 CONJUGATION SITE TO THE<br>LRB-LIKE REGION OF CUL1/2                | 61 |
| 13. ALIGNMENT OF SEQUENCES SHOWING SIMILARITY TO<br>THE LRBS                                   | 64 |
| 14. REFINED MSA OF THE CULLIN-LIKE AND LINKER-LIKE<br>REGIONS OF VARIOUS LRB PROTEIN HOMOLOGS  | 65 |
| 15. ALIGNMENT OF THE CUL <sup>CL</sup> REGION ON CULLINS                                       | 66 |
| 16. EDITED ALIGNMENT OF THE RBX <sup>LL</sup> REGION ON<br>RBX1 HOMOLOGS                       | 67 |

|   |     |
|---|-----|
| 17. OVERALL ALIGNMENT OF THE CULLIN CUL <sup>CL</sup> AREA AND THE CL REGION FROM LRB   | 70  |
| 18. ALIGNMENT AND PHYSICAL PROPERTIES OF THE RBX <sup>LL</sup> AND LL REGIONS   | 71  |
| 19. ALIGNMENT OF HUMAN CUL <sup>CL</sup> AND RBX <sup>LL</sup> AREAS WITH THEIR RESPECTIVE COUNTERPARTS IN <i>ARABIDOPSIS</i> | 73  |
| 20. ANAGLYPHIC IMAGES OF NATIVE CUL <sup>CL</sup> AND RBX <sup>LL</sup> AREAS IN THE CRL COMPLEX                              | 75  |
| 21. INTERACTION OF THE RBX <sup>LL</sup> REGION WITH NEDD8  | 76  |
| 22. ANAGLYPHIC STEREO VIEW OF <i>Ai</i> LRB PHYRE2 PROTEIN MODELS   | 80  |
| 23. <i>Ai</i> LRB PHYRE2 PROTEIN MODELS DISPLAYED VIA RESIDUE INDEX   | 81  |
| 24. COMPARISON OF THE CL PREDICTED STRUCTURE AND CUL <sup>CL</sup> NATIVE STRUCTURE   | 84  |
| 25. PREDICTED EVOLUTIONARY CONSERVATION OF FULL-LENGTH <i>Ai</i> LRB2   | 87  |
| 26. PREDICTED AMINO ACID CONSERVATION OF <i>Ai</i> LRB2N  | 88  |
| 27. PREDICTED AMINO ACID CONSERVATION OF THE AMINO-TERMINAL DOMAIN  | 89  |
| 28. ANAGLYPHIC MODEL OF THE PREDICTED PHOSPHORYLATION SITES ON <i>Ai</i> LRB2A  | 91  |
| 29. PHOSPHO-SHIFT ASSAY IN RED AND FAR-RED LIGHT  | 93  |
| 30. PROBING PURIFIED LRB2 FOR THE PRESENCE OF PHOSPHOSERINE RESIDUES  | 95  |
| 31. TREATMENT OF SEEDLINGS WITH THE NEDD8 INHIBITOR MLN4924   | 99  |
| 32. PROBING PURIFIED LRB2 FOR NEDD8   | 100 |
| 33. POTENTIAL MECHANISMS FOR BLOCKING CUL3 BINDING  | 108 |
| 34. PROPOSED MECHANISM OF <i>Ai</i> LRB NEDDYLATION   | 112 |

# NOMENCLATURE & ABBREVIATIONS

## GENERAL ABBREVIATIONS

- +**: DNA promoter region
- $\alpha/\beta$  Domain**: Site of Rbx1 association with Cullin, creating an  $\alpha/\beta$  hydrophobic core
- 3-Box/3BOX**: Conserved alpha-helices responsible for high-affinity interactions with Cul3
- 26S**: 26S Proteasome complex
- A**: Activated, refers to the amino-terminal LRB ‘bridge’ structure
- ACC Agreement**: Comparison of predicted vs calculated solvent accessibility
- ACCpro**: Server which predicts the relative solvent accessibility for protein residues
- APC2**: Anaphase Promoting Complex 2
- At(*protein*)**: The homologous protein counterpart in *Arabidopsis thaliana*
- AtLRB2A**: More accurate predicted structural model of AtLRB2 created using Phyre2
- AtLRB2B**: A less accurate predicted structural model of AtLRB2 created by Phyre2
- AtLRB2N**: Shortened amino-terminal AtLRB2A model (residues 1-144)
- AXR1/ECR1**: Proteins acting as the RUB-activating E1 enzyme for NEDD8
- B**: Blocked, refers to the amino-terminal LRB ‘bridge’ structure
- BACK Domain**: BTB and C-terminal Kelch domain
- BBK**: BTB-BACK-kelch proteins
- bHLH**: Basic Helix-Loop-Helix structural motif
- BLAST**: Basic Local Alignment Search Tool
- BLOSUM**: BLOcks Substitution Matrix used for aligning protein sequences.
- BTB Domain**: Bric-a-brac/Tram-track/Broad complex domain
- C $\beta$** : Carbon residue of protein backbone which attaches to the R group
- CAND1**: Cullin-Associated and Neddylation-Dissociated 1 Protein
- CH Domain**: Cullin Homology region containing the  $\alpha/\beta$  and WH-A domains.
- CL Motif**: The Cullin-Like region of LRB that resembles Cul1/2
- CLUSTALO**: Clustal Omega multiple sequence alignment program
- Col-0**: The Columbia early-flowering ecotype of *Arabidopsis thaliana*
- ConSurf**: Bioinformatics tool for displaying evolutionary conservation on a 3D structure
- COP1**: Constitutive Photomorphogenic 1 E3 ligase Protein
- CN Domain**: Cullin Neddylation or WH-A domain
- CR Domain**: Cullin Repeat-like domain
- CRL/CRL3**: Cullin-RING and Cul3-RING ubiquitin Ligase complexes, respectively
- CSI-BLAST**: Context-Specific Iterated BLAST
- Cul**: The scaffolding protein Cullin
- Cul<sup>CL</sup> region**: Region of Cul1/2 corresponding with the CL region of LRB
- Cul1/2**: Cul1 and Cul2 proteins
- DCN1**: Defective in Cullin Neddylation E3 enzyme for NEDD8 conjugation
- DSSP**: Defined Secondary Structure of Proteins database
- DUBs**: Deubiquitination enzymes
- E1/E2**: Ub activating enzyme, Ub conjugating enzyme,
- E3**: Ubiquitin protein ligase complex
- EMBOSS**: European Molecular Biology Open Software Suite
- Expresso**: T-coffee MSA tool which aligns protein sequences using structural information
- EZA1**: Histone-lysine N-methyltransferase protein

**FLC:** Flowering Locus C gene which represses flowering  
**FRI:** Coiled-coil scaffold protein FRIGIDA which upregulates FLC  
**GFP:** Green Fluorescent Protein tag  
**HHpred:** Protein homology detection server based on pairwise HMM comparisons  
**HMM:** Hidden Markov Model  
**Hs(Protein):** The homologous protein counterpart in *Homo sapiens*  
**I-TASSER:** Iterative Threading ASSEMBLY Refinement server for protein structure prediction  
**InterPro:** Protein sequence analysis and classification server  
**LL Motif:** The Linker-Like region of LRB that resembles Rbx1  
**LRBs:** Light-Response BTB proteins  
**LRB1/2:** LRB1 and LRB2 proteins  
***lrb12/lrb123:*** Transgenic *lrb* double/triple knockout mutants, respectively  
**MAD:** Mutually-Assured Destruction mechanism  
**Matcher:** EMBOSS pairwise sequence alignment program  
**Mdm2:** RING finger type E3 ubiquitin ligase which promotes neddylation of p53 in humans  
**MEME Suite:** Motif-based protein sequence analysis tool  
**MG132:** 26S proteasome inhibitor  
**MLN4924:** Analog of adenosine 5'-monophosphate which inhibits neddylation  
**MODELLER:** Comparative protein structure modeling program  
**MS:** Murashige and Skoog basal salts  
**MSA:** Multiple Sequence Alignment  
**MultiSeq:** Bioinformatics tool for aligning protein sequences in VMD  
**N8:** Abbreviation for the NEDD8 Protein  
**NEDD8:** RUB/Neural precursor cell Expressed, Developmentally Downregulated 8 Protein  
**NEEDLE:** EMBOSS tool for global pairwise sequence alignment  
**NLS:** Nuclear Localization Sequence  
**NIMIN-1:** Coiled-coil NIM1-Interacting protein  
**NS:** Nuclear speckles  
**P:** A site of Phosphorylation on a protein or in a MSA  
**p53:** Tumor suppressor gene in humans  
**PDB:** The RCSB Protein Data Bank archive  
**Pfr/Pr:** Active/inactive phy conformations, respectively  
**PhosPhAt 4.0:** The Arabidopsis Protein Phosphorylation site database  
**Phy:** Phytochrome  
**Phylogeny.fr:** Phylogenetic sequence analysis server  
**Phyre2:** Protein Homology/analogy Recognition Engine version 2.0  
**phyB<sup>Pfr</sup>/ phyB<sup>Pr</sup>:** Active/inactive phyB conformation in R/FR light, respectively  
**PIFs:** Phytochrome Interacting Factor proteins  
***pif3:*** PIF3 protein knockout mutant  
**POB1:** Alternative name for *AtLRB2*  
**POLYVIEW-3D:** Protein structure visualization server  
**PSIPRED:** Secondary structure prediction server  
**QMEAN:** Server which estimates the quality of protein structural models  
**R/FR:** Red light (660nm) and Far-Red light (730nm), respectively  
**RBX1/ROC:** RING-box 1 or Regulator of Cullin protein  
**Rbx<sup>LL</sup> region:** Region of Rbx1 corresponding with the LL region of LRB  
**RCE1:** RUB-conjugating E2 enzyme for NEDD8 conjugation  
**RING:** Really Interesting New Gene  
**RMSD:** Root-mean-square deviation  
**RUB:** Related to Ubiquitin/NEDD8 protein

**SAS:** Shade Avoidance Syndrome  
**SET10/SDG10:** Set Domain Group 10, alternative name for EZA1  
**SMART nrdb:** Simple Modular Architecture Research Tool non-redundant database  
**SSE Agreement:** Comparison of predicted vs calculated secondary structures  
**SWISS-MODEL:** Protein homology modelling server utilizing evolutionary information  
**SWN:** SWINGER protein, alternative name for EZA1  
**T-Coffee:** Tree-based Consistency Objective Function For AlignmEnt Evaluation MSA package  
**TAIR:** The Arabidopsis Information Resource database  
**TRAF Domain:** Tumor Necrosis Factor Receptor Associated Factors  
**Ub:** Ubiquitin  
**UniProt:** Universal Protein Resource database of protein sequence and function  
**UniProtKB:** UniProt Knowledgebase database of functional information for proteins  
**UniProtKB AC:** Accession number for entries in the UniProt Knowledgebase database  
**UPS:** Ubiquitin/26S Proteasome system  
**VMD:** Visual Molecular Dynamics program for visualizing protein structures  
**WH-A:** Cullin Winged-Helix A domain, alternative name for CN domain  
**WH-B:** Cullin Winged-Helix B domain  
**WT:** Wild-type Col-0 ecotype in *Arabidopsis thaliana*  
**WU-BLAST2:** Washington University BLAST version 2.0  
**Z-Score:** Estimated absolute quality for a model using crystal structure comparisons

## **ABBREVIATIONS FOR PLANT SPECIES**

**ARALL:** *Arabidopsis lyrata*  
**ARATH:** Mouse-ear cress (*Arabidopsis thaliana*)  
**BRARP:** Chinese cabbage (*Brassica rapa* subsp. *pekinensis* or *Brassica pekinensis*)  
**CARUB:** Pink shepherd's purse (*Capsella rubella*)  
**CICLE:** Clementine (*Citrus clementina*)  
**GLYMA:** Soybean (*Glycine max*)  
**MAIZE:** Corn (*Zea mays* subsp. *mays* or *Zea mays*)  
**ORYSJ:** Asian rice (*Oryza sativa* subsp. *japonica*)  
**PHYPA:** Physcomitrella moss (*Physcomitrella patens*)  
**PICSI:** Sitka spruce (*Picea sitchensis*)  
**POPTR:** California poplar or black cottonwood (*Populus trichocarpa*)  
**PRUPE:** Peach (*Prunus persica*)  
**RICCO:** Castor oil plant (*Ricinus communis*)  
**SEMLL:** Spikemoss (*Selaginella moellendorffii*)

# **I. BACKGROUND**

## **PHYTOCHROMES & RED LIGHT RESPONSE**

Plants require exposure to light in order to produce energy, and a plant's ability to sense and respond to different wavelengths of light is key for its survival. When a plant is exposed to white light, red and blue wavelengths are absorbed by chlorophyll to perform photosynthesis, while photons of other wavelengths, such as green or far-red, are filtered through the plant or reflected<sup>1</sup>. While green light may not have a large effect on plant growth, the amount of blue, red, or far-red light the plant perceives helps to provide specific information about its surroundings. For example, plants that are grown in close proximity to one another can sense an increase in far-red light reflected off neighboring plants, causing the plant to develop shade avoidance syndrome (**SAS**). SAS causes stem elongation, decreased leaf expansion, and increased petiole elongation as the plant tries to outgrow its neighbors and reach full sunlight on top of the canopy<sup>1,2</sup>. The amount of red light perceived also influences seedling germination, seedling establishment, initiation of flowering, pathogen resistance, and regulation of circadian clocks<sup>3,4</sup>.

Proteins bound to chromophores are used as a way for eukaryotes to detect light. Chromophores are molecules that can absorb a certain photon wavelength and, in doing so, undergo a conformational change which changes the function of the protein bound to it, signaling that a certain wavelength of light has been detected<sup>5</sup>. Whereas retinol is used as the sole chromophore for the photoreceptors in the human retina<sup>6</sup>, plants use multiple

chromophore protein receptors to detect different wavelengths of light<sup>4</sup>. Phototropins and cryptochromes are used to detect blue light, while phytochromes are able to detect red and far-red photon wavelengths<sup>4</sup>.

## Phytochromes

Plants are able to detect the amount of red light that is available by using phytochromes (**phy**), a class of photoreceptors responsible for detecting red and far-red wavelengths<sup>4</sup>. Phytochromes have two photoconvertible conformations: the active **Pfr** conformation, which absorbs far-red light, and the inactive **Pr** conformation, which absorbs red light<sup>4</sup> (**Figure 1A**). When red light is absorbed by the Pr phy conformation, the phytochrome becomes active and can signal to downstream effectors<sup>4,7</sup>. Conversely, when far-red light is absorbed by the Pfr phy conformation, the phytochrome becomes inactive<sup>4</sup>.

Phytochromes act as a way for plants to monitor their environments and exist as dimers in solution<sup>4</sup>. Phy exists exclusively in the cytoplasm as the Pr conformation in darkness, but once the plant is exposed to red light, there is a conversion from the inactive Pr form to the active Pfr form<sup>4</sup>. Phytochrome dimers containing at least one Pfr conformation can then move into the nucleus (**Figure 1B**)<sup>4</sup>. Any Pfr homodimers present in the nucleus can then interact with various proteins and accumulate in small nuclear speckles (**NS**)<sup>1,2,4</sup> (**Figure 1C**).

Five phy proteins, phyA-E, are found in *Arabidopsis*<sup>4</sup>. PhyA accumulates in dark-grown seedlings and is the primary photoreceptor responsible for seedling photomorphogenesis (the developmental response dark-grown seedlings undergo when

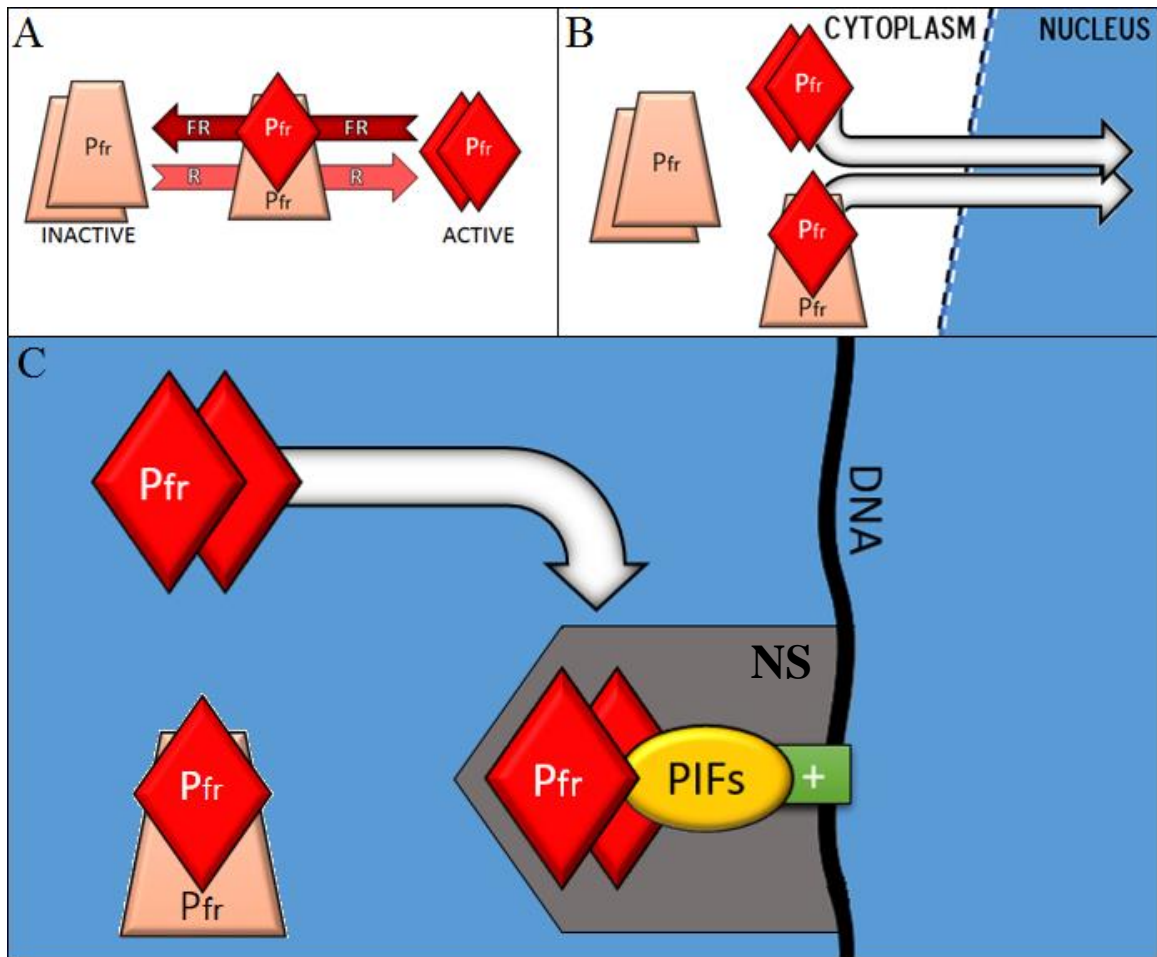


**Figure 1:** Phytochrome Response to Red Light

**A.** Photoconversion of inactive phytochrome (**Pr**) to the active (**Pfr**) form in response to red (**R**) light around  $660\text{nm}^8$ . When active **Pfr** is exposed to far-red (**FR**) light at around  $730\text{nm}^8$ , the phytochrome reverses and becomes inactive.

**B.** Both active and inactive forms of phytochrome remain as dimers in solution. As long as at least one member of the phy dimer is the active **Pfr** form, it can be transported into the nucleus.

**C.** Homodimers consisting of active phytochrome can interact with Phytochrome Interacting Factors (**PIFs**), which are transcription factor proteins that normally associate with certain promoter regions (+) of DNA that promote skotomorphogenesis or repress photomorphogenesis. The active phytochrome dimers coalesce and form structures known as nuclear speckles (**NS**) on various subnuclear foci.



exposed to light), but once seedlings are exposed to light, phyA is rapidly degraded<sup>4</sup>. PhyB-E are stable in white light conditions and are solely responsible for red light response, with phyB being the most influential light-stable phy<sup>1,4</sup>.

Exposure to red light influences almost every facet of the plant life cycle. When dark grown *Arabidopsis* seedlings are exposed to red light, approximately 10% of total gene expression is altered<sup>2</sup>. However, multiple factors determine how influential the exposure to red light will be, as the ratio of active (**phyB<sup>Pfr</sup>**) to inactive (**phyB<sup>Pr</sup>**) phyB creates different physiological responses<sup>2</sup>. Seedlings that are exposed to more far-red than red light have less active phyB<sup>Pfr</sup> in the nucleus, which may result in shade avoidance syndrome<sup>1</sup>. Conversely, seedlings exposed to high amounts of red light will have a large amount of active phyB<sup>Pfr</sup> in the nucleus<sup>1</sup>. With an increase in nuclear phyB<sup>Pfr</sup>, there is a decrease in stem elongation and an increase in the number and activity of chloroplasts<sup>1</sup>.

Although the ratio of red to far-red light controls the ratio of active and inactive phyB, the relative overall amount of phyB present in the nucleus was also found to create different physiological responses<sup>2,9</sup>. An increase in relative phyB levels as a result of phyB-overexpression or of knocking out negative regulators of phyB results in seedlings that are hypersensitive to red light, while a decrease in the level of phyB, as found in phyB knockdown or knockout mutants, results in a plant displaying red light insensitivity<sup>2,9</sup>, typically resulting in some degree of SAS.

## Phytochrome Interacting Factors

Phytochrome Interacting Factors (**PIFs**) are a family of nuclear-localized basic Helix-Loop-Helix (**bHLH**) transcription factor proteins that mediate various aspects of light signaling<sup>10</sup>. There are seven PIF protein members in *Arabidopsis*<sup>10</sup> and it is thought that their main function is to serve as negative regulators of photomorphogenesis<sup>1</sup>, with PIFs 1, 3, 4, and 5 being implicated in either promoting skotomorphogenesis<sup>11</sup> (the allocation of resources to hypocotyl elongation at the cost of root and cotyledon development when a seedling is grown in darkness<sup>7</sup>) or in photomorphogenic repression<sup>11</sup>. As such, the PIFs are specifically thought of as negative regulators of the phytochrome response pathway<sup>1,7,11,12</sup>.

In contrast to active phytochromes, the presence of PIF3 in the nucleus has been shown to promote accelerated hypocotyl elongation in shade<sup>1,7</sup>. PIF3, along with PIF1, PIF4, and PIF5, has been shown to promote hypocotyl elongation in prolonged red light exposure by both transcriptional regulation and by reducing the influence of phyB<sup>Pfr</sup> using feedback-loop-induced degradation<sup>1</sup>. Without PIF3, as shown in *pif3* knockout mutants, seedlings show hypersensitivity to R<sup>13</sup>, as PIF3 is required to prevent PhyB<sup>Pfr</sup> accumulation in the nucleus<sup>1</sup>.

A conserved amino-terminal region responsible for phyB binding, aptly named the Active PhyB Binding Motif, has been found in all seven PIF proteins<sup>11</sup>, and this motif allows for the high affinity binding of PIF3 to active phyB<sup>11</sup>. When phyB<sup>Pfr</sup> homodimers undergo nuclear translocation in red light, phyB<sup>Pfr</sup> is able to interact with the nuclear-localized PIF3, resulting in the colocalization of PIF3 and phyB<sup>Pfr</sup> in subnuclear photobodies<sup>11</sup> known as nuclear speckles (**NS, Figure 1C**).

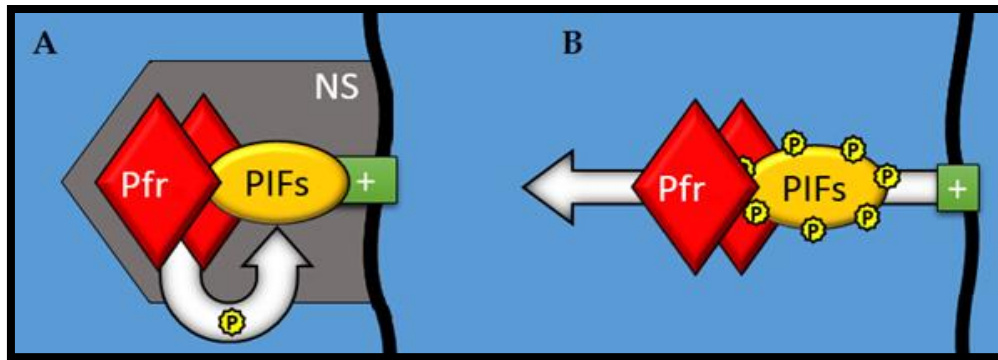


**Figure 2:** PhyB-PIF3 Interaction and Transphosphorylation

**A.** The interaction of photoactivated phytochrome with PIF proteins in the nucleus results in transphosphorylation (P) of the PIFs. The precise kinase responsible for phosphorylation is not known, but could be a result of an atypical kinase region on phytochromes as depicted<sup>4</sup>.

**B.** Transphosphorylation of the PIFs causes the release of the phyB<sup>Pfr</sup>/PIF complex from DNA. Transphosphorylation also blocks the PIFs from further interacting with any promoter regions, preventing any further NS colocalization.

### PhyB-PIF3 Phosphodegron

The regulation of proteins in the phytochrome signaling pathway using phosphorylation has been previously documented, as phyA is known to be an active kinase<sup>14</sup> and has been shown to directly phosphorylate proteins in the light response pathway such as Phytochrome Kinase Substrate 1, Auxin/Indole-3-Acetic Acid, and Nucleoside DiPhosphate Kinase 2<sup>15</sup>. Additionally, phosphorylation of phyA has been shown to prevent the interaction of phyA with PIF3, resulting in phyA degradation by the Constitutive Photomorphogenic 1 (COPI) E3 ubiquitin ligase complex<sup>15</sup>.

Phosphorylation was also found to control phyB and PIF3 stability, as both are degraded once PIF3 undergoes phosphorylation after interacting with phyB (Figure 2).

The breakdown of PIF3 occurs as part of a mutually-assured destruction (MAD) mechanism with phyB, where the interaction between PIF3 and phyB ultimately results

in the polyubiquitination and degradation of both<sup>11,16</sup>. The MAD mechanism is initiated when PIF3 is phosphorylated as a result of the interaction with photoactivated phyB (**Figure 2A**) in the nucleus, with PIF3 having the potential to be phosphorylated on up to 20 unique sites by a currently unidentified kinase<sup>11</sup>. The accumulated transphosphorylation of PIF3 provides a phosphodegron signal which grows stronger by each additional phosphorylation.

The phosphodegron signal is accompanied by the release of the phyB-PIF3 complex from DNA promoter regions<sup>11</sup> (**Figure 2B**). The phyB-PIF3 complex is then thought to recruit the Light-Response BTB proteins 1 and 2 (**LRB1** and **LRB2**, respectively) and create an active E3 complex<sup>16</sup>, which can then ubiquitinate the transphosphorylated PIF3 protein, marking PIF3 for degradation via the 26S proteasome system (**26S**)<sup>11</sup>. Mutant PIF3 proteins with phospho-null Ala mutations in 20 of the light-induced phosphorylation sites showed a significant reduction in ubiquitination, indicating that PIF3 transphosphorylation is necessary for interaction with and ubiquitination by the LRBs<sup>11,16</sup>. As the LRBs have been shown to interact with phyB<sup>Pfr</sup>, and the LRBs bind especially well when phyB<sup>Pfr</sup> is bound to transphosphorylated PIF3, it would seem that the LRBs would also ubiquitinate photoactive phyB in addition to transphosphorylated PIF3; however, no evidence has been found thus far that supports this hypothesis<sup>16</sup>.

In addition, PIF3 degradation is known to require a direct physical interaction between active PhyB<sup>Pfr</sup> and PIF3, as mutant PIF3 proteins that lacked the ability to bind phyB were not subject to light-induced degradation<sup>11</sup>. As such, the red light hypersensitivity phenotype that was found in the *pif3* knockout mutant seedlings was a result of the buildup of phyB<sup>Pfr</sup> in the nucleus, as there is an absence of the phyB<sup>Pfr</sup>-PIF3

interaction responsible for inducing the mutually-assured destruction negative feedback-loop that results in both PIF3 and phyB<sup>Pfr</sup> degradation<sup>1</sup>. Without PIF3, the PIF3-mediated-phyB<sup>Pfr</sup> degradation cannot occur, and the buildup of active phyB<sup>Pfr</sup> results in a red-light hypersensitive phenotype<sup>1</sup>.

## UBIQUITIN / 26S PROTEASOME SYSTEM

The protein ubiquitin (**Ub**) is vital for many signaling pathways due to its ability to selectively mark proteins for degradation via the 26S proteasome system, allowing for tightly-controlled regulation of various influential cellular processes. The Ub/26S proteasome system (**UPS**) has previously been implicated in phy-mediated signaling, as phosphorylated phyA is degraded by the COP1 E3-ubiquitin ligase complex<sup>15</sup>. It has also been shown that transcription factors PIF4, PIF5, and Long Hypocotyl in Far-Red 1, all of which are involved in the phytochrome response pathway, are degraded by the UPS after being phosphorylated<sup>15</sup>. Additionally, transphosphorylated PIF3 has been found to be ubiquitinated by the LRB E3 ligase complex<sup>16</sup>.

### Ubiquitin Conjugation Pathway

Ubiquitin is added to the protein using an ATP-dependent three-enzyme cascade mechanism composed of a ubiquitin activating enzyme (**E1**), ubiquitin conjugating enzyme (**E2**), and a ubiquitin protein ligase (**E3**)<sup>17</sup>. The E3 ligase family is composed of many different proteins that provide very specific target recognition and allow for diverse targets to be selectively degraded<sup>17</sup> (**Figure 3**). Approximately 5% of *Arabidopsis*' proteome is dedicated to the UPS<sup>18</sup>, with two E1 proteins, 37 E2 proteins, and potentially more than 1500 encoded E3 proteins in the genome<sup>17</sup>, illustrating the amount of target-specific diversity that is required to regulate protein breakdown.

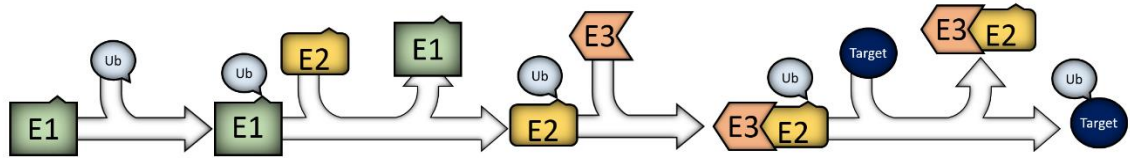


**Figure 3:** Simple Mechanism for the Ubiquitin Conjugation Cascade

Ubiquitin (**Ub**) is first attached to the Ubiquitin Activating Enzyme (**E1**) via a thioester bond in an ATP-dependent reaction. In the second step, ubiquitin is transferred to the Ubiquitin Conjugating Enzyme (**E2**). In the case of Cullin-RING Ligases, the E2 then binds to the Ubiquitin Protein Ligase (**E3**), forming a complex that is able to add ubiquitin to a lysine residue on a target protein.

### Degradative Effects of Ubiquitin Conjugation

Alteration of a protein by ubiquitin involves forming an isopeptide bond between an accessible lysine residue on the target protein and a glycine residue located on the carboxy-terminal end of Ub<sup>17</sup>. Ubiquitin itself can be ubiquitinated and form poly-Ub chains, with each ubiquitin protein containing several accessible lysine residues<sup>17</sup>. A single Ub conjugation to a protein<sup>19</sup>, or a poly-Ub chain conjugated to the Lys-63<sup>17,19</sup> of ubiquitin, will result in a non-proteolytic event<sup>19</sup> such as endocytosis of a protein<sup>17</sup>. Poly-Ub chains formed by conjugation of Ub to the Lys-48<sup>17,19</sup>, Lys-29<sup>19</sup>, or Lys-11<sup>17,19</sup> residue of another Ub will result in the degradation of the target protein by the 26S proteasome. The 26S proteasome releases poly-Ub chains from the target protein and degrades only the target<sup>20</sup>, allowing deubiquitination enzymes (**DUBs**) to cleave the poly-Ub chain down into single ubiquitin proteins. The release of ubiquitin chains by the 26S proteasome allows Ub to be recycled and reused to tag new proteins for degradation.

## Steric Effects of Ubiquitin Conjugation

The addition of a ubiquitin chain to a protein may also result in steric hindrance, as the bulky polyubiquitin chain can alter the structure of large multi-protein structures<sup>19</sup>. Ubiquitin also plays a large role in transcriptional regulation<sup>19</sup>. Steric consequences of ubiquitin attachment have been known to alter the structure of chromatin fibers<sup>19</sup>, and ubiquitination of different histone proteins by E3 ubiquitin ligase complexes might be partially responsible for the radical change in gene expression seen in *Arabidopsis* when active phyB<sup>Pfr</sup> is present in the nucleus<sup>11</sup>.

Some E3 proteins have also been shown to simultaneously function as transcriptional regulators and as adaptor proteins in Cullin-RING ligase complexes<sup>21</sup>. E3 ligase complexes can directly target transcription factors bound to DNA, RNA-binding proteins, or histone-methyltransferases for degradation via the UPS<sup>19,22</sup>.

The ubiquitination of histone proteins can have inhibitory effects on transcription or provide access to promoter regions through steric hindrance<sup>19</sup>. The monoubiquitination of histone H2B in yeast is associated with actively-transcribed euchromatin, and the addition of a ubiquitin molecule has been shown to induce structural changes in chromatin organization, ultimately providing new binding sites for chromatin regulators while simultaneously preventing other transcription factors from associating with chromatin<sup>19</sup>. Much like histone H2B, the addition of ubiquitin to histone H2A provides binding sites for transcription factors or blocks chromatin access for others, but this results in an overall repelling effect that prevents gene expression, promotes chromatin compaction, and silences gene expression<sup>19</sup>.



## CULLIN-RING LIGASE COMPLEXES

E3 ubiquitin ligase complexes are able to recognize both the substrate protein being targeted for degradation as well as the E2 enzyme that brings ubiquitin to the E3 complex<sup>23</sup>. One type of E3 ubiquitin ligase complex contains a member of the Cullin (**Cul**) family of scaffolding proteins. In *Arabidopsis*, there are five main types of known Cullins (**AtCul**) which include Cul1, Cul2, Cul3, Cul4, and **APC2**<sup>24,25</sup>. However, there are a total of 490 Cul-domain-containing proteins that have at least 60% sequence conservation located in the **SMART nrdb** database<sup>23</sup>, which helps to illustrate the ubiquitous presence of Cullin-like proteins in *Arabidopsis*.

### **General Characteristics of Cullin Proteins in *Arabidopsis thaliana***

All of the individual Cullin protein members are structurally very similar to one another and highly conserved, with all Cullin proteins sharing a similar domain and tertiary structure<sup>23</sup>. Cul1 through Cul4 contain a cylindrical amino-terminal domain which contains three repeats of the Cullin Repeat-like (**CR**) domain, as well as highly-conserved carboxy-terminal domains that include Cullin Homology (**CH**) and Cullin Neddylation (**CN**) domain<sup>23</sup> (**Figure 4A**). The CN region is made up of the Winged-Helix B (**WH-B**) domain and contains a highly-conserved lysine residue which is responsible for conjugation with NEDD8<sup>23</sup>, a small modifier protein which will be discussed in further detail in a later section.

The amino-terminal portion, which contains the three CR domains, has a long cylindrical shape for approximately 450 residues<sup>23,26</sup>. At the carboxy-terminal end of each Cullin rests a globular region which contains an  $\alpha/\beta$  domain and the two Winged-Helix domains; the latter lie on opposite sides of the protein from one another<sup>26</sup> (**Figure 4A-B**). The structure of Cullin, as well as the associated members of the E3 complex that Cul interacts with, have only been crystallized and resolved in mammalian proteins to date, but the structural models of both have been generally deemed applicable across all eukaryotic species based on the extreme conservation of the interactions between Cullins and their CRL partners determined using biochemical assays in systems ranging from humans to yeast<sup>23</sup>.

### **Genetic Diversity of Cullin Proteins**

A genome-wide study of Cullin proteins suggests that all eukaryotic Cul proteins arose from three genes, annotated *Cula*, *Cul $\beta$* , and *Culy*<sup>23</sup>. In humans, the *CUL1* and *CUL2* genes are thought to be descended from the *Cula* gene, while *CUL3* arose from *Cul $\beta$*  and *CULA* evolved from *Culy*<sup>23</sup>. As the structures and functions of Cullin proteins are thought to be almost completely conserved across all eukaryotic organisms, we can assume this is also true for *Arabidopsis*<sup>23</sup>.

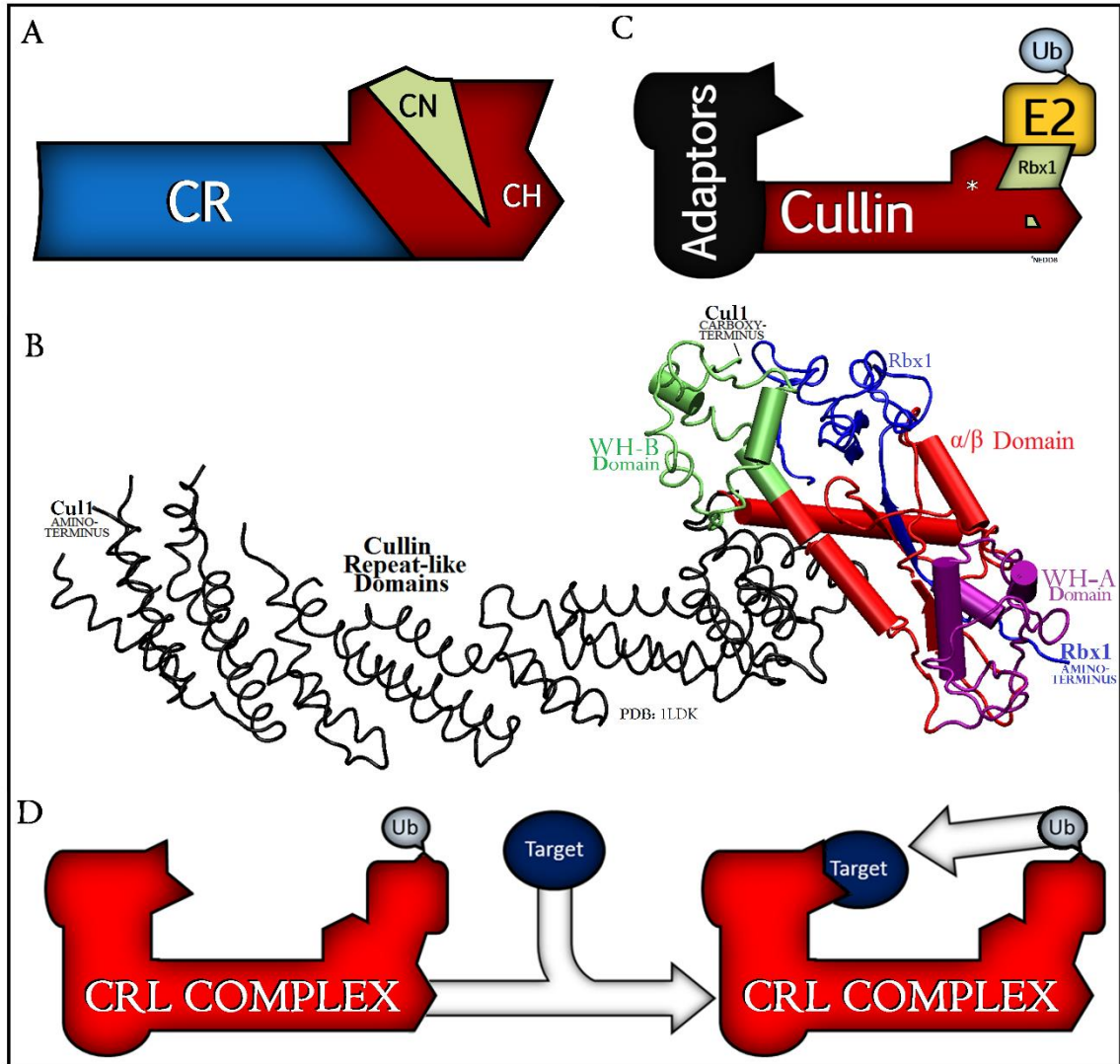


**Figure 4:** Structure of Cullin-RING Ligase Complexes

**A.** The amino-terminal portion of Cullin proteins contain three CR domains, which are collectively shown in blue<sup>23,26</sup>. A highly-conserved CH domain surrounds the winged-helix structure of the CN domain, shown in red and green, respectively<sup>23,26</sup>.

**B.** A model of crystalized Cul1/Rbx1 in *Homo sapiens* (PDB: 1LDK). The Cullin Repeat-like, Winged Helix, and  $\alpha/\beta$  domains are color coded<sup>26</sup>, with Rbx1 being depicted in blue. The threading of the amino-terminus of Rbx1 through the  $\alpha/\beta$  domain of Cul1 can also be observed.

**C.** The amino-terminal region of each type of Cullin protein is responsible for interacting with a different adaptor protein. Cullin's carboxy-terminal region focuses on interacting with Rbx1, which in turn recruits and associates with an ubiquitin-charged E2 enzyme. This multimeric complex of proteins is known as a CRL complex. The site of NEDD8 conjugation is marked with an asterisk.

**D.** When the adaptor protein in the CRL complex interacts with the target protein, the target is brought in close proximity to the Ub-charged E2 enzyme due to the ring-like shape of the CRL complex. The ubiquitin can then be transferred to a lysine residue on the target protein.

## Role of Cullin Proteins in the Formation of Cullin-RING Ligase Complexes

Cullin's carboxy-terminal domain binds to a Really Interesting New Gene (**RING**) partner called RING-box protein 1 (**Rbx1**), which can also be referred to as Regulator of Cullins (**ROC**)<sup>23</sup>. Rbx1 associates with Cullin by inserting its long amino-terminal extension through certain secondary elements in the  $\alpha/\beta$  domain on Cullin<sup>23</sup> (**Figure 4B**). The  $\beta$ -sheet of Rbx1 forms hydrogen bonds with the S1-3 strands of Cul1, creating an  $\alpha/\beta$  hydrophobic core that is the characteristic feature of Cullin-RING ligase complexes<sup>23</sup>.

Once Cullin is associated with Rbx1, the ubiquitin-charged E2 enzyme can be recruited to the carboxy-terminal portion of Cul<sup>23,27</sup>. Meanwhile, the amino-terminal CR1 region of Cul utilizes helices H2 and H5 to interact with specifically-designated adaptor proteins<sup>23</sup>, which differ from one Cullin protein to the other. The Cullin proteins that relate to this thesis will be discussed further in the next section.

The presence of Rbx1-E2-Ub at the carboxy-terminal of Cullin, in addition to the adaptor protein associated with the amino-terminal region, creates a multimeric structure that is known as a Cullin-RING ligase (**CRL**) complex<sup>27</sup> (**Figure 4C**). The adaptor protein can then interact with the target protein, which will be placed in close proximity to the Ub-charged E2 due to CRL's ring-like structure (**Figure 4D**), allowing the complex to ubiquitinate the target<sup>28</sup>.

## Crystal Structures of Native Cullin-RING Ligase Complexes

The native structure of three CRL complexes have been modeled in humans at 3.1Å resolution and will be later used for structural analysis. All three crystal structures were readily accessible from the Protein Data Bank (**PDB**). 1LDK and 4P5O both depict *HsCul1* in complex with *HsRbx1*<sup>26,29</sup>, while 2HYE depicts *HsCul4A* and *HsRbx1* associated with one another<sup>30</sup>. All three CRL complexes were unable to resolve the amino-terminal portion of Rbx1, but all models contain the portion of Rbx1 responsible for creating the  $\alpha/\beta$  hydrophobic core<sup>26,29,30</sup>. The crystal structure for 4P5O also includes the modifier protein Neural precursor cell Expressed, Developmentally Downregulated 8 (**NEDD8**) conjugated to Cul4A<sup>30</sup>. The implications of NEDD8 conjugation to Cullin proteins will be discussed in a later section.

## CUL3 & THE BTB DOMAIN

LRB proteins contain a Bric-a-brac/Tram-track/Broad (**BTB**) domain and have previously been shown to interact specifically with Cul3-RING ubiquitin ligase (**CRL3**) complexes preferentially in red-light<sup>2</sup>. Cul3 utilizes an amino-terminal extension sequence to specifically bind only substrate receptors that contain a BTB complex<sup>23</sup>. Previous genetic analysis of *Arabidopsis* shows various BTB subfamilies being responsible for the regulation of ethylene production<sup>27</sup>, development of gametophytes<sup>31</sup>, phototropism<sup>32</sup>, and other physiologically-important plant pathways. BTB domain E3 ligase complex adapter proteins are unique, however, due to their ability to dimerize and recruit two Cul3 subunits into the same Cullin-RING ligase complex, as well as their ability to recruit both Cul3 and a degradation target simultaneously via two distinct protein-interaction domains<sup>33</sup>.

### Characteristics of the BTB, BACK, and TRAF-Like Domains

The BTB fold motif is specifically targeted by Cul3<sup>34,35</sup>, and BTB proteins are also able to homodimerize at an area different from Cul3/BTB interaction, allowing both processes to occur at once<sup>35,36</sup>. It is the dimerization of the BTB domain at the  $\alpha 1$  helix<sup>36</sup> that allows two Cul3 proteins to be recruited in order to form one large CRL3 complex<sup>35</sup>. The BTB domain shares a common fold topology across all eukaryotes (**Figure 5A**); however, the surface residues of the domain are highly variable in order to obtain a large amount of different protein-protein interaction states<sup>34</sup>, allowing BTB proteins to be

selective in their dimerization partners. This prevents all BTB proteins from dimerizing with one another, but evidence suggests that closely-related BTB proteins are able to heterodimerize with one another in addition to homodimerization<sup>2</sup>.

A BTB and C-terminal Kelch (**BACK**) domain is commonly found immediately following the BTB domain<sup>2</sup>. The BACK domain is found mainly in BTB proteins that contain carboxy-terminal kelch repeats, called BTB-BACK-Kelch (**BBK**) proteins, but was found to be present in 11 BTB proteins in *Arabidopsis* that did not contain carboxy-terminal kelch repeats<sup>37</sup>. The LRB proteins contain a BTB domain and a BACK domain<sup>2</sup>, but no carboxy-terminal kelch repeat was detected.

Previously, the region carboxy-terminal to the BACK domain has been implicated in target recognition in BBK proteins<sup>34,35</sup>. It is also predicted that the BACK domain is necessary to correctly position the carboxy-terminal recognition region for substrate ubiquitination<sup>34</sup>. Despite a high amount of carboxy-terminal sequence conservation in the LRBs, the **SMART**<sup>38</sup> database could not recognize or predict the presence of any carboxy-terminal domains for LRB2. However, the InterPro database<sup>39</sup> entry for LRB2 in *Arabidopsis thaliana* (**UniProtKB AC: Q9FPW6**) predicts that the carboxy-terminal region contains a Tumor Necrosis Factor Receptor Associated Factors (**TRAF**)-like domain. TRAF proteins, as well as TRAF-like domains in other proteins, have been found to have roles in targeted degradation, with the domain typically containing a large, shallow groove that functions as the binding domain for a protein substrate<sup>40</sup>. The predicted TRAF-like domain further supports the theory that the carboxy-terminal end of the LRBs is responsible for recognizing and interacting with the target protein.

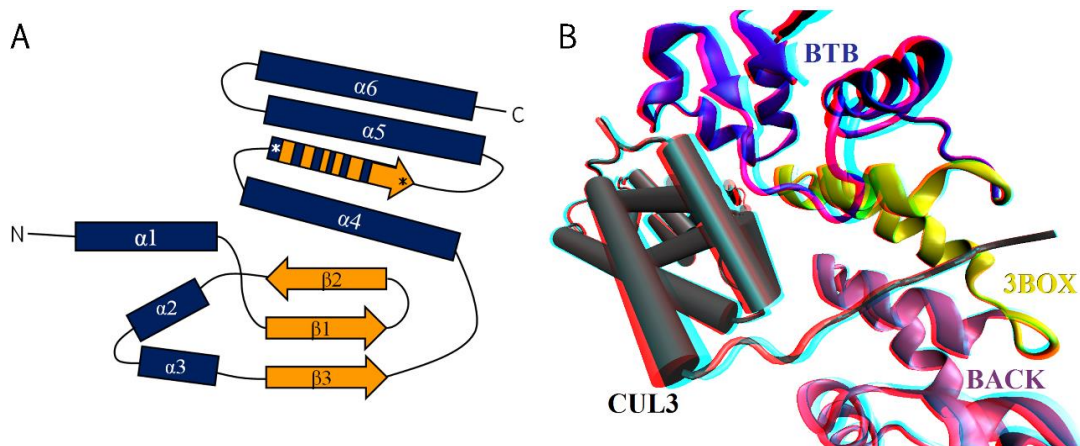


**Figure 5:** Conserved BTB Fold Topology and Interaction with Cul3

**A.** The fold topology for the well-conserved BTB domain<sup>34,36</sup>. All of the secondary structures for the BTB domain are shown and are drawn in agreement with previous BTB fold topologies published<sup>34,36</sup>, with the  $\alpha$ -helices denoted using a navy blue box and the  $\beta$ -sheets modeled using an orange arrow. The unlabeled structure marked with asterisks denotes a variable region in the domain that can be found as either an  $\alpha$ -helix or as a  $\beta$ -sheet, and it is drawn using both elements.

**B.** Anaglyphic image of the crystal structure for the PDB structure **4AP2** shows the layout of the BTB/3BOX/BACK domains of Kelch-like Protein 11 in relation to the amino-terminal extension of Cul3 at a 2.80Å resolution in humans<sup>35</sup>. Image was rendered using **VMD**<sup>41</sup>.

### Role of the 3-Box in Interactions with Cul3

Two conserved helices in the BTB domain,  $\alpha 5$  and  $\alpha 6$ , were determined to be responsible for high-affinity interaction with Cul3<sup>35,42</sup>. These helices, located at the carboxy-terminal portion of the BTB domain, were named the “**3-Box**” (**3BOX**)<sup>42</sup>. Two helices in the amino-terminal portion of the BACK domain,  $\alpha 7$  and  $\alpha 8$ , were also found to create the 3-Box motif and bind the two carboxy-terminal BTB helices in an antiparallel four-helix bundle<sup>35</sup> (**Figure 5B**). This 3-Box helix bundle contributes to the interaction with the carboxy-terminal portion of H2 and H5 of Cul3, and ultimately the helices of the BTB and BACK domains create a hydrophobic groove that allows the amino-terminal extension sequence that is unique to Cul3 to insert itself antiparallel to  $\alpha 7$ <sup>35</sup> of the 3-Box bundle. The majority of the interactions between the amino-terminal extension of Cul3 and the 3-Box were found to be hydrophobic<sup>35</sup>.



## NEDD8 & NEDDYLATION

One necessary modification for Cul proteins is the addition of the Related to Ubiquitin/Neural precursor cell Expressed, Developmentally Downregulated 8 (**RUB/NEDD8**) protein<sup>19,25,35</sup>, which will be referred to hereafter as only NEDD8. In *Arabidopsis thaliana*, two redundant genes, *UBQ15* and *UBQ7*, code for NEDD8, differing by only one amino acid<sup>25</sup>. Both encode a full-length protein that is cleaved in half to yield one ubiquitin and one NEDD8 protein. One additional gene, *UBQ16*, encodes for a protein 77.6% identical to *UBQ15* and *UBQ7*, but is only expressed in the stems and flower buds of plants<sup>25</sup>. Despite NEDD8 sharing 61.6% sequence identity with ubiquitin, alignments of the two proteins reveals that they have a structure that is almost identical to one another<sup>43</sup>, and it would seem that NEDD8 and Ub may having differing but overlapping roles in various cellular processes. The addition of NEDD8 to various proteins has been widely shown to result in an overall change of protein function<sup>44-46</sup>, but this phenomenon has not yet been well studied in *Arabidopsis thaliana*.

### The NEDD8 Conjugation Pathway

The covalent attachment of NEDD8 using its carboxy-terminal glycine residue to a conserved carboxy-terminal lysine in Cullin proteins occurs through a process much like the ubiquitin E1-E2-E3 conjugation cascade<sup>44</sup> (**Figure 6**). The NEDD8 conjugation cascade is less specific than its ubiquitin counterpart, as NEDD8 can be added to the ubiquitin E1 enzyme, transferred to the ubiquitin E2 enzyme, and ultimately incorporated

into ubiquitin chains via the activity of an E3 ligase<sup>45</sup>, though the consequences of this addition to a growing ubiquitin chain is not yet known. The opposite scenario is not true, however, as the proteins that act as the NEDD8 E1 or E2 enzymes do not recognize ubiquitin<sup>45</sup>. Each NEDD8 conjugation enzyme will therefore be referred to by its acronym to avoid any confusion.

NEDD8 is attached to the RUB-activating E1 by ATP-dependent conjugation<sup>25,45</sup>. In plants, the RUB-activating E1 enzyme is composed of heterodimeric Auxin-resistant 1 (**AXR1**) and E1 C-terminal-related 1 (**ECR1**) proteins<sup>25</sup>. This high-energy intermediate then transfers NEDD8 to the RUB-conjugating enzyme (**RCE1**) E2 protein<sup>17,25</sup>.

Circumstantial evidence has suggested that Rbx1 may provide the E3-like action necessary for the transfer of NEDD8 onto a conserved Cullin lysine residue. However, there has been no direct proof that Rbx1 is involved in the transfer of NEDD8 from RCE1 to Cullin, only that the RING domain of Rbx1 helps promote Cullin neddylation. Perhaps the addition of Rbx1 to Cullin provides NEDD8 with access to the appropriate lysine residue needed for conjugation. However, the Defective in Cullin Neddylation (**DCN1**) protein has been shown to provide the NEDD8 E3-ligase functions in both yeast and mammals<sup>44</sup>. DCN1 has been shown to interact with Rbx1, suggesting that DCN1 might cooperate with Rbx1 to enhance neddylation of Cullin proteins<sup>44</sup>. Much like the ubiquitin E3 ligase complex, DCN1 does not form thioester bonds with NEDD8 while interacting with RCE1 and Cullin, strongly suggesting that DCN1 is the NEDD8 E3 protein ligase responsible for the last step in NEDD8 conjugation<sup>44</sup> (**Figure 6**).

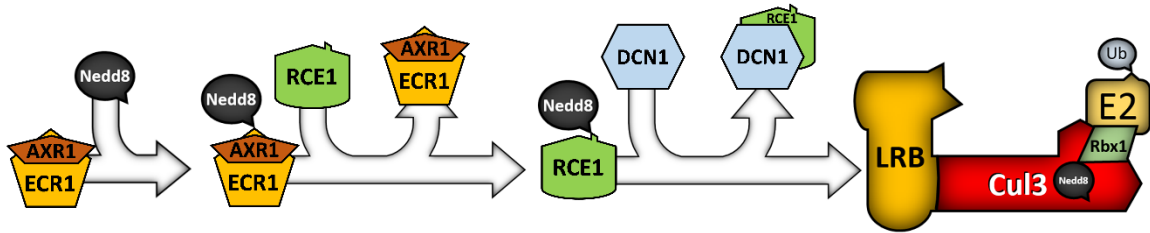


**Figure 6:** NEDD8 Conjugation Cascade

NEDD8 conjugation occurs very much like the conjugation of Ubiquitin to a target. First, free NEDD8 is attached to the heterodimeric Auxin-resistant 1 (**AXR1**) and E1 C-terminal-related 1 (**ECR1**) proteins. NEDD8 is then transferred from the high-energy E1 complex to the RUB-conjugating enzyme. Similarly to the Ub conjugation cascade, the NEDD8-charged RUB-conjugating E2 enzyme interacts with DCN1, which is able to neddylate a target protein without interacting directly with the NEDD8 itself. In the case of CRL complexes, DCN1 interacts with Rbx1 and Cullin, positioning itself in a way that allows the E2 to transfer the NEDD8 onto a conserved lysine residue that is present on all Cullin proteins.

### The Possible Effects of NEDD8 Conjugation

NEDD8 conjugation can induce a conformational change that ‘activates’ an enzyme, granting it flexibility and altering the function of the protein<sup>44</sup>. NEDD8 conjugation has been shown to cause a drastic conformational change in the Winged-Helix B region of Cullin proteins, conferring Rbx1 flexibility and placing the active Rbx1-bound E2 enzyme close to the target protein<sup>44</sup>. This close proximity of E2 with the target allows the transfer of ubiquitin to take place<sup>44</sup>, essentially activating the CRL complex. NEDD8 was also found to greatly stimulate ubiquitin chain elongation by creating a flexible activated Rbx1-E2 heterodimer that can be placed in different orientations and can add additional ubiquitin proteins to the elongated ubiquitin chain<sup>44</sup>.

NEDD8 can also result in direct steric hindrance or create a conformational change in the protein that limits its interactions with other proteins<sup>45</sup>. This effect can also

be seen when NEDD8 is attached to Cullin, as it creates steric hindrance that blocks the binding site of **CAND1**, a protein that sequesters unneddylated Cullin proteins and prevents them from creating Cullin-RING ligase complexes<sup>44</sup>. Also, the conformational change caused by NEDD8 that occurs in the winged-helix B region of Cullin grants Rbx1 flexibility by preventing the globular portion of Rbx1 from binding with Cullin<sup>44</sup>. Rbx1 remains tethered to the E3 complex by the amino-terminal extension embedded in the  $\alpha/\beta$  hydrophobic core of Cullin, and the flexibility and range granted to Rbx1 by NEDD8 ultimately activates the E3 complex<sup>44</sup>. Inactivation of a protein by NEDD8 occurs with human p53 protein, as NEDD8 creates steric hindrance that prevents p53 from binding to DNA, causing the protein to become inactive until NEDD8 is removed<sup>46</sup>.

## LIGHT-RESPONSE BTB PROTEINS

Despite its relative stability in light, phyB does undergo a slow degradation via the UPS<sup>2</sup>. The Light-Response BTB proteins 1 and 2 (**LRB1** and **LRB2**, respectively) are responsible for preventing phyB accumulation in red light, as an accumulation of phyB<sup>Pfr</sup> after the initial phyB signal propagation would cause the plant to become hypersensitive to red light<sup>2</sup>. LRB2 has been shown to interact with phyB<sup>Pfr</sup> in vitro, and this interaction is further enhanced in the presence of certain Phytochrome Interacting Factors<sup>16</sup>. However, a detailed mechanism regarding how the LRB proteins regulate phyB levels is still under investigation<sup>2,16,47</sup>.

The LRBs are E3 ligase linker proteins that were found to be involved in phytochrome-related processes. Due to their high sequence identity, LRB knockout mutant lines were created (*lrb1 lrb2*) which produced an interesting red light hypersensitive phenotype in *Arabidopsis thaliana*<sup>2</sup>. LRB1 and LRB2 shared 88% identity and an overall sequence similarity of 94% as determined using the global sequence alignment tool NEEDLE<sup>48</sup>. A third LRB protein, LRB3, was also identified, sharing 69% similarity and 55% identity with LRB1 and 2<sup>48</sup>, but the lack of robust expression and degree of overall sequence divergence implies that it is only a pseudogene<sup>2</sup>. All three LRB proteins were found to have the same overall domain distribution, with a proposed nuclear localization sequence (**NLS**) amino-terminal to the BTB domain as well as a carboxy-terminal BACK domain<sup>2</sup>.

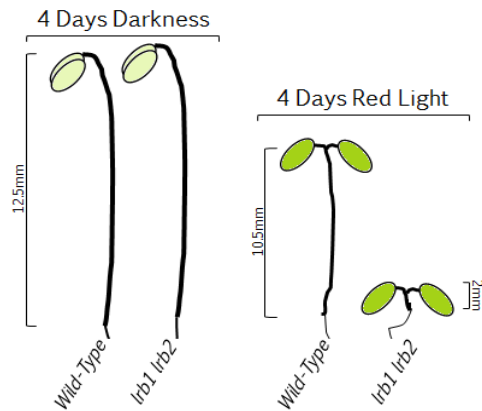


**Figure 7:** Photomorphogenic Differences of *lrb1 lrb2* Knockouts in *Arabidopsis*

Wild-type and *lrb1 lrb2* double knockout seedlings showed no noticeable differences when grown for 4 days in continuous darkness. When grown for 4 days in  $10 \frac{\mu\text{mole}}{\text{m}^2\text{s}}$  of red light, however, the *lrb1 lrb2* mutant showed significantly shorter hypocotyl length than the wild-type control<sup>2</sup>. There were no differences observed between plants grown in continuous far-red or blue light conditions<sup>2</sup> (*not shown*). Figure based on previously reported data and is not drawn to proportional scale<sup>2</sup>.

### Effects of *lrb1 lrb2* Double Knockout Mutants on Light Signaling

The nuclear-localized LRB1 and LRB2 proteins have previously been shown to negatively influence phyB and phyD activity *in planta*, as knocking out both *LRB1* and *LRB2* result in plants that are red-light hypersensitive<sup>2</sup> (**Figure 7**). Knocking out only *LRB1* or *LRB2* did not show an extreme phenotypic change, indicating that LRB1 and LRB2 act redundantly to negatively regulate red light responses. This redundancy could also be seen when LRB1 was reintroduced into the *lrb1 lrb2* double mutant knockout (*lrb12*), as Flag-LRB1 was able to rescue the *lrb12* phenotype, preventing the red light hypersensitivity normally seen in the double mutant knockout<sup>2</sup>.

Knocking out both LRB1 and LRB2 created plants extremely hypersensitive to red light. Additionally, the *lrb12* double knockouts were found to have higher amounts of chlorophyll present, as well as increased amounts of phyB and phyD when grown in red light<sup>2</sup>. Phenotypic differences in red-light grown *lrb12* mutants included shorter petioles, substantially shorter hypocotyls, and a delay in flowering<sup>2</sup>. Photomorphogenic defects, which included shorter hypocotyls, dwarfed rosettes, shorter petioles, and delayed

flowering, were found only when *lrb12* was exposed to red light (**Figure 7**). *lrb12* plants grown in continuous darkness or exposed to continuous blue or far-red light were indistinguishable from the wild-type control<sup>2</sup>, suggesting that the phy pathway was being affected in the *lrb12* double knockout plants.

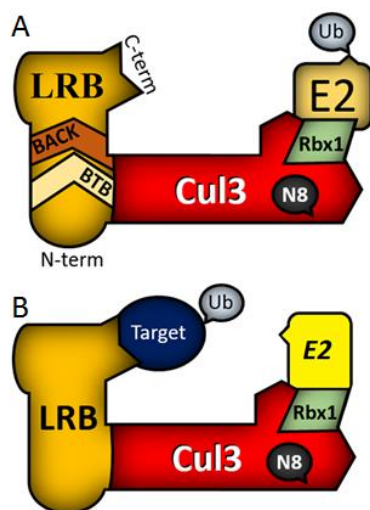
PhyB and phyD were found to be epistatic to the LRB proteins, as inactivating phyB and phyD in *lrb12* mutants saw a near complete suppression of the red-light hypersensitivity found in the *lrb12* mutant phenotype<sup>2</sup>, suggesting that LRB proteins act to suppress phyB and phyD. It was also shown that the LRBs increase the rate of phyB and phyD breakdown in the cell, as well as work through phyB to enhance phyA accumulation<sup>2</sup>. The breakdown of phyB after four days of continuous red light in the *lrb12* mutant was remarkably slower than wild type<sup>2,16</sup>. Additional treatment of the *lrb12* mutants with the 26S proteasome inhibitor MG132 resulted in further stabilization of phyB levels, implicating other E3 ligase activity, such as COP1, may also be responsible for phyB/D breakdown<sup>2</sup>.

### **LRB Protein Interactions in *Arabidopsis thaliana***

Both LRB1 and LRB2 interact with Cul3 *in vivo*, as predicted by the BTB/BACK domains present in both sequences<sup>2</sup> (**Figure 8A**). The interaction of the LRBs with Cul3 is dependent on light, with a stronger LRB/Cul3 interaction seen in response to red light as compared to dark-grown seeds<sup>2</sup>, which further supports the phenotypic differences observed in red light conditions. Also, as with all BTB proteins, LRB1 and LRB2 can form homodimers or heterodimers with one another, but were not found to interact with other types of BTB proteins<sup>2</sup>, indicating that dimerization is confined to other LRB proteins.

The LRBs have also been shown to interact with PIF3 *in vivo*<sup>16</sup>, suggesting that PIF3 is a target for the LRB CRL3 complex (**Figure 8B**). The interaction of PIF3 with LRB2 was found to be stronger with phosphorylated PIF3 *in vitro*, with LRB2 playing a role in the mutually assured destruction mechanism that degrades both PIF3 and phyB<sup>16</sup>. Additionally, LRB2 was able to interact with both forms of phyB *in vitro*, and this interaction was amplified with the addition of PIF3<sup>16</sup>. Interestingly, an *in vitro* immunoprecipitation of LRB3 showed that LRB3 can interact with the phospho-mimic PIF3 protein, which has an S/T→D mutation in 6 key phosphorylation locations and can mimic transphosphorylated PIF3, but this interaction was much weaker than was seen with LRB1 or LRB2<sup>16</sup>. However, LRB3 has never been detectable *in vivo* and was found to not be actively expressed, indicating that it might be a pseudogene<sup>2,16</sup>. Therefore it is currently unknown whether LRB3 can interact with Cul3 or dimerize.

**Figure 8:** The LRBs are the Adaptor Proteins in CRL3 Complexes



**A.** The LRB proteins interact with Cul3 to form the multimeric CRL3 complex. When bound to Cul3, the carboxy-terminal portion of LRB that is thought to be responsible for target recognition is positioned near the ubiquitin-charged E2. Once NEDD8 (**N8**) is conjugated to Cul3, the linker protein Rbx1 becomes flexible, and with the ring-like structure of the CRL3 complex, this brings the E2 into close proximity to the carboxy-terminus of LRB.

**B.** LRB proteins are able to selectively target other proteins for degradation, and when the target interacts with the carboxy-terminal end of the LRBs, the flexible and closely-located E2 protein can transfer Ub to the target protein.



## Effects of *lrb1 lrb2 lrb3* Triple Knockout Mutants on Light Signaling

Despite the *lrb1 lrb2 lrb3* triple knockout mutant (*lrb123*) having the same phenotypic characteristics as the *lrb12* mutant and no post-transcriptional data being available for LRB3<sup>2</sup>, the protein that was previously-dubbed a pseudogene may actually play a role in red light signaling<sup>16</sup>. LRB3 was previously detectable using reverse transcription PCR, indicating that it is actively transcribed<sup>2</sup>, but the LRB3 protein itself has yet to be detected by either immunoblotting or mass spectrometric analysis<sup>2,16</sup>. Despite this, the degradation of PIF3 was found to be reduced in the *lrb123* mutant, while PIF3 degradation was normal in the *lrb12* mutant<sup>16</sup>, suggesting that LRB3 is a functional gene that is able to cause PIF3 degradation in red light.

The amount of degradation for both native and phosphorylated PIF3 in the *lrb123* mutant after 60 minutes of red light irradiation was significantly decreased compared to the wild-type control, which had approximately 25% less PIF3 present than the triple mutant<sup>16</sup>. Additionally, phyB levels in the *lrb123* mutant were unaltered by red light. This phenomenon did not change in the PIF3-GFP transgenic lines, which contained an additional copy of PIF3 controlled by the very strong 35S promoter<sup>16</sup>, resulting in a massively high levels of PIF3 protein that should help to further abolish phyB. However, phyB levels remained unaltered in *lrb123* after four days of continuous exposure to red light, despite the increased degradation of phyB in the control line resulting from 35S-controlled PIF3 overexpression<sup>16</sup>.

### **Proposed Interaction of LRB with PHYB/PIF3 in Red Light**

The *lrb123* mutant was found to have less ubiquitinated PIF3 present than the wild-type control, and ubiquitinated phyB was not detectable at all in the *lrb123* mutant<sup>16</sup>, suggesting that the LRBs are solely responsible for phyB degradation and only assist in PIF3 ubiquitination. *In vitro* studies of the LRBs showed that LRB2 is able to interact with phosphorylated PIF3 and phyB<sup>Pfr</sup>, as well as with phyB<sup>Pr</sup> when phosphorylated PIF3 is also present<sup>16</sup>. Only PIF3 was found to be ubiquitinated by the LRB2 E3 complex *in vitro*, however, and neither phyB<sup>Pfr</sup> nor phyB<sup>Pr</sup> were found to be ubiquitinated in the same *in vitro* experiments<sup>16</sup>.

The ability of LRB2 to interact with phyB but not ubiquitinate it *in vitro* may suggest that phyB needs the phosphodegron signal propagated by phosphorylated PIF3 in order for phyB to be ubiquitinated. PhyB degradation was previously found to require direct physical interaction between phyB and PIF3, and without this interaction, a buildup of phyB was observed<sup>1</sup>. Another idea is that the LRBs must undergo a light-dependent modification in order to interact with Cul3, as LRB interacts with Cul3 strongly in red light. Therefore, without this light-induced modification to LRB, LRB cannot interact with Cul3 and cannot form an E3 ligase complex capable of ubiquitinating phyB<sup>Pfr</sup>.

### **The Region of the LRBs Found Amino-terminal to the BTB Domain is Important for Vernalization**

Recently, it was established that the amino-terminal portion of both *At*LRB1 and *At*LRB2, which was truncated at the start of the BTB domain (residue 136 for both),

interacts with a coiled-coil scaffold protein known as FRIGIDA (**FRI**) in yeast<sup>47</sup>. FRI is normally responsible for recruiting several chromatin modifiers that modify certain flowering genes after vernalization (the promotion of flowering in the spring after a plant has had exposure to an extended period of cold temperatures<sup>49</sup>) to initiate flowering. During vernalization, *AtLRB1/2* was found to assemble with FRI and Cul3 to promote FRI degradation via the 26S proteasome, but this was found to not be the case in the Columbia (**Col-0**) ecotype of *Arabidopsis thaliana*, which has an early-flowering phenotype due to a carboxy-terminal deletion allele at the *FRIGIDA* locus<sup>47</sup>.

As the established *lrb12* mutant phenotypes were observed in Col-0 *Arabidopsis* ecotypes<sup>2</sup>, the degradation of FRI cannot be responsible for the hypersensitivity found when plants were grown in red light. It is unclear what function the amino-terminal FRI protein plays in Col-0, and it is unknown whether truncated FRI is able to interact with the LRBs or what role it might have in phy signaling.

As well as demonstrating that there was a functional role for the amino-terminal portion of the LRBs, it was also established that the truncated amino-terminal portion of both LRB1 and LRB2 in *Arabidopsis thaliana* (***AtLRB1/2***) remains functional and is able to be co-purified with FRI<sup>47</sup>. Purifying truncated *AtLRB1/2* suggests that the amino-terminal portion of LRB folds correctly and is able to interact with the same proteins as full-length *AtLRB1/2*<sup>47</sup>. This evidence of truncated protein stability in the amino-terminal portion of *AtLRB* will be further investigated computationally as a way to further uncover any information on how this region may help to control the function of the LRBs.

## **Moving Forward by Investigating Whether the Amino-Terminal Region Can Regulate the Functional Role that the LRBs Play in Light Signaling**

Although the amino-terminal portion of the LRBs has been shown to interact with FRI, it is not yet known if it can regulate the functional role the LRBs play in light signaling. There are several intriguing aspects of the amino-terminal region that have yet to be studied in-depth, and may suggest an alternative function for this portion of the LRBs other than interacting with FRI. First, based on protein multiple sequence analysis, there seem to be several amino-terminal regions that may be conserved throughout the plant kingdom. Second, a preliminary sequence comparison analysis suggests that there are conserved portions of the amino-terminal region that may be similar to other E3 ligase components such as Cul1 and Rbx1. Lastly, it is well documented in the literature that monocots do not control flowering through the FRI, as a homologue has not been identified in these plants<sup>50</sup>. However, amino-terminal conservation was determined to be present in homologous LRB proteins across all land plants and not just conserved in eudicots. Taken together, these data suggests that the amino-terminal region may play a role in regulating light signaling. This thesis project aims to provide a more in-depth analysis of the amino-terminal portion of the LRBs to determine what role this region may play in light signaling.

## II. RESEARCH SIGNIFICANCE

Investigating the phytochrome pathway is significantly challenging, as it controls many different plant responses, including pathogen resistance, germination rates, efficiency of water use, shade avoidance response, seedling establishment, initiation of flowering, pathogen resistance, and regulation of circadian clocks<sup>1-4</sup>. One great example of the diverse phytochrome signaling pathway can be found in the shade avoidance response that is caused by the reflected far-red light from neighboring plants. The reflected far-red light from other nearby vegetation can cause a plant to undergo stem elongation, accelerated flowering, decreased leaf expansion, and increased petiole elongation as a way for the plant to try and outgrow any competition. As long as the plant senses a higher amount of far-red light than normal, even over a small area of the plant, some amount of shade avoidance mechanisms will be triggered. This phenomenon is modeled perfectly when looking at a field full of closely-planted rows of corn. Knowing the red light response pathway may help to design corn in the future that prevents it from wasting energy on trying to outgrow any neighboring plants.

Studying the mode of activation used by LRB2, a protein responsible for the negative regulation of the phytochrome response in red light, will help to shed some light on how plants use phytochromes to determine how to respond to light. Research into the LRBs could give new insights into the mechanisms used in the shade avoidance pathway in *Arabidopsis thaliana*, as discussed above, or may reveal new information on pathogen response and circadian rhythm regulation, as the phytochrome response pathway

encompasses a multitude of plant responses. Specifically, this project focused on detecting any modification of the LRBs that could be present in different light conditions, setting up a framework for understanding the mechanism of the red-light-dependent activation of the LRBs.

Additionally, research on the LRBs will help assist in pinning down the general mechanisms responsible for regulating certain protein degradation pathways. There are hundreds of E3 ligase proteins predicted in the *Arabidopsis* genome<sup>17</sup>, and the general mechanisms and structures of the core Cullin-RING Ligase complexes are thought to be equivalent across all CRL complexes of all origins<sup>23</sup>, including humans. With our understanding of all E3 ligase complexes still at its infancy, any research that investigates how any E3 ligase complex protein members are regulated helps to place one more piece into the E3 regulation pathway puzzle. This project was designed to determine if the LRBs were modified in red light, as knowing would increase the overall knowledge of how one family of E3 ligase complexes is regulated, helping to assist in uncovering general mechanisms responsible for protein degradation regulation.

Knowing the mechanics behind the function of the LRB proteins has a wide range of agricultural, environmental, and economical benefits. Identifying and manipulating the light-dependent mechanisms used by LRB proteins to selectively activate in certain light conditions would be applicable to almost every plant grown by man, as homologous LRB proteins are widely found in all types of land plants<sup>2</sup>. Therefore, understanding the mechanism of LRB activation and function could give rise to various groundbreaking applications such as the ubiquitous manipulation of the shade avoidance response in almost any member of the plant kingdom. This ability to manipulate red and far-red light response

pathways would present an opportunity to create plants that are better suited to grow in the harsh, stressful environments that might occur in the near future due to global climate change and as access to water becomes increasingly more difficult.

### III. PROJECT AIMS, OVERVIEW, AND OBJECTIVES

**AIM #1:** Use *in silico* methods to identify potentially functional segments of the amino-terminal regions of the LRB proteins in *Arabidopsis*.

- (A). Provide evidence that the LRB amino-terminus is conserved.
- (B). Investigate the relatedness of the LRB amino-terminal conserved sequence motifs to Cullin and Rbx1 proteins.
- (C). Create structural models of the LRB proteins to help predict function.

**AIM #2:** Investigate if phosphorylation is present on the LRBs in different light conditions which may be responsible for its preferential interaction with Cul3 in red light.

- (A). Identify potential phosphorylation sites on the LRBs.
- (B). Determine if light-dependent LRB phosphorylation occurs.
- (C). Determine if phosphorylation is present on purified LRB proteins.

**AIM #3:** Investigate if neddylation is present on the LRBs in different light conditions which may cause the LRBs to interact with Cul3 in a red-light-dependent manner.

- (A). Use the NEDD8 inhibitor MLN4924 to test for LRB neddylation.
- (B). Directly detect NEDD8 conjugation using purified LRB.



**AIM #1 OVERVIEW:** Use *in silico* methods to identify potentially functional segments of the amino-terminal regions of the LRB proteins in *Arabidopsis*.

***INTRODUCTION:***

Sequence conservation was predicted to be a reliable way to identify any portion of the protein important to the structure or function of the LRBs. Sequence analysis may also provide clues towards the possible mechanisms responsible for the light-specific interaction of the LRBs. The sequence for the BTB and BACK domains of LRB homologs are predicted to be very conserved, as both are established domains and must maintain the ability to selectively dimerize with other LRB proteins<sup>34</sup>. It is also predicted that the carboxy-terminus of LRB homologs will be highly conserved, as this is the predicted site of target recognition<sup>34,35</sup>. Accordingly, the amino-terminal portion of *AtLRB* proteins (residues 1-144 of *AtLRB2*) was thought to be of particular interest because it has no predicted function and does not contain any identifiable domains.

***HYPOTHESIS:***

The amino-terminal region of the *AtLRBs* contain two important contiguous regions that were found to be conserved across all land plant species<sup>2</sup>. We hypothesize that the amino-terminus of the LRBs may contain a novel regulatory site on LRBs. We will use *in silico* techniques to evaluate the amino-terminal sequence conservation in order to determine any possible similarity in structural characteristics of two contiguous regions, as preliminary data has suggested that each conserved regions contains a similar motif as found on Cullin and Rbx1 proteins, respectively.

## **OBJECTIVES FOR AIM #1:**

- (A.) Provide evidence that the LRB amino-terminus is conserved.** In order to provide evidence that the two contiguous amino-terminal regions (referred to as the Cullin-like and Linker-like regions, respectively) are conserved in all LRB proteins, *AtLRB* proteins will be compared to the LRBs in many diverse plant species by using the Basic Local Alignment Search Tool (**BLAST**) with the full-length LRB2 protein sequence in *Arabidopsis*. A multiple sequence alignment (**MSA**) will then be created using these homologous LRB proteins, providing an idea of which areas are important to the structure or function of the LRBs.
- (B.) Investigate the relatedness of the LRB amino-terminal conserved sequence motifs to Cullin and Rbx1 proteins.** Cul1 and Rbx1 proteins will also be compiled by using a protein BLAST with the Cul1 and Rbx1 protein sequences in *Arabidopsis*. Once compiled, a MSA will then be created for each to determine the degree of conservation in each of the regions associated with LRB. To definitively show that each of the amino-terminal domains of the LRB proteins remains similar to the Cul1 and Rbx1 in multiple plant species, a second MSA will be generated aligning the Cullin-like or linker-like regions of the LRBs with the corresponding areas on Cul1 or Rbx1. The known crystal structures of the Cul1/Rbx1 complex can then be used to investigate the location of the Cullin-like or Linker-like regions on Cul1 and Rbx1, respectively.
- (C.) Create structural models of the LRB proteins to help predict function.** The structure of the LRB proteins in *Arabidopsis thaliana* will be modeled using structural prediction software. Using homology models, sequence conservation will be displayed as a way to elucidate potential structural or functional roles for the two contiguous amino-terminal domains.

**AIM #2 OVERVIEW:** Investigate if phosphorylation is present on the LRBs in different light conditions which may be responsible for its preferential interaction with Cul3 in red light.

***INTRODUCTION:***

Phosphorylation has previously been shown to play a significant role in the red light signaling pathway<sup>11,14,15</sup> and, more specifically, has been found to be directly responsible for PIF-mediated phytochrome degradation<sup>11,16</sup>. Additionally, some evidence suggests that the phytochromes found in plants are atypical serine/threonine protein kinases<sup>12,14</sup>, and this kinase activity by the phytochromes might be the light-dependent modification that the LRBs need in order to become active in red light.

***HYPOTHESIS:***

Since the LRBs are able to interact with and ubiquitinate PIF3<sup>16</sup>, as well as interact with both active and inactive phytochromes<sup>16</sup>, both of which are closely tied to phosphorylation or kinase activity, it was hypothesized that LRB activation in red light could occur due to phosphorylation. This aim is designed to determine if phosphorylation is present on *AtLRB* and if the presence of phosphorylation occurs preferentially when exposed to red light (**Figure 9**).

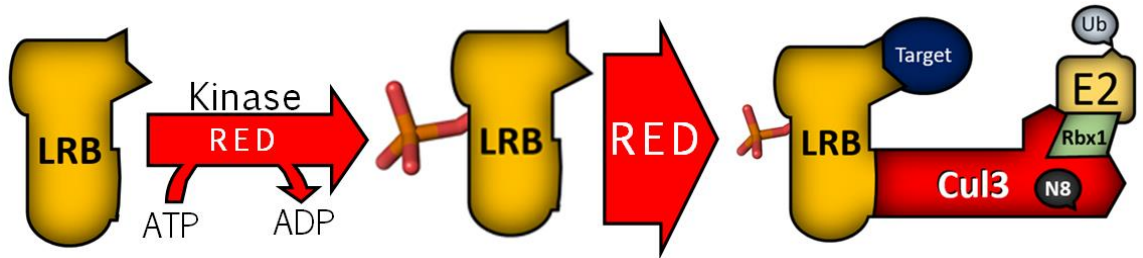


**Figure 9:** Potential Mechanism for LRB Activation in Red Light

When grown in complete darkness, LRB proteins do not form active E3 ubiquitin ligase complexes, but after exposure to red light, the LRBs are able to interact strongly with Cul3<sup>2,16</sup>. One potential mechanism to explain this phenomenon is that the phosphorylation of the LRBs may be responsible for LRB CUL3 complex formation in red light.

#### OBJECTIVES FOR AIM #2:

- (A.) Identify potential phosphorylation sites on the LRBs.** The light-dependent phosphorylation of LRB proteins by an unknown kinase could result in the activation and subsequent association of the LRBs with Cul3. *In silico* phosphorylation prediction methods will be used to investigate the probability that phosphorylation is responsible for the activation of the LRBs in red light. Predicted sites of phosphorylation will be modeled using the predicted protein structural models created in Aim #1C.
- (B.) Determine if light-dependent LRB phosphorylation occurs.** A phospho-shift assay using lambda phosphatase will be used to determine the phosphorylation status of LRB proteins extracted from plants grown in darkness, red light, or far-red light conditions. If phosphorylation is present on the LRBs, the tissue samples treated with the lambda phosphatase will have bands that run faster on a gel than the samples containing phosphatase inhibitors, as they will be influenced by a phosphorylation-dependent mobility shift<sup>51</sup>.
- (C.) Determine if phosphorylation is present on purified LRB proteins.** Purified LRB proteins extracted from plants grown in darkness, red light, or far-red light conditions will be probed with anti-phosphoserine antibodies in an attempt to detect any light-dependent phosphorylation present on the LRBs.

**AIM #3 OVERVIEW:** Investigate if neddylation is present on the LRBs in different light conditions which may cause the LRBs to interact with Cul3 in a red-light-dependent manner.

***INTRODUCTION:***

Since the amino-terminal end of the LRBs share some similarity to Cullin and Rbx1, one possibility is that the LRBs may be involved in neddylation. NEDD8 conjugation has been previously shown to create steric hindrance that prevents proteins from interacting with certain partners or grant flexibility and activate new functions for a protein<sup>44-46</sup>, either of which could be responsible for *AtLRB* activation and subsequent interaction with Cul3 when exposed to red light.

***HYPOTHESIS:***

This aim investigates the possibility that the LRB proteins are being conjugated in a light-dependent manner with the small modifier protein NEDD8. The two amino-terminal regions on *AtLRB* may be involved in helping to signal NEDD8 conjugation in red light.

**OBJECTIVES FOR AIM #3:**

- (A.) **Use MLN4924 to test for LRB neddylation.** To test the hypothesis that NEDD8 may be responsible for LRB activation in red light, the small-molecule NEDD8 inhibitor **MLN4924** will be used to inhibit the function of ECR1, the E1-like enzyme responsible for the first step in NEDD8 conjugation<sup>52</sup>. Transgenic seeds will be grown on MS media supplemented with the MLN4924 and exposed to red light or only darkness, and the apparent molecular weight of the LRB proteins will be assessed using Western blotting to identify the possible extent of NEDD8 presence in each light condition.

**(B.) Directly detect NEDD8 conjugation using purified LRB.** Purified LRB proteins extracted from *Arabidopsis thaliana* via immunoprecipitation will be probed with anti-NEDD8 antibodies on a Western blot to see if NEDD8 is conjugated to the LRBs.

## IV. RESULTS & DISCUSSION

### *IN SILICO* INVESTIGATIONS OF THE LRB PROTEINS

#### Two Conserved Amino-Terminal Regions Are Found in All LRB Homologs

Regions of conservation in the sequence of the amino-terminal portion of *AtLRB* may be the sites of any light-specific mechanisms or modifications that could be present. The BTB (residues 144-245) and BACK (residues 260-362) domains of *AtLRB2* were predicted to be conserved in a small number of LRB homologs, as both are well-known domains and contain the site of LRB dimerization and Cul3 interaction<sup>34</sup>; however, this was based on a limited sample size. It is also suggested, by the same limited alignment, that the carboxy-terminus of LRB homologs is also highly conserved, as this is the predicted site of target recognition<sup>34,35</sup>.

Current literature leaves the amino-terminus portion of *AtLRB2* (residues 1-144) unaccounted for, which contains no known domains or functions, and details regarding the functional role of this portion remain scarce. Amino-terminal *AtLRB* has been shown to interact with and cause the degradation of a transcription factor known as FRIGIDA in *Arabidopsis*<sup>47</sup>, supporting the hypothesis that the amino-terminal region is important for LRB function. Functional FRIGIDA proteins are only present in plants requiring vernalization<sup>53</sup>, so it is unclear what function the amino-terminal LRB region would play in non-biennial flowering plants.

Additionally, we do know that the *AtLRBs* are partially responsible for negatively regulating phyB accumulation in response to red light<sup>2</sup>, and they do so by ubiquitinating

phosphorylated PIF3 in a MAD pathway<sup>16</sup>. However, what we do not know is the mechanism used by the *At*LRBs to regulate their interaction with Cul3 in a red-light-dependent manner. Amino-terminal sequence conservation across all land plants would strengthen the argument that the amino-terminus has a role outside of vernalization and could be important for light signaling. This idea that the amino-terminal LRB portion is important and would be universally conserved in plants became our working hypothesis, so we began our investigation by determining amino-terminal sequence conservation in LRB protein homologs.

To carry out sequence analysis, full-length LRB protein homologs were chosen from different land plant species in each phylum. Out of 967 *At*LRB2 protein homologs, LRB proteins from 14 diverse land plant species were chosen. Members of the chosen species included flowering plants from both the eudicot and monocot subphyla, a conifer from the gymnosperm subphyla, a spikemoss from the lycophyte subphyla, and a non-vascular moss from the subdivision bryophyte. Proteins were collected from UniProtKB's database<sup>54,55</sup> after a protein BLAST search was performed using the full-length *At*LRB2 protein and default settings (**Supplemental Figure 1**). Any full-length LRB protein homologs sequences that were gathered in the protein BLAST were then used to create a multiple sequence alignment (**MSA, Supplemental Figure 2**) using default **T-coffee Expresso**<sup>56,57</sup> settings.

Essentially, three amino-terminal regions of LRB were found to be conserved across all plant phyla (**Figure 10**). The first conserved motif contained approximately 25 residues, and this motif was the most conserved of the three. The first two amino-terminal regions shown to be contiguous, with the second region containing the short NLS



sequence needed for nuclear localization<sup>2</sup>. However, the conservation of the second region spanned approximately 25 residues, a much larger area than the 5 amino acid NLS sequence, and this prompted us to further analyze that portion. The third conserved region contained a much shorter motif, consisting of approximately 15 residues, and was located in close proximity to the start of the BTB domain.

A phylogenetic tree<sup>58</sup> was used to infer evolutionary distance of one LRB homolog from another and to show the disproportionate amount of eudicot protein homologs used to create the MSA (**Figure 11**). The tree shows the diversity of the proteins chosen, while the strong bootstrap values indicate that the LRB proteins are conserved across all plant phyla, despite the disproportionate amount of eudicot proteins.

*AtLRB3*, previously thought to be a pseudogene<sup>2</sup>, along with two LRB3 protein homologs in *Capsella rubella* and *Arabidopsis lyrata*, contained extremely divergent sequences, enough to be marked as the outgroup in the tree, and based on their poor alignment in the MSA, they were removed from future sequence analysis. LRB homologs listed in red on the phylogenetic tree were removed from further multiple sequence alignments due to poor alignments with *AtLRB2* in the MSA, the presence of insertions or deletions in the protein sequence, or, in the case of *Physcomitrella patens* and *Selaginella moellendorffii*, the large evolutionary distance from *AtLRB2*.



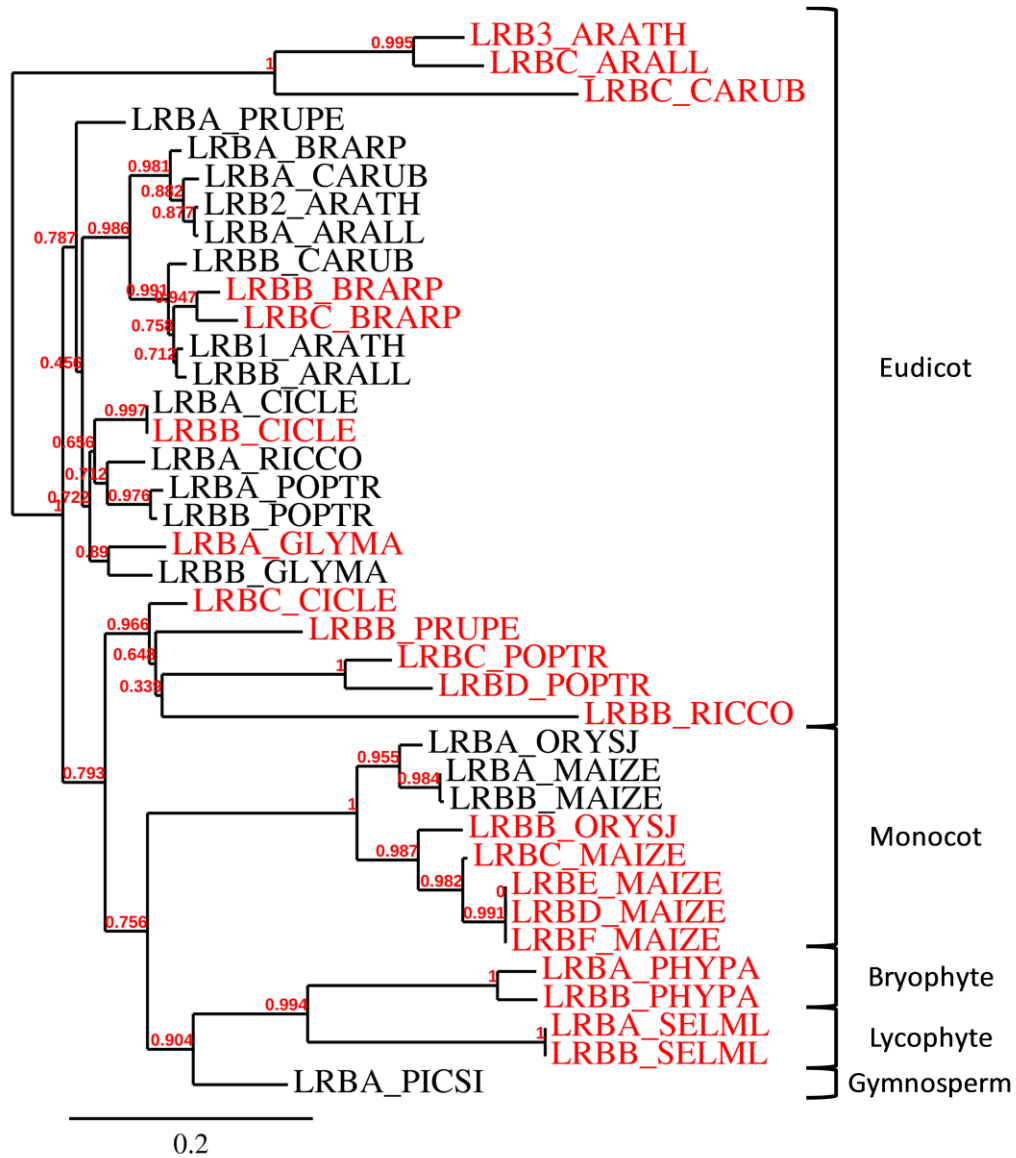


**Figure 11:** Phylogenetic Analysis and Division of LRB Protein Homologs

Phylogenetic analysis of the LRB proteins gathered using a UniProtKB protein BLAST<sup>54,55</sup> of *AtLRB2*. The LRB proteins were given generic names based on their similarity to *AtLRB2*. The length of each branch is proportional to the relative amount of divergence between each of the LRB proteins, with the scale at the top depicting 0.2 substitutions per sequence position. Branch support values are shown in red and display the amount of support for each node. *AtLRB3*, which is thought to be a pseudogene, was chosen as part of the outgroup by the Phylogeny.fr One Click tool<sup>58</sup>. Proteins were grouped together by phyla, as marked on the right. Proteins marked in red were removed from subsequent multiple sequence alignments.

Abbreviations for each plant species include *Arabidopsis thaliana* (ARATH), *Arabidopsis lyrata* (ARALL), *Brassica pekinensis* (BRARP), *Citrus clementina* (CICLE), *Populus trichocarpa* (POPTR), *Prunus persica* (PRUPE), *Ricinus communis* (RICCO), *Capsella rubella* (CARUB), *Glycine max* (GLYMA), *Oryza sativa subsp. japonica* (ORYSJ), *Zea mays* (MAIZE), *Picea sitchensis* (PICSI), *Physcomitrella patens* (PHYPA), and *Selaginella moellendorffii* (SELML).

## **Two of the Conserved Amino-terminal Regions of LRB1 and LRB2 Show Sequence Similarity to Other E3 Ligase Protein Members in *Arabidopsis thaliana***

The conserved amino-terminal motifs were investigated as a way to gain further insight into the functions each motif plays in the LRBs. Each of the conserved motifs, as well as the entire amino-terminal portion, were used to search for other proteins with similar conserved motifs. If proteins with similar motifs were detected, we would not be able to determine if the functions of both proteins are similar based solely on the sequence and amount of conservation. Related proteins may have the same functional role, but unfortunately, sequence conservation is not proof of similar functions<sup>59</sup>.

Each of the small conserved amino-terminal motifs of the *AtLRB2* proteins were used to perform a protein BLAST search using the **WU-BLAST2** tool on **TAIR**<sup>60</sup> (<http://arabidopsis.org>) to search for any other proteins in *Arabidopsis thaliana* containing similar sequences. The first of the two contiguous motifs on *AtLRB2* were found to be similar to those in Cullins 1 and 2 (**Figure 13A-B**), with 64 and 60% sequence similarity, respectively. Other hits from the WU-BLAST2 search included Trans-caffeoyl-CoA 3-O-methyltransferase, Asynaptic 1, and kelch repeat-containing protein At3g27220 (**Supplemental Figure 3A**). The second motif was found to be similar to a region on Rbx1 (**Figure 13A-B**), another member of the E3 ubiquitin ligase complex, with 64% similarity. Other proteins found in the search included **NIMIN-1**, Response to ABA and Salt 1, and Benzoic Acid Hypersensitive 1 (**Supplemental Figure 3B**). Statistical confidence in the amount of similarity is low for each of the motifs, as shown by the high E-values calculated (**Supplemental Figure 3A-B**), but this does not necessarily mean the functional role of the motifs on each protein is not similar. Low statistical confidence for each of the protein hits could indicate that the similarity is not

meaningful; however, it could also indicate that the similarity may be meaningful or that the motifs are a meaningful match with a meaningful function in all of the protein hits.

Interestingly, Region 1 was found to be similar to Cul1 and Cul2 but not similar to Cul3, which the LRBs have been shown to associate with when forming a CRL complex<sup>2</sup> (**Supplemental Figure 3C**). This discovery could relate back to the idea that Cul3 is a paralog of Cul1, with the Cul1/2 genes descended from the *Cula* gene, while Cul3 arose from the *Culβ* gene<sup>23</sup>. Also, the region of Cul1/2 sharing similarity to conserved Region 1 of the LRBs was found to be located directly upstream of the NEDD8 conjugation site that is found on all Cullin proteins (**Figure 12**).

A WU-BLAST2 search using the third conserved region did not turn up any viable results using variable lengths of the motif, suggesting that this portion may only be structurally significant to the LRBs or might be the site of a secondary modification such as phosphorylation or neddylation. Further investigation into the third conserved region will be touched on in later sections.

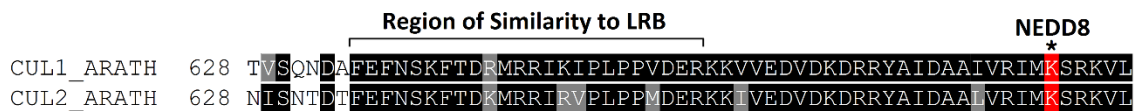


**Figure 12:** Proximity of the NEDD8 Conjugation Site to the LRB-like Region of Cul1/2  
 A pairwise alignment showing the area on Cullin that shares similarity to the Cullin-like region on the LRBs in brackets and its close proximity to the site of neddylation, which is highlighted in red and marked using an asterisk.

## The Amino-terminal Motifs in LRB Protein Homologs Retain Sequence Similarity to their Respective CRL Protein Members in All Land Plants

The first conserved motif on *AtLRB2* was found to be similar to a region on Cullins 1 and 2, while the second motif showed similarity to Rbx1. The next step in investigating these two amino-terminal regions was to determine if the similarity of the amino-terminal LRB motifs to E3 complex members (**Figure 13**) could also be found in homologous LRB proteins in different plant species and not just in *Arabidopsis thaliana*. In order to compare the LRB homologs to their respective Cul1/2 and Rbx1 proteins, the MSA was edited (**Figure 10, Supplemental Figure 2**) to exclude proteins with poor alignments in these two areas (**Figure 14, Supplemental Figure 4**), which will further be referred to as the Cullin-like (**CL**) and Linker-like (**LL**) regions or motifs, respectively.

Separate multiple sequence alignments were created of homologous Cul1/2 and homologous Rbx1 proteins as a way to view the overall sequence conservation of the regions found to be similar to the LRBs. In addition to determining the overall conservation of the motifs on Cul1/2 and Rbx1, we will also be aligning the conserved LRB motifs with their respective Cul1/2 and Rbx1 segments to show that the similarity between these E3 members is conserved across all land plants analyzed.

The area containing similarity to the CL region, further referred to as the **Cul<sup>CL</sup>** region (**Figure 15, Supplemental Figure 5**), showed very high sequence identity, with residues being either absolutely conserved (invariant) or containing substitutions similar in their physicochemical characteristics. Conservation of physicochemical characteristics is shown with the hydrophobic residues of *I/V* and *V/M*, as well as with the conservation of positively-charged basic residues with substitutions of *K/R*.

The alignment of the Rbx1 proteins at the region associated with the LL motif of the LRBs, denoted the **Rbx<sup>LL</sup>** motif (**Figure 16, Supplemental Figure 6**), showed an overall conservation of physicochemical properties of the first third of the motif with some substitutions of *A/G/S* and *A/V/S*. The middle portion of the alignment contained a region of variance with gaps in the alignment and only a few key serine residues, one lysine residue, and a positively-charged *K/R* substitution being conserved. The last half of the Rbx1 alignment retained a high amount of residue conservation, with only a single major *S/N* residue substitution.







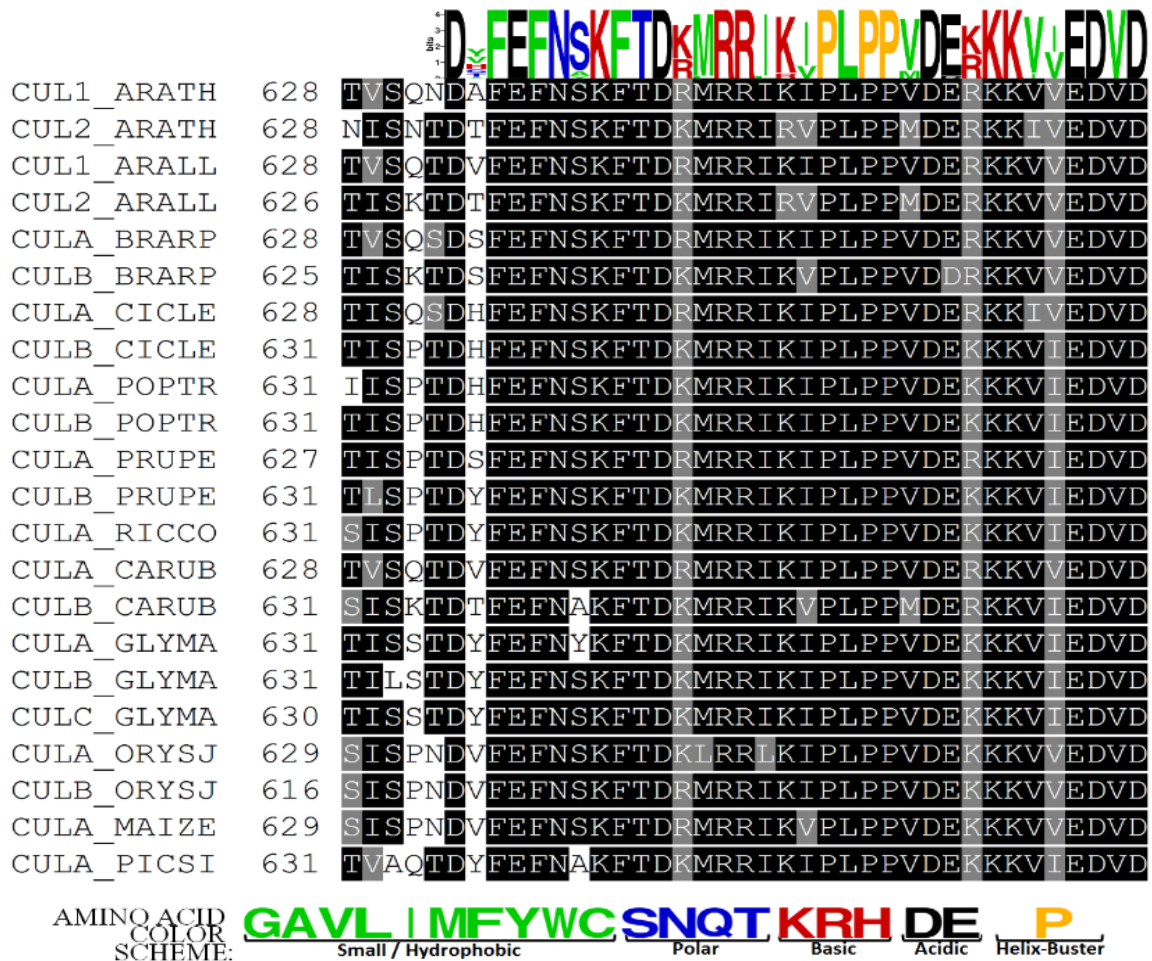


**Figure 15:** Alignment of the Cul<sup>CL</sup> Region on Cullins

An **Expresso**<sup>56,57</sup> MSA of the Cul<sup>CL</sup> region in proteins found to be homologous to *AtCul1* and *AtCul2*. Residues with a high overall conservation (above 70%) are shown highlighted in black, while residues that are conserved (above 70%) due to residue similarity consensus are shown in grey. Sequence conservation is also displayed directly above the alignment using a **MEME**<sup>61</sup> logo, with the height of each amino acid abbreviation being directly proportional to residue conservation.

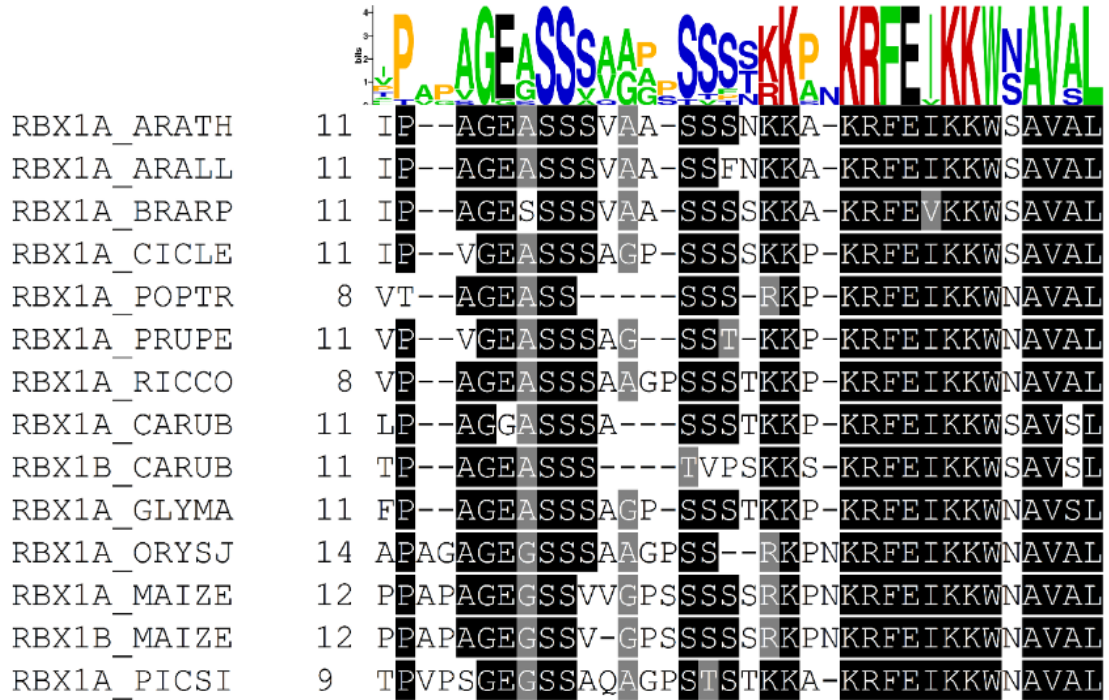


**Figure 16:** Edited Alignment of the Rbx<sup>LL</sup> Region on Rbx1 Homologs

An Expresso<sup>56,57</sup> alignment of the Rbx<sup>LL</sup> region of proteins (**Supplemental Figure 6A**) found to be homologous to *AtRbx1* which was edited manually for overall alignment (**Supplemental Figure 6B**). Residues with a high overall conservation (above 70%) are shown highlighted in black, while residues that are conserved (above 70%) by residue similarity consensus are shown highlighted in grey. Sequence conservation is also displayed directly above the alignment using a MEME<sup>61</sup> logo, with the height of each amino acid abbreviation being directly proportional to residue conservation.

To test if the amino-terminal regions of the LRB homologs retain similarities to Cul1/2 and Rbx1, additional MSAs were performed using the sequences for the CL or LL domain of the LRBs and the Cul<sup>CL</sup> (**Figure 17A**) or Rbx<sup>LL</sup> (**Figure 18A**) regions. The overall alignment of CL and Cul<sup>CL</sup> regions displayed complete conservation of 7 out of the 25 residues included in the alignment. Variant residue positions still retained a certain amount of physicochemical conservation when comparing Cullin sequences to the LRBs, with Cul/LRB substitutions such as *T/S* and *R/K/R* (site **9** and **11**, **Figure 17B**). Some basic physicochemical properties were also conserved, such as the polarity of *K/R/E* (site **16**, **Figure 17B**), while some residues that might be important for salt bridge formation contained *E/S* substitutions. A trio of hydrophobic residues were generally conserved, with overall substitutions of *PLP/MGG* (sites **18-20**, **Figure 17B**).

The overall alignment of the LL and Rbx<sup>LL</sup> areas had a small amount of complete residue conservation, with 3 out of the 37 residues being completely conserved. However, residue similarity in the LL alignment was quite substantial<sup>62</sup> (**Figure 18B**), despite a large variable region in the middle portion of the alignment due to the Rbx1 homologs. There is physicochemical conservation throughout the alignment, conserving hydrophobicity with *G/A* and *I/V/L/A* substitutions, charged residues with *R/K* and *E/D* substitutions, and polar residues with *N/S*, *S/T*, and *C/S* substitutions.

The similarity of the two conserved amino-terminal regions to CRL complex members was determined to be a phenomenon that was present in all land plants due to the overall amount of conservation between the CL and LL region of each LRB homolog and the associated regions on each respective Cullin and Rbx1 homolog. These two

amino-terminal sequences are conserved, and conservation of sequence implicates that these regions are vital for a structural or functional role for the LRBs. Regardless of the sequence comparisons between the LRBs, Cul1/2, and Rbx1, it is worth investigating both of the conserved amino-terminal regions to determine their role in LRB function or structure.



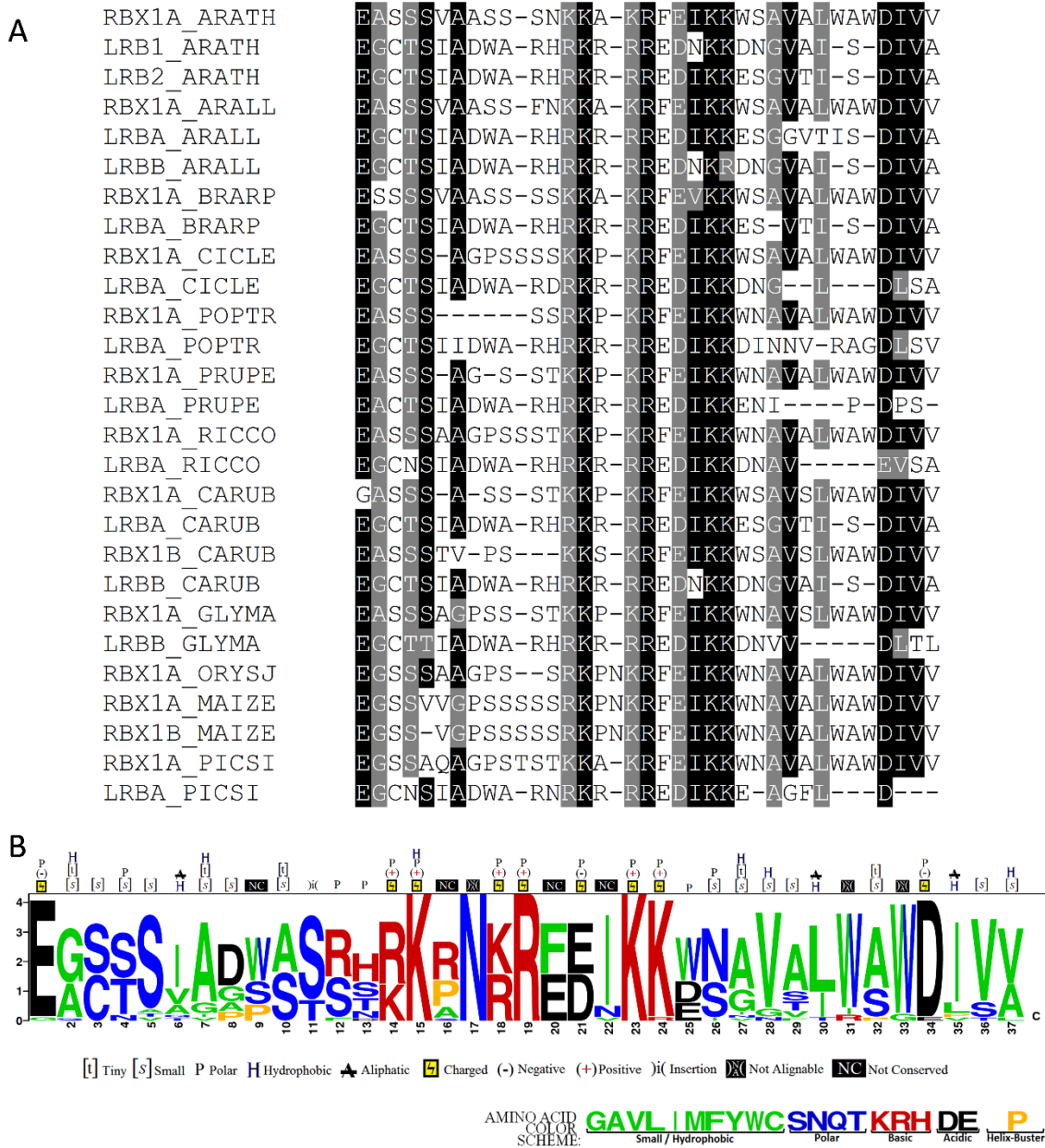


**Figure 18:** Alignment and Physical Properties of the Rbx<sup>LL</sup> and LL Regions

**A.** An Expresso<sup>56,57</sup> alignment of the LL region of the LRB proteins with the Rbx<sup>LL</sup> region on each respective Rbx1 protein. Conserved residues (above 70%) are shown highlighted in black, while residues that are mostly conserved and have consensus due to residue similarity (above 70%) are shown highlighted in grey.

**B.** A MEME<sup>61</sup> logo was also created in order to display the relative amount of sequence and basic chemical conservation. The height of each residue is directly proportional to the amount of residue conservation. Additionally, the conserved physicochemical properties for each residue at a given position is shown<sup>62</sup>.

## **The Cul<sup>CL</sup> and Rbx<sup>LL</sup> Regions are found to be in Close Proximity to One Another in Three Human CRL Complex Crystal Structures**

To understand the full biological role of a protein, both the structure and the function must be known<sup>63</sup>. Both Cul1 and Rbx1 have crystal structure models readily available in the Protein Data Bank<sup>64</sup> (**PDB**, *www.rcsb.org*) and the distribution of the Cul<sup>CL</sup> and Rbx<sup>LL</sup> regions on each of their respective proteins can be viewed simultaneously, as both proteins form CRL complexes. We know that the Cul<sup>CL</sup> region is upstream from the site of neddylation, but little is known about the location of the Rbx<sup>LL</sup> region. It would be beneficial to know where the Cul<sup>CL</sup> and Rbx<sup>LL</sup> regions reside at on the Cullin and Rbx1 structures, as mapping these motifs may help us to understand the functional meaning of the similarity to the LRBs that is found at either region. However, there are currently no CRL complex structures from plant species found in the PDB.

All CRL complexes found in PDB were crystalized using human CRL complex proteins, but despite a large evolutionary distance between humans and plants, there is evidence that the Cullin scaffolding functions and structure are highly conserved, and as such, the CRL complexes modeled in humans is thought to be equivalent to Cullin protein homologs from all origins<sup>23</sup>. The crystal structures of three different CRL complexes (2HYE<sup>30</sup>, 1LDK<sup>26</sup> and 4P5O<sup>29</sup>) were chosen to provide information on the exact location of the conserved Cul<sup>CL</sup> and Rbx<sup>LL</sup> motifs. 2HYE<sup>30</sup> contained the crystal structure for human Cul4/Rbx1 in complex, while both 1LDK<sup>26</sup> and 4P5O<sup>29</sup> contained models of human Cul1/Rbx1. The structure for 4P5O also contained NEDD8 attached to Cul1 at the conserved neddylation site<sup>29</sup>.



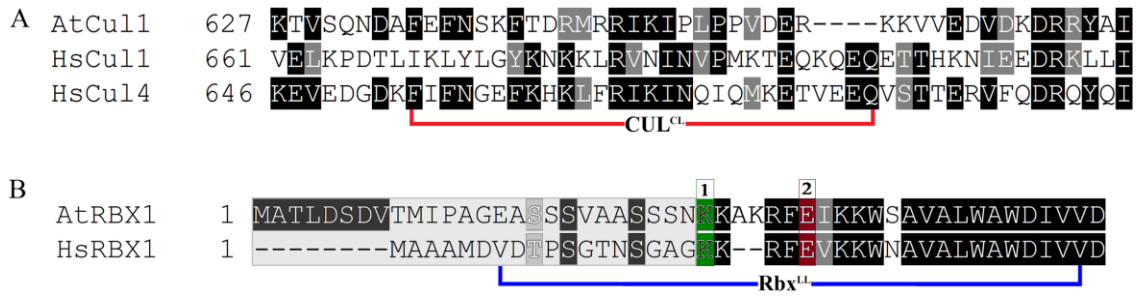


**Figure 19:** Alignment of Human Cul<sup>CL</sup> and Rbx<sup>LL</sup> Areas with their Respective Counterparts in *Arabidopsis*

**A.** A MSA showing the alignment of the Cul1 protein in *Arabidopsis thaliana* with two homologous proteins, Cul1 and Cul4A, in *Homo sapiens*, which are modeled in the PDB structures 2HYE<sup>30</sup>, 1LDK<sup>26</sup>, and 4P5O<sup>29</sup>. The portion of the alignment corresponding to the Cul<sup>CL</sup> region is marked below in red.

**B.** A pairwise alignment of *AtRbx1* with the Rbx1 protein homolog in *Homo sapiens*. The *HsRbx1* protein is modeled in complex with the Cullin proteins in all three of the previously mentioned PDB structures, and the region corresponding to the Rbx<sup>LL</sup> area is marked below the alignment in blue. A structure for the amino-terminal portion of *HsRbx1* remains unresolved and highlighted with grey. The first modeled residue in both the 1LDK<sup>26</sup> and 2HYE<sup>30</sup> crystal structures are boxed in green and marked [1], while the first residue of the 4P5O<sup>29</sup> *HsRbx1* crystal structure is boxed in dark red and marked [2] on the alignment.

An alignment of *AtCul1* with both *HsCul1* and *HsCul4* was created in order to account for any variations in the protein sequence (**Figure 19A**) and provided further justification for our use of human CRL complexes to model plant protein motifs. *AtCul1* was found to share a sequence identity score of 31% with *HsCul4* and 23.0% with *HsCul1*, as determined using UniProt's CLUSTALO alignment program<sup>54,55</sup>. The sequences for *AtRbx1* and *HsRbx1* were very similar (**Figure 19B**), with a sequence identity score of 75% being calculated using CLUSTALO<sup>54,55</sup>.

Using VMD<sup>41</sup>, a 3-dimensional anaglyphic image was created for each of the relevant proteins in the three crystalized CRL complexes (**Figure 20**). In all three of the structures, a general pattern was observed with respect to the mutual orientation of the Cul<sup>CL</sup> and Rbx<sup>LL</sup> motifs, and this general pattern showed that the Cul<sup>CL</sup> and Rbx<sup>LL</sup> areas

were in close proximity to one another, with the Cul<sup>CL</sup> area maintaining a horseshoe-like shape that was not dependent on NEDD8 conjugation (4P5O) (**Figure 20**).

The first half of the Rbx<sup>LL</sup> region was found to be the region where Rbx1 inserts itself into Cullin, with the amino-terminal portion entering on the top of the  $\alpha/\beta$  domain of Cul1 closest to NEDD8 conjugation and exiting from the far end of the Cul1 WH-A (**Figure 4B, Figure 20**). Interestingly, one portion of the Rbx<sup>LL</sup> region was found to be in direct contact with NEDD8 (**Figure 21A**). The residues that interacted with NEDD8 (D36, I37, V38, V39 of *HsRbx1*) were found to be very well conserved across the eudicot LRB homologs, with the residues of the other homologous LL regions showing an overall conservation of chemical properties across the alignment (**Figure 21B**).

The amino-terminal portion of the Rbx<sup>LL</sup> region was unresolved on *HsRbx1* due to lack of crystal structure (**Figure 19B**). This was most likely due to high mobility for this span of residues on *HsRbx1*. This unresolved area was also the region which contained the most divergence in the MSA of the homologous LL regions of LRBs with their corresponding Rbx<sup>LL</sup> regions (**Figure 18**). This could suggest that only the first 8 amino acids in the MSA alignment might be important for signaling or protein function, while the six or more Rbx1 residues that reside in the space immediately outside of the Cullin WH-A threading region (residues 20 to 26 of *AtRbx1*) might not be as important.

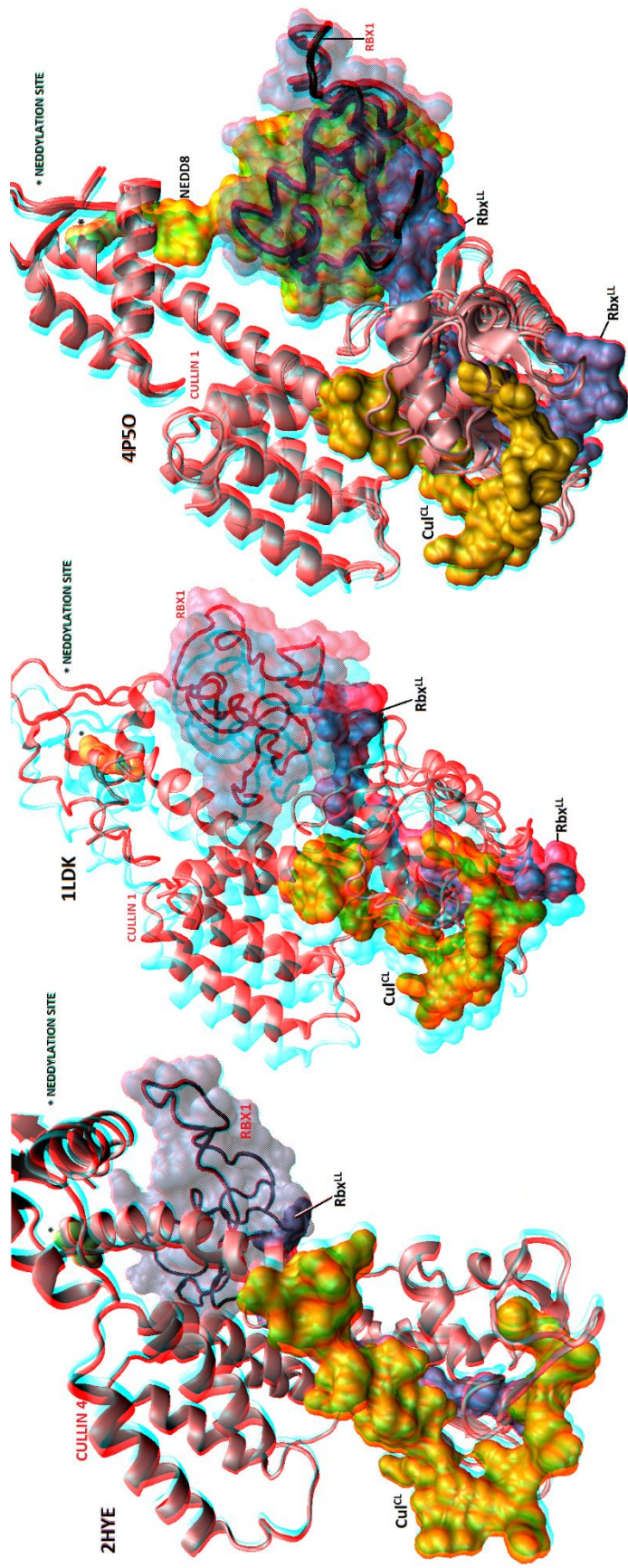


**Figure 20:** Anaglyph Images of Native Cull<sup>CL</sup> and Rbx<sup>LL</sup> Areas in the CRL Complex

Anaglyphic cartoon images of three CRL crystal structures. The first structure, 2HYE, shows human Cull4 in complex with human Rbx1. The second and third structures, 1LDK and 4P50, depicts human Cull1 in complex with Rbx1, with 4P50 showing the neddylated form of the CRL complex. The Cull<sup>CL</sup> and Rbx<sup>LL</sup> regions in each case are shown in solid surface format, while Rbx1 is shown as a ribbon structure inside a transparent surface. NEDD8 is shown as a solid yellow structure, with the Neddylolation site for each Cullin marked with a green surface residue and an asterisk. All three structural models were created using the anaglyphic capabilities of VMD.

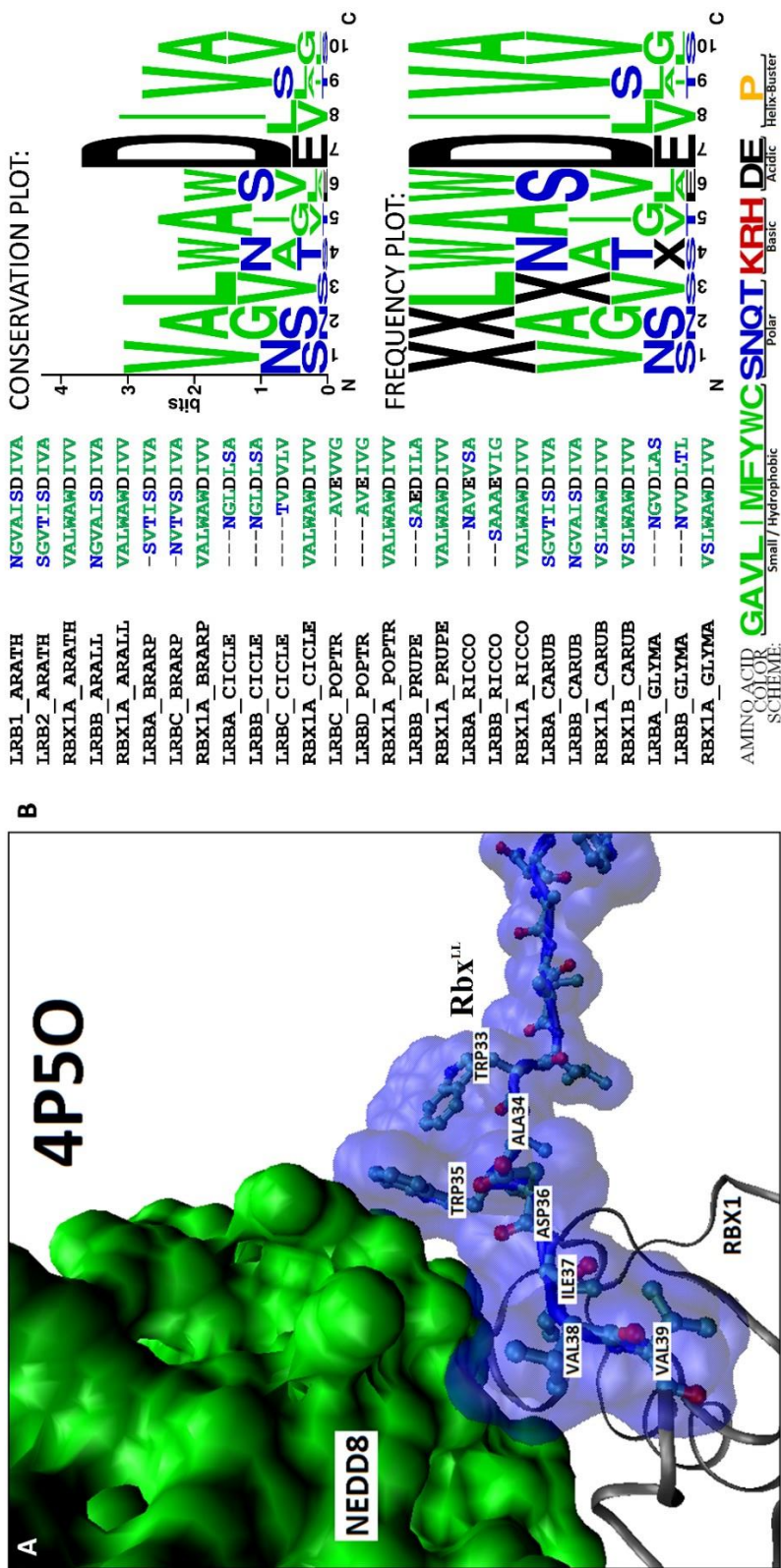


**Figure 21:** Interaction of the Rbx<sup>LL</sup> Region with NEDD8

**A.** The residues of the Rbx<sup>LL</sup> area of *Hs*Rbx1 that interact with *Hs*NEDD8 are shown, as determined by the PDB structure 4P5O. The WAWDIVV motif is involved with NEDD8 interaction. Structure was visualized using VMD.

**B.** The multiple sequence alignment of the Rbx<sup>LL</sup> regions of homologous Rbx1 and the respective LL regions in homologous LRB proteins. As this region contained multiple gaps in the original MSA, the MSA was edited by cutting the alignment 6 amino acids upstream from the aligned Aspartic Acid (D) and trimming away all the gaps. A MEME conservation plot is depicted on the top right, showing the relative amount of conservation present around the WAWDIVV motif in Rbx1 and the area of the LL region corresponding to it on homologous LRBS. The MEME frequency plot, shown at the bottom right, shows the amount of residue frequency, with an X signifying a gap in the alignment.

## ***IN SILICO* Structural Models of the *At*LRB Proteins**

In the previous section, it was established that both Cul1 and Rbx1 share sequence similarity with the amino-terminal portion of the LRBs. The Rbx<sup>LL</sup> motif was also found to interact with NEDD8, as both Cul1 and Rbx1 had crystal structures readily available in the Protein Data Bank<sup>64</sup> (**Figure 20**). It would be beneficial to not only know where the Cul<sup>CL</sup> and Rbx<sup>LL</sup> regions reside on each respective protein, but also where the CL and LL regions are located on the amino-terminal portion of the LRB proteins. However, there is no crystal structure currently available for the LRB proteins. In an attempt to try and better understand the significance of the CL and LL motifs, protein structure prediction software was used to create homology models for the three LRB proteins in *Arabidopsis*.

Homology models for each of the three *At*LRB proteins were created using various open-source homology modeling programs, including **Phyre2**<sup>65</sup>, **HHpred/Modeller**<sup>66</sup>, **I-TASSER**<sup>67</sup>, and **Swiss-Model**<sup>68</sup>. Phyre2 was the only program able to produce atomic coordinates for the entire *At*LRB sequences, which wasn't unexpected, as Phyre2 is known to be able to collect and combine multiple templates to cover the full protein sequence length (**Supplemental Table 1**)<sup>69</sup>. Using multiple templates usually results in an increased root-mean-square deviation (**RMSD**) of atomic positions, which is the measure of the average distance between the backbone atoms of the model superimposed onto the original template, but this method has been able to create highly reliable *in silico* structures of a modeled protein in the past<sup>69</sup>. Phyre2 also uses a Hidden Markov Model (**HMM**) database of known structures that is able to reliably detect remote homology and create accurate protein models, even at sequence identities of 15% or less<sup>70,71</sup>. However, Phyre2 was also the program that provided the

least amount of control over determining the structure, as the structural templates are chosen by the program and cannot be adjusted by the user. The homology models created by Phyre2 served as representations of the overall structure of the *AtLRB* proteins, despite multiple caveats. Problems with the predicted structure included low sequence identity between the templates and the *AtLRB* protein sequences, ambiguous alignment of the individual templates with the protein, ambiguous alignment of the templates with the overall protein sequences, and the need for Phyre2 to use multiple templates from distant protein homologs.

Two different models of the same *AtLRB2* isoform (UniProtKB AC: **Q9FPW6-1**) were produced by Phyre2<sup>65</sup>, as the HMM database of known structures is constantly being updated to include any new structures added to PDB. One model, created on February 9<sup>th</sup>, 2015 using 8 template structures (**Supplemental Figure 7A, Supplemental Table 1**), had 98% of the residues modeled with a confidence of >90%. This model was labeled ***AtLRB2A*** (**Figure 22A, 23A**). The second model, denoted ***AtLRB2B*** (**Figure 22B, 23B**), was created on April 7<sup>th</sup>, 2015, and had a total of 97% of the residues reported as being modelled with a confidence of >90% by Phyre2<sup>65</sup> (**Supplemental Figure 7B**). *AtLRB2B* was created using only three template structures (**Supplemental Table 1**). With fewer overlapping structures, Phyre2 cannot overlap the protein templates and tends to make more errors in the overall predicted structure, requiring more *ab initio* modeling<sup>69</sup>. Also, the second model had less residue coverage, creating a less reliable carboxy-terminal end with more *de novo* modeling required (**Supplemental Figure 7B, Supplemental Table 1**).

The models for *AtLRB1* (**Figure 22C, 23C**) and *AtLRB3* (**Figure 22D, 23D**) were both created on April 4<sup>th</sup>, 2015. Both structural models showed much less confidence, however, than the *AtLRB2* models, with only 84% and 81% of residues being

modelled at greater than 90% confidence, respectively. Both *AtLRB1/3* had large amino-terminal gaps in sequence template coverage, and *AtLRB1* also had a large carboxy-terminal gap immediately following the BACK domain (**Supplemental Table 1**). It was decided that only the two *AtLRB2* predicted structures would be used due to their higher overall model coverage and decreased number of residues modeled by *ab initio* methods.

Unfortunately, a high amount of confidence does not translate to a high level of accuracy in the model, but instead refers to the quality of prediction of the overall fold and the placement of residues in the core of the protein<sup>72</sup>. Therefore, confidence alone should not be the deciding factor when choosing between *AtLRB2A* and *AtLRB2B*. The overall number of templates used also indicates model reliability, as a greater number of templates creates a model with a higher number of caveats.

**QMEAN**, a web server that performs comprehensive model evaluation and calculates scoring functions, was used to gauge the overall quality of each of the *AtLRB2* models<sup>73-75</sup> as a way to select which model was more appropriate to use based on residue reliability and overall structural integrity. Despite a similar overall QMEAN score for both models, *AtLRB2A* was predicted to have modeled the C $\beta$  and all-atom interactions more accurately than *AtLRB2B* (**Supplemental Figure 8A-B**). The overall propensity of a residue for being exposed to the solvent was also predicted to be modeled much more accurately in *AtLRB2A* than in *AtLRB2B* (**Supplemental Figure 8A-B**). An overall assessment of the residue error for each model showed a much higher probability that *AtLRB2A* is more reliable than *AtLRB2B*, especially over the region amino-terminal to the BTB domain (residues 1-120, **Supplemental Figure 8C-D**).

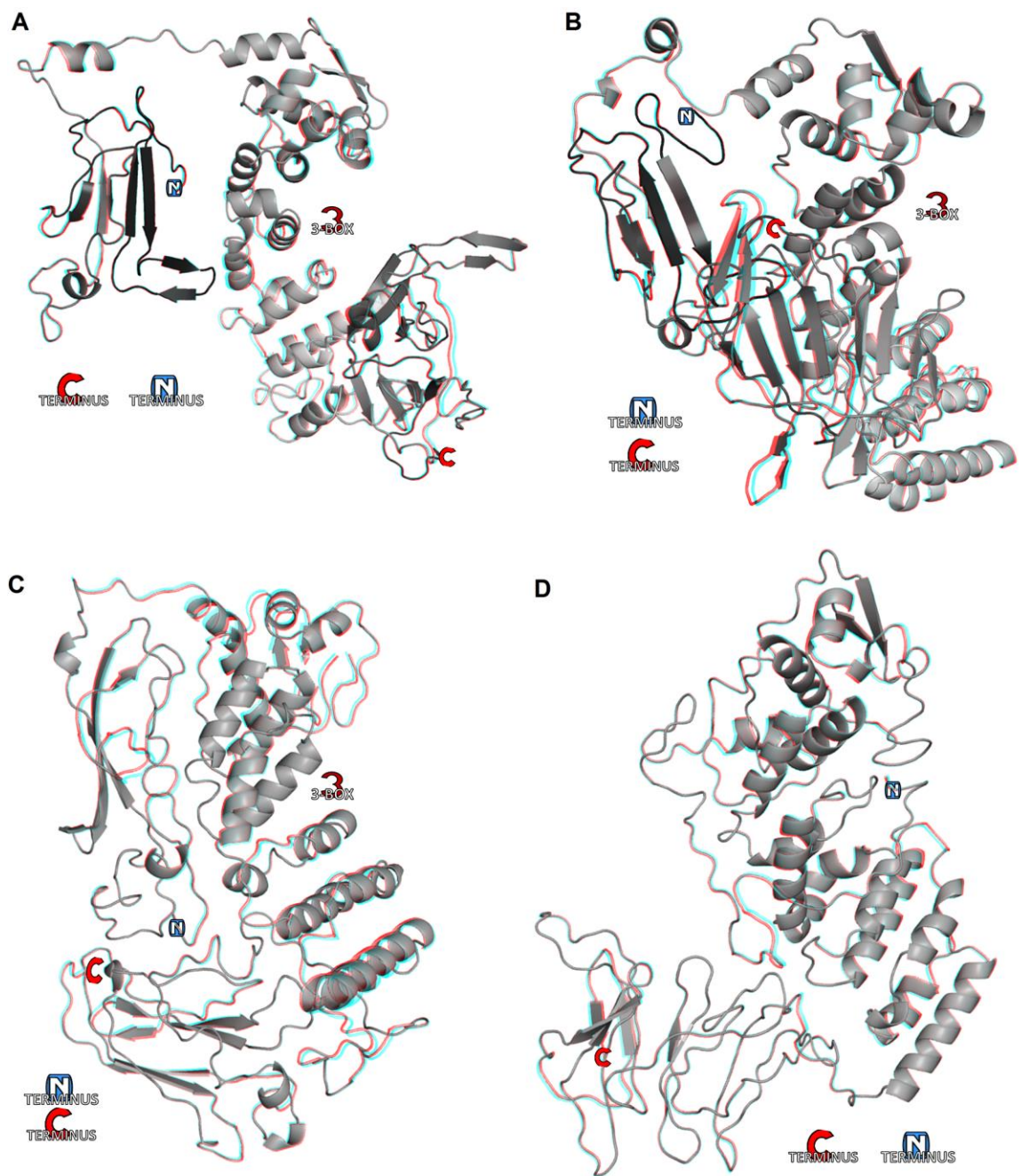


**Figure 22:** Anaglyphic Stereo View of *AtLRB* Phyre2 Protein Models

Anaglyphic stereo view of the (A) *AtLRB2A*, (B) *AtLRB2B*, (C) *AtLRB1*, and (D) *AtLRB3* models created using the intensive mode of the protein homology modeling program Phyre2<sup>65</sup>. Each model was developed by combining and overlapping the known structural templates of multiple protein structures found in PDB<sup>64</sup> (**Supplemental Table 1**). Anaglyphic structural models were then created using POLYVIEW-3D<sup>76</sup>.



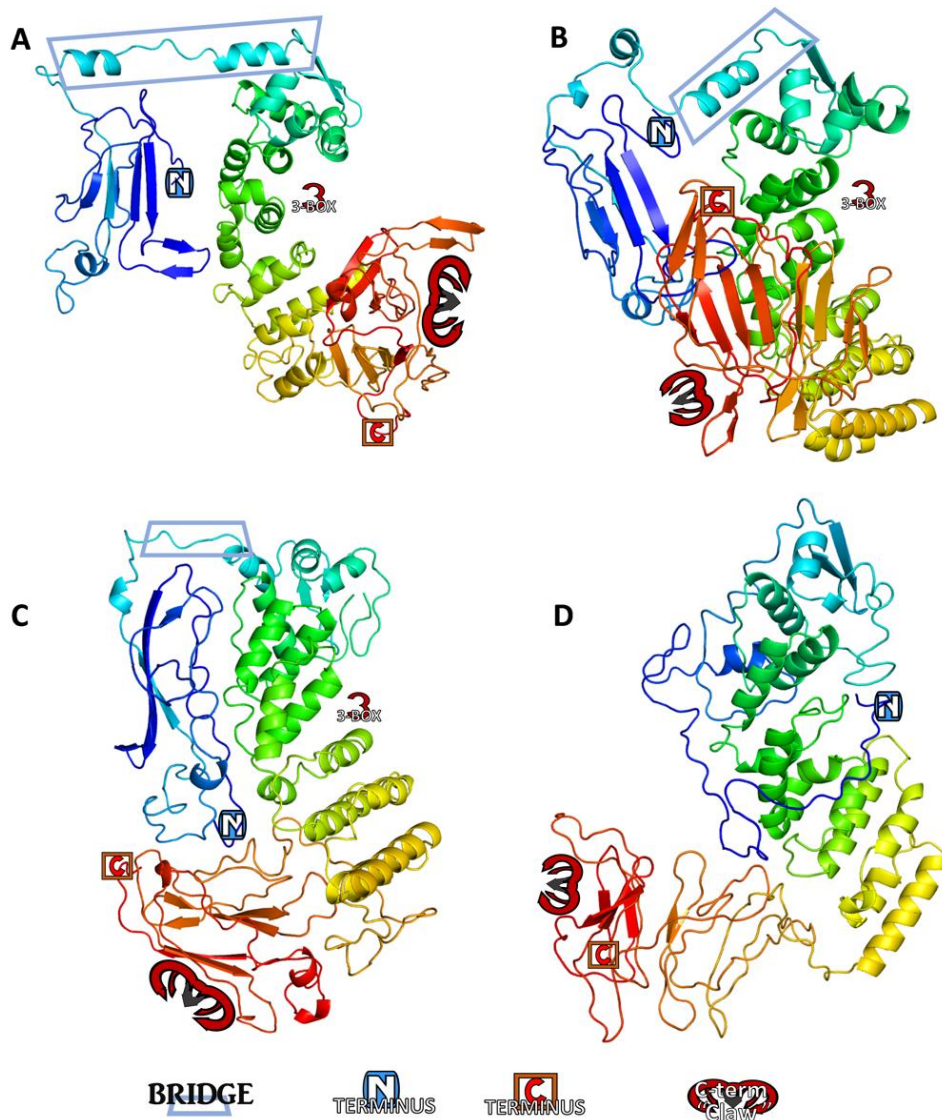


**Figure 23:** *AtLRB* Phyre2 Protein Models Displayed via Residue Index

Model of the (A) *AtLRB2A*, (B) *AtLRB2B*, (C) *AtLRB1*, and (D) *AtLRB3* structures that were created using the intensive mode of the protein homology modeling program Phyre2<sup>65</sup>. Amino-terminal residues are displayed in blue, while carboxy-terminal residues are displayed in red. The amino-terminus, carboxy-terminus, amino-terminal “bridge”, C-term “claw”, and 3-Box regions are also marked. Models were created using the structural rendering web-based interface program POLYVIEW-3D<sup>76</sup>.

The sequence beginning carboxy-terminal to the BACK domain (approximately residue 350) showed a high probability of residue error for both *AtLRB2* models, but *AtLRB2A* contained fewer and less frequent spikes in the amount of predicted residue error. With this, *AtLRB2A* was chosen to be the model that would be used to create all future figures.

### **Analyzing the *AtLRB* *IN SILICO* Structural Models**

Despite the caveats previously discussed, the *AtLRB1* and both *AtLRB2* models created using Phyre2<sup>65</sup> offered several insights into the possible structure and functional mechanism of the LRBs. The BTB domain of the *AtLRB2A* structure was examined to determine if the domain architecture was correctly predicted<sup>34,36</sup>. By using the Kelch-like Protein 11, we were able to compare known BTB/3BOX/BACK architecture to the *AtLRB2A* predicted model (**Supplemental Figure 9**). The topology expected to be found in the BTB domain corresponds well to the BTB domain topology in *AtLRB2A* (**Supplemental Figure 9A-B**). This region was modeled using templates containing MATH/BTB (PDB ID: **3HU6**)<sup>42</sup> or BTB/BACK (PDB ID: **3I3N, 3HVE**)<sup>42</sup> domains, both of which are known to associate with Cul3 in humans, so we would expect this region to be accurately modeled.

Another feature that was readily found in all three models was the 3-Box motif, which resides in the cleft between the BTB and BACK domains<sup>35,42</sup> (**Supplemental Figure 9C**). The grooved area that corresponds to the 3-Box marks the site at which amino-terminal Cul3 creates a high-affinity interaction with the BTB domain of the LRBs<sup>35,42</sup> (**Figure 5B**). The 3-Box region was found to be modeled as expected, with the

two carboxy-terminal  $\alpha$ -helices creating an antiparallel four-helix bundle with the two amino-terminal  $\alpha$ -helices of the BACK domain<sup>34</sup> (**Supplemental Figure 9C**).

A third structural feature that was found to be consistent in each model was a carboxy-terminal structure resembling a claw, as the structure of the claw consists of a shallow groove surrounded by multiple finger-like protrusions (**Figure 23**). This carboxy-terminal claw structure is predicted to be responsible for target recognition and interaction, as the carboxy-terminal region has already been well established as being responsible for target recruitment<sup>34,35,40</sup>. The claw is based solely on observations from the predicted model, however, and has no evidence to support its existence at this time.

Finally, the most notable feature that was found in all three of the models was an amino-terminal bridge or loop (residues 108 to 138) that seemed to separate the amino-terminal portion of *AtLRB* from the BTB domain (**Figure 23**). The amino-terminal loop structure (residues 108 to 138) was consistently found in all *AtLRB2* models created by Phyre2<sup>65</sup>, and each model had varied orientation to the region amino-terminal to the loop in subsequent models created using Phyre2<sup>65</sup> (*not shown*).

Interestingly, neither *HsCul1* nor *HsRbx1* were chosen as templates for the amino-terminal portion of the *AtLRBs*. This may mean that our hypothesis that the *LRBs* share homology with  $\text{Cul}^{\text{CL}}$  and  $\text{Rbx}^{\text{LL}}$  is not correct. However, the motifs may be homologous but were simply judged to be unsuitable templates due to their small size and therefore neither were chosen as templates by the program. The overall layout of the CL region of *AtLRB2* was directly compared to the native layout of the  $\text{Cul}^{\text{CL}}$  crystal structure (**Figure 24**). The horseshoe-like shape of the CL region was found in both the predicted *AtLRB2* model and in the region of the 1LDK crystal structure associated with

the CL region. If the predicted *AtLRB2* model is found to be an accurate model of the *AtLRBs*, this similarity between the CL region of *AtLRB2* and the Cul<sup>CL</sup> region of Cul1 could signify a conservation of function between the two proteins in this region.

Overall, this is a very difficult case for homology modeling. The *AtLRB2A* predicted structure that we have decided to use should not be thought of as highly reliable or of good quality. There is no structural information to make the model any more accurate. However, in terms of overall fold in the BTB/3BOX/BACK domains, the predicted structural models are usable.

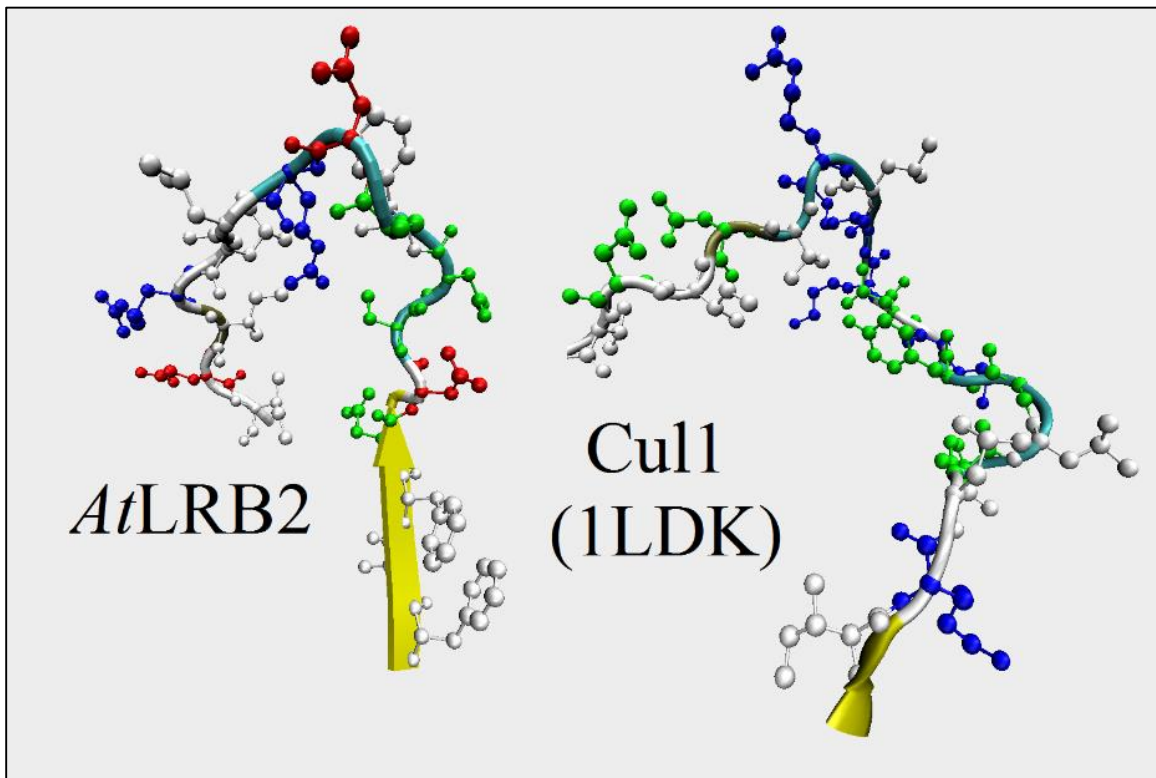


**Figure 24:** Comparison of the CL Predicted Structure and Cul<sup>CL</sup> Native Structure

The CL region of *AtLRB2* is shown next to the Cul<sup>CL</sup> region of Cul1<sup>26</sup>. Amino acid side chains are colored by type using VMD<sup>41</sup>, with hydrophobic residues in white, acidic residues in red, polar residues in green, and basic residues in blue.

## Using ConSurf to Map the Relative Evolutionary Conservation of the CL & LL Motifs onto Full-Length *AtLRB2A* Model

The bioinformatics program **ConSurf**<sup>77</sup> was used in an attempt to merge the *AtLRB2A* model created by Phyre2<sup>65</sup> with previous data on sequence conservation identified through MSA. Combining sequence conservation and a three-dimensional model will provide us with further insight into the function of the amino-terminal motifs.

Additionally, ConSurf has the ability to go one step further than the MSAs that were created previously using Expresso<sup>57,77</sup>, as ConSurf runs a context-specific iterated BLAST (**CSI-BLAST**) on *AtLRB2* to find homologous protein sequences, then clusters them together, with highly similar sequences being removed along the way. ConSurf then uses Expresso to create a MSA, which is then used to construct a phylogenetic tree and create position-specific conservation scores that range from 1 to 9, with 9 being the most conserved (**Figure 25A**). Once the evolutionary conservation of *AtLRB2* was determined, the amount of conservation was then written into the *AtLRB2A* structural model and could then be visualized using **POLYVIEW-3D**<sup>76</sup> (**Figure 25B**).

The ability to display evolutionary sequence conservation on the predicted three-dimensional LRB2 protein structure helps to further provide insight into which regions are important for the overall function of the LRBs. Accordingly, the BTB and BACK domains were found to be the most well conserved portions of the protein. Unfortunately, despite the 45% minimum cutoff value for percent identity, the MSA created by ConSurf contained a multitude of protein sequences that did not contain any residues amino-terminal to the BTB or BACK domains resulting in very low relative scores for all amino-terminal residues (**Figure 25A**). In order to determine the evolutionary sequence

conservation of the region amino-terminal to the BTB domain, the PDB file for *AtLRB2A* was edited to contain only the first 144 residues. This shortened amino-terminal structure was then investigated using ConSurf.

### **Analysis of Relative Evolutionary Conservation of the CL & LL Motifs Using ConSurf and Only the Amino-terminal Portion of *AtLRB2***

The shortened amino-terminal *AtLRB2A* model was denoted as *AtLRB2N* and ran using ConSurf. Our new dataset contained only sequences relevant to the amino-terminus of LRB, resulting in a more accurate representation of sequence similarity across the dataset, particularly in the Cullin-like region (**Figure 26A**). Additionally, the amount of evolutionary conservation representation in the Linker-like region was also higher in the *AtLRB2N* model, extending beyond the 5 residues responsible for nuclear localization (residues 74-78) and encompassing much more of the full Linker-like region.

Additionally, the updated evolutionary conservation scores were written onto the newly-created *AtLRB2N* structural file and visualized using POLYVIEW-3D<sup>76</sup> (**Figure 26B, 26C**). The *AtLRB2N* structure was also used to visualize the CL and LL regions (**Figure 26B, 26C**). In the spacefill models of *AtLRB2N*, the CL region can be seen creating a “horseshoe” around the LL motif (**Figure 27A**), and together, the two regions form a prominent and compact structural area on the amino-terminal *AtLRB2* domain.

The *AtLRB2N* structure modeling the conservation predicted by ConSurf<sup>77</sup> analysis (**Figure 27**) also showed the conservation of some of the residues residing in the amino-terminal ‘loop’ or ‘bridge’ region (residues 108 to 138) that was previously postulated to control the orientation of the amino-terminal structure (**Figure 24**). However, the residues that were conserved did not appear to be sites for potential

modifications. Only a single serine residue was relatively conservation, indicating a potential target site for phosphorylation. A conformational shift in the LRB “bridge” region could be due to a modification placed anywhere on the LRBs, so a lack of complete conservation does not necessarily disprove the hypothesis that the bridge could be a regulatory site.

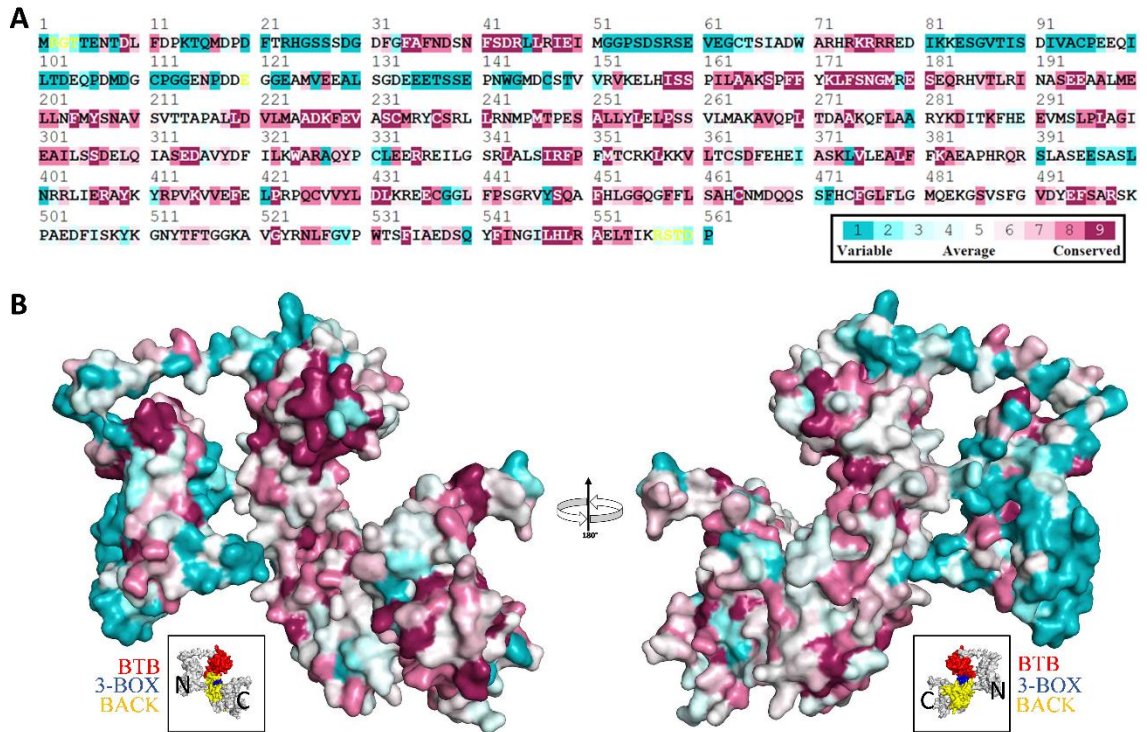


**Figure 25:** Predicted Evolutionary Conservation of Full-Length *AtrLRB2*

**A.** The relative amount of LRB2 residue conservation as predicted by ConSurf<sup>77</sup>. Residues scoring 9 (scarlet) are predicted to be the most conserved, while a score of 1 (cyan) signifies a high amount of residue variability. Residues highlighted in yellow contain unreliable scores.

**B.** The front and rear surface view of *AtrLRB2A*. Residues are colored based on the ConSurf scores assigned to them. The small model in the box below the ConSurf structures shows the locations of the BTB, 3-BOX, and BACK domains. Structures were rendered using POLYVIEW-3D<sup>76</sup>.

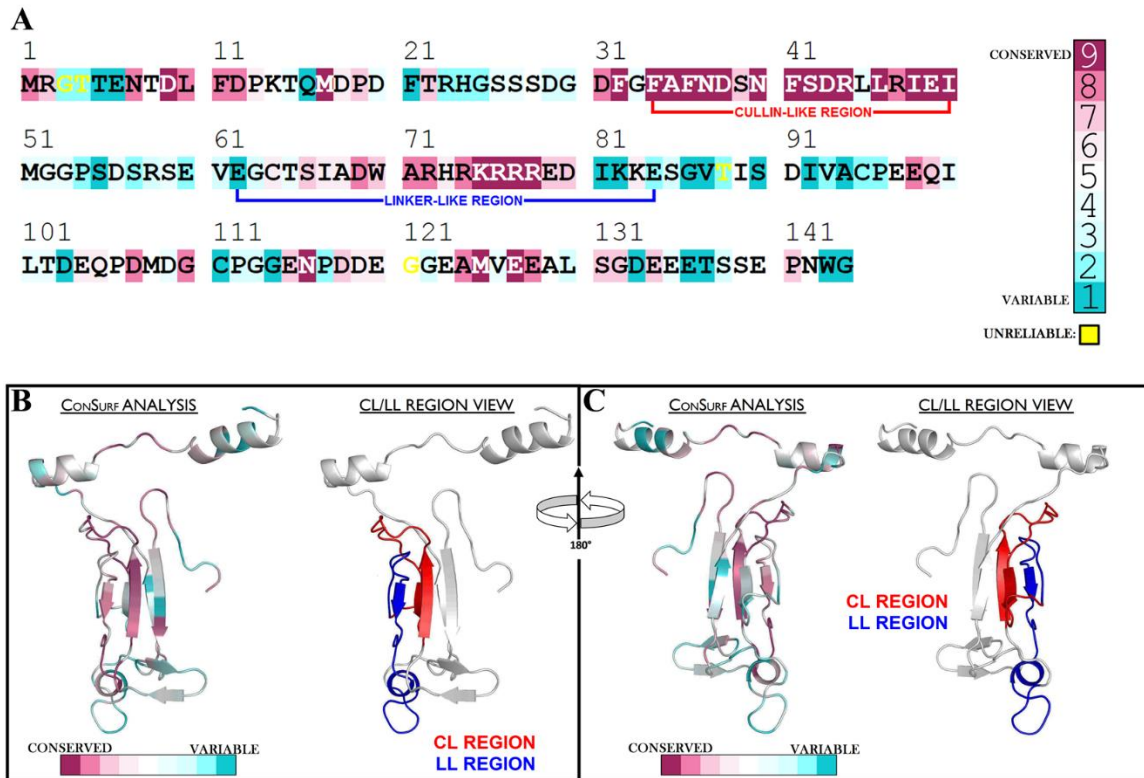


**Figure 26:** Predicted Amino Acid Conservation of *AtLRB2N*

**A.** The relative amino acid conservation of the *AtLRB2N* sequence, as determined by ConSurf<sup>77</sup>. The areas corresponding to the Cullin-like and Linker-like regions are also marked. Residues scoring 9 are predicted to be the most conserved, while a score of 1 signifies a high amount of residue variability.

**B.** The front cartoon views of *AtLRB2N*. Residues on the figures to the left are colored based on the ConSurf<sup>77</sup> scores assigned to them. The structure on the right shows the area of the amino-terminal region associated with the CL and LL regions, which are colored in red and blue, respectively.

**C.** The back cartoon views of *AtLRB2N* after rotating the model 180°. Residues on the figures to the left are colored based on the ConSurf<sup>77</sup> scores assigned to them, with conserved residues being marked scarlet. The structure on the right shows the area of the amino-terminal region associated with the CL and LL regions, which are colored in red and blue, respectively. All of the structural models created were rendered using POLYVIEW-3D<sup>76</sup>.



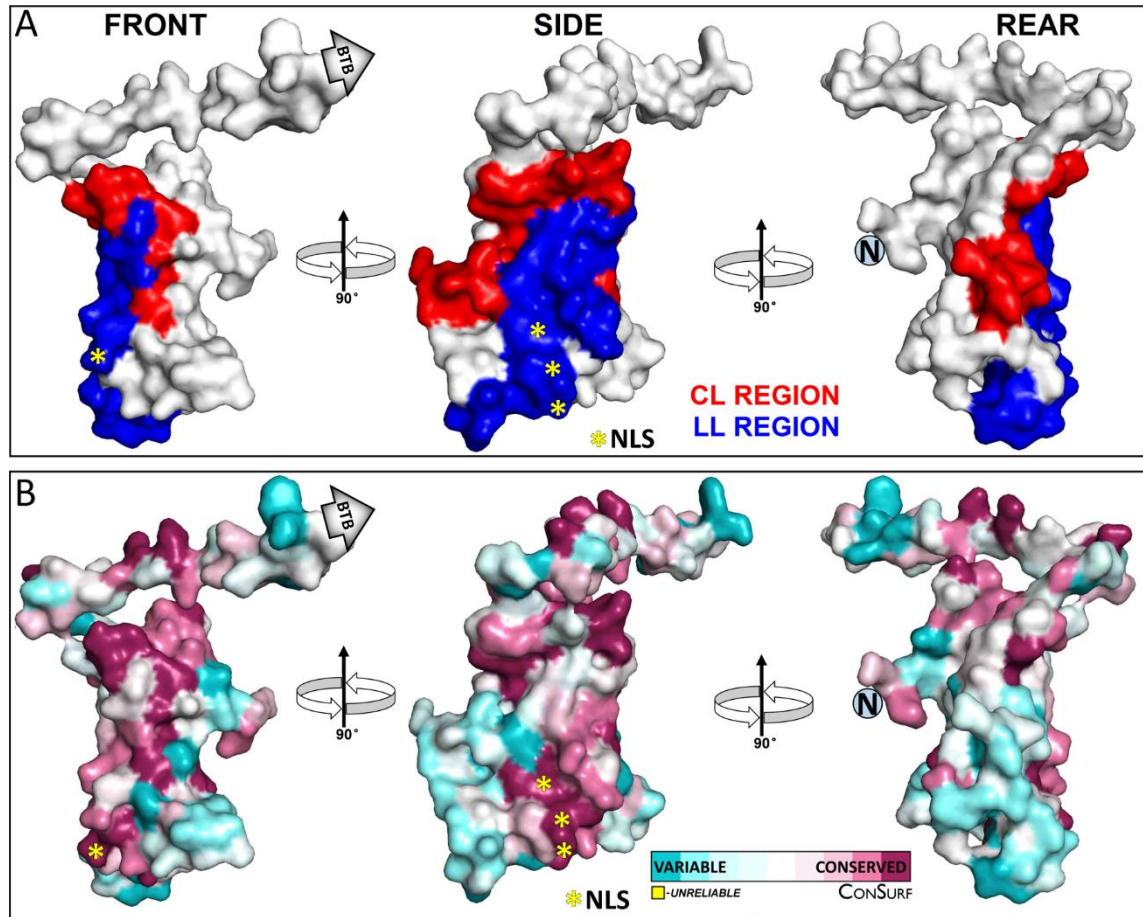


**Figure 27:** Predicted Amino Acid Conservation of the Amino-terminal Domain

**A.** The front, side, and rear surface views of *AtLRB2N*, which was achieved by rotating each structure 90° each time. The structural areas of the amino-terminal region associated with the CL and LL regions, which are colored in red and blue, respectively, are shown. The location of the NLS sequence is marked with yellow asterisks, while the amino-terminus is marked with an N inside a light-blue-colored circle. The start of the BTB domain is also shown.

**B.** The front, side, and rear surface views of *AtLRB2N*, which was achieved by rotating each structure 90° each time. ConSurf<sup>77</sup> was used to determine sequence conservation, with the conserved residues colored scarlet and variable residues colored cyan. The location of the NLS sequence is marked with yellow asterisks, while the amino-terminus is marked with an N inside a light-blue circle. The start of the BTB domain is also shown. All of the structural models of *AtLRB2N* created were rendered using POLYVIEW-3D<sup>76</sup>.

## DETERMINING THE ROLE OF PHOSPHORYLATION ON LRB FUNCTION

### Three Predicted Phosphorylation Sites Are Completely Conserved in All LRB Protein Homologs

Phosphorylation is known to play a significant role in the phy signaling pathway, with the phosphorylation of PIF3 being directly responsible for PIF-mediated phytochrome degradation<sup>11,16</sup>. There is also evidence to suggest that plant phytochromes act as atypical serine/threonine protein kinases<sup>12,14</sup>. Phosphorylation is known to play a major role in triggering the MAD mechanism responsible for PIF3<sup>16</sup> and phyB<sup>2,16</sup> degradation, and since we know that the LRBs directly interact with both PIF3 and phyB, it was hypothesized that phosphorylation may also play a role in regulating LRB function.

First, we wanted to identify any potential phosphorylation sites that were present on the conserved regions of the LRBs. Using the Arabidopsis Protein Phosphorylation Site Database<sup>78,79</sup> (**PhosPhAt 4.0**, <http://phosphat.uni-hohenheim.de/>), each of the LRB protein sequences that were used to create the edited MSA previously (**Supplemental Figure 4**) were individually tested for any potential regions where phosphorylation could occur. Then, the multiple sequence alignment of the homologous LRB proteins was used to predict potential phosphorylation sites using regions of conservation (**Supplemental Figure 10**). Only three conserved sites on the LRB alignment showed a high probability of being phosphorylated (sites **H**, **U**, **W**, **Supplemental Table 2**), with three other sites showing almost complete conservation and moderate phosphorylation potential (sites **O**, **S**, **V**, **Supplemental Table 2**). One particular serine residue, *S131* in *AtLRB2* (site **H**,

**Supplemental Table 2**), was located at the end of the third conserved amino-terminal region and was predicted to have a high probability of being phosphorylated. The remaining conserved residues predicted to be phosphorylated appeared on the carboxy-terminal portion of the LRBs (residues 513 through 516 in *AtLRB2*) in the form of a highly-conserved *YTFT* sequence (sites *U*, *V*, *W*, **Supplemental Table 2**). *S131* and the *YTFT* sequence were both projected onto the *AtLRB2A* model in order to determine their placement in proximity to known or predicted structural features (**Figure 28**).

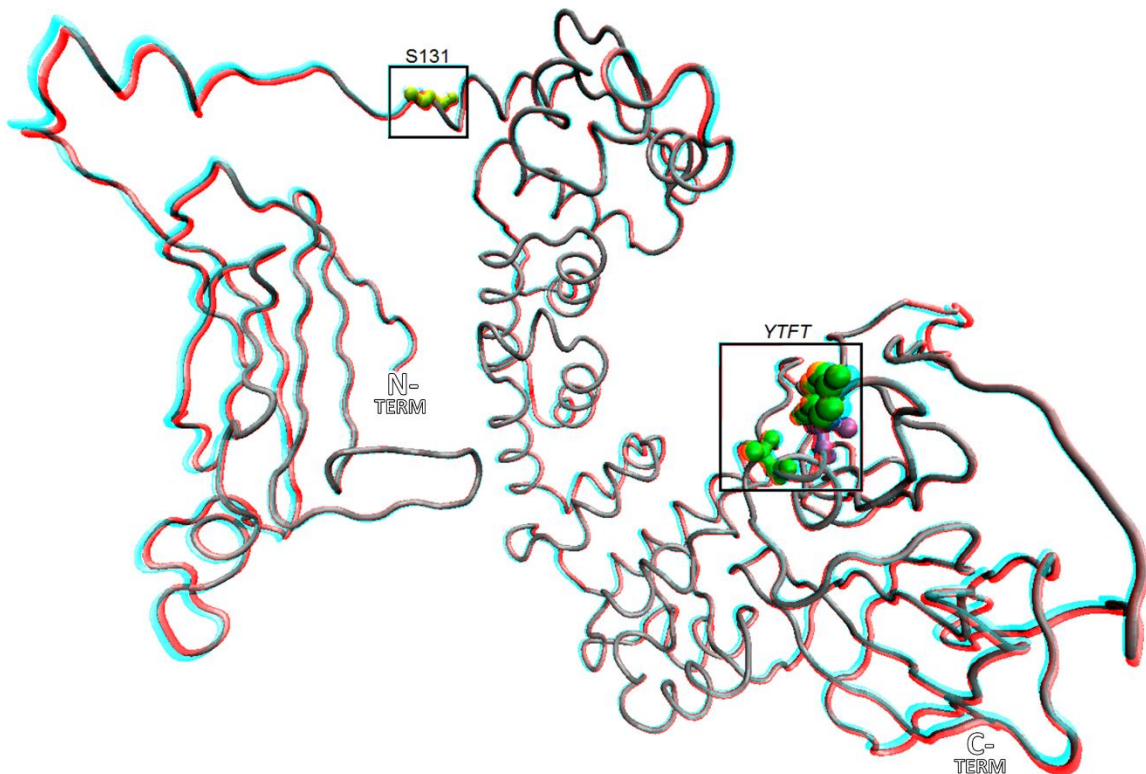


**Figure 28:** Anaglyphic Model of the Predicted Phosphorylation Sites on *AtLRB2A*

An anaglyphic model of the two phosphorylation regions found to be conserved across all LRB land plant homologs. The serine-131 residue (S131) is displayed in yellow, while the tyrosine-513, threonine-514, and threonine-516 residues from the conserved *YTFT* sequence are displayed in green. Phosphorylation sites were determined by the PhosPhAt<sup>78,79</sup> database, while the model was created using the *AtLRB2A* structure and the anaglyphic stereo option of VMD<sup>41</sup>.

Two other clusters of predicted phosphorylation sites, known as phosphorylation “hotspots”, were found in LRB and contained fairly-conserved potential phosphorylation residues. Each hotspot was found immediately before the CL or LL regions (sites *A/B/C* and *D/E/F* in **Supplemental Figure 10**), contained at least three predicted phosphorylation residues in close proximity to one another, and each hotspot had high predicted phosphorylation values in two out of the three potential sites (**Supplemental Table 2**).

### **The Phospho-Shift Assay Did Not Present Evidence that Transgenic LRB1 Proteins are Phosphorylated**

To test the phosphorylation state of LRB proteins in response to different light conditions, a phospho-shift assay was performed on an *Arabidopsis thaliana* transgenic line overexpressing LRB1-GFP that was grown in red or far-red light conditions. Phosphorylated proteins have previously been shown to sometimes run higher on an acrylamide gel by repelling the negatively-charged SDS molecules<sup>80</sup>. However, a negative result, i.e. no shift detected, would not necessarily mean there is no difference in phosphorylation<sup>81</sup>, as some proteins simply do not show a phosphorylation shift. The protein lysate from seedlings grown in different light conditions (**Figure 29A**) was treated with a  $\lambda$ -protein phosphatase and compared to a non-treated plant grown in the same light conditions using immunoblotting. In theory, the  $\lambda$ -protein phosphatase will remove any phosphorylation present on any proteins in the lysate. Immunoblot analysis following SDS-PAGE using anti-GFP antibodies could reveal any differences in phosphorylation state of the LRBs between red, far-red, and dark-grown seedlings<sup>81</sup>.

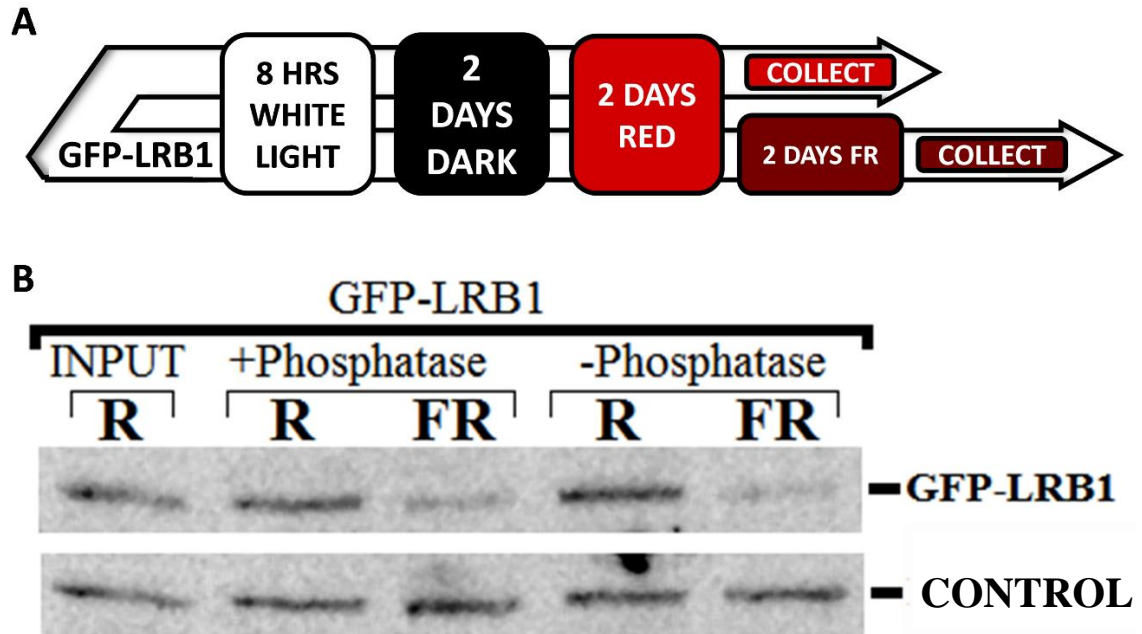


**Figure 29:** Phospho-Shift Assay in Red and Far-Red Light

**A.** A graphic showing the duration and type of light exposure each GFP-LRB1 treatment group was exposed to and when each sample was collected.

**B.** Plant lysates from plants treated with red light and then isolated immediately (“R”) or after a further 2 day treatment with Far-red light (“FR”) were treated with (“+Phosphatase”) or without (“-Phosphatase”) a  $\lambda$ -protein phosphatase and analyzed using Western blotting with anti-GFP antibodies. The INPUT lane represents lysates immediately after isolation, with a non-specific band used as a loading control.

The phospho-shift assay did not show any dephosphorylation after 15 minutes of incubation (**Figure 29B**). The lack of shifting in band size could indicate that there was no phosphorylation present on GFP-LRB1, as there is not a noticeable difference in band migration between the zero and 15 minute timepoints for samples treated with  $\lambda$ -protein phosphatase or between the inhibitor controls. A lack of band shifting could also indicate that either the samples were not incubated long enough to remove the phosphate from any active GFP-LRB1, the phosphatase was non-functional, or that the phosphorylated

proteins do not run higher on the gel as expected. However, there is a noticeable difference between the intensity of the red and far-red light samples, as the band is visibly brighter in red light than it is in far-red light conditions. Despite the same strength in the non-specific band, the difference in banding strength could be due to the seedlings that were exposed to two days of far-red light for a total of 6 days of growth, compared to the red light seedlings, which were collected after 4 days of treatment (**Figure 29B**).

### **Anti-Phosphoserine Antibodies Did Not Reveal the Presence of Phosphoserine Residues on Purified GFP-LRB2 Proteins**

The *in silico* phosphorylation site prediction software PhosPhAt 4.0<sup>78,79</sup> predicted a high probability of phosphorylation occurring on multiple different sites on the *AtLRBs* (**Supplemental Figure 10**). The phospho-shift assay was unable to support this, showing inconclusive results (**Figure 29**), but the lack of a shift does not correlate to a lack of phosphorylation<sup>81</sup>. A more direct approach, such as directly detecting phosphorylation on purified LRB proteins, would be needed to determine if phosphorylation was present on the *AtLRBs*.

LRB proteins purified by immunoprecipitation from plants grown in darkness, red light, or far-red light conditions were investigated using Western blotting and probed with anti-phosphoserine antibodies in an attempt to detect any light-dependent phosphorylation present on the LRBs. Although we were able to purify the GFP-LRB2 proteins, none of the purified samples from the GFP-LRB2 immunoprecipitation cross-reacted with the anti-phosphoserine antibodies under our conditions (**Figure 30**). This supports the conclusion from the phospho-shift assay that the LRBs may not be

phosphorylated, despite the *in silico* data predicting otherwise. However, definitive interpretation of these results is difficult, because phosphorylation present on the *YTFT* sequence (*Y513*, *T514*, and *T516* in *AtLRB2*) would not be identifiable when probing for phosphoserine, since the phosphoserine antibody targets only phosphorylated serine residues.

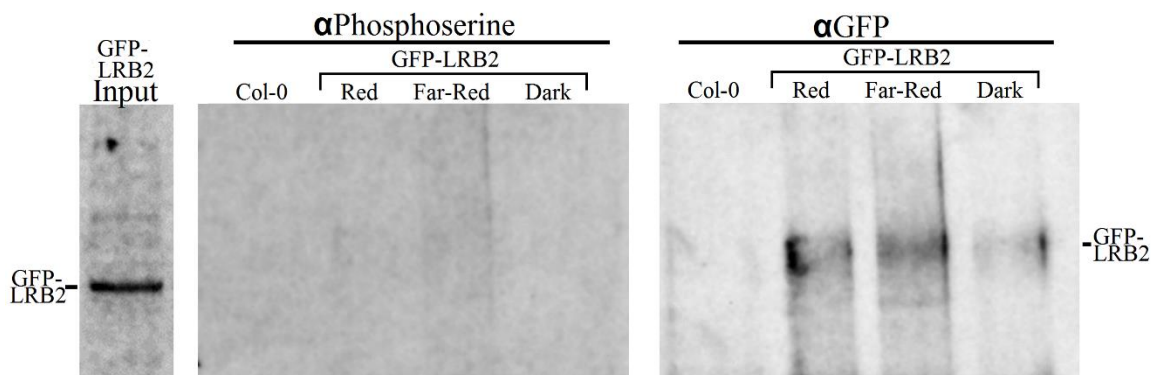


**Figure 30:** Probing Purified LRB2 for the Presence of Phosphoserine Residues

Immunoprecipitated GFP-LRB2 proteins extracted from *Arabidopsis* seedlings grown in darkness or exposed exclusively to R or FR light were analyzed using SDS-PAGE and immunoblotting. The purified GFP-LRB2 eluates were probed with anti-phosphoserine antibodies, then reprobed with anti-GFP antibodies. The crude input for GFP-LRB2 grown in FR light was probed using anti-GFP antibodies.

## NEDD8 CONJUGATION PREDICTED ON *At*LRB2

### Disrupting Neddylation Using MLN4924 Shows an Accumulation of GFP-LRB1 in Red Light Conditions

Since we see that the CL and LL domains in LRBs are similar to regions found in both CUL and RBX, and these regions are adjacent to and may play a role in the neddylation of Cullin, we wanted to investigate the possibility that the LRBs may be neddylated. The interaction of the Rbx<sup>LL</sup> region with NEDD8 also suggests that the LRBs can also interact with NEDD8 at the LL region (**Figure 21**). Additionally, GFP-tagged *At*LRB2 tends to run at around approximately 105kDa in an SDS-PAGE gel, despite only being 90kDa in size (27kDa GFP + 63kDa *At*LRB2). This suggests that the LRBs are modified in some form, which may support the hypothesis that light-dependent neddylation occurs.

The small-molecule NEDD8-inhibitor **MLN4924** will be used as a way to indirectly test for NEDD8 conjugation on GFP-tagged *At*LRB proteins, as MLN4924 binds to ECR1 to prevent the first step of NEDD8 conjugation<sup>52</sup>. If the *At*LRB proteins are conjugated with NEDD8, which is approximately 9kDa in size, treatment with MLN4924 should inhibit NEDD8 conjugation and show an overall change in the molecular weight of the *At*LRBs when visualized using Western blotting.

Exposure to a 50 $\mu$ M concentration of MLN4924 by 4-day-old etiolated GFP-LRB2 seedlings for four days resulted in an accumulation of only GFP-LRB1 in red light (**Figure 31**). Without NEDD8 conjugation, Cullin proteins would not be able to form functional CRL complexes, preventing the attachment of Ubiquitin and the subsequent



degradation of any proteins targeted by Cullin-RING E3 Ubiquitin ligases<sup>52</sup>. As it was previously established that the *AtLRBs* undergo degradation via the UPS<sup>2</sup>, an accumulation of the GFP-tagged *AtLRBs* would be expected.

A molecular weight band shift could not be detected after MLN4924 treatment in any light condition (**Figure 31A**). Despite a lack of band shift after MLN4924 treatment, the MLN4924 treatment worked, as the plants treated with the inhibitor had decreased hypocotyl lengths and showed increased root hair growth when exposed to 50 $\mu$ M MLN4924 as was observed in previous studies<sup>52</sup>. Seeds placed on 100 $\mu$ M MLN4924 did not germinate even after 6.5 days of growth (**Figure 31B**). The absence of a band shift in the seedlings treated with MLN4924 could indicate that no NEDD8 modification is present in any light condition. However, the GFP-tagged *AtLRB* proteins continue to run approximately 15kDa higher than expected, so to rule out NEDD8 conjugation completely, the LRBs will need to be purified and probed with anti-NEDD8 antibodies.

Preliminary results suggest the amount of GFP-tagged *AtLRB1* and *AtLRB2* protein accumulation after treatment with MLN4924 may be different between the two transgenic lines. GFP-LRB2 levels in both dark and red light conditions did not increase noticeably after MLN4924 treatment, while the inhibitor caused a pronounced accumulation of GFP-LRB1 in red light (**Figure 31**). Despite having a non-specific control band with considerably less intensity, the MLN4924-treated GFP-LRB1 sample had a much darker GFP band than its untreated GFP-LRB1 counterpart. *AtLRB1* has previously been shown to be less effective at rescuing the hypersensitive phenotype found in the *lrb12* double mutant than *AtLRB2*. The *lrb2* single knockout mutant also showed rosette compaction when grown in short day conditions, whereas the *lrb1* single

knockout did not show any obvious change in phenotype from the wild-type<sup>2</sup>. This may suggest that LRB1 and LRB2 do not operate identically to one another and may have two separate mechanisms for regulating phytochrome and PIF levels, or possibly that each of the LRBs have an additional protein-specific function in the red light response pathway that the other does not.

### **NEDD8 Conjugation Was Detected on Purified GFP-LRB2 Proteins**

The *AtLRB* predicted models and alignments, along with the *HsCul* crystal structure models, consistently suggested that NEDD8 conjugation or the NEDD8 signaling pathway was important to the overall function of the LRBs. Since the CL region of *AtLRB2* shares sequence and structural similarities with the region of *AtCul1/2* which sits in close proximity to the site of Cullin neddylation, in addition to the similarities seen with the LL region and the region of *AtRbx1* which has been shown to physically interact with NEDD8<sup>29</sup> (**Figure 21**), a direct method for detecting NEDD8 was devised. Additionally, the 15kDa increase in the molecular weight of *AtLRB* found when using SDS-PAGE analysis could be the result of NEDD8 conjugation, despite the lack of support for NEDD8 conjugation that was found in the MLN4924 NEDD8 inhibitor experiment (**Figure 31**).

GFP-tagged *AtLRB2* proteins were purified from plants grown for 4 days in darkness, then exposed to 4 additional days of either darkness, red light, or far-red light. Special care was taken to prevent Cul3 from being pulled down, with total protein lysates being boiled prior to immunoprecipitation. Under these conditions, neddylated Cul3 should be prevented from interacting with GFP-LRB2, and this is especially important,

given that Cullin and GFP-LRB2 have similar molecular weights and can't be differentiated from one another when probing with anti-NEDD8 antibody.

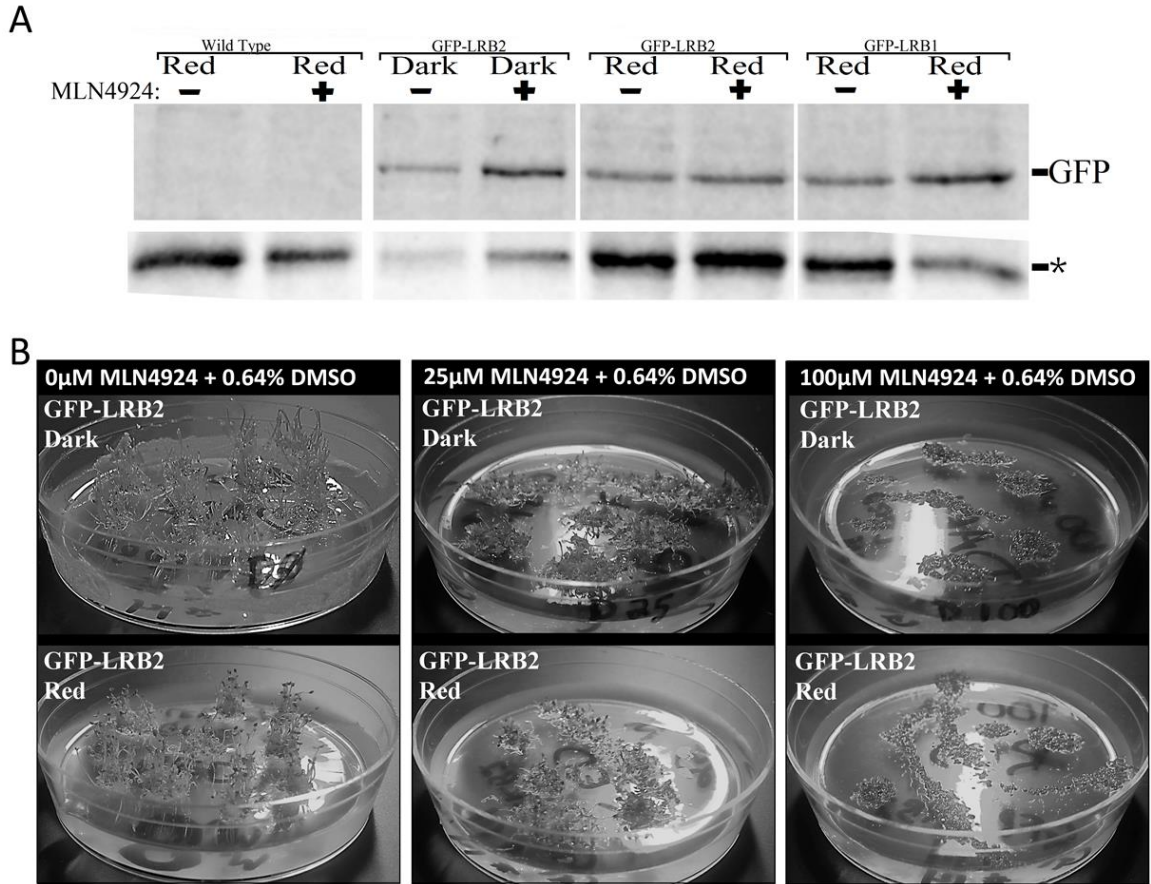


**Figure 31:** Treatment of seedlings with the NEDD8 Inhibitor MLN4924

**A.** Etiolated 4-day-old *Arabidopsis* seedlings were treated with 50 $\mu$ M of MLN4924 and exposed to different light conditions for four additional days. Total protein extracts were analyzed via Western blotting using anti-GFP antibodies. An asterisk marks the non-specific band used to compare protein loading between each pair of related samples.

**B.** Transgenic GFP-LRB2 *Arabidopsis* seeds were planted on plates containing 0.64% DMSO and 100 $\mu$ M MLN4924, 25 $\mu$ M MLN4924, or 0 $\mu$ M of the inhibitor. Seeds were exposed to 2.5 days of white light, placed in darkness for 3 days, then either remained in darkness or were exposed to red light for 24 hours. All plates were photographed after 6.5 days of total growth.

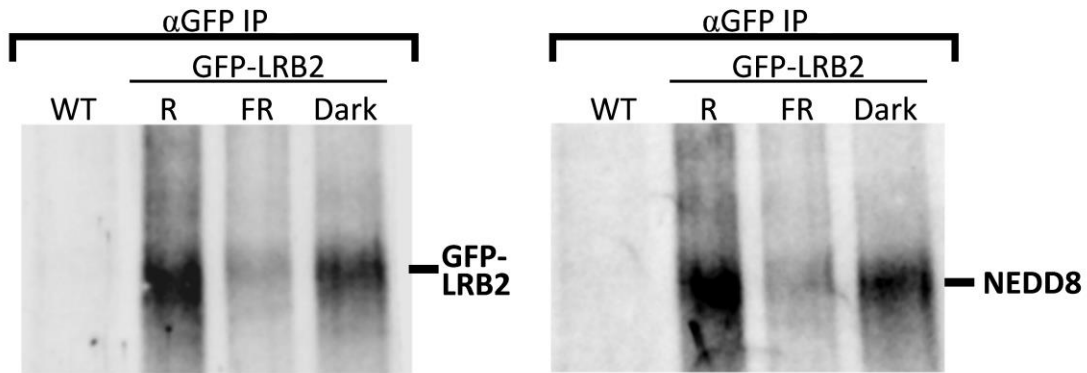


**Figure 32:** Probing Purified LRB2 for NEDD8

GFP-LRB2 proteins immunoprecipitated with anti-GFP antibodies from seedlings grown exclusively in darkness or continuous R or FR light were probed with anti-GFP (left) and anti-NEDD8 (right) antibodies. The WT lane contains immunoprecipitated proteins from the *Col-0* ecotype and was used as a negative control.

Samples were investigated via Western blotting, with the purified *AtLRB2* eluates each being probed with anti-GFP and anti-*HsNEDD8* antibodies in two separate blots in an attempt to detect any NEDD8 conjugated to the LRBs (**Figure 32**). Despite the noticeable absence of any shift in molecular weight on the LRBs when using the NEDD8 inhibitor MLN4924, the anti-NEDD8 antibody was able to detect the presence of NEDD8 on the purified GFP-LRB2 samples in all three light conditions (**Figure 32**).

Quantification values were obtained for each light treatment by using the Odyssey FC Image Studio Lite 5.0 program<sup>82</sup> (**Supplemental Figure 11A-B**). Quantification values for each treatment were normalized to the lane containing the wild-type *Col-0* ecotype in each blot to address any differences in the exposure times of the two blots. The normalized quantification values for each light treatment could be compared between blots, but the quantification values could not be compared between light conditions, as the far-red GFP immunoprecipitation yielded significantly less GFP-LRB2 than the

immunoprecipitations performed on the red or dark treatment groups (**Supplemental Figure 11B**). The ratio of  $\alpha$ NEDD8 to  $\alpha$ GFP (and vice-versa) can provide an estimate of the distribution of NEDD8 that is found between each light condition.

The normalized GFP probe signal intensity was determined to be 1.41 times stronger than the signal intensity found when probing for NEDD8 in plants grown in red light, and 1.08 times more intense with seedlings grown in far-red light. Interestingly, the signal intensity for GFP was found to be 0.77x as intense as NEDD8 signaling in dark-grown seedlings (**Supplemental Figure 11C**). The dark-grown seedlings were found to have a  $\alpha$ GFP: $\alpha$ NEDD8 ratio that was less intense than in the other two treatment groups, which could signify that NEDD8 conjugation occurs mainly in darkness. However, the experiment must be performed again before the ratios could be considered significant.

## V. CONCLUSIONS

The two highly-conserved Light-Response BTB proteins are quickly becoming known as key members of the red light signaling pathway in *Arabidopsis thaliana*<sup>2,16</sup>. This project used a two-pronged approach to show that the amino-terminal portion of the LRBs are highly conserved in at least two regions in all land plants, and these conserved regions may play a role in LRB neddylation.

### TWO AMINO-TERMINAL REGIONS FOUND TO BE CONSERVED IN ALL LRB PROTEIN HOMOLOGS

A multiple sequence alignment of homologous LRB proteins taken from various land plant species revealed two amino-terminal regions that were highly conserved across all land plant species. Amino-terminal conservation was not unexpected, as a recent paper established that the amino-terminal portion of *AtLRB1/2* interacts with a coiled-coil scaffold protein FRIGIDA (FRI)<sup>47</sup>. FRI is normally responsible for recruiting several chromatin modifiers that modify several flowering genes after vernalization to initiate flowering, but this was found to not be the case in the Columbia (**Col-0**) ecotype of *Arabidopsis thaliana*, which has an early-flowering phenotype due to a carboxy-terminal deletion allele at the *FRIGIDA* locus<sup>47</sup>. As the established *lrb12* mutant phenotypes were observed in *Col-0 Arabidopsis* ecotypes, the degradation of FRI cannot be responsible for the hypersensitivity to red light<sup>2</sup>, implying that the LRBs have multiple roles in distinct signaling pathways.

If the amino-terminal portion of LRB interacted solely with FRI, we would not expect to see the two regions of conservation in the LRB proteins from monocots and non-flowering plant species, as the proteins that make up the FRI signaling pathway are only found in eudicots<sup>50</sup>. Transgenic *Arabidopsis* plants containing a truncated version of *AtLRB2* could be used to further support the hypothesis that the conserved amino-terminal LRB regions are important for LRB function. Just observing the phenotype expressed by plants containing the truncated amino-terminal (residues 1-140) or carboxy-terminal (residues 140-561) *AtLRB2* protein transgene could provide valuable insight into the role that the amino-terminal portion plays in light signaling.

#### **CONSERVED AMINO-TERMINAL LRB REGIONS SHOW SEQUENCE SIMILARITY TO OTHER CRL PROTEIN MEMBERS**

To narrow down the potential mechanisms that could be utilized to regulate the LRB proteins in different light conditions, both of the conserved amino-terminal regions were used as queries to search for other proteins that share a similar sequence. The two conserved regions of LRB were found to be similar to regions on Cul1 and Rbx1 proteins, and this similarity between sequences was conserved across all land plants. By using CRL complex crystal structures, we determined that the distribution of the Cul<sup>CL</sup> and Rbx<sup>LL</sup> regions on their respective CRL proteins were in close proximity to one another, and the Rbx<sup>LL</sup> region directly interacts with NEDD8. The Cul<sup>CL</sup> region was also located in close proximity to the NEDD8 conjugation site on *AtCul1*, and this prompted our later investigation of NEDD8 conjugation on the *AtLRBs*.

To determine the functional role of the amino-terminal portion of the LRBs, a carboxy-terminal *AtLRB2* (residues 140-561) transgene could be placed in the *lrb12* double knockout seed lines. The phenotype observed in red light would provide insight into the role that the amino-terminal LRB region plays in phyB accumulation/degradation. The amount of Cul3 interaction that occurs in the carboxy-terminal *AtLRB2* mutant could also be investigated, as a significant decrease in Cul3-LRB interaction would implicate the amino-terminal region as being responsible for Cul3-LRB interaction.

### **LRB HOMOLOGY MODELS REPRESENT THE OVERALL FOLD OF THE BTB/3BOX/BACK DOMAINS**

Homology models were created by Phyre2<sup>65</sup> to serve as representations of the overall structure of the *AtLRB* proteins (**Figure 22**). While *AtLRB2A* was predicted to be the more comprehensive model, a majority of the overall structural features (exposure of certain residues to solvent, secondary and tertiary structure) in *AtLRB2A* were consistent with both *AtLRB1* and *AtLRB2B*. A comparison of the *AtLRB2A* predicted BTB/3BOX/BACK domain structure with the known crystal structure for 4AP2<sup>35</sup> revealed that the overall fold of the protein in these domains was usable (**Supplemental Figure 9**). The LRB homology models were used as representations of the overall structure of the *AtLRB* proteins, despite multiple caveats regarding template alignments and low sequence identity during the creation of each model.

The overall shape and sidechain arrangement of the CL region was found in both the predicted *AtLRB2* model and in the Cul<sup>CL</sup> region of the 1LDK crystal structure<sup>26</sup>



(**Figure 24**). If the predicted *AtLRB2* homology model structures are found to be accurate, the similarities between the CL region of *AtLRB2* and the Cul<sup>CL</sup> region of Cull1 could signify a conservation of function between the two proteins in this region. Cullin was not chosen as a template for the *AtLRB2A* homology model, yet there was found to be a convergent arrangement of residues in this region (**Figure 24**). This observation strengthens our hypothesis that there is some parallel in function or identity between the LRBs and Cullins in the CL motif.

Beyond the BTB/3BOX/BACK domains, we were able to observe structural features on each of the homology models. One of the prominent features observed on the *AtLRB2A* homology model was an amino-terminal ‘bridge’ (residues 108-138) structure (**Figure 23A**), and the bridge seemed to be conserved on the *AtLRB1* and *AtLRB2B* homology models as well (**Figure 23B-C**). A carboxy-terminal ‘claw’ structure was also found on each of the models and was predicted to be the site of target recognition<sup>34,35,40</sup> (**Figure 23A-C**).

The *AtLRB2A* ‘bridge’ gave rise to many ideas about the possible function of the amino-terminal LRB region. Residues 20 to 128 of *AtLRB2A* were modeled after the MATH domain, a subset of TRAF-like domains, of one PDB structure (PDB ID: **3HU6**)<sup>42</sup>. MATH domains are known to be flexibly tethered to the BTB domain, suggesting that if the model for the *AtLRBs* is correct, the amino-terminal region may be equivalent to MATH domains and the possibly flexible “loop” or “tether” structure could be used to control the orientation and placement of the amino-terminal *AtLRB* region<sup>42</sup> (**Figure 33A**). If this ‘loop’ is indeed responsible for amino-terminal orientation, a light-dependent modification on or near the loop could result in a change in the orientation of

the amino-terminal region and could be responsible for the red-light-dependent interaction with Cul3 (**Figure 33B**)<sup>2,16</sup>. However, there is currently no evidence to support this theory outside from the predicted structures created using Phyre2<sup>65</sup>.

Two hypotheses were created to explain the potential placement of the amino-terminal domain when no red light is present that would essentially inactivate the LRBs. As Cul3 is known to only interact with the LRBs after exposure to red light<sup>2</sup>, and the 3-Box on the LRBs are responsible for high-affinity Cul3 binding<sup>35</sup>, it was predicted that the amino-terminal LRB structure could be physically blocking Cul3 from interacting with the 3-Box on the LRBs. The two ways that this physical 3-Box blocking phenomenon was predicted to occur was through changing the overall shape of the LRBs through target recognition site promiscuity (**Figure 33C**) or through a direct interaction of the amino-terminal LRB domain with the 3-Box area (**Figure 33D**).

The amino-terminal region of the LRBs could be targeted by the carboxy-terminal recognition region through binding site promiscuity. If the carboxy-terminal “claw” responsible for target recognition were to bind the amino-terminal portion of LRB, the entire shape of the protein may be altered, and this conformational change could block access to the 3-Box (**Figure 33C**).

A more simple method of blocking the 3-Box from access, however, could simply be that the amino-terminal region of LRB is oriented in such a way that it creates a physical barrier that prevents Cul3 from interacting with the 3-Box (**Figure 33D**). A direct physical barrier would also leave the carboxy-terminal “claw” region free to bind to any target proteins, and binding the target may ultimately be the modification that is

needed for the LRBs to reorient the amino-terminal domain and allow Cul3 to bind the 3-Box.

The distribution of the LL and CL regions on the amino-terminal portion of *AtLRB2* should be investigated further, but the crystal structure of *AtLRB2* would first need to be determined. *AtLRB* homology models were created to provide a three-dimensional view of the *AtLRBs*, but the predicted structures contained large caveats and may not be accurate. By crystalizing the *AtLRBs*, the native distribution of the CL and LL regions could then be identified in the native structure and compared to the native distribution of Cul<sup>CL</sup> and Rbx<sup>LL</sup>, removing all of the caveats associated with the predicted homology models of the *AtLRBs*.

If the distributions of the Cul<sup>CL</sup> and Rbx<sup>LL</sup> regions were found to be identical or similar to the native placement of the CL and LL regions on the *AtLRB* crystal structure, then we could start to hypothesize that the CL and LL regions are ‘mimicking’ the structure of Cul1/2 in complex with Rbx1. However, further investigation would be needed to determine if the mimicking caused by the CL/LL region interacts with proteins in the same way the Rbx1/Cul1/2 complex does.

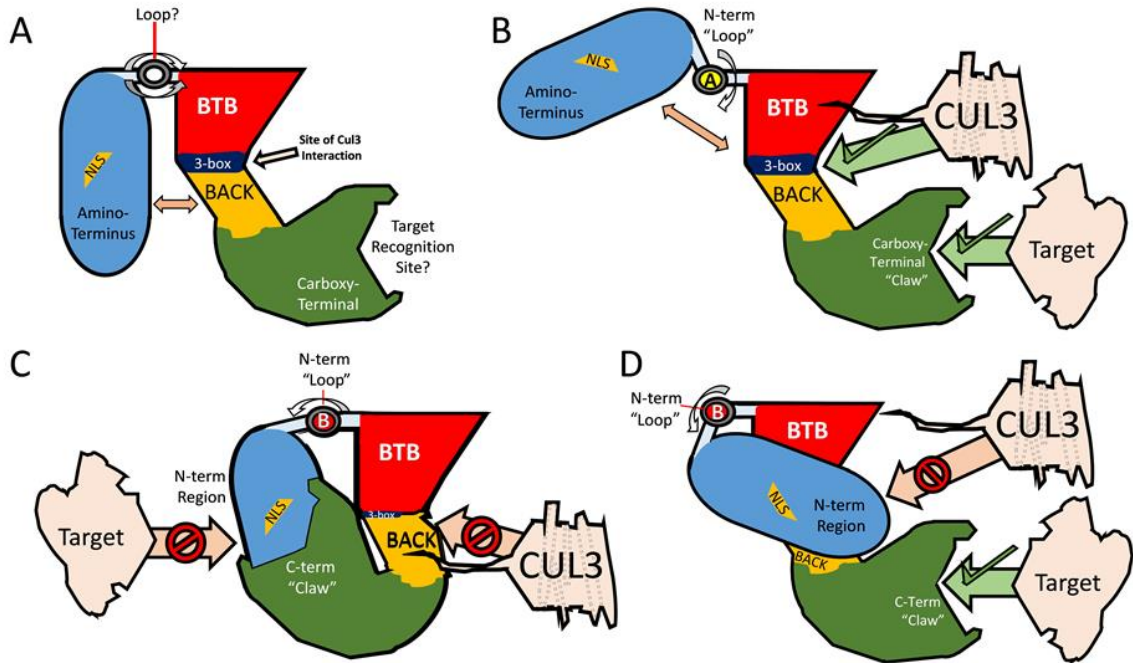


**Figure 33:** Potential Mechanisms for Blocking Cul3 Binding

**A.** A predictive model showing the overall structural characteristics of the LRBs, with specific emphasis on *AtLRB2A*, that were determined using the structural prediction models created by Phyre2<sup>65</sup>. Notable features included an independently-folded amino-terminal domain, an amino-terminal ‘loop’ (or ‘bridge’), the 3-Box region, and a carboxy-terminal ‘claw’ structure, which may be the site of target recognition.

**B.** A predictive model showing the possible movement of the amino-terminal region by activation of the loop. When activated (A), the loop could be used to control the orientation and placement of the amino-terminal LRB structure, allowing Cul3 to bind to the 3-Box or allowing the carboxy-terminal claw to interact with the target.

**C.** This predictive model shows binding site promiscuity at the carboxy-terminus of the LRBs, which could result in the amino-terminal domain being targeted by the carboxy-terminal ‘claw’, in turn preventing the target from binding to the target recognition site. Additionally, when the LRBs interact in this manner, the protein could adopt a different conformation, blocking access to the 3-Box and preventing Cul3 from interacting. In this model, the amino-terminal loop region is blocked (B) from moving the amino-terminal domain and breaking the carboxy-terminal LRB binding site promiscuity.

**D.** A second model depicting the amino-terminal region of the LRBs directly blocking (B) the 3-Box from interacting with Cul3. In this model, the amino-terminal loop would orient the amino-terminal LRB domain so that it would block the 3-Box. Upon activation of the loop, the orientation of the amino-terminal domain would be altered, allowing for Cul3 interaction with the 3-Box. This scenario depicts the carboxy-terminal claw as open, as the binding of the target to the target recognition site might be the activation needed to reorient the amino-terminal LRB region away from the 3-Box.

## **NEDD8 MAY HAVE A ROLE IN THE FUNCTION OR REGULATION OF THE LRB PROTEINS**

The conjugation of NEDD8 to the LRBs was hypothesized after investigating the two conserved amino-terminal LRB regions and the similarities they shared with Cullin and Rbx1. The Cul<sup>CL</sup> region was found to be located directly upstream from the site of NEDD8 conjugation on Cullin, while the Rbx<sup>LL</sup> region was found to directly interact with NEDD8, and this led to the hypothesis that the amino-terminal region of LRB may also be neddylated.

The small-molecule NEDD8-inhibitor MLN4924, which binds to ECR1 and blocks the NEDD8 conjugation pathway, was used to indirectly test the *At*LRBs for NEDD8 conjugation. Treatment of MLN4924 gave inconclusive results when investigated using immunoblotting, as no band shift was observed. However, we know that the MLN4924 treatment was effective from the distinct phenotype which was observed in the seedlings treated with MLN4924. Exposure to the NEDD8-inhibitor resulted in decreased hypocotyl expansion, stunted root growth, and, at higher concentrations, prevented germination from occurring altogether.

An overall accumulation of GFP-LRB proteins in MLN4924-treated dark-grown seedlings could be detected, but the lack of an adequate control line provides reasonable doubt to the validity of this observation. The accumulation of GFP-LRB proteins in the presence of MLN4924 would be expected, however, because it has been previously shown that the *At*LRBs are degraded via the UPS<sup>2</sup>, which relies on Cul3-NEDD8 conjugation to form the active CRL E3 complex required for ubiquitination and subsequent protein degradation<sup>44</sup>.

It is also known that some E3 proteins that are conjugated with NEDD8 are also able to conjugate with ubiquitin interchangeably. **Mdm2** is able to autoubiquitinate and autoneedylate itself<sup>45</sup>, and it has been shown to conjugate with NEDD8 and ubiquitin interchangeably<sup>46</sup>. By doing so, Mdm2 promotes either the neddylation or ubiquitination of p53<sup>45,46</sup>. The same may be true for the *At*LRBs, as the lack of band shift in the seedlings treated with MLN4924 could be due to the same number of ubiquitin and NEDD8 proteins being conjugated to the *At*LRBs, as both proteins are approximately the same size.

For a more direct approach, enriched GFP-tagged *At*LRB2 proteins were probed with anti-NEDD8 antibodies. NEDD8 was detected in the purified GFP-LRB2 samples, suggesting that the LRBs are neddylated. A second immunoprecipitation will need to be done in order to show reproducibility in these results, as well as provide further evidence that the quantification values and signal intensity ratios in each light treatment are significant. Also, detecting the presence of GFP-tagged *At*LRB1/2 after performing an anti-NEDD8 immunoprecipitation prepared using the same method of boiling samples prior to immunoprecipitation would provide undeniable *in vivo* evidence that the LRBs are neddylated.

Despite the lack of immunoprecipitated proteins appearing in the far-red GFP-LRB2 samples, the ratio of GFP signal intensity to NEDD8 signal intensity within each individual light treatment sample was calculated and compared. However, the experiment will need to be performed multiple times before the ratio can be considered viable. The diminishing signal intensity ratio of  $\alpha$ GFP: $\alpha$ NEDD8 when comparing the quantification values of red, far-red, and dark-grown seedlings respectively suggests that NEDD8 conjugation may be primarily found in darkness (**Figure 34A**) as a means to control LRB

function (**Figure 34B**). The removal of NEDD8 from the LRBs in a light-dependent manner (**Figure 34C**) could be the modification that allows the LRBs to interact with Cul3 (**Figure 34D**), as protein neddylation has been found to inhibit protein-protein interactions, decrease protein stability, and even antagonize ubiquitination<sup>44-46,83</sup>.

The theory behind using the signal intensity ratio of  $\alpha$ GFP: $\alpha$ NEDD8 to determine the amount of NEDD8 conjugation occurring in one light condition compared to another could be modified by using MLN4924. After transgenic GFP-LRB2 seedlings are treated with MLN4924 and exposed to a specific set of light conditions, immunoblotting could be used to detect both NEDD8 and GFP. If a decrease in  $\alpha$ NEDD8 signal intensity is discovered after MLN4924 treatment for each light condition, we could be fairly certain that neddylation of the LRBs is occurring via the NEDD8 conjugation cascade (**Figure 6**), as MLN4924 blocks NEDD8 from reaching the first step of the conjugation cascade.

Additionally, before the *At*LRBs can be confirmed as authentic targets of NEDD8 conjugation, the lysine (or lysines) that serve as the site of attachment on the *At*LRBs must first be identified using mutagenesis or by mass spectrometric analysis<sup>45,83</sup>. Also, the criteria currently published for determining the authenticity of NEDD8 protein targets state that NEDD8 conjugation must be found to occur *in planta* and must rely on the specific neddylation enzymes and/or deneddylases *in vivo*<sup>45,83</sup> (**Figure 34A, 34C**). If NEDD8-conjugation is confirmed to be present on the *At*LRBs, this would be a very big discovery, as few neddylated proteins have been discovered in plants. Also, the conjugation of NEDD8 to the *At*LRBs may provide a very clear pathway for studying the LRBs, as they could be investigated using the same approach as the E3 proteins that have been identified in humans.

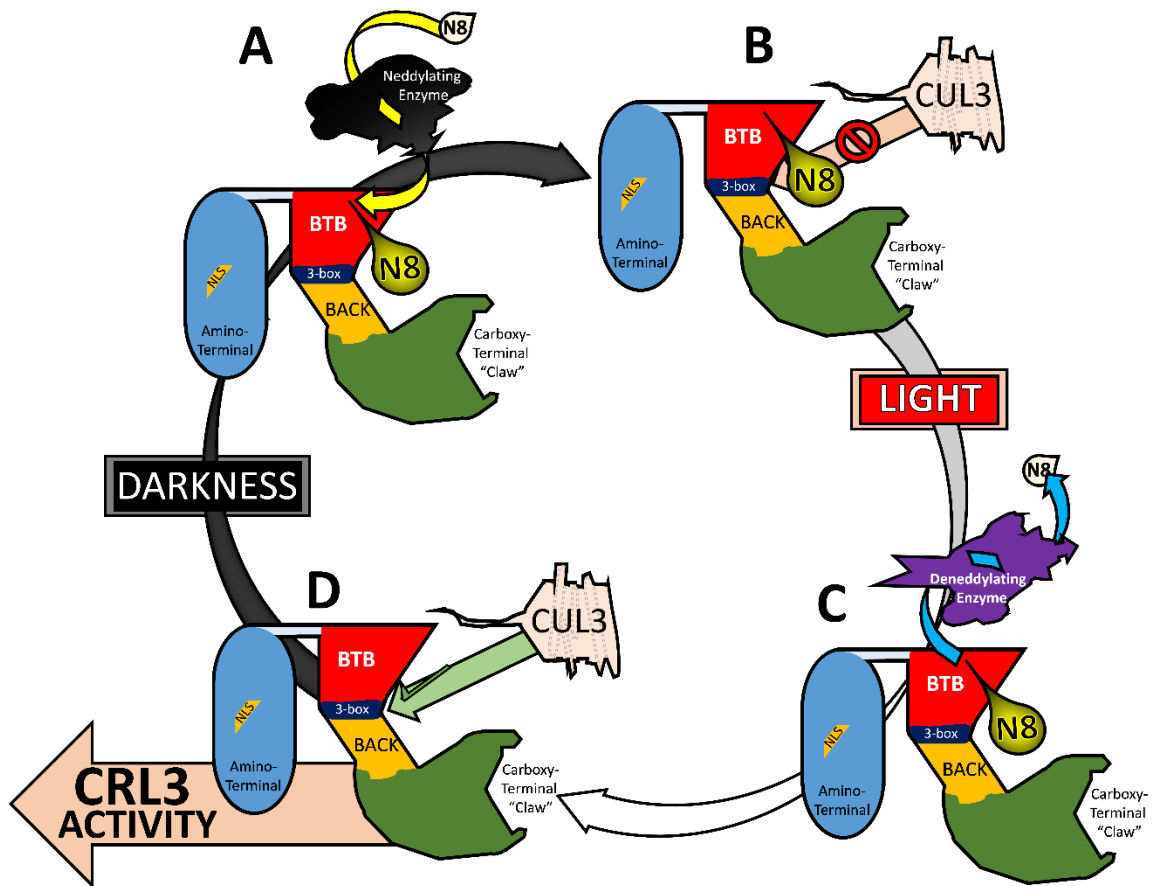


**Figure 34:** Proposed Mechanism of *AtLRB* Neddylation

**A.** NEDD8 conjugation to the LRB proteins by a NEDD8 ligase enzyme is thought to primarily be found in darkness.

**B.** The conjugation of NEDD8 to the LRBs blocks Cul3 from interacting with the 3-Box region and prevents CRL3 formation. In addition to inhibiting Cul3 interaction, neddylation may cause the LRBs to become flexible, allowing them to interact with other proteins (*not shown*).

**C.** The removal of NEDD8 from the LRBs occurs after exposure to R or FR light. In a light-dependent manner, a deneddylating enzyme would remove NEDD8, allowing proteins to access the 3-Box region once again.

**D.** Once NEDD8 is removed, the LRBs are free to interact with Cul3 and can once again form active CRL3 complexes.



It is currently unknown whether NEDD8 conjugation is responsible for the red-light dependent activation of the *At*LRBs, nor is it known if NEDD8 plays an inhibitory role in *At*LRB function. Further investigation will need to be performed in order to discern the role that the neddylation of *At*LRB proteins plays in a plant's ability to sense light and respond to it.

### ***At*LRB PHOSPHORYLATION COULD NOT BE DETECTED DESPITE IN SILICO PHOSPHORYLATION SITE PREDICTIONS**

The LRB proteins are thought to undergo distinct changes after exposure to red light. The increased interaction between LRB and Cul3 after red light irradiation demonstrates how the LRBs change in response to light. This change may be a result of the LRBs interacting with phyB<sup>Pfr</sup> or PIF, or could be due to some other modification brought about by red light irradiation. One of the possibilities is phosphorylation, as phosphorylation has already been found to play a large role in many light signaling pathways.

*In silico* phosphorylation site prediction data, in combination with the LRB multiple sequence alignment, suggested that there could be three possible phosphorylation sites on *At*LRB2. A phospho-shift assay performed using a bacterial  $\lambda$ -protein phosphatase showed no conclusive results, but this does not necessarily mean there is no phosphorylation present, as some proteins simply do not show a phosphorylation shift<sup>81</sup>. Also, phosphorylation is removed from proteins at different rates by the  $\lambda$ -protein phosphatase, so a 15 minute treatment may not have been adequate for dephosphorylation of the GFP-tagged *At*LRB1 protein.

Despite a lack of band shift after exposure to the  $\lambda$ -protein phosphatase, there was a noticeable difference in band strength between the phospho-shift samples that were grown in red and far-red light conditions, but this could be due to the difference in growth time between the two groups. Half of the seedlings were grown in red light and collected after four days of irradiation, while the second half were grown for four days in red and then exposed to far-red light for an additional two days. Future experiments should be designed so that the seedlings are collected at the same timepoint, regardless of light conditions.

A more direct approach was devised to specifically detect any phosphoserine residues that could be present on the *AtLRB* proteins. No phosphoserine residues were detected when probing enriched *AtLRB2* with anti-phosphoserine antibodies, but this could be due to a number of different factors. A human phosphoserine immunogen was used to create the phosphoserine antibody that was used, so it is possible that the human anti-phosphoserine antibody is not able to detect phosphoserine residues in *Arabidopsis thaliana*. Without a positive phosphoserine control, we cannot be certain that the antibody can detect phosphoserine-specific phosphorylated residues in plants. Phosphorylation present in the *YTFT* sequence (*Y513*, *T514*, and *T516* in *AtLRB2*), which was predicted in the *in silico* analysis of the *AtLRBs* using PhosPhAt 4.0 prediction software, would not be identifiable when probing for phosphoserine. Probing purified *AtLRB2* with anti-tyrosine or anti-threonine antibodies could implicate the *YTFT* sequence as the site of phosphorylation.

The proximity of the *YTFT* sequence to the predicted carboxy-terminal “claw” could suggest that any phosphorylation found in that particular area would relate to target

recognition, but could also be the result of the Serine/Threonine kinase activity that has been found previously in eukaryotic phytochromes<sup>14</sup>. The creation of phospho-mimic ( $Y/T \rightarrow D$ ) or phospho-null ( $Y/T \rightarrow F/A$ ) mutations at each residue in the *YTFT* sequence would need to be performed in order to confirm that the *YTFT* sequence is the site of phosphorylation. Also, any phenotypic changes witnessed in the phospho-mutant lines would give valuable insight into the modification on the LRBs that may regulate the red light signaling pathway.

With a lack of *in vivo* evidence to support or definitively reject phosphorylation as a modification present on the *AtLRB* proteins using the phospho-shift assay or by immunoblot analysis of purified LRB2 proteins using a phosphoserine antibody, no overall conclusion could be drawn about the phosphorylation state of the *AtLRBs*.

#### **THE INTERACTION BETWEEN LRB1 AND HISTONE-LYSINE N-METHYLTRANSFERASE EZA1 SHOULD BE INVESTIGATED FURTHER**

Ubiquitin plays a large role in transcriptional regulation<sup>19</sup>. The ubiquitination of histone proteins can have inhibitory effects on transcription, such as preventing elongation of a transcript from occurring, preventing RNA polymerase from reaching promoters, recruiting repressive factors, or blocking histone-methyltransferases from initiating transcription by methylating histones<sup>19</sup>. However, ubiquitination on a different histone protein can provide a binding site for histone-methyltransferases, prevent DNA compaction, provide access to promoter regions for RNA polymerase through steric hindrance, or repress the expression of pro-oncogenes<sup>19</sup>. Additionally, E3 ligase

complexes can directly target transcription factors bound to DNA, RNA-binding proteins, or histone-methyltransferases for degradation via the 26S proteasome<sup>19,22</sup>.

The *At*LRBs are able to interact with the coiled-coil domain of the transcriptional activator protein FRI<sup>47</sup>, as well as the basic Helix-Loop-Helix transcription factor protein PIF3<sup>16</sup>. Previous unpublished experimentation performed by Dr. Christians revealed that *At*LRB1 is able to interact with histone-lysine N-methyltransferase EZA1 (also known as SWINGER (**SWN**), CURLY LEAF-LIKE 1, or SET DOMAIN GROUP 10 (**SET10**)). EZA1 helps to control Flowering Locus C (**FLC**) expression during and after vernalization<sup>84</sup>. While FRI is responsible for increasing FLC transcript levels and suppressing flowering until after vernalization<sup>53</sup>, EZA1 down-regulates FLC expression after prolonged exposure to the cold<sup>84</sup>, working against FRI and FLC to allow flowering to occur. Further investigation into the interactions between EZA1 and the LRBs could help to unlock the complex and growing role that the LRBs play in regulating vernalization in addition to red light response in *Arabidopsis*.

## VI. MATERIALS & METHODS

### Protein BLAST, LRB Sequence Alignments, and Phylogenetic Analysis

The UniProtKB BLAST program<sup>54</sup> was used to identify homologous LRB proteins. The entry for LRB2 in *Arabidopsis thaliana* (**UniProtKB AC: Q9FPW6**) was used to probe the UniProtKB Plant database for proteins containing regions of local sequence similarity. Using a BLOSUM62 matrix, an expectation value threshold of 10, and filtering for low complexity regions, the BLAST presented 641 proteins that shared local sequence similarity with the LRBs ranging from 99% to 27%. Closely-related LRB homologs were chosen based on overall sequence conservation and lack of gaps in the alignment, while the homologous proteins in some additional plant species were chosen due to genetic variation.

A multiple sequence alignment was created with homologous LRB protein sequences from *Arabidopsis thaliana* (ARATH), *Arabidopsis lyrata* (ARALL), *Brassica pekinensis* (BRARP), *Citrus clementina* (CICLE), *Populus trichocarpa* (POPTR), *Prunus persica* (PRUPE), *Ricinus communis* (RICCO), *Capsella rubella* (CARUB), *Glycine max* (GLYMA), *Oryza sativa subsp. japonica* (ORYSJ), *Zea mays* (MAIZE), *Picea sitchensis* (PICSI), *Physcomitrella patens* (PHYPA), and *Selaginella moellendorffii* (SELML) using the default settings of the multiple sequence alignment tool Expresso<sup>56</sup>.

Phylogenetic analysis was performed on the same homologous LRB sequences using the One Click phylogeny analysis tool at Phylogeny.fr<sup>58</sup>, which is designed to perform robust phylogenetic analysis for non-specialists<sup>58</sup>.

## Refining the Homologous LRB Multiple Sequence Alignment

The MSA of homologous LRB proteins was refined by removing protein sequences that deviated substantially from *AtLRB2*. *LRBC\_BRARP* was removed for containing large gaps in the total protein sequence. The pseudogenes *LRB3\_ARATH*, *LRBC\_ARALL*, and *LRBC\_CARUB* were removed, as they contained multiple deviations from the other LRB sequence. *LRBB\_RICCO* was removed for containing a large insertion in the carboxy-terminal portion of its protein sequence. The bryophytes (*LRB\_PHYPA*) and lycophytes (*LRB\_SELML*) were removed, as the amino-terminal LRB sequences for these proteins contained very little conservation at the LL region. Diverging LRB proteins, as determined by phylogenetic analysis, were also removed, but only when more than one copy of the LRBs were found in an organism, resulting in the removal of *LRBA\_GLYMA*, *LRBC\_CICLE*, *LRBB\_PRUPE*, *LRBC\_POPTR*, *LRBD\_POPTR*, *LRBB\_BRARP*, *LRBB\_RICCO*, *LRBB\_ORYSJ*, *LRBC\_MAIZE*, *LRBE\_MAIZE*, *LRBD\_MAIZE*, and *LRBF\_MAIZE*. Finally, *LRBB\_CICLE* was removed, as it was found to be an identical copy of *LRBA\_CICLE*.

## Alignment of the CL and LL Sequences with Cul<sup>CL</sup> and Rbx<sup>LL</sup> Sequences

The alignment of Cul1 and Cul2 proteins with the CL motif sequence of each of the *AtLRB* proteins (amino acids 34-61 of *AtLRB2*) was found using a BLOSUM90 matrix of the **EMBOSS** pairwise sequence alignment tool **Matcher**<sup>85,86</sup>. Additionally, homologous Cul1 and Cul2 were found using a UniProtKB protein BLAST<sup>54</sup> search of *AtCul1* and *AtCul2*, pulling out any full-length Cullin proteins that were found in the other 13 plant species that were used. An alignment of these Cullin sequences was

performed using the default settings of the MSA tool Expresso<sup>56</sup> was used to determine the overall alignment of Cullin at the area associated with the CL region of the LRBs, and this short region was then aligned with the shortened CL region using default Expresso<sup>56</sup> settings. Each of the alignments were also visualized using the program **MEME SUITE**<sup>61</sup>.

Similarly, an alignment of RING-box 1 (**Rbx1**) proteins in *Arabidopsis thaliana* with the Linker-Like sequence of LRB proteins (amino acids 62-89 of *AtLRB2*) was found using a BLOSUM90 matrix of the pairwise sequence alignment tool **Matcher**<sup>85,86</sup>. Homologous Rbx1 proteins were found using a UniProtKB protein BLAST<sup>54</sup> search of *AtRbx1*, and any full-length Rbx1 proteins that were found in the other 13 plant species that were used. The homologous Rbx1 proteins were aligned using the multiple sequence alignment tool Expresso<sup>56</sup>. The short region with similarity to the LL region was then aligned with the actual LL region of the LRBs using default Expresso settings. Both of the multiple sequence alignments were visualized using the program MEME SUITE<sup>61</sup>.

### **Structural Prediction of the LRB Proteins in *Arabidopsis***

Phyre2<sup>65</sup> predictive protein modeling software was used to create each model of the LRB proteins. The models were created using the intensive setting, allowing the use of multiple templates to be used to cover the full protein sequence length. The *AtLRB2* models produced was determined to be more reliable, as the models for *AtLRB1* and *AtLRB3* had a smaller amount of homologous template coverage. A QMEAN structural analysis was also used to assess the quality of the two *AtLRB2* protein models, with *AtLRB2A* being chosen as the more reliable model between the two. All structures were

displayed using POLYVIEW-3D<sup>76</sup>, a free online protein structure rendering program, or by using the VMD program<sup>41</sup>.

### **Modeling the Conservation of LRB Sequence**

Sequence conservation of full-length LRB2 was projected onto the predicted model *AtLRB2A* using the ConSurf<sup>77</sup> program (<http://consurf.tau.ac.il/>). ConSurf was able to determine conservation by building a MSA from 3 iterations of CSI-BLAST with a 0.0001 E-value cutoff using the UniProt protein database. Homologs collected contained sequence identity between 98% and 45%, and these sequences were aligned using Expresso. The calculation method used for the rate of evolution at each site in the MSA was the Bayesian method, with the default JTT model used as the evolutionary substitution model.

To determine conservation of the region amino-terminal to the BTB domain (residues 1-144), the PDB file for *AtLRB2A* was modified to include only the amino-terminal domain. ConSurf was then used to build a MSA from 3 iterations of CSI-BLAST searches with a 0.0001 E-value cutoff using the UniProt protein database. Homologs collected contained sequence identity between 98% and 35%, and these sequences were aligned using Expresso. The calculation method used for the rate of evolution at each site in the MSA was the Bayesian method, with the default JTT model used as the evolutionary substitution model.



## Displaying the Cul<sup>CL</sup> and Rbx<sup>LL</sup> Regions on Crystallized CRL Complexes

The multiple sequence alignments that were created used *AtCul1* (UniProtKB AC: **Q94AH6-1**), *HsCul1* (UniProtKB AC: **Q13616-1**) and *HsCul4A* (UniProtKB AC: **Q13619-1**) for the Cullin alignments, and *AtRbx1A* (UniProtKB AC: **Q940X7-1**) with *HsRbx1* (UniProtKB AC: **P62877-1**) to align Rbx1. The full sequence for each of these proteins can be found using the UniProtKB ACC numbers given in parenthesis. Default Expresso<sup>56</sup> settings were used to create both alignments. The three PDB structures that were used were **1LDK**<sup>26</sup>, **4P5O**<sup>29</sup>, and **2HYE**<sup>30</sup>. Modeller<sup>87</sup> was used to create a homology model of *HsCul1* and *HsRbx1* for the PDB structure 4P5O, as the original PDB structure contained multiple gaps in vital portions of both structures. By creating two homology models that could be aligned with the original structure, 4P5O was able to be used to model the Cul<sup>CL</sup> and Rbx<sup>LL</sup> regions after neddylation had occurred. The updated structures were then aligned to 4P5O using the **MultiSeq**<sup>88</sup> option on VMD<sup>41</sup>. VMD was also used to visualize the other two structures.

## Determining Phosphorylation Sites Using *In Silico* Analysis

The Arabidopsis Protein Phosphorylation Site Database<sup>78,79</sup> software PhosPhAt 4.0 was used to find any known or highly-suggestive phosphorylation motifs present on *AtLRB1* and *AtLRB2*. To achieve this, each of the LRB protein sequences that were used to create the edited MSA previously were individually tested using the PhosPhAt 4.0 software to find any potential regions where phosphorylation could occur. This information was then recorded on the full multiple sequence alignment of the homologous LRB proteins as a means to isolate any overall regions of phosphorylation

conservation. Phosphorylation sites were then modeled using the AtLRB2A structure and visualized using the anaglyphic stereo option on VMD<sup>41</sup>.

### **General Planting and Growth Procedures of *Arabidopsis thaliana* Seedlings**

All *Arabidopsis thaliana* seedlings were surface sterilized using 70% ethanol and 3% bleach. Seeds were grown on plates of Murashige and Skoog Basal Media with Sucrose and Agar (*Sigma, cat# M9274-10L*), pH=5.7, which were covered with a layer of sterile cellophane. Incubation of the plated seedlings occurred at 21.0° C under different light conditions dependent on experimental requirements.

### **General SDS-PAGE Procedure**

SDS-PAGE stacking and resolving gel recipes were obtained using the polyacrylamide gel recipe calculator provided at the Cytographica website (<http://www.cytographica.com/lab/acryl2.html>). Resolving gels were made using 18mΩ water, 40% acrylamide (*BioRad, cat# 161-0146*), 2.0M Tris (pH=8.8), 10% SDS, 10% APS, and TEMED (*Sigma, cas# 110-18-9*). Stacking gels were made using 0.5M Tris (pH=6.8) instead of 2.0M Tris. Isopropanol was used to flatten the resolving gel and allow for complete polymerization. Gels were run on a Mini-PROTEAN Tetra Vertical Electrophoresis Cell (*BioRad, product #1658006FC*) in 1xTris/Glycine/SDS buffer. Current, voltage, and running time varied for each experiment.

## General Western Transfer Procedure

Proteins separated using SDS-PAGE were transferred from a gel onto a membrane to prepare for Western blotting. An Immobilon-FL membrane (*cat# IPFL10100, pore size 0.45um*) was first activated in 100% methanol for two minutes, then placed in 1xPBS for ten minutes. The SDS-PAGE gel was then covered with the Immobilon-FL membrane, sandwiched between two sheets of Whatman paper, and placed into the Mini-PROTEAN Tetra Vertical Western Transfer Cell. Western transfer was performed in 1x Tris/Glycine along with an icepack. Current, voltage, and time varied for each experiment. After transfer, membranes were washed in 1xPBS for 5 minutes, then dried for one hour at 37°C. Before blocking, membranes were reactivated in 100% methanol for one minute, placed in 1xPBS for ten minutes, and then placed in a blocking solution containing 50% Odyssey Blocking Buffer (*Licor, cat #T1753*) and 50% 1xPBS. Blocking took place for one hour with agitation at room temperature.

## $\lambda$ -Phosphatase Treatment and Phospho-Shift Assay

Transgenic *lrb1-1 lrb2-1* plants containing a *GFP-LRB2* transgene<sup>2</sup> were grown in 8 hours of white light, left in darkness for 2 days, exposed to 2 days of red light, then an additional 2 days of far-red light. Wild-type Col-0 control plants were grown in darkness. Seedlings were ground up in protein extraction buffer containing 100mM HEPES-KOH (*RPI, cas# 7365-45-9*), 5% glycerol (*EMD, cas# 56-81-5*), 0.5% PVP (*Acros Organics, cas# 9003-39-8*), 1mM PMSF (*Sigma, cas# 329-98-6*), and 1x Protease Inhibitor Cocktail (*Sigma, P9599-1mL*) adjusted to pH=7.53. Extraction buffer was added at a 1:1 ratio of grams of tissue to milliliters of extraction buffer and spun down for 2 minutes at

10,000RCF at room temperature. Protein extracts were then treated with an  $\lambda$ -phosphatase (*New England BioLabs*, #BO7615), an inhibitor cocktail containing 500mM EDTA ( $pH=8$ ) and 500mM NaF (*Sigma-Aldrich*, cas# 7681-49-4), both the  $\lambda$ -phosphatase and the inhibitor cocktail, or using neither the phosphatase nor the inhibitor cocktail. Treatment lasted for fifteen minutes in a water bath at 30°C before the addition of a phosphatase-stopping cocktail (2.5% SDS, 250mM EDTA, 250mM NaF).

Samples were boiled in 300uL SDS Sample Buffer (26mM Tris, 4.16% Glycerol, 1.66% SDS, 0.02% Bromophenol Blue, 10% $\beta$ ME) for ten minutes before proteins were separated using SDS-PAGE (4% stacking, 8% resolving gels). Proteins were then transferred onto an Immobilon-FL membrane, and subsequent Western blotting utilized rabbit anti-GFP primary antibodies (*Abcam ab290*, 1:4000 dilution) and goat anti-rabbit secondary antibodies (*Licor IRDye800CW*, 1:8000 dilution). Blot was visualized using the 800nm channels on the Odyssey FC machine (*Licor*).

### **MLN4924 Treatment and Immunoblotting**

Seeds were grown for 4 days in darkness as previously described, then the cellophane was transferred to plates containing 8mLs of MS agar ( $pH=5.7$ ) along with either 25.6uL of 15.6mM MLN4924 (*ChemieTek*, cat# CT-M4924) stock solution for a concentration of 50uM MLN4924 or 25.6uLs of DMSO (*Sigma*, cas# 67-68-5). Seedlings treated with the inhibitor for 4 days in either red light or remained in darkness. Seedlings were prepared in a 1:1 ratio of denaturing buffer:tissue, with the denaturing buffer containing 100mM MOPS ( $pH=7.6$ ), 50mM Na Metabisulfite, 2% SDS, 10% glycerol, and 4mM EDTA ( $pH=8$ ). SDS sample buffer was added at a ratio of 0.5mL SDS sample

buffer: 1 gram of tissue before sample was boiled for 10 minutes and ground up using clean pestles. Proteins were separated using SDS-PAGE and transferred onto an Immobilon-FL membrane as previously described. Immunoblotting was performed using rabbit polyclonal antibodies to GFP (*Abcam290, 1:2000 dilution*) and goat anti-rabbit secondary antibodies (*Licor IRDye800CW, 1:5000 dilution*). Blot was visualized using the 800nm channel on the Odyssey FC machine (*Licor*).

### **Immunoprecipitation and Immunoblotting**

Seedlings were grown for 4 days in darkness then exposed to 4 additional days of the specific light treatment (red, far-red, or darkness). Under a green safelight, samples were ground in liquid nitrogen before adding a 1:1 ratio of pre-chilled Non-Denaturing MOPs Buffer containing 100mM MOPs (*pH=7.6*), 50mM NaF (*Sigma-Aldrich, cas# 7681-49-4*), 150mM NaCl, 1% Triton X100, 1mM PMSF (*Sigma, cas# 329-98-6*), Protease Inhibitors (*Sigma, cat# P9599-1mL, added at 50uL inhibitor per 1mL sample*), 10 uM Leupeptin (*Sigma, cat# SLBL7867V*), 0.3uM Aprotinin (*Sigma, cat# SLBJ6925V*), and 15mM Iodoacetimide (*Sigma, cat# SLBJ8175V*). Samples were boiled 10 minutes to denature proteins, then ran through a cheese cloth and centrifuged at 13000 RCF for 10 minutes. Rabbit polyclonal antibody to GFP (*Abcam290, 1:1750 dilution*) was added to the supernatant and the solution was left in the darkroom for two hours with agitation. Solutions were treated with Pierce protein A/G magnetic beads (*Pierce, prod# 88802*) at a rate of 18uL beads per 1mL supernatant and left overnight in darkness at 4°C. Beads were collected using magnetism and washed thrice with non-denaturing MOPs buffer. The beads were boiled for ten minutes in a 100uL solution containing a 66% non-

denaturing MOPs buffer and 33% SDS sample buffer. Proteins were separated using SDS-PAGE with a 10% resolving and 5% stacking gel. Immunoblotting for GFP-LRB2 was performed using rabbit polyclonal antibodies to GFP (*Abcam290, 1:2000 dilution*) and goat anti-rabbit secondary antibodies (*Licor IRDye800CW, 1:5000 dilution*). Immunoblotting for NEDD8 utilized rabbit polyclonal antibodies to NEDD8 (*Abcam Ab139468, 1:1000 dilution*) and goat anti-rabbit secondary antibodies (*Licor IRDye800CW, 1:5000*). Immunoblotting for Phosphoserine residues was performed using mouse anti-phosphoserine antibodies (*BD Biosciences, 1:1000 dilution*) and goat anti-mouse secondary antibodies (*Licor IRDye680LT, 1:5000 dilution*).

### **Quantifying Immunoblot Signaling Intensity**

Quantification values were obtained for each light treatment by using the Odyssey FC Image Studio Lite 5.0 program<sup>82</sup> (**Supplemental Figure 11**). Quantification values for each treatment were normalized to the wild-type lane in each blot to address any differences in the exposure times of the two blots. After normalization, the ratio of normalized band intensities for each light treatment sample was calculated.

## VII. SUPPLEMENTAL INFORMATION

| <u>UniProtKB AC#</u> | <u>LRB Name</u> | <u>UniProtKB AC#</u> | <u>LRB Name</u> |
|----------------------|-----------------|----------------------|-----------------|
| <b>O82343</b>        | LRB1_ARATH      | <b>B9RCL7</b>        | LRBB_RICCO      |
| <b>Q9FPW6-1</b>      | LRB2_ARATH*     | <b>R0FMM2</b>        | LRBA_CARUB      |
| <b>O04615</b>        | LRB3_ARATH      | <b>R0FV79</b>        | LRBB_CARUB      |
| <b>D7LSC0</b>        | LRBA_ARALL      | <b>R0FK01</b>        | LRBC_CARUB      |
| <b>D7LDY0</b>        | LRBB_ARALL      | <b>I1MKP3</b>        | LRBA_GLYMA      |
| <b>D7M4Y3</b>        | LRBC_ARALL      | <b>I1NCH4</b>        | LRBB_GLYMA      |
| <b>M4CGX6</b>        | LRBA_BRARP      | <b>Q5Z9M6</b>        | LRBA_ORYSJ      |
| <b>M4C889</b>        | LRBB_BRARP      | <b>Q6K229</b>        | LRBB_ORYSJ      |
| <b>M4CK17</b>        | LRBC_BRARP      | <b>C0HG55</b>        | LRBA_MAIZE      |
| <b>V4U2A9</b>        | LRBA_CICLE      | <b>B6T8V9</b>        | LRBB_MAIZE      |
| <b>V4U7L7</b>        | LRBB_CICLE      | <b>B4FHV1</b>        | LRBC_MAIZE      |
| <b>V4TS09</b>        | LRBC_CICLE      | <b>K7V570</b>        | LRBD_MAIZE      |
| <b>B9GQF7</b>        | LRBA_POPTR      | <b>B7ZYR2</b>        | LRBE_MAIZE      |
| <b>B9I8T4</b>        | LRBB_POPTR      | <b>C0P6I9</b>        | LRBF_MAIZE      |
| <b>B9GX53</b>        | LRBC_POPTR      | <b>A9NUY5</b>        | LRBA_PICSI      |
| <b>B9GKA4</b>        | LRBD_POPTR      | <b>A9SYT5</b>        | LRBA_PHYPA      |
| <b>M5XM81</b>        | LRBA_PRUPE      | <b>A9S1Y2</b>        | LRBB_PHYPA      |
| <b>M5WCM9</b>        | LRBB_PRUPE      | <b>D8SJ32</b>        | LRBA_SELML      |
| <b>B9RE12</b>        | LRBA_RICCO      | <b>D8QNY9</b>        | LRBB_SELML      |

### Supplemental Figure 1: UniProt Accession Numbers for Homologous LRB Proteins

The UniProtKB Accession number (**UniProtKB AC**) is given in bold on the left side of each column. The right side of the column features the LRB name assigned to each of the LRB protein homologues. The organism's abbreviated name is separated from the assigned LRB name by an underscore, with the abbreviated names listed below. LRB2\_ARATH used the protein sequence for Isoform 1 and is marked with an asterisk.

Species are abbreviated as ARATH (*Arabidopsis thaliana*), ARALL (*Arabidopsis lyrata*), BRARP (*Brassica pekinensis*), CICLE (*Citrus clementina*), POPTR (*Populus trichocarpa*), PRUPE (*Prunus persica*), RICCO (*Ricinus communis*), CARUB (*Capsella rubella*), GLYMA (*Glycine max*), ORYSJ (*Oryza sativa subsp. japonica*), MAIZE (*Zea mays*), PICSI (*Picea sitchensis*), PHYPA (*Physcomitrella patens*), and SELML (*Selaginella moellendorffii*).

```

LRB1_ARATH 1 MR-GS--NNTDLDFPK-T--E-----MDS--NFS--RHG--S-----SSEGD5GFAPNDSNFSDRLRLRIEINGGPS-----SRSD-A-EG
LRB2_ARATH 1 MR-GTENTDLDFPK-T--Q-----MDP--DFH--RHG--S-----SSDGD5GFAPNDSNFSDRLRLRIEINGGPS-----SRSE-V-EG
LRB3_ARATH 1 MR-GTENTDLDFPK-T--Q-----MDL--DFH--RHG--S-----LSSGD5GFAPNDSNFSDRLRLRIEINGGPS-----G--E-VI
LRBA_ARALL 1 MR-GTENTDLDFPK-T--Q-----MDP--DFH--RHG--S-----SSDGD5GFAPNDSNFSDRLRLRIEINGGPS-----SRSD-V-EG
LRBB_ARALL 1 MR-GS--NNTDLDFPK-T--D-----MDS--NFS--RHG--S-----SSEGD5GFAPNDSNFSDRLRLRIEINGGPS-----SRSD-G-EG
LRBC_ARALL 1 MR-GS--NNTDLDFPK-T--D-----MDL--NFS--RHG--S-----LSSGD5GFAPNDSNFSDRLRLRIEINGGPS-----G--D-E-VI
LRBA_BRARP 1 MR-GG-ENTDLDFPK-T--Q-----MDS--DFS--RHG--S-----SSEGD5GFAPNDSNFSDRLRLRIEINGGPS-----SRSD-V-EG
LRBB_BRARP 1 MR-G----SDLDFPK-TSTD-----MDS--ILS--PRD--S-----SPGAD5GFAPNDSNFSDRLRLRIEINGGPS-----SRPD-G-DCC
LRBC_BRARP 1 MR-GSSNDADLDFPK-T--E-----MDS--NFS--RHG--S-----SSS--SSSEGD5GFAPNDSNFSDRLRLRIEINGGPS-----STSDVGECC
LRBA_CICLE 1 MR-DV--NTDLDFPK-T--E-----MDS--DIS--RSA--S-----SSDGD5GFAPNDSNFSDRLRLRIEINGGPS-----SRSD-G-EG
LRBB_CICLE 1 MR-DV--NTDLDFPK-T--E-----MDS--DIS--RSA--S-----SSDGD5GFAPNDSNFSDRLRLRIEINGGPS-----SRSD-G-EG
LRBA_POPTR 1 MRGS--NTDLDFPK-T--E-----MDS--DFS--RGS--S-----ASDGD5GFAPNDSNFSDRLRLRIEINGGSA-----NRAD-G-EG
LRBB_POPTR 1 MRGS--NSDLDFPK-T--E-----MDS--DFS--RGS--S-----ASDGD5GFAPNDSNFSDRLRLRIEINGGSA-----SRAD-G-EG
LRBC_POPTR 1 MR-LP--GADLDFPK-T--E-----MDS--DFS--RGS--S-----ASDGD5GFAPNDSNFSDRLRLRIEINGGSA-----NRAD-G-EG
LRBD_POPTR 1 MR-LP--GADLDFPK-T--E-----MDS--DFS--RGS--S-----ASDGD5GFAPNDSNFSDRLRLRIEINGGSA-----SRAD-G-EG
LRBA_PRUPE 1 MR-KE--LNTDLDFPK-T--L-----MDP--DQS--RDATPSAD--ADADD5GFAPNDSNFSDRLRLRIEINGDTP-----SRPD-S-EG
LRBB_PRUPE 1 MR-KP--NVDLDFPK-T--I-----MDS--DQS--RDATPSAD--ADADD5GFAPNDSNFSDRLRLRIEINGDTP-----SRPD-S-EG
LRBA_RICCO 1 MR-GS--NSDLDFPK-T--E-----MDS--DFS--RGS--S-----ASDGD5GFAPNDSNFSDRLRLRIEINGGSA-----NRAD-G-EG
LRBB_RICCO 1 MR-LP--SVDLDFPK-T--I-----MDS--DFS--RGS--S-----ASDGD5GFAPNDSNFSDRLRLRIEINGGSA-----SRAD-G-EG
LRBA_CARUB 1 MR-GAANDLDFPK-T--I--Q-----MDS--DFS--RHG--S-----SSDGD5GFAPNDSNFSDRLRLRIEINGGPS-----SRSD-V-EG
LRBB_CARUB 1 MR-GS--NNTDLDFPK-T--E-----MDS--DFS--RHG--S-----SSEGD5GFAPNDSNFSDRLRLRIEINGGPS-----SRSD-G-EG
LRBC_CARUB 1 MR-GS--NNTDLDFPK-T--E-----MDS--DFS--RHG--S-----SSEGD5GFAPNDSNFSDRLRLRIEINGGPS-----SRSD-G-EG
LRBA_GLYMA 1 MR-K--DSNSNDLDFPK-T--M--A-----MDS--DFS--RGS--S-----ASDGD5GFAPNDSNFSDRLRLRIEINGGSA-----NRAD-G-EG
LRBB_GLYMA 1 MR-K--DF--NSDLDFPK-T--V-----MDS--DFS--RGS--S-----ASDGD5GFAPNDSNFSDRLRLRIEINGGSA-----NRAD-G-EG
LRBA_ORYSJ 1 MR-GS--EA-AAAQE-A--E-----MDP--DFS--RGS--S-----ASDGD5GFAPNDSNFSDRLRLRIEINGGSA-----NRAD-G-EG
LRBB_ORYSJ 1 MR-GS--EA-AAAQE-A--E-----MDP--DFS--RGS--S-----ASDGD5GFAPNDSNFSDRLRLRIEINGGSA-----NRAD-G-EG
LRBA_MAIZE 1 MR-GS--EA-AAAQE-A--E-----MDP--DFS--RGS--S-----ASDGD5GFAPNDSNFSDRLRLRIEINGGSA-----NRAD-G-EG
LRBB_MAIZE 1 MR-GS--EA-AAAQE-A--E-----MDP--DFS--RGS--S-----ASDGD5GFAPNDSNFSDRLRLRIEINGGSA-----NRAD-G-EG
LRBA_MAIZE 1 MR-GS--EA-AAAQE-A--E-----MDP--DFS--RGS--S-----ASDGD5GFAPNDSNFSDRLRLRIEINGGSA-----NRAD-G-EG
LRBB_MAIZE 1 MR-GS--EA-AAAQE-A--E-----MDP--DFS--RGS--S-----ASDGD5GFAPNDSNFSDRLRLRIEINGGSA-----NRAD-G-EG
LRBA_MAIZE 1 MR-GS--EA-AAAQE-A--E-----MDP--DFS--RGS--S-----ASDGD5GFAPNDSNFSDRLRLRIEINGGSA-----NRAD-G-EG
LRBB_MAIZE 1 MR-GS--EA-AAAQE-A--E-----MDP--DFS--RGS--S-----ASDGD5GFAPNDSNFSDRLRLRIEINGGSA-----NRAD-G-EG
LRBA_PICSI 1 MR-LE--PSE-VQPL-T--AESRNTNRIGGSGGAFMDS--SPYSASA--S-----APPN5GFAPNDSNFSDRLRLRIEINGSGP-----SKSD-G-EG
LRBA_PHYPA 1 MR-LE--PSE-VQPL-T--AESRNTNRIGGSGGAFMDS--SPYSASA--S-----APPN5GFAPNDSNFSDRLRLRIEINGSGP-----SKSD-G-EG
LRBB_PHYPA 1 MR-LE--PSE-VQPL-T--AESRNTNRIGGSGGAFMDS--SPYSASA--S-----APPN5GFAPNDSNFSDRLRLRIEINGSGP-----SKSD-G-EG
LRBA_SEMLL 1 MR-LE--PSE-VQPL-T--AESRNTNRIGGSGGAFMDS--SPYSASA--S-----APPN5GFAPNDSNFSDRLRLRIEINGSGP-----SKSD-G-EG
LRBB_SEMLL 1 MR-LE--PSE-VQPL-T--AESRNTNRIGGSGGAFMDS--SPYSASA--S-----APPN5GFAPNDSNFSDRLRLRIEINGSGP-----SKSD-G-EG

```

```

LRB1_ARATH 63 CSISLDWARRRKRRRE NKK NGV-AISDIV-ACA-----EQQ TDNNQPM DCPGG NLDIE GBAM BEA--LS-----D-D D--ASS PNAAGMC
LRB2_ARATH 64 CSISLDWARRRKRRRE NKK SGV-TISDIV-ACP-----EQQ TD-EQPM DCPGG NLDIE GBAM BEA--LS-----D-D E-ETSS PNAAGMC
LRB3_ARATH 39 CSISLDWARRRKRRRE VNNNSN---NK-----EQQ TD-EQPM DCPGG NLDIE GBAM BEA--LS-----D-D DE-NE -RLTNNN
LRBA_ARALL 64 CSISLDWARRRKRRRE NKK SGGVTISDIV-ACP-----EQQ TD-EQPM DCPGG NLDIE GBAM BEA--LS-----D-D E-ETSS PNAAGMC
LRBB_ARALL 63 CSISLDWARRRKRRRE NKK NGV-AISDIV-ACA-----EQQ TDNNQPM DCPGG NLDIE GBAM BEA--LS-----D-D D--ASS PNAAGMC
LRBC_ARALL 40 CSISLDWARRRKRRRE DMSNKK-----EQQ TD-EQPM DCPGG NLDIE GBAM BEA--LS-----D-D DH-IE -ERVINN
LRBA_BRARP 63 CSISLDWARRRKRRRE NKK SVT--ISDIV-ACP-----EQQ TD-EQPM DCPGG NLDIE GBAM BEA--LS-----D-D E-DTSS PNAAGMC
LRBB_BRARP 64 CSISLDWARRRKRRRE NKK KNNK-----DIV-ACP-----EQQ TDNNRPM DCPGG NLDIE GBAM BEA--LS-----D-D D-DESS PNAAGMC
LRBA_CICLE 70 CSISLDWARRRKRRRE NKK KDNV-TVSDIV-ACP-----EQQ TDNNQPM DCPGG NLDIE GBAM BEA--LS-----D-D D--ASS PNAAGMC
LRBB_CICLE 62 CSISLDWARRRKRRRE NKK NGL--DLS-ACP-----EQQ TD--NQP M DCVGC NQDEE-VBAM BGS--PS-----D-D A-ANGN SSASMC
LRBA_CICLE 62 CSISLDWARRRKRRRE NKK NGL--DLS-ACP-----EQQ TD--NQP M DCVGC NQDEE-VBAM BGS--PS-----D-D A-ANGN SSASMC
LRBC_CICLE 59 CSISLDWARRRKRRRE NKK TVD--VL--VQ-----EQQ QC-NMP T DGVAYNQDEE-PBAM BES--PADVGLNLKQC--E-A TGNI PNASMCL
LRBA_POPTR 63 CSISLDWARRRKRRRE NKK INNVRAGDLS-VGA-----EQQ SGS-IQP M DCVGC NQDEE-ABAM BGS--PS-----D-D A-ADGT SSASMC
LRBB_POPTR 63 CSISLDWARRRKRRRE NKK NNN-----GA-----EQQ SGS-NQP M DCVGC NQDEE-GBAM BGS--PS-----D-D A-GDGN SSASMC
LRBA_PRUPE 62 CSISLDWARRRKRRRE NKK KAV--EIVGQNK-----EQQ NF-NIP T NNVAYNQVE-AVVM BGS--PTDAQLDHQR--D-AA GPSS SSASMC
LRBB_PRUPE 68 CSISLDWARRRKRRRE NKK NIP--DPS-ECP-----EQQ ND-NQP M DCEGC NQDEE-AVAM BES--PS-----D-D A-ANSN SDGSMC
LRBA_RICCO 62 CSISLDWARRRKRRRE NKK NAV--EVS-AGA-----EQQ L--NQP M DCVGC NQDEE-AVAM BEP--PS-----D-D A-VDSN STASMC
LRBB_RICCO 65 CSISLDWARRRKRRRE NKK SAA-A--EVI-GQS-----EQQ SC-NMP T DAVVYNQDEE-PMAM BEP--PTDNQ-----D-D D-ETSS PNAAGMC
LRBA_CARUB 64 CSISLDWARRRKRRRE NKK SGV-TISDIV-ACP-----EQQ TD-EQPM DCPGG NLDIE GBAM BEA--LS-----D-D D-ETSS PNAAGMC
LRBB_CARUB 63 CSISLDWARRRKRRRE NKK NGV-AISDIV-ACA-----EQQ TDNNQPM DCPGG NLDIE GBAM BEA--LS-----D-D D-VSS PNAAGMC
LRBC_CARUB 40 SNTLDLVRKRRRE NSNKH-----EQA-LVIMSOK--PQS-----C-ODENEYSNCGLITNP
LRBA_GLYMA 65 SNTLDLVRKRRRE NKK NGV--DLA-SVP-----EQQ NG-HQS V EC--NQDEE-PBAM BEP--HS-----D-D A-TNSN SDGSMC
LRBB_GLYMA 65 SNTLDLVRKRRRE NKK NVV--DLT-LLP-----EQQ NE-NQP M DFVPS NQDEE-AVAM BEP--PS-----D-D A-ANSN SNAGMC
LRBA_ORYSJ 49 CSISLDWARRRKRRRE NKK KES--GK--YT-----LE-TC--KV A ECDTY ENQE-PVAM BES--PPDIG-----QDG-D-GDCS SSASMC
LRBB_ORYSJ 67 AGSISLDWARRRKRRRE NKK KES--EA--VMP-----Q--NC--KV P ECDAY ENQE-PVAM DS--PPSVG-----PDG-D-GPSM SPGGV
LRBA_MAIZE 49 CSISLDWARRRKRRRE NKK KES--RK--YMP-----PA-NC--KV A ECDAY E-GNE-PVAM BES--PPDIE-----DG-D-GKSS SYCSMC
LRBB_MAIZE 49 CSISLDWARRRKRRRE NKK KES--RK--YMP-----PA-NC--KV A ECDAY E-GNE-PVAM BES--PPDIE-----DG-D-GKSS SYCSMC
LRBA_MAIZE 49 GGGSDWARRRKRRRE NKK KES--TT--HMS-----Q--NF-NEV A ECDAY ENQE-PVAM BES--PPDVG-----QDG-D-CQGI PSRAVV
LRBB_MAIZE 48 GGGSDWARRRKRRRE NKK KES--TT--YMS-----Q--NF-NEV A ECDAY ENQE-PVAM BGS--PPDVG-----QDG-D-CQGI PSRAVV
LRBA_PICSI 78 SNTLDLVRKRRRE NKK AGF-LD-----GCBH HES-SHP T DAAAY NFD E E-AVAM BES--PTTVAMLSSP--A--D-CGHGSSASMC
LRBA_PHYPA 45 ---GASRQ KRRRAHRS AGS-GVSKLL-GGPVEAQLGEGQBEQ MVV-GE-----DVAPOEADEE-AVAM BEP--HG-----N-SM-FSALGGTANLDT
LRBB_PHYPA 45 ---GTSRQ KRRRAHRS AGS-GVSKLL-GGASETQLGEGQBEQ MVV-AE-----DVAPOEADEE-AVAM BEP--YGVTF-----G-D-GTSSGSMNLT
LRBA_SEMLL 47 SNTLDLVRKRRRGADAK KGT-LFSCLF-FY-----LSFBEQ MTG-TQ-----PEP DABE-GDVM BES--PTSMA-----N-QD-QMSTSSANSSES
LRBB_SEMLL 47 SNTLDLVRKRRRGADAK KGT-LFSCLF-FY-----LSFBEQ MTG-TQ-----PEP DABE-GDVM BES--PTSMA-----N-QD-QMSTSSANSSES

```







```

LRB1 ARATH 479 -----MDEKGVMS--FGVDYEFPAARDKSTK--BBLVSK
LRB2 ARATH 481 -----MDEKGVMS--FGVDYEFPAARDKSTK--BBLVSK
LRB3 ARATH 427 -----MDEKGVMS--FGVDYEFPAARDKSTK--BBLVSK
LRBA ARALL 482 -----MDEKGVMS--FGVDYEFPAARDKSTK--BBLVSK
LRBB ARALL 479 -----MDEKGVMS--FGVDYEFPAARDKSTK--BBLVSK
LRBC ARALL 426 -----MDEKGVMS--FGVDYEFPAARDKSTK--BBLVSK
LRBA BRARP 478 -----MDEKGVMS--FGVDYEFPAARDKSTK--BBLVSK
LRBB BRARP 473 -----MDEKGVMS--FGVDYEFPAARDKSTK--BBLVSK
LRBC_BRARP 433 -----MDEKGVMS--FGVDYEFPAARDKSTK--BBLVSK
LRBA CICLE 473 -----MDEKGVMS--FGVDYEFPAARDKSTK--BBLVSK
LRBB CICLE 474 -----MDEKGVMS--FGVDYEFPAARDKSTK--BBLVSK
LRBC CICLE 479 -----MDEKGVMS--FGVDYEFPAARDKSTK--BBLVSK
LRBA POPTR 480 -----MDEKGVMS--FGVDYEFPAARDKSTK--BBLVSK
LRBB POPTR 472 -----MDEKGVMS--FGVDYEFPAARDKSTK--BBLVSK
LRBC POPTR 485 -----MDEKGVMS--FGVDYEFPAARDKSTK--BBLVSK
LRBD POPTR 485 -----MDEKGVMS--FGVDYEFPAARDKSTK--BBLVSK
LRBA PRUPE 481 -----MDEKGVMS--FGVDYEFPAARDKSTK--BBLVSK
LRBB PRUPE 479 -----MDEKGVMS--FGVDYEFPAARDKSTK--BBLVSK
LRBA RICCO 473 -----MDEKGVMS--FGVDYEFPAARDKSTK--BBLVSK
LRBB RICCO 557 VPGYSMLTAVVGFPMVFNASNAKAKIKRISLDTNRRNIIIHFNALTFPHERLISEAKVAFSENGTFHLSEINQLNVCYSQIQGHFS--VVMKPKR-----K--GEQGRK
LRBA CARUB 482 -----MDEKGVMS--FGVDYEFPAARDKSTK--BBLVSK
LRBB CARUB 478 -----MDEKGVMS--FGVDYEFPAARDKSTK--BBLVSK
LRBC CARUB 451 -----MDEKGVMS--FGVDYEFPAARDKSTK--BBLVSK
LRBA GLYMA 477 -----MDEKGVMS--FGVDYEFPAARDKSTK--BBLVSK
LRBB GLYMA 477 -----MDEKGVMS--FGVDYEFPAARDKSTK--BBLVSK
LRBA ORYSJ 459 -----MDEKGVMS--FGVDYEFPAARDKSTK--BBLVSK
LRBB ORYSJ 479 -----MDEKGVMS--FGVDYEFPAARDKSTK--BBLVSK
LRBA MAIZE 459 -----MDEKGVMS--FGVDYEFPAARDKSTK--BBLVSK
LRBB MAIZE 459 -----MDEKGVMS--FGVDYEFPAARDKSTK--BBLVSK
LRBC MAIZE 461 -----MDEKGVMS--FGVDYEFPAARDKSTK--BBLVSK
LRBD MAIZE 460 -----MDEKGVMS--FGVDYEFPAARDKSTK--BBLVSK
LRBE MAIZE 460 -----MDEKGVMS--FGVDYEFPAARDKSTK--BBLVSK
LRBF MAIZE 416 -----MDEKGVMS--FGVDYEFPAARDKSTK--BBLVSK
LRBA PICSI 495 -----MDEKGVMS--FGVDYEFPAARDKSTK--BBLVSK
LRBA PHYPA 459 -----MDEKGVMS--FGVDYEFPAARDKSTK--BBLVSK
LRBB PHYPA 463 -----MDEKGVMS--FGVDYEFPAARDKSTK--BBLVSK
LRBA SELML 460 -----MDEKGVMS--FGVDYEFPAARDKSTK--BBLVSK
LRBB SELML 460 -----MDEKGVMS--FGVDYEFPAARDKSTK--BBLVSK

```

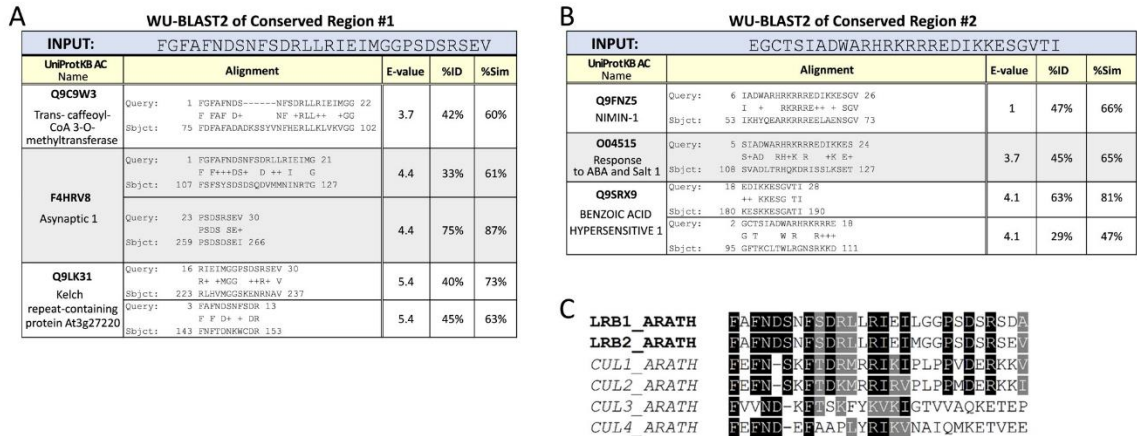
```

LRB1 ARATH 508 YKGNVYTFGGKA VGYRNLF IPWTSE A DSOHPFING LHLRAELT I RSTDL--H
LRB2 ARATH 509 YKGNVYTFGGKA VGYRNLF IPWTSE A DSOHPFING LHLRAELT I RSTDL--P
LRB3 ARATH 457 YKGNVYTFGGKA VGYRNLF IPWTSE A DSOHPFING LHLRAELT I RSTDL--P
LRBA ARALL 510 YKGNVYTFGGKA VGYRNLF IPWTSE A DSOHPFING LHLRAELT I RSTDL--P
LRBB ARALL 508 YKGNVYTFGGKA VGYRNLF IPWTSE A DSOHPFING LHLRAELT I RSTDL--H
LRBC ARALL 456 YKGNVYTFGGKA VGYRNLF IPWTSE A DSOHPFING LHLRAELT I RSTDL--P
LRBA BRARP 506 YKGNVYTFGGKA VGYRNLF IPWTSE A DSOHPFING LHLRAELT I RSTDL--P
LRBB BRARP 501 YKGNVYTFGGKA VGYRNLF IPWTSE A DSOHPFING LHLRAELT I RSTDL--P
LRBC BRARP 461 YKGNVYTFGGKA VGYRNLF IPWTSE A DSOHPFING LHLRAELT I RSTDL--P
LRBA CICLE 501 YKGNVYTFGGKA VGYRNLF IPWTSE A DSOHPFING LHLRAELT I RSTDL--P
LRBB CICLE 502 YKGNVYTFGGKA VGYRNLF IPWTSE A DSOHPFING LHLRAELT I RSTDL--P
LRBC CICLE 507 YKGNVYTFGGKA VGYRNLF IPWTSE A DSOHPFING LHLRAELT I RSTDL--P
LRBA POPTR 508 YKGNVYTFGGKA VGYRNLF IPWTSE A DSOHPFING LHLRAELT I RSTDL--P
LRBB POPTR 500 YKGNVYTFGGKA VGYRNLF IPWTSE A DSOHPFING LHLRAELT I RSTDL--P
LRBC POPTR 513 YKGNVYTFGGKA VGYRNLF IPWTSE A DSOHPFING LHLRAELT I RSTDL--P
LRBD POPTR 513 YKGNVYTFGGKA VGYRNLF IPWTSE A DSOHPFING LHLRAELT I RSTDL--P
LRBA PRUPE 509 YKGNVYTFGGKA VGYRNLF IPWTSE A DSOHPFING LHLRAELT I RSTDL--P
LRBB PRUPE 507 YKGNVYTFGGKA VGYRNLF IPWTSE A DSOHPFING LHLRAELT I RSTDL--P
LRBA RICCO 501 YKGNVYTFGGKA VGYRNLF IPWTSE A DSOHPFING LHLRAELT I RSTDL--P
LRBB RICCO 657 HSLWAVLHIFIVGSGGLALVGRFVAVSKLLRQKIQVMERQAL EDMVLEHIV--GNSKMPSAHRTQPTT--ESGGFP--
LRBA CARUB 510 YKGNVYTFGGKA VGYRNLF IPWTSE A DSOHPFING LHLRAELT I RSTDL--P
LRBB CARUB 507 YKGNVYTFGGKA VGYRNLF IPWTSE A DSOHPFING LHLRAELT I RSTDL--H
LRBC CARUB 479 YKGNVYTFGGKA VGYRNLF IPWTSE A DSOHPFING LHLRAELT I RSTDL--H
LRBA GLYMA 505 YKGNVYTFGGKA VGYRNLF IPWTSE A DSOHPFING LHLRAELT I RSTDL--P
LRBB GLYMA 505 YKGNVYTFGGKA VGYRNLF IPWTSE A DSOHPFING LHLRAELT I RSTDL--P
LRBA ORYSJ 487 YKGNVYTFGGKA VGYRNLF IPWTSE A DSOHPFING LHLRAELT I RSTDL--P
LRBB ORYSJ 507 YKGNVYTFGGKA VGYRNLF IPWTSE A DSOHPFING LHLRAELT I RSTDL--P
LRBA MAIZE 487 YKGNVYTFGGKA VGYRNLF IPWTSE A DSOHPFING LHLRAELT I RSTDL--P
LRBB MAIZE 487 YKGNVYTFGGKA VGYRNLF IPWTSE A DSOHPFING LHLRAELT I RSTDL--P
LRBC MAIZE 489 YKGNVYTFGGKA VGYRNLF IPWTSE A DSOHPFING LHLRAELT I RSTDL--P
LRBD MAIZE 488 YKGNVYTFGGKA VGYRNLF IPWTSE A DSOHPFING LHLRAELT I RSTDL--P
LRBE MAIZE 488 YKGNVYTFGGKA VGYRNLF IPWTSE A DSOHPFING LHLRAELT I RSTDL--P
LRBF MAIZE 444 YKGNVYTFGGKA VGYRNLF IPWTSE A DSOHPFING LHLRAELT I RSTDL--P
LRBA PICSI 523 YKGNVYTFGGKA VGYRNLF IPWTSE A DSOHPFING LHLRAELT I RSTDL--P
LRBA PHYPA 487 YKGNVYTFGGKA VGYRNLF IPWTSE A DSOHPFING LHLRAELT I RSTDL--P
LRBB PHYPA 491 YKGNVYTFGGKA VGYRNLF IPWTSE A DSOHPFING LHLRAELT I RSTDL--P
LRBA SELML 489 YKGNVYTFGGKA VGYRNLF IPWTSE A DSOHPFING LHLRAELT I RSTDL--M
LRBB SELML 489 YKGNVYTFGGKA VGYRNLF IPWTSE A DSOHPFING LHLRAELT I RSTDL--M

```

## Supplemental Figure 2: Multiple Sequence Alignment of All LRB Protein Homologues

The MSA of all LRB protein homologues discovered using *AtLRB2* as the query sequence to perform a UniProtKB<sup>54,55</sup> protein BLAST. This alignment was ultimately used to create a phylogenetic tree and to observe the regional conservation present in the amino-terminal region. Proteins are abbreviated as listed in Supplemental Figure 1.



### Supplemental Figure 3: Alignments of *AtLRB2* with BLAST Search Results

**A.** Results of the WU-BLAST2 search using the first conserved region of *AtLRB2*. UniProtKB AC, protein name, alignment, E-value, percent identity, and percent similarity are provided for each match.

**B.** Results of the WU-BLAST2 search using the second conserved region of *AtLRB2*. UniProtKB AC, protein name, alignment, E-value, percent identity, and percent similarity are provided for each match.

**C.** A MSA of the CL region of *AtLRB1/2* with the  $Cu1^{CL}$  region of all four Cullin proteins found in *Arabidopsis thaliana*. Residues with a high overall conservation (above 66%) are shown highlighted in black, while residues that are mostly conserved and have consensus due to residue similarity (above 66%) are shown highlighted in grey.

```

LRB1_ARATH 1 M-RGS-NMIDLFDP--T-----EMDS--NFSRHSSS--GGDFGFANDSNFSDRLRLRIETGGPS--SRSDAEGCTSIADWAR
LRB2_ARATH 1 M-RGTENIDLFDP--T-----QMDP--DFIRHSSS--GGDFGFANDSNFSDRLRLRIETGGPS--SRSEVGGCTSIADWAR
LRBA_ARALL 1 M-RGTENIDLFDP--T-----QMDP--DFIRHSSS--GGDFGFANDSNFSDRLRLRIETGGPS--SRSDVGGCTSIADWAR
LRBB_ARALL 1 M-RGS-NMIDLFDP--T-----EMDS--NFSRHSSS--GGDFGFANDSNFSDRLRLRIETGGPS--SRSEVGGCTSIADWAR
LRBA_BRARP 1 M-RGG-ENIDLFDP--T-----QMDS--DFSRRHSSS--GGDFGFANDSNFSDRLRLRIETGGPS--SRSDVGGCTSIADWAR
LRBA_CICLE 1 M-R-D-VNIDLFDP--T-----EMDS--DFIRHSSS--GGDFGFANDSNFSDRLRLRIETGGPP--SRSDGGGCTSIADWAR
LRBA_POPTR 1 M-R-G-SMIDLFDP--T-----EMDS--DFIRHSSS--GGDFGFANDSNFSDRLRLRIETGGSAE--NRADGGGCTSIADWAR
LRBB_POPTR 1 M-R-G-SMIDLFDP--T-----EMDS--DFIRHSSS--GGDFGFANDSNFSDRLRLRIETGGSAE--SRADGGGCTSIADWAR
LRBA_PRUPE 1 M-RGAEINIDLFDP--S-----LMDP--DFSRA--SADADADDF--FANDSNFSDRLRLRIETGGTPE--SRDSEVGGCTSIADWAR
LRBA_RICCO 1 M-R-G-SMIDLFDP--T-----EMDS--VFSRGSSS--GGDFGFANDSNFSDRLRLRIETGGSP--NRDGGGCTSIADWAR
LRBA_CARUB 1 M-RGAEINIDLFDP--I-----QMDS--DFSRRHSSS--GGDFGFANDSNFSDRLRLRIETGGPS--SRSDVGGCTSIADWAR
LRBB_CARUB 1 M-RGS-NMIDLFDP--T-----EMDS--NFSRHSSS--GGDFGFANDSNFSDRLRLRIETGGPS--SRSDVGGCTSIADWAR
LRBB_GLYMA 1 M-R-D-FNIDLFDP--G-M-----VMDSSSS--SRSS--GGDFGFANDSNFSDRLRLRIETGGPVE--ARPEGGCTSIADWAR
LRBA_ORYSJ 1 -----MDP--DFSRA--SR--GPS--FANFNSVNFSDRLRLRIETGGDDAAGAKGAGGCS--ADWAH
LRBA_MAIZE 1 -----MDP--DFSRA--SG--GPS--FANFNSVNFSDRLRLRIETGGDDALGAKGATGCGCS--ADWAC
LRBB_MAIZE 1 -----MDP--DFSRA--SG--GPS--FANFNSVNFSDRLRLRIETGGDDALGAKGATGCGCS--ADWAC
LRBA_PICSI 1 M-R-L-EPSE-VQEL--AESRNTNRIGSGGGAFVSD--SP--SAS--SA--PPNF--FANFNSVNFSDRLRLRIETGGPTE--SRSDGGGCTSIADWAR

```

```

NLS BTB DOMAIN
LRB1_ARATH 72 HRKRRREDNKKKNG--VAISDVAQAEQIITDNNOPMDPAPGGNLDDE--EAMEE--ALSGD-----D-ASS--PNAG--DCS--VVRVKELHI
LRB2_ARATH 73 HRKRRREDNKKKSG--VTISDVAQAEQIITD--POPMDCCPGG--NDDDE--EAMEE--ALSGD-----EETS--SE--PNAGMDCS--VVRVKELHI
LRBA_ARALL 73 HRKRRREDNKKKSGG-VTISDVAQAEQIITD--POPMDCCPGG--NDDDE--EAMEE--ALSGD-----EETS--SE--PNAGMDCS--VVRVKELHI
LRBB_ARALL 72 HRKRRREDNKKKNG--VAISDVAQAEQIITDNNOPMDPAPGGNLDDE--EAMEE--ALSGD-----D-ASS--PNAG--DCS--VVRVKELHI
LRBA_BRARP 72 HRKRRREDNKKKSV--TISDVAQAEQIITD--POPMDCCPGG--NDDDE--EAMEE--SLSGD-----BEDT--SE--PSAGMDCS--VVRVKELHI
LRBA_CICLE 71 HRKRRREDNKKKNG---ID--SAGPEEQIL---NOPMDCCVCC--NDDDE--VAMEE--G--SPSGD-----EAANGN--SSAGMDCS--VVRVKELHI
LRBA_POPTR 72 HRKRRREDNKKKINN-VRACD--SVGAEQILGS--IOPMDCCVCC--NDDDE--EAMEE--G--SPSGD-----EAADGT--SSAGMDCS--VVRVKELHI
LRBB_POPTR 72 HRKRRREDNKKKNN-----NGAEQILGS--NOPMDCCVCC--NDDDE--EAMEE--V--SPSGD-----EAGDGN--SSAGMDCS--VVRVKELHI
LRBA_PRUPE 77 HRKRRREDNKKKNI---P--PSE--PEEQIIND--NOPMDCCVCC--NDDDE--VAMEE--G--SPSGD-----EAANGN--SDAGMDCS--VVRVKELHI
LRBA_RICCO 71 HRKRRREDNKKKNA--V---SAGAEQIIL---NOPMDCCVCC--NDDDE--VAMEE--P--SPSGD-----EAVDGN--STAGMDCS--VVRVKELHI
LRBA_CARUB 73 HRKRRREDNKKKSG--VTISDVAQAEQIITD--POPMDCCPGG--NDDDE--EAMEE--EALSGD-----EETS--SE--PNAGMDCS--VVRVKELHI
LRBB_CARUB 72 HRKRRREDNKKKNG--VAISDVAQAEQIITDNNOPMDPAPGGNLDDE--EAMEE--ALSGD-----D-VSS--PNAG--DCS--VVRVKELHI
LRBB_GLYMA 74 HRKRRREDNKKKNNV---VD--TLLPEEQILNE--NOPMDCCVCC--NDDDE--VAMEE--P--SPSGD-----EAANGN--SNAGMDCS--VVRVKELHI
LRBA_ORYSJ 58 HRKRRREDNKKKESGK-YTD--ET--K-----VAAECDDTY--EGNE--PVAMEE--S--PPDIE---ADG--EDGK--SS--SYCSM--C--QV--RVKYS--YI
LRBA_MAIZE 58 HRKRRREDNKKKESRKYMP--PANCK-----VAAECDDTY--EGNE--PVAMEE--S--PPDIE---ADG--EDGK--SS--SYCSM--C--QV--RVKYS--YI
LRBB_MAIZE 58 HRKRRREDNKKKESRKYMP--PANCK-----VAAECDDTY--EGNE--PVAMEE--S--PPDIE---ADG--EDGK--SS--SYCSM--C--QV--RVKYS--YI
LRBA_PICSI 87 NRKRRREDNKKKAG--F---D--GCE--H--IS--SH--P--D--AA--Y--N--F--E--E--VAMEE--S--P--TVAMLSSPAAD--C--GHGSS--SS--MDCS--VVRVKELHI

```

```

BTB DOMAIN BTB DOMAIN 3-BOX
LRB1_ARATH 157 SSPILAAKSPFFYKLFSGMRESEQRHVTLRINASEEALMELLNFMYSNLSTTTAPALLDVLMAADKFEVASCRCYRSLRLRNPMTESALLYLELP
LRB2_ARATH 159 SSPILAAKSPFFYKLFSGMRESEQRHVTLRINASEEALMELLNFMYSNLSTTTAPALLDVLMAADKFEVASCRCYRSLRLRNPMTESALLYLELP
LRBA_ARALL 160 SSPILAAKSPFFYKLFSGMRESEQRHVTLRINASEEALMELLNFMYSNLSTTTAPALLDVLMAADKFEVASCRCYRSLRLRNPMTESALLYLELP
LRBB_ARALL 157 SSPILAAKSPFFYKLFSGMRESEQRHVTLRINASEEALMELLNFMYSNLSTTTAPALLDVLMAADKFEVASCRCYRSLRLRNPMTESALLYLELP
LRBA_BRARP 156 SSPILAAKSPFFYKLFSGMRESEQRHVTLRINASEEALMELLNFMYSNLSTTTAPALLDVLMAADKFEVASCRCYRSLRLRNPMTESALLYLELP
LRBA_CICLE 151 SSPILAAKSPFFYKLFSGMRESEQRHVTLRINASEEALMELLNFMYSNLSTTTAPALLDVLMAADKFEVASCRCYRSLRLRNPMTESALLYLELP
LRBA_POPTR 158 SSPILAAKSPFFYKLFSGMRESEQRHVTLRINASEEALMELLNFMYSNLSTTTAPALLDVLMAADKFEVASCRCYRSLRLRNPMTESALLYLELP
LRBB_POPTR 150 SSPILAAKSPFFYKLFSGMRESEQRHVTLRINASEEALMELLNFMYSNLSTTTAPALLDVLMAADKFEVASCRCYRSLRLRNPMTESALLYLELP
LRBA_PRUPE 159 SSPILAAKSPFFYKLFSGMRESEQRHVTLRINASEEALMELLNFMYSNLSTTTAPALLDVLMAADKFEVASCRCYRSLRLRNPMTESALLYLELP
LRBA_RICCO 151 SSPILAAKSPFFYKLFSGMRESEQRHVTLRINASEEALMELLNFMYSNLSTTTAPALLDVLMAADKFEVASCRCYRSLRLRNPMTESALLYLELP
LRBA_CARUB 160 SSPILAAKSPFFYKLFSGMRESEQRHVTLRINASEEALMELLNFMYSNLSTTTAPALLDVLMAADKFEVASCRCYRSLRLRNPMTESALLYLELP
LRBB_CARUB 156 SSPILAAKSPFFYKLFSGMRESEQRHVTLRINASEEALMELLNFMYSNLSTTTAPALLDVLMAADKFEVASCRCYRSLRLRNPMTESALLYLELP
LRBB_GLYMA 156 SSPILAAKSPFFYKLFSGMRESEQRHVTLRINASEEALMELLNFMYSNLSTTTAPALLDVLMAADKFEVASCRCYRSLRLRNPMTESALLYLELP
LRBA_ORYSJ 139 SSAILAASPFFYKLFSGMRESEQRHATLRINASEEALMELLNFMYSGKLTNQPTVLLDMLMADKFEVASCRCYRSLRLRNPMTESALLYLELP
LRBA_MAIZE 139 SSAILAASPFFYKLFSGMRESEQRHATLRINASEEALMELLNFMYSGKLTNQPTVLLDMLMADKFEVASCRCYRSLRLRNPMTESALLYLELP
LRBB_MAIZE 139 SSAILAASPFFYKLFSGMRESEQRHATLRINASEEALMELLNFMYSGKLTNQPTVLLDMLMADKFEVASCRCYRSLRLRNPMTESALLYLELP
LRBA_PICSI 175 SSAILAASPFFYKLFSGMRESEQRHATLRINASEEALMELLNFMYSGKLTNQPTVLLDMLMADKFEVASCRCYRSLRLRNPMTESALLYLELP

```

```

3-BOX BACK DOMAIN BACK DOMAIN
LRB1_ARATH 257 SSVLMABAVOPLTDAAKQLAARYKDTKPEEVMALPLAGIEAILSSDDLOASEDAVYDFLKWARYOYSSLEERREILGRLALYIRFPMTCRKLL
LRB2_ARATH 259 SSVLMABAVOPLTDAAKQLAARYKDTKPEEVMALPLAGIEAILSSDDLOASEDAVYDFLKWARYOYCLEERREILGRLALYIRFPMTCRKLL
LRBA_ARALL 260 SSVLMABAVOPLTDAAKQLAARYKDTKPEEVMALPLAGIEAILSSDDLOASEDAVYDFLKWARYOYCLEERREILGRLALYIRFPMTCRKLL
LRBB_ARALL 257 SSVLMABAVOPLTDAAKQLAARYKDTKPEEVMALPLAGIEAILSSDDLOASEDAVYDFLKWARYOYSSLEERREILGRLALYIRFPMTCRKLL
LRBA_BRARP 256 SSVLMABAVOPLTDAAKQLAARYKDTKPEEVMALPLAGIEAILSSDDLOASEDAVYDFLKWARYOYSSLEERREILGRLALYIRFPMTCRKLL
LRBA_CICLE 251 SSVLMABAVOPLTDAAKQLAARYKDTKPEEVMALPLAGIEAILSSDDLOASEDAVYDFLKWARYOYRREERREILGRLALYIRFPMTCRKLL
LRBA_POPTR 258 SSVLMABAVOPLTDAAKQLAARYKDTKPEEVMALPLAGIEAILSSDDLOASEDAVYDFLKWARYOYRREERREILGRLALYIRFPMTCRKLL
LRBB_POPTR 250 SSVLMABAVOPLTDAAKQLAARYKDTKPEEVMALPLAGIEAILSSDDLOASEDAVYDFLKWARYOYRREERREILGRLALYIRFPMTCRKLL
LRBA_PRUPE 259 SSVLMABAVOPLTDAAKQLAARYKDTKPEEVMALPLAGIEAILSSDDLOASEDAVYDFLKWARYOYRREERREILGRLALYIRFPMTCRKLL
LRBA_RICCO 251 SSVLMABAVOPLTDAAKQLAARYKDTKPEEVMALPLAGIEAILSSDDLOASEDAVYDFLKWARYOYRREERREILGRLALYIRFPMTCRKLL
LRBA_CARUB 260 SSVLMABAVOPLTDAAKQLAARYKDTKPEEVMALPLAGIEAILSSDDLOASEDAVYDFLKWARYOYRREERREILGRLALYIRFPMTCRKLL
LRBB_CARUB 256 SSVLMABAVOPLTDAAKQLAARYKDTKPEEVMALPLAGIEAILSSDDLOASEDAVYDFLKWARYOYRREERREILGRLALYIRFPMTCRKLL
LRBB_GLYMA 256 SSVLMABAVOPLTDAAKQLAARYKDTKPEEVMALPLAGIEAILSSDDLOASEDAVYDFLKWARYOYRREERREILGRLALYIRFPMTCRKLL
LRBA_ORYSJ 239 SSVLMABAVOPLTDAAKQLAARYKDTKPEEVMALPLAGIEAILSSDDLOASEDAVYDFLKWARYOYRREERREILGRLALYIRFPMTCRKLL
LRBA_MAIZE 239 SSVLMABAVOPLTDAAKQLAARYKDTKPEEVMALPLAGIEAILSSDDLOASEDAVYDFLKWARYOYRREERREILGRLALYIRFPMTCRKLL
LRBB_MAIZE 239 SSVLMABAVOPLTDAAKQLAARYKDTKPEEVMALPLAGIEAILSSDDLOASEDAVYDFLKWARYOYRREERREILGRLALYIRFPMTCRKLL
LRBA_PICSI 275 SSVLMABAVOPLTDAAKQLAARYKDTKPEEVMALPLAGIEAILSSDDLOASEDAVYDFLKWARYOYRREERREILGRLALYIRFPMTCRKLL

```

```

LRB1_ARATH 357 KVLTCDFDHHVASKVLEALFFKAEAPHQRRLAAEBSA LNRRRERAYKYRVPKVVVEFELPRQCQVVYLDLKREECAGLFPSSGRVYSQAFHLGGQGF
LRB2_ARATH 359 KVLTCDFDHHVASKVLEALFFKAEAPHQRRLAAEBSA LNRRRERAYKYRVPKVVVEFELPRQCQVVYLDLKREECAGLFPSSGRVYSQAFHLGGQGF
LRBA_ARALL 360 KVLTCDFDHHVASKVLEALFFKAEAPHQRRLAAEBSA LNRRRERAYKYRVPKVVVEFELPRQCQVVYLDLKREECAGLFPSSGRVYSQAFHLGGQGF
LRBB_ARALL 357 KVLTCDFDHHVASKVLEALFFKAEAPHQRRLAAEBSG LNRRRERAYKYRVPKVVVEFELPRQCQVVYLDLKREECAGLFPSSGRVYSQAFHLGGQGF
LRBA_BRARP 356 KVLTCDFDHHVASKVLEALFFKAEAPHQRRLAAEBSA LNRRRERAYKYRVPKVVVEFELPRQCQVVYLDLKREECAGLFPSSGRVYSQAFHLGGQGF
LRBA_CICLE 351 KVLTCDFDHHVASKVLEALFFKAEAPHQRRLAAEBSV LNRRRERAYKYRVPKVVVEFELPRQCQVVYLDLKREECANLFPSSGRVYSQAFHLGGQGF
LRBA_POPTR 358 KVLTCDFDHHVASKVLEALFFKAEAPHQRRLAAEBSA LNRRRERAYKYRVPKVVVEFELPRQCQVVYLDLKREECANLFPSSGRVYSQAFHLGGQGF
LRBB_POPTR 350 KVLTCDFDHHVASKVLEALFFKAEAPHQRRLAAEBSA LNRRRERAYKYRVPKVVVEFELPRQCQVVYLDLKREECANLFPSSGRVYSQAFHLGGQGF
LRBA_PRUPE 359 KVLTCDFDHHVASKVLEALFFKAEAPHQRRLAAEBSA LNRRRERAYKYRVPKVVVEFELPRQCQVVYLDLKREECANLFPSSGRVYSQAFHLGGQGF
LRBA_RICCO 351 KVLTCDFDHHVASKVLEALFFKAEAPHQRRLAAEBSA LNRRRERAYKYRVPKVVVEFELPRQCQVVYLDLKREECANLFPSSGRVYSQAFHLGGQGF
LRBA_CARUB 360 KVLTCDFDHHVASKVLEALFFKAEAPHQRRLAAEBSA LNRRRERAYKYRVPKVVVEFELPRQCQVVYLDLKREECAGLFPSSGRVYSQAFHLGGQGF
LRBB_CARUB 356 KVLTCDFDHHVASKVLEALFFKAEAPHQRRLAAEBSA LNRRRERAYKYRVPKVVVEFELPRQCQVVYLDLKREECAGLFPSSGRVYSQAFHLGGQGF
LRBB_GLYMA 356 KVLTCDFDHHVASKVLEALFFKAEAPHQRRLAAEBSA LNRRRERAYKYRVPKVVVEFELPRQCQVVYLDLKREECANLFPSSGRVYSQAFHLGGQGF
LRBA_ORYSJ 339 KVLACDDLHQARCVTEALLKADAPHQRRLAAAVL--TKRYAERAYKYRVPKVVVEFELPRQCQVVYLDLKREECANLFPSSGRVYSQAFHLGGQGF
LRBA_MAIZE 339 KVLACDDLHQARCVTEALLKADAPHQRRLAAAVM--TKRYAERAYKYRVPKVVVEFELPRQCQVVYLDLKREECANLFPSSGRVYSQAFHLGGQGF
LRBB_MAIZE 339 KVLACDDLHQARCVTEALLKADAPHQRRLAAAVM--TKRYAERAYKYRVPKVVVEFELPRQCQVVYLDLKREECANLFPSSGRVYSQAFHLGGQGF
LRBA_PICSI 375 KVLTCDFDHHVASKVLEALFFKAEAPHQRRLAAEBSA LNRRRERAYKYRVPKVVVEFELPRQCQVVYLDLKREECAGLFPSSGRVYSQAFHLGGQGF

LRB1_ARATH 457 FLSAHCNMDQSSFHCFGLFLGMOEKGVSFTVDYEFFAARAK--PGEER--SKYKGNVYFTGGKAVGYRNLFIPTWTF--ADSDPFIQGLHHLRAELTIKRSSDLH--
LRB2_ARATH 459 FLSAHCNMDQSSFHCFGLFLGMOEKGVSFTVDYEFFAARAK--PGEER--SKYKGNVYFTGGKAVGYRNLFIPTWTF--ADSDPFIQGLHHLRAELTIKRSTD---P
LRBA_ARALL 460 FLSAHCNMDQSSFHCFGLFLGMOEKGVSFTVDYEFFAARAK--PGEER--SKYKGNVYFTGGKAVGYRNLFIPTWTF--ADSDPFIQGLHHLRAELTIKRSTD---P
LRBB_ARALL 457 FLSAHCNMDQSSFHCFGLFLGMOEKGVSFTVDYEFFAARAK--PGEER--SKYKGNVYFTGGKAVGYRNLFIPTWTF--ADSDPFIQGLHHLRAELTIKRSSDLH--
LRBA_BRARP 456 FLSAHCNMDQSSFHCFGLFLGMOEKGVSFTVDYEFFAARAK--PGEER--SKYKGNVYFTGGKAVGYRNLFIPTWTF--ADSDPFIQGLHHLRAELTIKRSTDPPPQ
LRBA_CICLE 451 FLSAHCNMDQSSFHCFGLFLGMOEKGVSFTVDYEFFAARAK--PGEER--SKYKGNVYFTGGKAVGYRNLFIPTWTF--ADSDPFIQGLHHLRAELTIKR--
LRBA_POPTR 458 FLSAHCNMDQSSFHCFGLFLGMOEKGVSFTVDYEFFAARAK--PGEER--SKYKGNVYFTGGKAVGYRNLFIPTWTF--ADSDPFIQGLHHLRAELTIKR--
LRBB_POPTR 450 FLSAHCNMDQSSFHCFGLFLGMOEKGVSFTVDYEFFAARAK--PGEER--SKYKGNVYFTGGKAVGYRNLFIPTWTF--ADSDPFIQGLHHLRAELTIKR--
LRBA_PRUPE 459 FLSAHCNMDQSSFHCFGLFLGMOEKGVSFTVDYEFFAARAK--PGEER--SKYKGNVYFTGGKAVGYRNLFIPTWTF--ADSDPFIQGLHHLRAELTIKR--
LRBA_RICCO 451 FLSAHCNMDQSSFHCFGLFLGMOEKGVSFTVDYEFFAARAK--PGEER--SKYKGNVYFTGGKAVGYRNLFIPTWTF--ADSDPFIQGLHHLRAELTIKR--
LRBA_CARUB 460 FLSAHCNMDQSSFHCFGLFLGMOEKGVSFTVDYEFFAARAK--PGEER--SKYKGNVYFTGGKAVGYRNLFIPTWTF--ADSDPFIQGLHHLRAELTIKRSTD---P
LRBB_CARUB 456 FLSAHCNMDQSSFHCFGLFLGMOEKGVSFTVDYEFFAARAK--PGEER--SKYKGNVYFTGGKAVGYRNLFIPTWTF--ADSDPFIQGLHHLRAELTIKRSTDH--
LRBB_GLYMA 455 FLSAHCNMDQSSFHCFGLFLGMOEKGVSFTVDYEFFAARAK--PGEER--SKYKGNVYFTGGKAVGYRNLFIPTWTF--ADSDPFIQGLHHLRAELTIKR--
LRBA_ORYSJ 437 FLSAHCNMDQSSFHCFGLFLGMOEKGVSFTVDYEFFAARAK--PGEER--SKYKGNVYFTGGKAVGYRNLFIPTWTF--ADSDPFIQGLHHLRAELTIKR--
LRBA_MAIZE 437 FLSAHCNMDQSSFHCFGLFLGMOEKGVSFTVDYEFFAARAK--PGEER--SKYKGNVYFTGGKAVGYRNLFIPTWTF--ADSDPFIQGLHHLRAELTIKR--
LRBB_MAIZE 437 FLSAHCNMDQSSFHCFGLFLGMOEKGVSFTVDYEFFAARAK--PGEER--SKYKGNVYFTGGKAVGYRNLFIPTWTF--ADSDPFIQGLHHLRAELTIKR--
LRBA_PICSI 473 FLSAHCNMDQSSFHCFGLFLGMOEKGVSFTVDYEFFAARAK--PGEER--SKYKGNVYFTGGKAVGYRNLFIPTWTF--ADSDPFIQGLHHLRAELTIKR--

```

**Supplemental Figure 4: Refined MSA of Homologous LRB Proteins**

A refined MSA that excludes LRB homologues that deviate substantially in the overall alignment. Sequences that contained large insertions or deletions were also excluded from the alignment. If all homologues for a particular plant species deviated substantially, the LRB homologue that deviated the least was used in the alignment. If two protein sequences were found to be identical, as was found with *LRBA\_CICLE* and *LRBB\_CICLE*, then the second protein sequence was removed from the alignment. Residues with a high overall conservation (above 70%) are shown highlighted in black, while residues that are mostly conserved and have consensus due to residue similarity (above 70%) are shown highlighted in grey.

CUL1\_ARATH 1 M---ERKTIIDLEQGWDMCTGITKLRIRLEGLPEPAFDSEQYMMLYTTIYNMCTQKPPHDYSQQLYDKYR  
 CUL2\_ARATH 1 M---AKKDSVLEAGWSVMEAGVAKLORILEEVPEPPDFVQRMLYTTVENLCTQKPEINDYSQQLYDRYR  
 CUL1\_ARALL 1 M---ERKTIIDLEQGWDMCTGITKLRIRLEGLPEPAFDSEQYMMLYTTIYNMCTQKPPHDYSQQLYDKYR  
 CUL2\_ARALL 1 M---SRGITVLEEGWPFMEAGVTKLHRIRLELPEPAFDSVQYNNLYTTIYNMCTQKPPHDYSQQLYDKYR  
 CULA\_BRARP 1 M---ERKTIIDLEQGWDMCTGITKLRIRLEGLPEPAFDSEQYMMLYTTIYNMCTQKPPHDYSQQLYDKYR  
 CULB\_BRARP 1 MSFSNRKPIITLEDGFKLIDAAVTKLIRIIEGKPEPPFLFEFYIGNYTIYNMCTQKPPHDYSQQLYDKYR  
 CULA\_CICLE 1 M---DRKTIIDLEQGWDMCKGITKLRIRLEGLPEPSPFSSEYMMLYTTIYNMCTQKPPHDYSQQLYDKYR  
 CULB\_CICLE 1 MTMNERKTIIDLEQGWDFMCKGITKLRIRLEGLPEPQFSSSEYMMLYTTIYNMCTQKPPHDYSQQLYDKYR  
 CULA\_POPTR 1 MAINERKTIIDLEQGWDFMCKGITKLRIRLEGLPEPQFSSSEYMMLYTTIYNMCTQKPPHDYSQQLYDKYR  
 CULB\_POPTR 1 MTMNERKTIIDLEQGWDFMCKGITKLRIRLEGLPEPQFSSSEYMMLYTTIYNMCTQKPPHDYSQQLYDKYR  
 CULA\_PRUPE 1 M---ERKTIIDLEQGWDMCKGITKLRIRLEGLPEPQFSSSEYMMLYTTIYNMCTQKPPHDYSQQLYDKYR  
 CULB\_PRUPE 1 MTMNERKTIIDLEQGWDFMCKGITKLRIRLEGLPEPQFSSSEYMMLYTTIYNMCTQKPPHDYSQQLYDKYR  
 CULA\_RICCO 1 MTMNERKTIIDLEQGWDFMCKGITKLRIRLEGLPEPQFSSSEYMMLYTTIYNMCTQKPPHDYSQQLYDKYR  
 CULA\_CARUB 1 M---ERKTIIDLEQGWDMCTGITKLRIRLEGLPEPAFDSEQYMMLYTTIYNMCTQKPPHDYSQQLYDKYR  
 CULB\_CARUB 1 ILSLQMKSTIEEQGWSVMEAGVAKLORILELPEPPFLFEFYNNQYTTIYNMCTQKPEINDYSQQLYDKYS  
 CULA\_GLYMA 1 MSMSERKTIIDLEQGWDFMLKGITKLRIRLEGLPEPQFSSSEYMMLYTTIYNMCTQKPPHDYSQQLYDKYR  
 CULB\_GLYMA 1 MSMSERKTIIDLEQGWDFMCKGITKLRIRLEGLPEPQFSSSEYMMLYTTIYNMCTQKPPHDYSQQLYDKYR  
 CULC\_GLYMA 1 MSMSERKTIIDLEQGWDFMCKGITKLRIRLEGLPEPQFSSSEYMMLYTTIYNMCTQKPPHDYSQQLYDKYR  
 CULA\_ORYSJ 1 MATHERKTIIDLEQGWDFMCKGITKLRIRLEGLPEPQFSSSEYMMLYTTIYNMCTQKPPHDYSQQLYDKYR  
 CULB\_ORYSJ 1 MGVHEHPR-QARATLRGHDHDA---LHPPPP---PPP---PPGTTIYNMCTQKPPHDYSQQLYDKYR  
 CULA\_MAIZE 1 MAGQER-RTDLEEGWAFMCKGITKLRIRLEGLPEPQFSSSEYMMLYTTIYNMCTQKPPHDYSQQLYDKYR  
 CULA\_PICSI 1 MTMSERKTIIDLEAGWDFMCKGITKLRIRLEGNPEQQINSEYMMLYTTIYNMCTQKPEINDYSQQLYDRYR

CUL1\_ARATH 68 EAFEEYINSTVLPALREKHDEFMLRELKRWSNHKVMVRWLSRFFYYLDRYFIARRSLPLNEVGLTCFR  
 CUL2\_ARATH 68 GVVVDYINKQTVLPALREKHGEFMLRELVKRWANQKILVRWLSHFFYYLDRYFTRRCSHPTLSAVGFISFR  
 CUL1\_ARALL 68 EAFEEYINSTVLPALREKHDEFMLRELKRWSNHKVMVRWLSRFFYYLDRYFIARRSLPLNEVGLTCFR  
 CUL2\_ARALL 68 GVIDDYINKQTVLPALREKHGEFMLRELVKRWANHKVIVRWLSRFFDYLDRYFVPRRNLITLNSVGLTSFR  
 CULA\_BRARP 68 EAFEEYINSTVLPALREKHDEFMLRELKRWSNHKVMVRWLSRFFYYLDRYFIARRSLPLNEVGLTCFR  
 CULB\_BRARP 71 AILQAMDKLITLPSLMEKHDEFMLREMSRWEINKIMVRWLSHFFYYLDRYFIARRSLPLNEVGLTCFR  
 CULA\_CICLE 68 QAFEEYISSMVLPSLSEKHDEFMLRELVKRWANHKVMVRWLSRFFYYLDRYFIARRSLPLNEVGLTCFR  
 CULB\_CICLE 71 ESFEEYISSMVLPSLREKHDEFMLRELKRWSNHKVMVRWLSRFFYYLDRYFIARRSLPLNEVGLTCFR  
 CULA\_POPTR 71 ESFEEYITSTVLPALREKHDEFMLRELKRWANHKVMVRWLSRFFYYLDRYFIARRSLPLNEVGLTCFR  
 CULB\_POPTR 71 ESFEEYITSTVLPALREKHDEFMLRELKRWANHKVMVRWLSRFFYYLDRYFIARRSLPLNEVGLTCFR  
 CULA\_PRUPE 68 EAFEEYITSTVLPALREKHDEFMLRELKRWANHKVMVRWLSRFFYYLDRYFIARRSLPLNEVGLTCFR  
 CULB\_PRUPE 71 ESFEEYITSTVLPALREKHDEFMLRELKRWANHKVMVRWLSRFFYYLDRYFIARRSLPLNEVGLTCFR  
 CULA\_RICCO 71 ESFEEYITSTVLPALREKHDEFMLRELKRWANHKVMVRWLSRFFYYLDRYFIARRSLPLNEVGLTCFR  
 CULA\_CARUB 68 EAFEEYINSTVLPALREKHDEFMLRELKRWANHKVMVRWLSRFFYYLDRYFIARRSLPLNEVGLTCFR  
 CULB\_CARUB 71 EVIATYINKQTVLPALREKHDEFMLRELKRWANHKVIVRWLSRFFDYLDRYFIARRSLPLNEVGLTCFR  
 CULA\_GLYMA 71 ESFEEYIVSTVLPALREKHDEFMLRELKRWANHKIMVRWLSRFFYYLDRYFIARRSLPLNEVGLTCFR  
 CULB\_GLYMA 71 ESFEEYIVSTVLPALREKHDEFMLRELKRWANHKIMVRWLSRFFYYLDRYFIARRSLPLNEVGLTCFR  
 CULC\_GLYMA 71 ESFEEYIVSTVLPALREKHDEFMLRELKRWANHKIMVRWLSRFFYYLDRYFIARRSLPLNEVGLTCFR  
 CULA\_ORYSJ 70 ESFEEYITSMVLPALREKHDEFMLRELKRWSNHKVMVRWLSRFFYYLDRYFIARRSLPLNEVGLTCFR  
 CULB\_ORYSJ 56 ESFEEYITSMVLPALREKHDEFMLRELKRWANHKIMVRWLSRFFYYLDRYFIARRSLPLNEVGLTCFR  
 CULA\_MAIZE 69 ESFEEYITSMVLPALREKHDEFMLRELKRWANHKIMVRWLSRFFYYLDRYFIARRSLPLNEVGLTCFR  
 CULA\_PICSI 71 ESFEEYITSMVLPALREKHDEFMLRELKRWANHKIMVRWLSRFFYYLDRYFIARRSLPLNEVGLTCFR

CUL1\_ARATH 138 DLVYNEIHSKVKEAVIALDKEREQEIDRALLKNVLDIFVEIGMGOMERYEEDFESEFMLQDTSYYSRK  
 CUL2\_ARATH 138 DLVYQEIQSNAKDAVIALTHKEREQEIDRALLKNVLDIVYCGNMGCEMVRKYEEDFESEFLEDTSASYSRN  
 CUL1\_ARALL 138 DLVYNEIHSKVKEAVIALDKEREQEIDRALLKNVLDIFVEIGMGOMERYEEDFESEFMLQDTSYYSRK  
 CUL2\_ARALL 138 DLVYQEIQSNAKDAVIALTHKEREQEIDRSLLKNVLDIVYCGNMGCEMVRKYEEDFESEFLEDTSASYSRK  
 CULA\_BRARP 138 DLVYNEIHSKVKEAVIALDKEREQEIDRALLKNVLDIFVEIGMGOMERYEEDFESEFMLQDTSYYSRK  
 CULB\_BRARP 141 DHVYEKWHFNKQVAVIALTHKEREQEIDRALLKNVLDIFVQNGMGOMERYEEDFEDEFFLETNSYYSRK  
 CULA\_CICLE 138 EQVYDAIKNAKDAVIALDKEREQEIDRALLKNVLDIFVEIGMGOMERYEEDFESEFMLQDTSYYSRK  
 CULB\_CICLE 141 DLVYTEINGKVRDAVITLIDQEREQEIDRALLKNVLDIFVEIGMGOMERYEEDFEDEFFLETNSYYSRK  
 CULA\_POPTR 141 DLVYQEIINGKVRDAVISLIDQEREQEIDRALLKNVLDIFVEIGMGOMERYEEDFESEFMLQDTSYYSRK  
 CULB\_POPTR 141 NOVYQEIINGKVRDAVISLIDQEREQEIDRALLKNVLDIFVEIGMGOMERYEEDFESEFMLQDTSYYSRK  
 CULA\_PRUPE 138 DLVYREINANARVAVIGLIDQEREQEIDRALLKNVLDIFVEIGMGOMERYEEDFESEFMLQDTSYYSRK  
 CULB\_PRUPE 141 DLVYQEIINAKVRDAVISLIDQEREQEIDRALLKNVLDIFVEIGMGOMERYEEDFESEFMLQDTSYYSRK  
 CULA\_RICCO 141 DLVYQEIINAKVRDAVISLIDQEREQEIDRALLKNVLDIFVEIGMGOMERYEEDFESEFMLQDTSYYSRK  
 CULA\_CARUB 138 DLVYNEIHSKVKEAVIALDKEREQEIDRALLKNVLDIFVEIGMGOMERYEEDFESEFMLQDTSYYSRK  
 CULB\_CARUB 141 DLVYQEIQSNAKDAVIALTHKEREQEIDRALLKNVLDIVYCGNMGCEMVRKYEEDFESEFLEDTSASYSRK  
 CULA\_GLYMA 141 DLVYKEINGKVRDAVISLIDQEREQEIDRALLKNVLDIFVEIGMGOMERYEEDFESEFMLQDTSYYSRK  
 CULB\_GLYMA 141 DLVYKEINGKVRDAVISLIDQEREQEIDRALLKNVLDIFVEIGMGOMERYEEDFESEFMLQDTSYYSRK  
 CULC\_GLYMA 141 DLVYKEINGKVRDAVISLIDQEREQEIDRALLKNVLDIFVEIGMGOMERYEEDFESEFMLQDTSYYSRK  
 CULA\_ORYSJ 139 DLVYQEIINGKVRDAVISLIDQEREQEIDRALLKNVLDIFVEIGMGOMERYEEDFESEFMLQDTSYYSRK  
 CULB\_ORYSJ 126 DLVYQEIINGKVRDAVISLIDQEREQEIDRALLKNVLDIFVEIGMGOMERYEEDFESEFMLQDTSYYSRK  
 CULA\_MAIZE 139 DLVYQEIINGKVRDAVISLIDQEREQEIDRALLKNVLDIFVEIGMGOMERYEEDFESEFMLQDTSYYSRK

CUL1\_ARATH 208 ASSWIQEDSCPDYMLKSEECLEKREKRVVAHYLHSSSEPKLVEKVOHELLVVYASOLLEKEHSGCRALLRD  
 CUL2\_ARATH 208 ASRWNOENSCPDYMLKAEESLPILEKERVNTYLHSTTEPKLVAKVONELLVVYAKOLTEENEGSGCRALLRD  
 CUL1\_ARALL 208 ASSWIQEDSCPDYMLKSEECLEKREKRVVAHYLHSSSEPKLVEKVOHELLVVYASOLLEKEHSGCRALLRD  
 CUL2\_ARALL 208 ASKWSQEDSCPDYMLKAECECLKEKREKRVVAHYLHSSSEPKLVEKVOHELLVVYAKOLTEENEGSGCRALLRD  
 CULA\_BRARP 208 ASSWIQEDSCPDYMLKSEECLEKREKRVVAHYLHSSSEPKLVEKVOHELLVVYANOLLEKEHSGCRALLRD  
 CULB\_BRARP 211 ASSWIQEDSCPEYMLKAEESLKKKEKRVSHYLHSDTEPKLVANVOTNLLVSVAKOLLEKENSGCSALLRD  
 CULA\_CICLE 208 ASNWILEDSCPEYMLKAECECLKEKREKRVSHYLHSSSEPKLVEKVOHELLVVYATELLEKEHSGCRALLRD  
 CULB\_CICLE 211 ASNWILEDSCPDYMLKAECECLKEKREKRVSHYLHSSSEPKLVEKVOHELLSVYANOLLEKEHSGCHALLRD  
 CULA\_POPTR 211 ASNWILEDSCPDYMLKAECECLKEKREKRVSHYLHSSSEPKLVEKVOHELLSVYATOLLEKEHSGCHALLRD  
 CULB\_POPTR 211 AANWILEDSCPDYMLKAECECLKEKREKRVSHYLHSSSEPKLVEKVOHELLSVYANOLLEKEHSGCHALLRD  
 CULA\_PRUPE 208 ASNWILEDSCPDYMLKAECECLKEKREKRVSHYLHSSSEPKLVEKVOHELLVVYATOLLEKEHSGCRALLRD  
 CULB\_PRUPE 211 ASNWILEDSCPDYMLKAECECLKEKREKRVVAHYLHSSSEPKLVEKVOHELLSVYATOLLEKEHSGCHALLRD  
 CULA\_RICCO 211 ASNWILEDSCPDYMLKAECECLKEKREKRVVAHYLHSSSEPKLVEKVOHELLSVFANOLLEKEHSGCHALLRD  
 CULA\_CARUB 208 ASSWIQEDSCPDYMLKSEECLEKREKRVVAHYLHSSSEPKLVEKVOHELLVVYANOLLEKEHSGCRALLRD  
 CULB\_CARUB 211 ASKWIQEDSCPDYMLKSEECLEKREKRVSHYLHVAATEPKLVEKVOHELLVVYAKRIETENEGSGCRALLRD  
 CULA\_GLYMA 211 ASNWILEDSCPDYMLKAECECLKEKREKRVVAHYLHSSSEPKLVEKVOHELLSVYANOLLEKEHSGCHALLRD  
 CULB\_GLYMA 211 ASNWILEDSCPDYMLKAECECLKEKREKRVVAHYLHSSSEPKLVEKVOHELLSVYANOLLEKEHSGCHALLRD  
 CULC\_GLYMA 211 ASNWILEDSCPDYMLKAECECLKEKREKRVVAHYLHSSSEPKLVEKVOHELLSVYANOLLEKEHSGCHALLRD  
 CULA\_ORYSJ 209 AQTWILEDSCPDYMLKAECECLKEKREKRVVAHYLHSSSEPKLVEKVOHELLVQYASOLLEKEHSGCRALLRD  
 CULB\_ORYSJ 196 AQSWILEDSCPDYMLKAECECLKEKREKRVVAHYLHSSSEPKLVEKVOHELLVQYATFELLEKEHSGCFALLRD  
 CULA\_MAIZE 209 AQSWILEDSCPDYMLKAECECLKEKREKRVVAHYLHSSSEPKLVEKVOHELLVQYATFELLEKEHSGCSALLRD  
 CULA\_PICSI 211 AASWILEDSCPDYMLKAECECLKEKREKRVVAHYLHSSSEPKLVEKVOHELLVQYASOLLEKEHSGCHALLRD

CUL1\_ARATH 278 DKVDDLARMYRLYHKILRGLPEVANIIFKQHVTAEGNALVQQAEDTAINQVANTASVQEQVLRIRKVIELHD  
 CUL2\_ARATH 278 DKMDDLARMYRLYHPIQGLDPVADLFKQHTVVEGSALIKQATEAATDKAASGLKVOQVLRIRKVIELHD  
 CUL1\_ARALL 278 DKVDDLARMYRLYHKILRGLPEVANIIFKQHVTAEGNTLVQQAEDTAINQAANTASVQEQVLRIRKVIELHD  
 CUL2\_ARALL 278 DKMDDLARMYRLYHPIQGLDPVADLFKQHVTAEGNALIKQAADAATNQDAS--GVQDHLVLRKVIELHD  
 CULA\_BRARP 278 DKVDDLARMYRLYHKILRGLPEVANIIFKQHVTAEGNALVQQAEDTAINHAANTASVQEQVLRIRKVIELHD  
 CULB\_BRARP 281 DKVDDLARMYRLYHPIQGLPEVAVAFRLHVTAEGNLSLQQAEDAATSG----IVEEQVLRIRKVIELHD  
 CULA\_CICLE 278 DKVEDLSRMRYLHKIPKGLPEVANIIFKQHTAEGTVLVQQAEDAATNQGESSGAVQEQVLRIRKVIELHD  
 CULB\_CICLE 281 DKVEDLSRMERLFSKIPRGLDPVSNIFKQHVTAEGTALVKLAEDAASNKKAEEVGLQEQVLRIRKVIELHD  
 CULA\_POPTR 281 DKVEDLSRMERLFSKIPRGLDPVSGIFKQHVTAEGTALVKQAEDAASNKKADVVGLQEQVLRIRKVIELHD  
 CULB\_POPTR 281 DKVEDLSRMERLFSKIPRGLDPVSSIIFKQHVTAEGTALVKQAEDAASSKKADVVGLQEQVLRIRKVIELHD  
 CULA\_PRUPE 278 DKVEDLSRIYRLYKIPKGLPEVSSIIFKQHVTAEGTALVQQAEDVASNQTS--GAGTQEQVLRIRKVIELHD  
 CULB\_PRUPE 281 DKVDDLARMERLFSKIPRGLDPVSSIIFKQHVTAEGTALVKQAEDAASNRRKAEVGLQEQVLRIRKVIELHD  
 CULA\_RICCO 281 DKVEDLSRMERLFSKIPRGLDPVSSIIFKQHVTAEGTALVKLAEDAASNKKAEEVGLQEQVLRIRKVIELHD  
 CULA\_CARUB 278 DKVDDLARMYRLYHKILRGLPEVANIIFKQHVTAEGNALVQQAEDTAINQAANTASVQEQVLRIRKVIELHD  
 CULB\_CARUB 281 DKMDDLARMYRLYHPIQGLDPVADLFKQHVTAEGNALIKQAADAATNQDASGVQVQVLRIRKVIELHD  
 CULA\_GLYMA 281 DKVEDLSRMERLFSKIPRGLDPVSNIFKQHVTEGMALVKQAEDAASNKKAEEVGLQEQVLRIRKVIELHD  
 CULB\_GLYMA 281 DKVEDLSRMERLFSKIPRGLDPVSSIIFKQHVTEGMALVKHAEDAASNKKAEEVGLQEQVLRIRKVIELHD  
 CULC\_GLYMA 281 DKVEDLSRMERLFSKIPRGLDPVSSIIFKQHVTEGMALVKLAEDAV--STKAEIVGLQEQVLRIRKVIELHD  
 CULA\_ORYSJ 279 DKVDDLARMYRLYHPIQGLPEVSIIFKQHVTEGNTALVKQAEDAASNKKPEIVGLQEQVLRIRKVIELHD  
 CULB\_ORYSJ 266 DKVEDLSRMYRLFSKINRGLPEPTANMFKHTVHTNEGTALVKQAEDSASNKKPEMVGQEQVLRIRKVIELHD  
 CULA\_MAIZE 279 DKVEDLSRMYRLFSKISRGLPEPTSNMFKHTVHTNEGTALVKQAEDSASNKKPEIVGMQEQVLRIRKVIELHD  
 CULA\_PICSI 281 DKVDDLARMYRLYHPIKGLPEVSLIFKQHVTEGTSLVKHAEDAASNKKAEEVGLQEQVLRIRKVIELHD

CUL1\_ARATH 348 KYMAYVTECFQNHFLFHKALKEAFEVFCNKTAVAGSSSAELLATFCDNILKKGSEKLSDEATEETLEKVV  
 CUL2\_ARATH 348 KEMAYVTECFQKHSFLFHKALKEAFEVFCNKTAVAGVSSAELLATYCDNILKTTGGTEKLENEDELEETLEKVV  
 CUL1\_ARALL 348 KYMAYVTECFQNHFLFHKALKEAFEVFCNKTAVAGSSSAELLATFCDNILKKGSEKLSDEATEETLEKVV  
 CUL2\_ARALL 346 KYMAYVTECFQKHSFLFHKALKEAFEVFCNKTAVAGVSSAELLATYCDNILKTTGGSEKLSFEVTEETLEKVV  
 CULA\_BRARP 348 KYMAYVTECFQNHFLFHKALKEAFEVFCNKTAVAGSSSAELLATFCDNILKKGSEKLSDEATEETLEKVV  
 CULB\_BRARP 346 KYMAYVTECFQNHFLFHKSLSKEAFEVFCNKTAVAGSSSAELLATFCDNVFKKAANKSNDLSTESTIDNVV  
 CULA\_CICLE 348 KYMEYVTECFQNHFLFHKALKEAFEVFCNKTAVAGSSSAELLATFCDNILKKGSEKLSDEATEETLEKVV  
 CULB\_CICLE 351 KYLAYVTECFQNHFLFHKSLSKEAFEVFCNKTAVAGSSSAELLATFCDNILKKGSEKLSDEATEETLEKVV  
 CULA\_POPTR 351 KYLAYVTECFQNHFLFHKALKEAFEVFCNKTAVAGSSSAELLATFCDNILKKGSEKLSDEATEETLEKVV  
 CULB\_POPTR 351 KYLAYVTECFQNHFLFHKALKEAFEVFCNKTAVAGSSSAELLATFCDNILKKGSEKLSDEATEETLEKVV  
 CULA\_PRUPE 347 KYMAYVTECFQNHFLFHKALKEAFEVFCNKTAVAGSSSAELLATFCDNILKKGSEKLSDEATEETLEKVV  
 CULB\_PRUPE 351 KYLAYVTECFQNHFLFHKALKEAFEVFCNKTAVAGSSSAELLATFCDNILKKGSEKLSDEATEETLEKVV  
 CULA\_RICCO 351 KYLAYVTECFQNHFLFHKALKEAFEVFCNKTAVAGSSSAELLATFCDNILKKGSEKLSDEATEETLEKVV  
 CULA\_CARUB 348 KYMAYVTECFQKHSFLFHKALKEAFEVFCNKTAVAGSSSAELLATFCDNILKKGSEKLSDEATEETLEKVV  
 CULB\_CARUB 351 KYMAYVTECFQKHSFLFHKALKEAFEVFCNKTAVAGSSSAELLATYCDNILKKGSEKLSDEATEETLEKVV  
 CULA\_GLYMA 351 KYLAYVTECFQNHFLFHKALKEAFEVFCNKTAVAGSSSAELLATFCDNILKKGSEKLSDEATEETLEKVV  
 CULB\_GLYMA 351 KYLAYVTECFQNHFLFHKALKEAFEVFCNKTAVAGSSSAELLATFCDNILKKGSEKLSDEATEETLEKVV  
 CULC\_GLYMA 350 KYLAYVTECFQNHFLFHKALKEAFEVFCNKTAVAGSSSAELLATFCDNILKKGSEKLSDEATEETLEKVV  
 CULA\_ORYSJ 349 KYMAYVTECFQGHFLFHKALKEAFEVFCNKTAVAGSSSAELLATFCDNILKKGSEKLSDEATEETLEKVV  
 CULB\_ORYSJ 336 KYMAYVTECFQGHFLFHKALKEAFEVFCNKTAVAGSSSAELLATFCDNILKKGSEKLSDEATEETLEKVV  
 CULA\_MAIZE 349 KYMAYVTECFQGHFLFHKALKEAFEVFCNKTAVAGSSSAELLATFCDNILKKGSEKLSDEATEETLEKVV

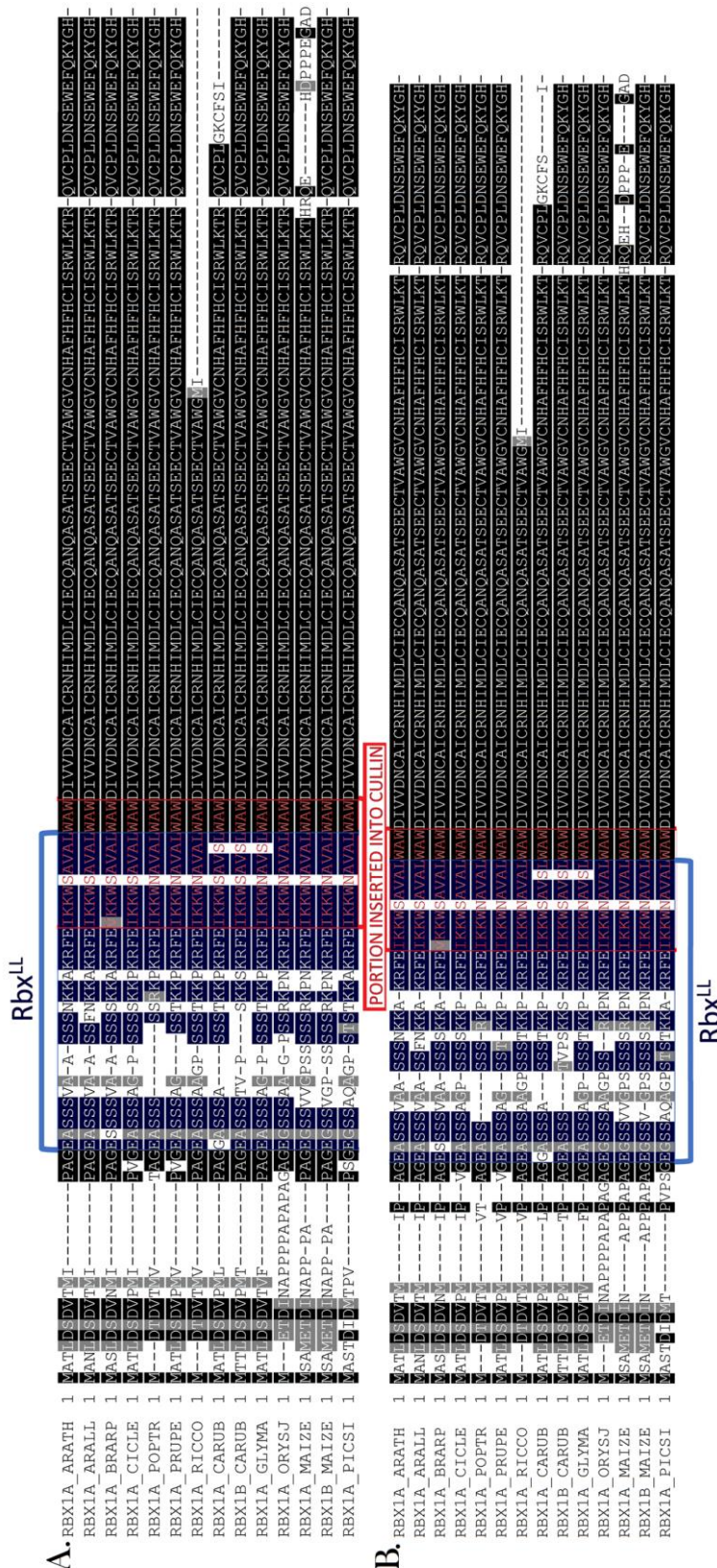


CUL1\_ARATH 418 KLLAYISDKDLFAEFYRKKLARLLFDRSANDDHERSILTKLKQCCGGQFTSKMEGMVDTLTLARENQNS  
 CUL2\_ARATH 418 KLLVYISDKDLFAEFYRKKARLLFDRSANDDHERSILTKLKQCCGGQFTSKMEGMVDTLTLAREHOTN  
 CUL1\_ARALL 418 KLLAYISDKDLFAEFYRKKLARLLFDRSANDDHERSILTKLKQCCGGQFTSKMEGMVDTLTLARENQNS  
 CUL2\_ARALL 416 KLLVYISDKDLFAEFYRKKARLLFDRSANDDHERSILTKLKQCCGGQFTSKMEGMVDTLTLAREQOCTN  
 CULA\_BRARP 418 KLLAYISDKDLFAEFYRKKLARLLFDRSANDDHERSILTKLKQCCGGQFTSKMEGMVDTLTLARENQNS  
 CULB\_BRARP 416 KLLDYISDKDLFAEFYRKKLARLLFGKF-SDDHERSILTKLKQCCGGQFTSKMEGMVDTLTLAREKDOCTG  
 CULA\_CICLE 418 KLLAYISDKDLFAEFYRKKLARLLFDRSANDDHERSILTKLKQCCGGQFTSKMEGMVDTLTLARENQTS  
 CULB\_CICLE 421 KLLAYISDKDLFAEFYRKKLARLLFDRSANDDHERSILTKLKQCCGGQFTSKMEGMVDTLTLARENQTS  
 CULA\_POPTR 421 KLLAYISDKDLFAEFYRKKLARLLFDRSANDDHERSILTKLKQCCGGQFTSKMEGMVDTLTLARENQTS  
 CULB\_POPTR 421 KLLAYISDKDLFAEFYRKKLARLLFDRSANDDHERSILTKLKQCCGGQFTSKMEGMVDTLTLARENQTS  
 CULA\_PRUPE 417 KLLAYISDKDLFAEFYRKKLARLLFDRSANDDHERSILTKLKQCCGGQFTSKMEGMVDTLTLARDNOAN  
 CULB\_PRUPE 421 KLLAYISDKDLFAEFYRKKLARLLFDRSANDDHERSILTKLKQCCGGQFTSKMEGMVDTLTLARENQAS  
 CULA\_RICCO 421 KLLAYISDKDLFAEFYRKKLARLLFDRSANDDHERSILTKLKQCCGGQFTSKMEGMVDTLTLARENQTS  
 CULA\_CARUB 418 KLLAYISDKDLFAEFYRKKLARLLFDRSANDDHERSILTKLKQCCGGQFTSKMEGMVDTLTLARENQNS  
 CULB\_CARUB 421 KLLVYISDKDLFAEFYRKKARLLFDRSANDDHERSILTKLKQCCGGQFTSKMEGMVDTLTLARDNQTS  
 CULA\_GLYMA 421 KLLAYISDKDLFAEFYRKKLARLLFDRSANDDHERSILTKLKQCCGGQFTSKMEGMVDTLTLARENQTS  
 CULB\_GLYMA 421 KLLAYISDKDLFAEFYRKKLARLLFDRSANDDHERSILTKLKQCCGGQFTSKMEGMVDTLTLARENQTS  
 CULC\_GLYMA 420 KLLAYISDKDLFAEFYRKKLARLLFDRSANDDHERSILTKLKQCCGGQFTSKMEGMVDTLTLARENQTS  
 CULA\_ORYSJ 419 RLLAYISDKDLFAEFYRKKLARLLFDRSANDDHERSILTKLKQCCGGQFTSKMEGMVDTLTLARDHQAQ  
 CULB\_ORYSJ 406 RLLAYISDKDLFAEFYRKKLARLLFDRSANDDHERSILTKLKQCCGGQFTSKMEGMVDTLTLARDHQAQ  
 CULA\_MAIZE 419 RLLAYISDKDLFAEFYRKKLARLLFDRSANDDHERSILTKLKQCCGGQFTSKMEGMVDTLTLARDHQAQ  
 CULA\_PICSI 421 KLLAYISDKDLFAEFYRKKLARLLFDRSANDDHERSILTKLKQCCGGQFTSKMEGMVDTLTLARENQCTN

CUL1\_ARATH 488 FEYILGNSNPAANPGIDLTVTLTGGFWPSYKSFIDLNLSEMIKCEVVFKGFYETKTKHRKLTWYISLGTG  
 CUL2\_ARATH 488 FEYELSVNKTKKLGMDFVTVTLTGGFWPSYKTFIDLNLSEMIKCEVVFKGFYETKTKHRKLTWYISLGTG  
 CUL1\_ARALL 488 FEYILGNSNPAANPGIDLTVTLTGGFWPSYKSFIDLNLSEMIKCEVVFKGFYETKTKHRKLTWYISLGTG  
 CUL2\_ARALL 486 FEYILSASLTTKLIDLTVTLTGGFWPSYKTFIDLNLSEMIKCEVVFKGFYETKTKHRKLTWYISLGTG  
 CULA\_BRARP 488 FEYILGNSNPAANPGIDLTVTLTGGFWPSYKSFIDLNLSEMIKCEVVFKGFYETKTKHRKLTWYISLGTG  
 CULB\_BRARP 485 FEYILKNATGKPKGMDFVTVTLTGGFWPSYKTFIDLNLSEMIKCEVVFKGFYETKTKHRKLTWYISLGTG  
 CULA\_CICLE 488 FEYILSNQNAHPGIDLTVTLTGGFWPSYKSFIDLNLSEMIKCEVVFKGFYETKTKHRKLTWYISLGTG  
 CULB\_CICLE 491 FEYILSNPNANPGIDLTVTLTGGFWPSYKSFIDLNLSEMIKCEVVFKGFYETKTKHRKLTWYISLGTG  
 CULA\_POPTR 491 FEYILSNPNANPGIDLTVTLTGGFWPSYKSFIDLNLSEMIKCEVVFKGFYETKTKHRKLTWYISLGTG  
 CULB\_POPTR 491 FEYILSNPNANPGIDLTVTLTGGFWPSYKSFIDLNLSEMIKCEVVFKGFYETKTKHRKLTWYISLGTG  
 CULA\_PRUPE 487 FEYILHNPNVNPMDLTVTLTGGFWPSYKSFIDLNLSEMIKCEVVFKGFYETKTKHRKLTWYISLGTG  
 CULB\_PRUPE 491 FEYILSNPNANPGIDLTVTLTGGFWPSYKSFIDLNLSEMIKCEVVFKGFYETKTKHRKLTWYISLGTG  
 CULA\_RICCO 491 FEYILSNPNANPGIDLTVTLTGGFWPSYKSFIDLNLSEMIKCEVVFKGFYETKTKHRKLTWYISLGTG  
 CULA\_CARUB 488 FEYILGHNPANPGIDLTVTLTGGFWPSYKSFIDLNLSEMIKCEVVFKGFYETKTKHRKLTWYISLGTG  
 CULB\_CARUB 491 FEYILSTNTNTKLGIDLTVTLTGGFWPSYKTFIDLNLSEMIKCEVVFKGFYETKTKHRKLTWYISLGTG  
 CULA\_GLYMA 491 FEYILSNPNANPGIDLTVTLTGGFWPSYKSFIDLNLSEMIKCEVVFKGFYETKTKHRKLTWYISLGTG  
 CULB\_GLYMA 491 FEYILSNPNANPGIDLTVTLTGGFWPSYKSFIDLNLSEMIKCEVVFKGFYETKTKHRKLTWYISLGTG  
 CULC\_GLYMA 490 FEYILSNPNANPGIDLTVTLTGGFWPSYKSFIDLNLSEMIKCEVVFKGFYETKTKHRKLTWYISLGTG  
 CULA\_ORYSJ 489 FEYILSTHSELNPGIALAVTVTLTGGFWPSYKTFIDLNLSEMIKCEVVFKGFYETKTKHRKLTWYISLGTG  
 CULB\_ORYSJ 476 FEYFVAHQELNPGIDLAVTVTLTGGFWPSYKTFIDLNLSEMIKCEVVFKGFYETKTKHRKLTWYISLGTG  
 CULA\_MAIZE 489 FEYFVAGHPNPNPGIDLAVTVTLTGGFWPSYKTFIDLNLSEMIKCEVVFKGFYETKTKHRKLTWYISLGTG  
 CULA\_PICSI 491 FEYILNENPLAHPGIDLTVTLTGGFWPSYKSFIDLNLSEMIKCEVVFKGFYETKTKHRKLTWYISLGTG

CUL1\_ARATH 558 HINGKFDQKAEELIVSTYQAAVLLLFNTIDKLSYTEILAQNLNLSHEDIVRLLHLSLSCAKYKILKEPNTK  
 CUL2\_ARATH 558 QLAGKFFDKKTEELIVVTYQAAVLLLFNTIRLSYTEILAEQNLNLSHEDIVRLLHLSLSCAKYKILKEPMSR  
 CUL1\_ARALL 558 HINGKFDQKAEELIVSTYQAAVLLLFNTIDKLSYTEILAQNLNLSHEDIVRLLHLSLSCAKYKILKEPSTK  
 CUL2\_ARALL 556 HINGKFFDKKTEELIVSTYQAAVLLLFNNAIRLSYTEILAEQNLNLSHEDIVRLLHLSLSCAKYKILKEPMSR  
 CULA\_BRARP 558 HINGKFDQKAEELIVSTYQAAVLLLFNTIDKLSYTEILAQNLNLSHEDIVRLLHLSLSCAKYKILKEPSTK  
 CULB\_BRARP 555 NETARFDAPTEELIVSTYQAAVLCFNFHTIRLTYQELIDQNLNLSHEDIVRLLHLSLSCAKYKILKEPMSR  
 CULA\_CICLE 558 NINGKFFDKKTEELIVSTYQAAVLLLFNTIDKLSYTEILAEQNLNLSHEDIVRLLHLSLSCAKYKILKEPNTK  
 CULB\_CICLE 561 NINGKFFDKKTEELIVTYQASALLLFNSDRLSYSEIMTQNLNLSHEDIVRLLHLSLSCAKYKILKEPNTK  
 CULA\_POPTR 561 NINGKFFDKKTEELIVTYQASALLLFNSDRLSYSEIMTQNLNLSHEDIVRLLHLSLSCAKYKILKEPNTK  
 CULB\_POPTR 561 NINGKFFDKKTEELIVTYQASALLLFNSDRLSYSEIMTQNLNLSHEDIVRLLHLSLSCAKYKILKEPNTK  
 CULA\_PRUPE 557 NINGKFFDKKTEELIVTYQAAVLLLFNTIDKLSYTEILAEQNLNLSHEDIVRLLHLSLSCAKYKILKEPNTK  
 CULB\_PRUPE 561 NINGKFFDKKTEELIVTYQASALLLFNSDRLSYSEIMTQNLNLSHEDIVRLLHLSLSCAKYKILKEPNTK  
 CULA\_RICCO 561 NINGKFFDKKTEELIVTYQASALLLFNSDRLSYSEIMTQNLNLSHEDIVRLLHLSLSCAKYKILKEPNTK  
 CULA\_CARUB 558 HINGKFDQKAEELIVSTYQAAVLLLFNTIDKLSYTEILAEQNLNLSHEDIVRLLHLSLSCAKYKILKEPSTK  
 CULB\_CARUB 561 HINGKFFDKKTEELIVSTYQAAVLLLFNTIRLSYTEILAEQNLNLSHEDIVRLLHLSLSCAKYKILKEPMSR  
 CULA\_GLYMA 561 NINGKFFDKKTEELIVTYQASALLLFNSDRLSYSEIMTQNLNLSHEDIVRLLHLSLSCAKYKILKEPNTK  
 CULB\_GLYMA 561 NINGKFFDKKTEELIVTYQASALLLFNSDRLSYSEIMTQNLNLSHEDIVRLLHLSLSCAKYKILKEPNTK  
 CULC\_GLYMA 560 NINGKFFDKKTEELIVTYQASALLLFNSDRLSYSEIMTQNLNLSHEDIVRLLHLSLSCAKYKILKEPNTK  
 CULA\_ORYSJ 559 NINGKFFDKKTEELIVTYQAAVLLLFNNGVDRLSYSEIMTQNLNLSHEDIVRLLHLSLSCAKYKILKEPNTK  
 CULB\_ORYSJ 546 NINGKFFDKKTEELIVTYQAAVLLLFNNGVDRLSYSEIMTQNLNLSHEDIVRLLHLSLSCAKYKILKEPNTK  
 CULA\_MAIZE 559 NINGKFFDKKTEELIVTYQAAVLLLFNNGVDRLSYSEIMTQNLNLSHEDIVRLLHLSLSCAKYKILKEPNTK

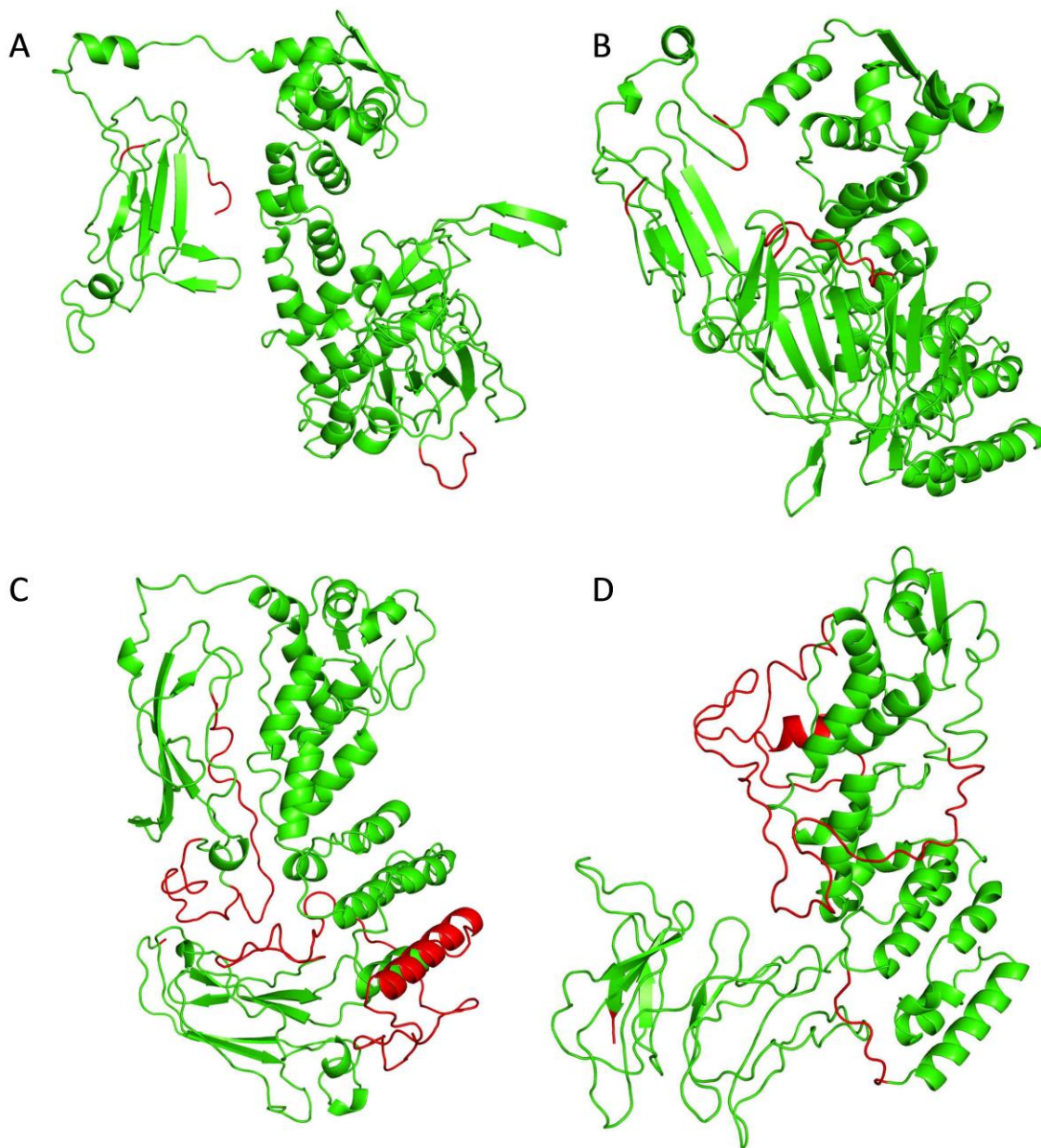




**Supplemental Figure 6: Multiple Sequence Alignments of *At*Rbx1 Homologs**

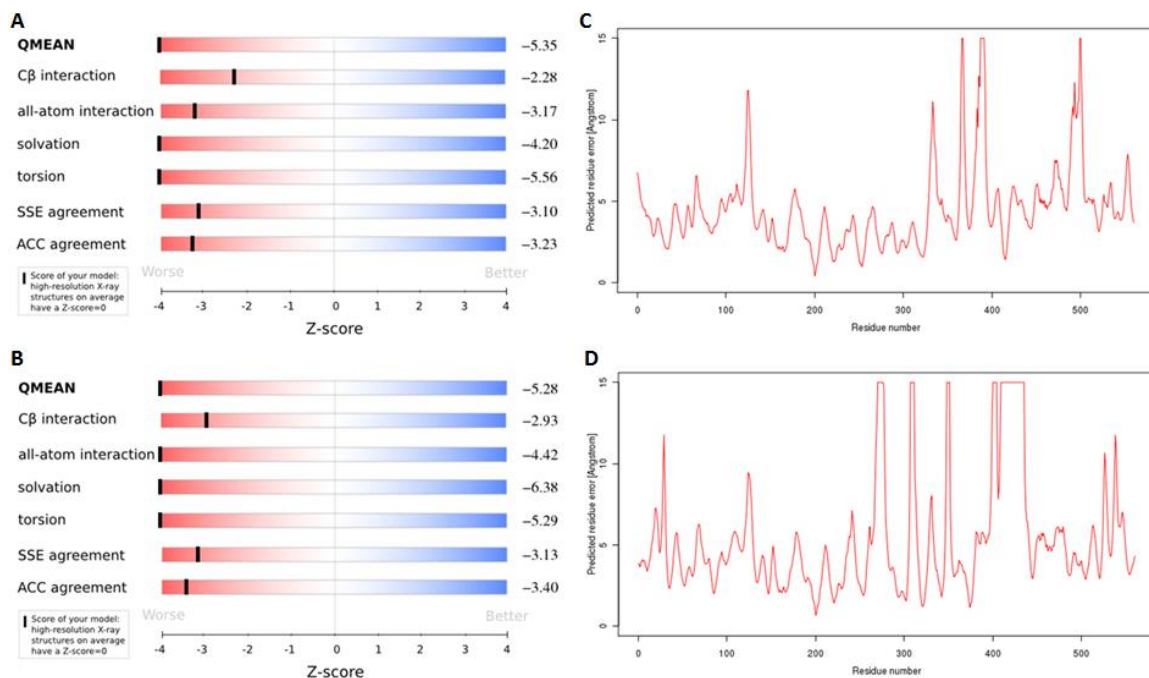
**A.** A MSA of Rbx1 proteins homologous to *At*Rbx1. Alignment was created using default Expresso<sup>55</sup> settings. The region of the alignment associated with the LL region of the LRBs is marked in blue and labeled as Rbx<sup>LL</sup>. Additionally, the portion of Rbx1 that is known to be inserted inside of Cullin proteins in CRL complexes<sup>25,28,29</sup> is labeled below the alignment and marked in red. Residues with a high overall conservation (above 70%) are shown highlighted in black, while residues that are mostly conserved and have consensus due to residue similarity (above 70%) are shown highlighted in grey. Gaps in the alignment are denoted by a dash (-).

**B.** A manually edited MSA of Rbx1 proteins homologous to *At*Rbx1. The alignment also marked the Rbx<sup>LL</sup> region in blue and the portion of Rbx1 inserted into Cullin in red. Residues with an overall conservation above 70% are shown highlighted in black, while residues that have consensus due to residue similarity (above 70%) are shown highlighted in grey. Gaps in the alignment are denoted by a dash (-).



**Supplemental Figure 7: *AtLRB* Phyre2 Models Displayed by Percent Confidence**

A figure showing the (A) *AtLRB2A*, (B) *AtLRB2B*, (C) *AtLRB1*, and (D) *AtLRB3* models created using the intensive mode of the protein homology modeling program Phyre2<sup>65</sup>. Each model was developed by combining and overlapping the known structural templates of multiple protein structures found in PDB<sup>64</sup> (**Supplemental Table 1**). Models are colored based on percent confidence given by Phyre2<sup>72</sup>, with residues that are modeled with >90% confidence colored in green, while residues modeled using de novo methods are colored in red. Protein images were created using POLYVIEW-3D<sup>76</sup>.

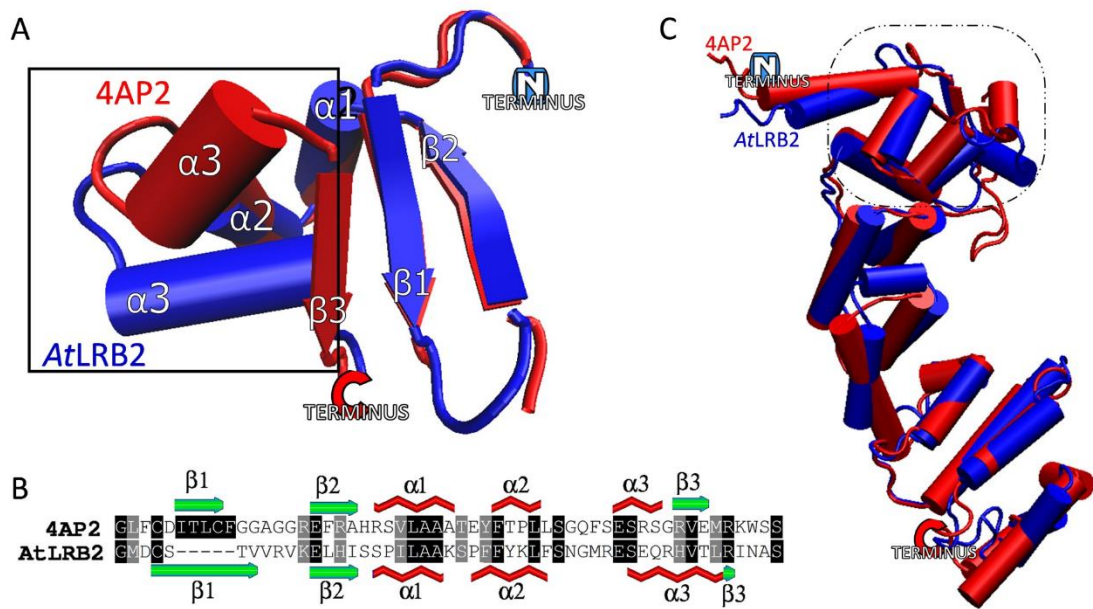


### Supplemental Figure 8: QMEAN Structural Analysis of *AtLRB2* Models

Z-score analysis of the (A.) *AtLRB2A* and (B.) *AtLRB2B* homology models that were created on February 9<sup>th</sup>, 2015 and April 7<sup>th</sup>, 2015, respectively, using Phyre2<sup>65</sup>.

The amount of residue error present in the (C.) *AtLRB2A* and (D.) *AtLRB2B* homology models that were created using Phyre2<sup>65</sup>. The plot on the right displays the amount of residue error present for each protein sequence, with a higher predicted error being associated with higher probability of region unreliability.

The QMEAN analysis<sup>73,74</sup> for each model has a plot on the left depicting the relative Z-score for the overall **QMEAN** (a linear combination of the six following scores), **C $\beta$  interactions** score (interaction potentials determined by the secondary-structure-specific interactions made by the C $\beta$  atoms<sup>89</sup>), **all-atom interactions** score (interaction potentials determined by the secondary-structure-specific interactions made by any atoms in the protein), the **solvation** score (the potential for certain residue types to have a specific degree of exposure to the solvent when not buried), and the **extended torsion potential** (the torsion angle over three residues in order to test the propensity for certain amino acids to conform to a certain local geometries compared to other residues). The **SSE agreement** is scored by the difference between the predicted secondary structures of the model (using the **PSIPRED** web server<sup>90</sup>) and the calculated secondary structures of the model (using **DSSP**, which contains all secondary structure alignments for all proteins in PDB<sup>91</sup>). The **ACC agreement** compares the predicted solvent accessibility that is determined using the ACCpro solvent accessibility prediction server<sup>92</sup> and the calculated solvent accessibility determined by **DSSP**<sup>89</sup>. A higher **Z-score** is associated with a better structural model, as the Z-score estimates the amount of ‘nativeness’ in a model, presenting the overall likelihood of the model being comparable to reference structures that have already been crystalized.



### Supplemental Figure 9: Comparative Structural Modeling of the BTB/BACK Domains

**A.** Overlay of the BTB domain from the predicted LRB2 model *AtLRB2A* (blue) with the known crystal structure of the BTB domain of the Kelch-like Protein 11 (red, PDB ID: **4AP2**<sup>35</sup>) using MultiSeq<sup>88</sup>. Model is labeled according to the fold topology diagram described in **Figure 5**. A box was used to show the region of the BTB domain containing major differences in structure.

**B.** Sequence alignment of the BTB domains from **4AP2** and *AtLRB2* (residues 143-190). Secondary structure for both proteins is shown, with fold topology labeled as shown in **A**.

**C.** Overall structural alignment of the BTB, 3-Box, and BACK domains for *AtLRB2A* (residues 126-380) and **4AP2**. The BTB domain is enclosed within the dotted oval.

**PHOS SITE:**

```
LRB1_ARATH 1 M-RGS-NNTDLFDPK-TEMDS---NFSRHGSSS---EGDFGFANFNSNFSDRLLRIEIL
LRB2_ARATH 1 M-RGTENTDLFDPK-TQMDP---DFTRHGSSS---DGDFGFANFNSNFSDRLLRIEIM
LRBA_ARALL 1 M-RGTNENTDLFDPK-TQMDP---DFTRHGSSS---DGDFGFANFNSNFSDRLLRIEIM
LRBB_ARALL 1 M-RGS-NNTDLFDPK-TDMDS---NFSRHGSSS---EGDFGFANFNSNFSDRLLRIEIL
LRBA_BRARP 1 M-RGG-ENTDLFDPK-TQMDP---DFSRHGSSS---EGDFGFANFNSNFSDRLLRIEIM
LRBA_CICLE 1 M-R-D-VNTDLFDPK-TEMDS---DISRSASSS---DGDFGFANFNSNFSDRLLRIEIM
LRBA_POPTR 1 MLR-G-SNTDLFDPK-TEMDS---DFTRHGSSAS---DGDFGFANFNSNFSDRLLRIEIM
LRBB_POPTR 1 MMR-G-SNSDLFDPK-TEMES---DSTRGGSSAS---DGDFGFANFNSNFSDRLLRIEIM
LRBA_PRUPE 1 M-MKE-LNTDLFDPK-STLMDP---DFSRTDTPSADADADDFAFANFNSNFSDRLLRIEIM
LRBA_RICCO 1 M-R-G-SNSDLFDPK-TEMES---VYSRGAASSS---DGDFGFANFNSNFSDRLLRIEIM
LRBA_CARUB 1 M-RGAADNTDLFDPK-IQMDS---DFSRHGSSS---DGDFGFANFNSNFSDRLLRIEIM
LRBB_CARUB 1 M-RGS-NNTDLFDPK-TEMDS---TFSRHGSSP---EGDFGFANFNSNFSDRLLRIEIL
LRBB_GLYMA 1 M-K-D-FNSDLFDPG-MVMDSSSSDYSRASASSS---DADFGFANFNSNFSDRILRIEIM
LRBA_ORYSJ 1 -----MDP---DFSRA--SR---GPSFAFANFNSVNFSDRVLRIEIV
LRBA_MAIZE 1 -----MDP---DFSRA--SG---GPSFEFANFNSVNFSDRVLRIEIV
LRBB_MAIZE 1 -----MDP---DFSRA--SG---GPSFEFANFNSVNFSDRVLQIEIV
```

**PHOS SITE:**

```
LRB1_ARATH 51 GGPSSD---SRSDAEGCTSADWARHRKRREDNKKDNG--VAISDIVACAEQILTDNNQ
LRB2_ARATH 52 GGPSSD---SRSEVEGCTSADWARHRKRREDIKKESG--VTISDIVACPEEQILTDEQ
LRBA_ARALL 52 GGPSSD---SRSDVEGCTSADWARHRKRREDIKKESGG-VTISDIVACPEEQILTDEQ
LRBB_ARALL 51 GGPSSD---SRSDGEGCTSADWARHRKRREDNKRDN--VAISDIVACAEQILTDNNQ
LRBA_BRARP 51 GNPSSD---SRSDVEGCTSADWARHRKRREDIKKESV---TISDIVACPEEQILTDEQ
LRBA_CICLE 50 GDPPE---SRSDGEGCTSADWARDKRREDIKKDN----GLDLSACPEEQILTDNQ
LRBA_POPTR 51 GGSAE---NRADGEGCTSIIDWARHRKRREDIKKDINN-VRAGDLSVGAEEQILGS-NQ
LRBB_POPTR 51 GGSAE---SRADGEGCTSIIDWARHRKRREDIKKDNN-----NGAEEQILGS-NQ
LRBA_PRUPE 56 GDTPPE---SRPDSEACTSIADWARHRKRREDIKKEN----IPDPSECPEEQILNDNQ
LRBA_RICCO 50 DESPD---NRCDGEGCNSIADWARHRKRREDIKKDNA--V---EVSAGAEQILTDNQ
LRBA_CARUB 52 GGPSSD---SRSDVEGCTSADWARHRKRREDIKKESG--VTISDIVACPEEQILTDEQ
LRBB_CARUB 51 GGPSSD---SRSDGEGCTSADWARHRKRREDNKKDNG--VAISDIVACAEQILTDNNQ
LRBB_GLYMA 53 GDPVE---ARPDSEGGTTIADWARHRKRREDIKKDN----VVDLTLPPDEQILNE-NQ
LRBA_ORYSJ 34 AGDDAAGAKGAAGEGCSSLADWAHQRRREELRREKESGK--YTDLETCKV-----
LRBA_MAIZE 34 AGDDALGAKGATGEGCSSLADWACHRKRREELRRDKESRKYMPDPANCKV-----
LRBB_MAIZE 34 AGDDALGAKGATGEGCSSLADWACHRKRREELRRDKESRKYMPDPANCKV-----
```

**PHOS SITE:**

```
LRB1_ARATH 106 PDMDDAPGGDNLDE-GEAMVEE--ALSGD---DD-ASSEPNWGDICSTVVRVKELHIS
LRB2_ARATH 106 PDMDCPGGENPDEEGEAMVEE--ALSGD---EEEISSSEPNWGMDCSTVVRVKELHIS
LRBA_ARALL 107 PDMDCPGGENLDDEGEAMVEE--ALSGD---EEEISSSEPNWGMDCSTVVRVKELHIS
LRBB_ARALL 106 PDMDDPGGGDNLDE-GEAMVEE--ALSGD---DD-ASSEPNWGDICSTVVRVKELHIS
LRBA_BRARP 104 PDMDCPGGGDNLDE-GEAMIEE--SISGD---EEDTSSSEPSWGMDCSKVVRVIELHIS
LRBA_CICLE 99 PDMDDCVGCENQDEE-VEAMIEG--SPSGD---EAANGNESSWSMDCSTVVRVKTLHIS
LRBA_POPTR 106 PDMDDCVGCDNQDEE-AEAMVEG--SPSGD---EAADGIESWSMDCSTVVRVKTLHIS
LRBB_POPTR 98 PDMDDCVVGDNQDEE-GEAMVEV--SPSDD---EAGDGNNESSWSMDCSTVVRVKTLHIS
LRBA_PRUPE 107 PDMDDCEGCENQDEE-AVAMVEE--SPSGD---EAANSNDSDWGMDCSTVVRVKTLHIS
LRBA_RICCO 99 PDMDDCVGCENQDED-AVAMIEE--PPSGD---EAVDGNESWWSMDCSTVVRVKTLHIS
LRBA_CARUB 106 PDMDCPGGENIDDE-GEAMVEEEALSGD---EDEISSSEPNWGMDCSTVVRVKELHIS
LRBB_CARUB 106 PDMDDCPGGDNLDE-GEAMVEE--ALSGD---DD-VSSSEPNWGDICSTVVRVKELHIS
LRBB_GLYMA 104 PDMDDFVPSENQDED-AVAMVEE--PPSGD---EAANSNDSNWNMDCSAVVRVRTLHIS
LRBA_ORYSJ 84 -EAECDTYEENNEE-PVAMIEE--SPPDIGQDGEDGSDSSWSMECTQVLRVKSIYIS
LRBA_MAIZE 85 -EAECDAYEEG-NE-PVAMIEE--SPPDIEADGEDGKSSDSYCSMECTQVLRVKSMYIS
LRBB_MAIZE 85 -EAECDAYEEG-NE-PVAMIEE--SPPDIEADGEDGKSSDSYCSMECTQVLRVKSMYIS
```

PHOS SITE:

|            |     |   |   |   |   |   |   |   |   |   |   |   |   |   |   |   |   |   |   |   |   |   |   |   |   |   |   |   |   |   |   |   |   |   |   |   |   |   |   |   |   |   |   |   |   |   |   |   |   |   |   |   |   |   |   |   |   |   |   |   |
|------------|-----|---|---|---|---|---|---|---|---|---|---|---|---|---|---|---|---|---|---|---|---|---|---|---|---|---|---|---|---|---|---|---|---|---|---|---|---|---|---|---|---|---|---|---|---|---|---|---|---|---|---|---|---|---|---|---|---|---|---|---|
| LRB1_ARATH | 158 | S | P | I | L | A | A | K | S | P | F | F | Y | K | L | F | S | N | G | M | R | E | S | E | Q | R | H | V | T | L | R | I | S | A | Q | E | E | G | A | L | M | E | L | L | N | F | M | Y | S | N | S | L | S | V | T | T | A | P | A | L |
| LRB2_ARATH | 160 | S | P | I | L | A | A | K | S | P | F | F | Y | K | L | F | S | N | G | M | R | E | S | E | Q | R | H | V | T | L | R | I | N | A | S | E | E | A | A | L | M | E | L | L | N | F | M | Y | S | N | A | V | S | V | T | T | A | P | A | L |
| LRBA_ARALL | 161 | S | P | I | L | A | A | K | S | P | F | F | Y | K | L | F | S | N | G | M | R | E | S | E | Q | R | H | V | T | L | R | I | N | A | S | E | E | A | A | L | M | E | L | L | N | F | M | Y | S | N | A | V | S | V | T | T | A | P | A | L |
| LRBB_ARALL | 158 | S | P | I | L | A | A | K | S | P | F | F | Y | K | L | F | S | N | G | M | R | E | S | E | Q | R | H | V | T | L | R | I | N | A | S | E | E | A | A | L | M | E | L | L | N | F | M | Y | S | N | S | L | S | V | T | T | A | P | A | L |
| LRBA_BRARP | 157 | S | P | I | L | A | A | K | S | P | F | F | Y | K | L | F | S | N | G | M | R | E | S | E | Q | R | H | V | T | L | R | I | N | A | S | E | E | A | A | L | M | E | L | L | N | F | M | Y | S | N | V | S | V | A | T | A | P | A | L |   |
| LRBA_CICLE | 152 | S | P | I | L | A | A | K | S | P | F | F | Y | K | L | F | S | N | G | M | K | E | S | E | Q | R | H | V | A | L | R | I | N | A | S | E | E | A | A | L | M | E | L | L | N | F | M | Y | S | N | T | L | S | T | T | A | A | P | A | L |
| LRBA_POPTR | 159 | S | P | I | L | A | A | K | S | P | F | F | Y | K | L | F | S | N | G | M | R | E | S | E | Q | R | H | V | T | L | R | I | N | A | S | E | E | A | A | L | M | E | L | L | N | F | M | Y | S | N | T | L | T | A | S | Q | A | P | Q | L |
| LRBB_POPTR | 151 | S | P | I | L | A | A | K | S | P | F | F | Y | K | L | F | S | N | G | M | R | E | S | E | Q | R | H | V | T | L | R | I | N | A | S | E | E | A | A | L | M | E | L | L | N | F | M | Y | S | N | T | L | T | A | S | Q | A | P | Q | L |
| LRBA_PRUPE | 160 | S | P | I | L | A | A | K | S | P | F | F | Y | K | L | F | S | N | G | M | R | E | S | E | Q | R | H | V | T | L | R | I | N | A | S | E | E | A | A | L | M | E | L | L | N | F | M | Y | R | N | S | L | T | T | T | S | A | P | A | L |
| LRBA_RICCO | 152 | S | P | I | L | A | A | K | S | P | F | F | Y | K | L | F | S | N | G | M | R | E | S | E | Q | R | H | V | T | L | R | I | N | A | S | E | E | A | A | L | M | E | L | L | N | F | M | Y | S | N | S | L | S | T | N | T | A | P | G | L |
| LRBA_CARUB | 161 | S | P | I | L | A | A | K | S | P | F | F | Y | K | L | F | S | N | G | M | R | E | S | E | Q | R | H | V | T | L | R | I | N | A | S | E | E | A | A | L | M | E | L | L | N | F | M | Y | S | N | A | V | S | V | T | T | A | P | A | L |
| LRBB_CARUB | 157 | S | P | I | L | A | A | K | S | P | F | F | Y | K | L | F | S | N | G | M | R | E | S | E | Q | R | H | V | T | L | R | I | N | A | S | E | E | G | A | L | M | E | L | L | N | F | M | Y | S | N | S | L | S | V | T | T | A | P | G | L |
| LRBB_GLYMA | 157 | S | P | I | L | A | A | K | S | P | F | F | Y | K | L | F | S | N | G | M | R | E | S | E | Q | R | H | V | T | L | R | I | N | A | S | E | E | A | A | L | M | E | L | L | N | F | M | Y | S | N | T | L | S | I | T | S | P | P | A | L |
| LRBA_ORYSJ | 140 | S | A | I | L | A | A | E | S | P | F | F | Y | K | L | F | S | N | G | M | K | E | S | D | Q | R | H | A | T | L | R | I | T | A | S | E | N | A | L | M | E | L | L | S | F | M | Y | S | G | K | L | T | T | N | O | P | T | L | L |   |
| LRBA_MAIZE | 140 | S | A | I | L | A | A | K | S | P | F | F | Y | K | L | F | S | N | G | M | K | E | S | D | Q | R | H | A | T | L | R | I | T | A | S | E | N | A | L | M | E | L | L | S | F | M | Y | S | G | K | L | T | T | N | O | P | T | V | L | L |
| LRBB_MAIZE | 140 | S | A | I | L | A | A | K | S | P | F | F | Y | K | L | F | S | N | G | M | K | E | S | D | Q | R | H | A | T | L | R | I | T | A | S | E | N | A | L | M | E | L | L | S | F | M | Y | S | G | K | L | T | T | N | O | P | T | V | L | L |

PHOS SITE:

|            |     |   |   |   |   |   |   |   |   |   |   |   |   |   |   |   |   |   |   |   |   |   |   |   |   |   |   |   |   |   |   |   |   |   |   |   |   |   |   |   |   |   |   |   |   |   |   |   |   |   |   |   |   |   |   |   |   |   |   |   |   |
|------------|-----|---|---|---|---|---|---|---|---|---|---|---|---|---|---|---|---|---|---|---|---|---|---|---|---|---|---|---|---|---|---|---|---|---|---|---|---|---|---|---|---|---|---|---|---|---|---|---|---|---|---|---|---|---|---|---|---|---|---|---|---|
| LRB1_ARATH | 218 | D | V | L | M | A | A | D | K | F | E | V | A | S | C | M | R | Y | C | S | R | L | L | R | N | M | P | M | T | P | D | S | A | L | L | Y | L | E | L | P | S | S | V | L | M | A | E | A | V | Q | P | L | T | D | A | A | K | Q | F | L | A |
| LRB2_ARATH | 220 | D | V | L | M | A | A | D | K | F | E | V | A | S | C | M | R | Y | C | S | R | L | L | R | N | M | P | M | T | P | E | S | A | L | L | Y | L | E | L | P | S | S | V | L | M | A | K | A | V | Q | P | L | T | D | A | A | K | Q | F | L | A |
| LRBA_ARALL | 221 | D | V | L | M | A | A | D | K | F | E | V | A | S | C | M | R | Y | C | S | R | L | L | R | N | M | P | M | T | P | E | S | A | L | L | Y | L | E | L | P | S | S | V | L | M | A | K | A | V | Q | P | L | T | D | A | A | K | Q | F | L | A |
| LRBB_ARALL | 218 | D | V | L | M | A | A | D | K | F | E | V | A | S | C | M | R | Y | C | S | R | L | L | R | N | M | P | M | T | P | D | S | A | L | L | Y | L | E | L | P | S | S | V | L | M | A | E | A | V | Q | P | L | T | D | A | A | K | Q | F | L | A |
| LRBA_BRARP | 217 | D | V | L | M | A | A | D | K | F | E | V | A | S | C | M | R | Y | C | S | R | L | L | R | N | M | P | M | T | P | E | S | A | L | L | Y | L | E | L | P | S | S | V | L | M | A | K | A | V | Q | P | L | T | D | A | A | K | Q | F | L | A |
| LRBA_CICLE | 212 | D | V | L | M | A | A | D | K | F | E | V | A | S | C | M | R | Y | C | S | R | L | L | R | N | M | P | M | T | P | E | S | A | L | L | Y | L | E | L | P | S | S | V | L | M | G | E | A | V | Q | P | L | T | D | A | A | R | Q | Y | L | A |
| LRBA_POPTR | 219 | D | V | L | M | A | A | D | K | F | E | V | A | S | C | M | R | Y | C | S | R | Q | L | R | N | L | P | M | K | P | E | S | A | L | L | Y | L | E | L | P | S | S | V | L | M | A | E | A | V | Q | P | L | T | D | A | A | K | Q | Y | L | A |
| LRBB_POPTR | 211 | D | V | L | M | A | A | D | K | F | E | V | A | S | C | M | R | Y | C | S | R | Q | L | R | N | L | S | M | T | P | E | S | A | L | L | Y | L | E | L | P | S | S | V | L | M | A | E | A | V | Q | P | L | T | D | A | A | K | Q | Y | L | A |
| LRBA_PRUPE | 220 | D | V | L | M | A | A | D | K | F | E | V | A | S | C | M | R | Y | C | S | R | L | L | R | N | M | P | M | T | P | E | S | A | L | L | Y | L | E | L | P | S | S | V | L | M | A | E | A | V | Q | A | L | T | D | A | A | K | Q | Y | L | A |
| LRBA_RICCO | 212 | D | V | L | M | A | A | D | K | F | E | V | A | S | C | M | R | Y | C | S | R | Q | L | R | N | M | S | M | T | P | E | S | A | L | L | Y | L | E | L | P | S | S | V | L | M | A | E | A | V | Q | P | L | T | D | A | A | K | Q | Y | L | A |
| LRBA_CARUB | 221 | D | V | L | M | A | A | D | K | F | E | V | A | S | C | M | R | Y | C | S | R | L | L | R | N | M | S | M | T | P | E | S | A | L | L | Y | L | E | L | P | S | S | V | L | M | A | K | A | V | Q | P | L | T | D | A | A | K | Q | F | L | A |
| LRBB_CARUB | 217 | D | V | L | M | A | A | D | K | F | E | V | A | S | C | M | R | Y | C | S | R | Q | L | R | N | M | P | M | T | P | D | S | A | L | L | Y | L | E | L | P | S | S | V | L | M | A | E | A | V | Q | P | L | T | D | A | A | K | Q | F | L | A |
| LRBB_GLYMA | 217 | D | V | L | M | A | A | D | K | F | E | V | A | S | C | M | R | Y | C | S | R | L | L | R | N | I | P | M | T | P | E | S | A | L | L | Y | L | E | L | P | S | S | V | L | M | A | D | A | V | Q | P | L | T | D | A | A | K | Q | Y | L | A |
| LRBA_ORYSJ | 200 | D | I | L | M | I | A | D | K | F | E | V | V | S | C | M | R | H | C | S | Q | L | L | R | S | L | P | M | T | T | E | S | A | L | L | Y | L | D | L | P | S | S | I | S | M | A | A | V | Q | P | L | T | D | T | A | K | A | F | L | A |   |
| LRBA_MAIZE | 200 | D | I | L | M | I | A | D | K | F | E | V | G | S | C | M | R | H | C | S | Q | L | L | R | N | L | P | M | T | T | E | S | A | L | L | Y | L | D | L | P | S | S | I | S | M | A | A | V | Q | P | L | T | D | T | A | K | E | F | L | A |   |
| LRBB_MAIZE | 200 | D | I | L | M | I | A | D | K | F | E | V | G | S | C | M | R | H | C | S | Q | L | L | R | N | L | P | M | T | T | E | S | A | L | L | Y | L | D | L | P | S | S | I | S | M | A | A | V | Q | P | L | T | D | T | A | K | E | F | L | A |   |

PHOS SITE:

|            |     |   |   |   |   |   |   |   |   |   |   |   |   |   |   |   |   |   |   |   |   |   |   |   |   |   |   |   |   |   |   |   |   |   |   |   |   |   |   |   |   |   |   |   |   |   |   |   |   |   |   |   |   |   |   |   |   |   |   |   |
|------------|-----|---|---|---|---|---|---|---|---|---|---|---|---|---|---|---|---|---|---|---|---|---|---|---|---|---|---|---|---|---|---|---|---|---|---|---|---|---|---|---|---|---|---|---|---|---|---|---|---|---|---|---|---|---|---|---|---|---|---|---|
| LRB1_ARATH | 278 | S | R | Y | K | D | I | T | K | F | H | E | V | M | A | L | P | L | A | G | I | E | A | I | L | S | S | D | L | Q | I | A | S | E | D | A | V | Y | D | F | V | L | K | W | A | R | G | O | S | S | L | E | D | R | R | E | I | L |   |   |
| LRB2_ARATH | 280 | A | R | Y | K | D | I | T | K | F | H | E | E | V | M | S | L | P | L | A | G | I | E | A | I | L | S | S | D | E | L | Q | I | A | S | E | D | A | V | Y | D | F | I | L | K | W | A | R | A | O | S | P | C | L | E | R | R | E | I | L |
| LRBA_ARALL | 281 | A | R | Y | K | D | I | T | K | F | H | E | E | V | M | T | L | P | L | A | G | I | E | A | I | L | S | S | D | L | Q | I | A | S | E | D | A | V | Y | D | F | I | L | K | W | A | R | A | O | S | P | C | L | E | R | R | E | I | L |   |
| LRBB_ARALL | 278 | S | R | Y | K | D | I | T | K | F | H | E | V | M | A | L | P | L | A | G | I | E | A | I | L | S | S | D | L | Q | I | A | S | E | D | A | V | Y | D | F | V | L | K | W | A | R | G | O | S | S | L | E | D | R | R | E | I | L |   |   |
| LRBA_BRARP | 277 | A | R | Y | K | D | I | T | K | F | Q | E | E | V | M | S | L | P | L | A | G | I | E | A | I | L | S | S | D | L | Q | I | A | S | E | D | A | V | Y | D | F | I | L | K | W | A | R | A | O | S | P | S | L | E | R | R | E | I | L |   |
| LRBA_CICLE | 272 | S | R | Y | K | D | M | T | K | F | Q | E | V | M | A | L | P | L | A | G | V | E | A | I | L | S | S | D | L | Q | I | A | S | E | D | A | V | Y | D | F | V | L | K |   |   |   |   |   |   |   |   |   |   |   |   |   |   |   |   |   |



PHOS SITE:

LRB1\_ARATH 338 GSRLALYIRFPYMTCRKLKVVLTCSDFEHEVASKQVLEALFFKAEAPHRQRILAAEGSDS  
 LRB2\_ARATH 340 GSRLALSIRFPFMTCRKLKVVLTCSDFEHEIASKLVLEALFFKAEAPHRQRILAAEESAS  
 LRBA\_ARALL 341 GSRLALSIRFPFMTCRKLKVVLTCSDFEHEIASKLVLEALFFKAEAPHRQRILAAEESAS  
 LRBB\_ARALL 338 GSRLALYIRFPYMTCRKLKVVLTCSDFEHEVASKQVLEALFFKAEAPHRQRILAAEGSGS  
 LRBA\_BRARP 337 GSRLALSIRFPFMTCRKLKVVLTCSDFDHEIASKLVLEALFFKAEAPHRQRILAAEESAS  
 LRBA\_CICLE 332 GSRLARFIRFPHMTCRKLKVVLTCSDFDHDVASKLVLEALFFKAEAPHRQRILAAEESVT  
 LRBA\_POPTR 339 GARLARYIRFPYMTCRKLKVVLTCTDFEHDAAASKLVLEALFFKGEPPHRQRILAAEESAT  
 LRBA\_POPTR 331 GARLARYIRFPYMTCRKLKVVLTCTDFEHDAAASKLVLEALFFKGEPPHRQRILAAEESAT  
 LRBA\_PRUPE 340 GSRLARYIRFPYMTCRKLKVVLTCSDFDHDAAASKLVLEALFFKAEAPHRQRILAAEESAT  
 LRBA\_RICCO 332 GARLARFIRFPYMTCRKLKVVLTCSDFDHDVASKLVLEALFFKAEAPHRQRILAAEESAS  
 LRBA\_CARUB 341 GSRLALSIRFPFMTCRKLKVVLTCSDFDHEIASKLVLEALFFKAEAPHRQRILAAEETAS  
 LRBB\_CARUB 337 GSRLALYIRFPYMTCRKLKVVLTCSDFEHEVASKQVLEALFFKAEAPHRQRILAGEGSDS  
 LRBB\_GLYMA 337 GTRLARLIRFPYMTCRKLKVVLTCSDFDHDVASKLVLEALFFKAEAPHRQRILAAE--SAS  
 LRBA\_ORYSJ 320 GTRLLPLVRFCHMTCRKLKVVLTACNDLDHEQATKCVTEALLYKADAPHRQRILAAADV--L  
 LRBA\_MAIZE 320 GTRLLPLVRFCHMTCRKLKVVLTACNDLDHEQATKCVTEALLYKADAPHRQRALAAADV--M  
 LRBB\_MAIZE 320 GTRLLPLVRFCHMTCRKLKVVLTACNDLDHEQATKCVTEALLYKADAPHRQRALAAADV--M

PHOS SITE:

LRB1\_ARATH 398 MNRRFIERAYKYRPPVKVVEFELPRPQCQVYLDLKKREECAGLFPSSGRVYSQAFHLGGQGF  
 LRB2\_ARATH 400 LNRRLIERAYKYRPPVKVVEFELPRPQCQVYLDLKKREECGLFPSSGRVYSQAFHLGGQGF  
 LRBA\_ARALL 401 LNRRLIERAYKYRPPVKVVEFELPRPQCQVYLDLKKREECGLFPSSGRVYSQAFHLGGQGF  
 LRBB\_ARALL 398 LNRRFIERAYKYRPPVKVVEFELPRPQCQVYLDLKKREECAGLFLSGRVYSQAFHLGGQGF  
 LRBA\_BRARP 397 VNRRLIERAYKYRPPVKVVEFELPRPQCQVYLDLKKREECAGLFPSSGRVYSQAFHLGGQGF  
 LRBA\_CICLE 392 LNRRFVERAYKYRPPVKVVEFERPRQCQVYLDLKKREECENLFPSSGRVYSQAFHLGGQGF  
 LRBA\_POPTR 399 LNRRFVERAYKYRPPVKVVEFELPRQCQVYLDLKKREECVNLFPSSGRVYSQAFHLGGQGF  
 LRBB\_POPTR 391 SNRRFVERAYKYRPPVKVVEFELPRQCQVYLDLKKREECANLFPSSGRVYSQAFHLGGQGF  
 LRBA\_PRUPE 400 LNRRFVERAYKYRPPVKVVEFDLPRQCQVYLDLKKREECANLFPSSGRVYSQAFHLGGQGF  
 LRBA\_RICCO 392 LNRRFVERAYKYRPPVKVVEFELPRQCQVYLDLKKREECANLFPSSGRVYSQAFHLGGQGF  
 LRBA\_CARUB 401 LNRRLIERAYKYRPPVKVVEFELPRPQCQVYLDLKKREECGLFPSSGRVYSQAFHLGGQGF  
 LRBB\_CARUB 397 MNRRFIERAYKYRPPVKVVEFELPRPQCQVYLDLKKREECAGLFPSSGRVYSQAFHLGGQGF  
 LRBB\_GLYMA 396 FNRLFVERAYKYRPPVKVVEFELPRQCQVYLDLKKREECTNLFPSSGRVYSQAFHLGGQGF  
 LRBA\_ORYSJ 378 TCRKYAERAYKYRPLKVVVEFDRPYRQCIAYLDLKKREEC SRLFPSSGRIYSQAFHLAGQGF  
 LRBA\_MAIZE 378 TCRKYAERAYKYRPLKVVVEFDRPYRQCIAYLDLKKREEC SRLFPSSGRIYSQAFHLAGQGF  
 LRBB\_MAIZE 378 TCRKYAERAYKYRPLKVVVEFDRPYRQCIAYLDLKKREEC SRLFPSSGRIYSQAFHLAGQGF

PHOS SITE:

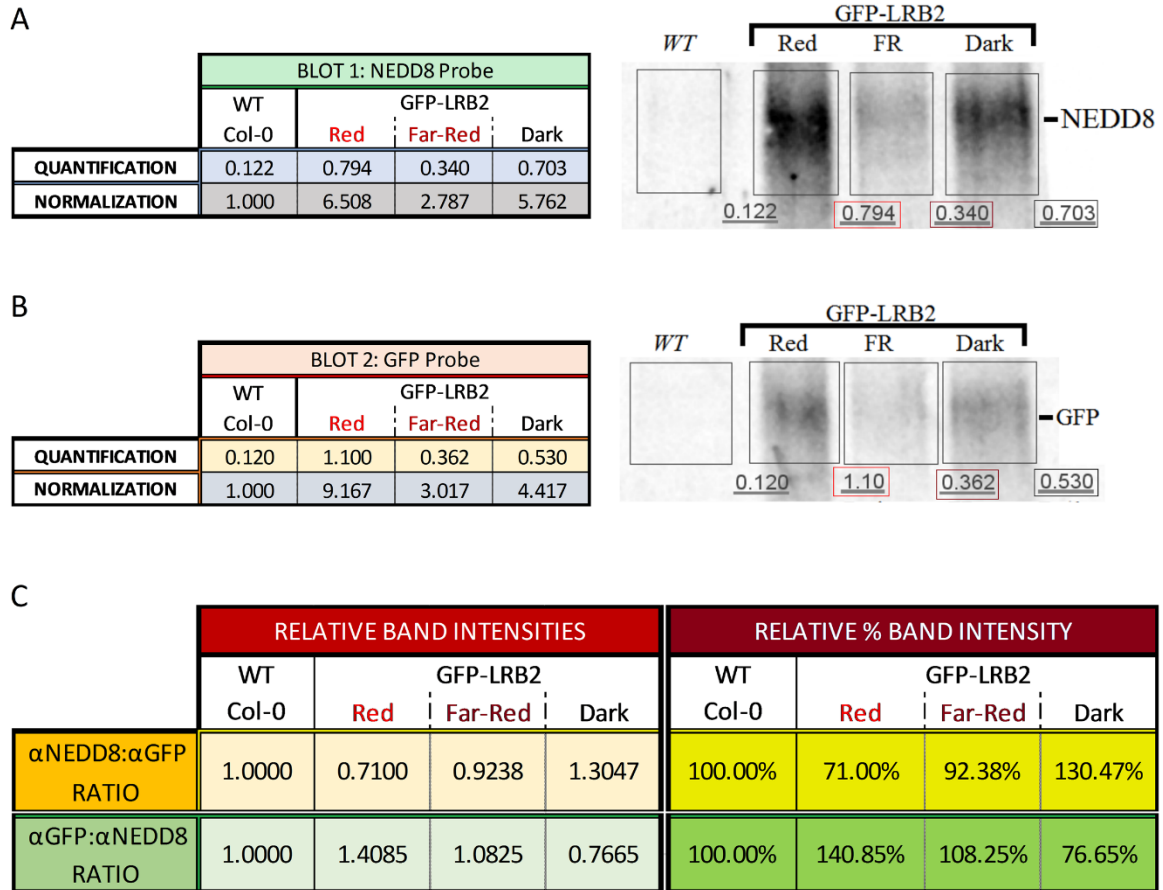
LRB1\_ARATH 458 LSAHCNMDQSSFHCFGLFLGMQEKGVAVSFGVDYEF AARDKRSSTKEEYVSKYKGN YTFHGG  
 LRB2\_ARATH 460 LSAHCNMDQSSFHCFGLFLGMQEKGSV SFGVDYEF SARKS-PAEDFISKYKGN YTFHGG  
 LRBA\_ARALL 461 LSAHCNMDQSSFHCFGLFLGMQEKGSV SFGVDYEF SARKS-PAEDFISKYKGN YTFHGG  
 LRBB\_ARALL 458 LSAHCNMDQSSFHCFGLFLGMQEKGVAVSFGVDYEF AARDKKSSEEYVSKYKGN YTFHGG  
 LRBA\_BRARP 457 LSAHCNMDQSSFHCFGLFLGMQEKGSV SFGVDYEF SARKS-PSEEFISKYKGN YTFHGG  
 LRBA\_CICLE 452 LSAHCNMDQSSFHCFGLFLGMQEKGSV SFAVDYEF AARSK-PTEEFVSKYKGN YTFHGG  
 LRBA\_POPTR 459 LSAHCNMDQSSFHCFGLFLGMQEKGSV SFAVDYEF AARSK-PTEEFVSKYKGN YTFHGG  
 LRBB\_POPTR 451 LSAHCNMDQSSFHCFGLFLGMQEKGSV SFAVDYEF AARSK-PTEEFVSKYKGN YTFHGG  
 LRBA\_PRUPE 460 LSAHCNMDQSSFHCFGLFLGMQEKGSV SFAVDYEF AARSK-PTEEFISKYKGN YTFHGG  
 LRBA\_RICCO 452 LSAHCNMDQSSFHCFGLFLGMQEKGNV SFAVDYEF AARAK-PTEEFVSKYKGN YTFHGG  
 LRBA\_CARUB 461 LSAHCNMDQSSFHCFGLFLGMQEKGSV SFGVDYEF SARKS-PAEDFISKYKGN YTFHGG  
 LRBB\_CARUB 457 LSAHCNMDQSSFHCFGLFLGMQEKGVAVSFAVDYEF AARENKPGEEFVSKYKGN YTFHGG  
 LRBB\_GLYMA 456 LSAHCNMDQSSFHCFGLFLGMQEKGSV SFAVDYEF AARSR-PTEEFVSKYKGN YTFHGG  
 LRBA\_ORYSJ 438 LSAHCNMDQSSAFHCFGLFLGMQEKGST SVTVDYEF AARTR-PSGEFVSKYKGY YTFHGG  
 LRBA\_MAIZE 438 LSAHCNVDQSSAFYCFGLFLGMQEKGST SVTVDYEF AARTR-PSGEFVSKYKGY YTFHGG  
 LRBB\_MAIZE 438 LSAHCNVDQSSAFYCFGLFLGMQEKGST SVTVDYEF AARTR-PSGEFVSKYKGY YTFHGG

**PHOS SITE:**

```
LRB1_ARATH 518 KAVGYRNLFVIPWTSFIAEDSQHFINGILHLRAELTIKRSSDLH--
LRB2_ARATH 519 KAVGYRNLFVVPWTSFIAEDSQYFINGILHLRAELTIKRSTDP---
LRBA_ARALL 520 KAVGYRNLFVVPWTSFIAEDSQYFINGILHLRAELTIKRSTDP---
LRBB_ARALL 518 KAVGYRNLFVIPWTSFIAEDSQHFINGILHLRAELTIKRSSDLH--
LRBA_BRARP 516 KAVGYRNLFVIPWTSFIAEDSLYFINGILHLRAELTIKRSTDPPPQ
LRBA_CICLE 511 KAVGYRNLFVIPWTSFMADDSLYFINGILHLRAELTIRH-----
LRBA_POPTR 518 KAVGYRNLFVIPWTSFMAEDSPYFINGVLHLRAELTIRH-----
LRBB_POPTR 510 KAVGYRNLFVIPWTSFMAEDSLYFINGVLHLRAELTIRL-----
LRBA_PRUPE 519 KAVGYRNLFVIPWTSFMAEDSLYFINGVLHLRAELTIRH-----
LRBA_RICCO 511 KAVGYRNLFVIPWTSFMADDSLYFINGVLHLRAELTIRH-----
LRBA_CARUB 520 KAVGYRNLFVIAWTSFIAEDSQYFINGILHLRAELTIKRSTDP---
LRBB_CARUB 517 KAVGYRNLFVVPWTSFMAEDSLHFINGILHLRAELTIKRSTDLH--
LRBB_GLYMA 515 KAVGYRNLFVIPWTFMAEDSLYFINGVLHLRAELTIRH-----
LRBA_ORYSJ 497 KAVGYRNLFVIPWSSFMADDSLFFIEGVLHLRAELTIKQP-----
LRBA_MAIZE 497 KAVGYRNLFVIPWPLFMADDSLFFIDGVLHLRAELTIKQP-----
LRBB_MAIZE 497 KAVGYRNLFVIPWPLFMADDSLFFIDGVLHLRAELTIKQP-----
```

**Supplemental Figure 10: Phosphorylation Site Prediction using PhosPhAt 4.0**

The edited MSA was used to show the amount of conservation for each phosphorylation site predicted using the PhosPhAt 4.0 program<sup>78,79</sup>. Each phosphorylation site was highlighted in alternating yellow or black (to distinguish between closely-located phosphorylation sites) and given a letter that corresponds to a specific phosphorylation value. The exact phosphorylation values predicted for each phosphorylation site can be found listed in **Supplemental Table 2**.



**Supplemental Figure 11: Quantification Results for  $\alpha$ GFP *At*LRB2 Immunoprecipitation**

**A.** Immunoprecipitated GFP-LRB2 proteins purified from 8-day-old *Arabidopsis* seedlings grown exclusively in darkness or 4 days in darkness followed by 4 days of continuous R or FR light were investigated using Western blotting probed with anti-NEDD8 antibodies. The quantification and normalization values are provided. Blot was visualized on the Odyssey FL system using IRDye800 secondary antibodies. Quantification for each band was found using the Odyssey FC Image Studio Lite 5.0 program<sup>82</sup>, while normalization values were calculated for each blot individually by taking the quantification values for each independent light treatment and dividing it by the WT Col-0 quantification value for that individual blot.

**B.** Immunoprecipitated GFP-LRB2 proteins were probed with anti-GFP antibodies. The quantification and normalization values are provided. Blot was visualized on the Odyssey FL system using IRDye800 secondary antibodies. Quantification for each band was found using the Odyssey FC Image Studio Lite 5.0 program<sup>82</sup>.

**C.** Relative banding intensity ratio values for each light treatment. The ratio of  $\alpha$ NEDD8 to  $\alpha$ GFP and  $\alpha$ GFP to  $\alpha$ NEDD8 are provided, with the relative percent band intensity listed to the right.

**Supplemental Table 1:** Template Coverage of Phyre2 Homology Models

| PDB<br>Template                       | At LRB1     |      |          | At LRB2A    |      |          | At LRB2B    |      |          | At LRB3     |      |          |
|---------------------------------------|-------------|------|----------|-------------|------|----------|-------------|------|----------|-------------|------|----------|
|                                       | Conf (%)    | % ID | Residues | Conf (%)    | % ID | Residues | Conf (%)    | % ID | Residues | Conf (%)    | % ID | Residues |
| * 3HU6.b                              | 99.9        | 21   | 20-279   | 100         | 21   | 5-281    | 100         | 21   | 5-281    | -           | -    | -        |
| * 3I3N.a                              | 100         | 20   | 129-385  | 100         | 19   | 128-387  | 100         | 19   | 128-387  | 100         | 19   | 84-331   |
| 3HVE.a                                | 100         | 17   | 142-360  | -           | -    | -        | -           | -    | -        | -           | -    | -        |
| 2CR2.a1                               | 96.5        | 17   | 442-558  | -           | -    | -        | -           | -    | -        | -           | -    | -        |
| 2F1Z.b                                | 95.4        | 10   | 442-560  | -           | -    | -        | -           | -    | -        | -           | -    | -        |
| 2F1X.b                                | 95.2        | 9    | 444-554  | -           | -    | -        | -           | -    | -        | -           | -    | -        |
| 3H7.a                                 | -           | -    | -        | 99.3        | 16   | 394-549  | -           | -    | -        | 96.7        | 6    | 342-503  |
| 2XN4.a                                | -           | -    | -        | 99.4        | 16   | 397-549  | -           | -    | -        | 96.8        | 10   | 343-446  |
| 1X2R.a                                | -           | -    | -        | 99.4        | 10   | 397-550  | -           | -    | -        | 96.5        | 3    | 346-437  |
| 2VPJ.a                                | -           | -    | -        | 99.4        | 19   | 400-550  | -           | -    | -        | 96.3        | 9    | 343-437  |
| 1ZGK.a1                               | -           | -    | -        | 99.3        | 11   | 397-548  | -           | -    | -        | 97.2        | 5    | 340-497  |
| 2WOZ.a                                | -           | -    | -        | 99.4        | 15   | 387-553  | -           | -    | -        | -           | -    | -        |
| 4YY8.b                                | -           | -    | -        | -           | -    | -        | 100         | 12   | 147-549  | -           | -    | -        |
| 4ASC.a                                | -           | -    | -        | -           | -    | -        | -           | -    | -        | 96.3        | 7    | 362-503  |
| <i>Ab initio</i>                      | 0           | 0    | 1-19     | 0           | 0    | 1-4      | 0           | 0    | 1-4      | 0           | 0    | 1-83     |
| <i>Ab initio</i>                      | 0           | 0    | 83-100   | 0           | 0    | 65-66    | 0           | 0    | 65-66    | 0           | 0    | 332-339  |
| <i>Ab initio</i>                      | 0           | 0    | 361-441  | 0           | 0    | 554-561  | 0           | 0    | 550-561  | 0           | 0    | 504-505  |
| <i>Ab initio</i>                      | 0           | 0    | 561      | -           | -    | -        | -           | -    | -        | -           | -    | -        |
| Total<br><i>ab initio</i>             | 89 residues |      |          | 13 residues |      |          | 17 residues |      |          | 97 residues |      |          |
| <b>Overall<br/>Model<br/>Coverage</b> | <b>84%</b>  |      |          | <b>98%</b>  |      |          | <b>97%</b>  |      |          | <b>81%</b>  |      |          |

The PDB template identifiers for the known crystal structures used by Phyre2<sup>65</sup> to make the predicted structures for the AtLRBs. The confidence, percent identity, and residues of the query sequence that are covered are provided for each PDB template used. Residues that were modeled using *ab initio* methods are also listed. The percent of the overall coverage modeled with >90% confidence was calculated by Phyre2 and presented at the bottom of the table. An asterisk marks the only two templates used to create both AtLRB1 and AtLRB2.

**Supplemental Table 2:** Predicted Phosphorylation Site Values for LRB Homologs

| Phosphorylation Site:                     | A        | B        | C        | D        | E        | F        | G        | H        | I        | J        | K        | L        | M        | N        | O        | P        | Q        | R        | S        | T        | U        | V        | W        |
|---|----------|----------|----------|----------|----------|----------|----------|----------|----------|----------|----------|----------|----------|----------|----------|----------|----------|----------|----------|----------|----------|----------|----------|
| LRB1_ARATH                                | 0.93     | --       | 0.75     | 0.41     | 0.57     | 0.87     | 1.43     | 1.22     | --       | 0.53     | --       | 0.43     | 0.53     | 0.83     | 0.81     | 0.05     | --       | 0.37     | 0.78     | 1.06     | 0.67     | 0.1      | 0.88     |
| LRB2_ARATH                                | 0.97     | 0.09     | 1.03     | 0.48     | 0.79     | 0.26     | 0.41     | 1.37     | 0.36     | 0.45     | --       | 0.43     | 0.53     | 0.67     | 0.3      | --       | 0.72     | 0.2      | 0.07     | --       | 0.67     | 0.1      | 0.88     |
| LRBA_ARALL                                | 0.97     | 0.09     | 1.03     | 0.51     | 0.75     | 0.52     | 0.41     | 1.37     | 0.36     | 0.45     | --       | 0.43     | 0.53     | 0.67     | 0.3      | --       | 0.72     | 0.2      | 0.07     | --       | 0.67     | 0.1      | 0.88     |
| LRBB_ARALL                                | 0.93     | --       | 0.75     | 0.53     | 0.48     | 1.01     | 1.43     | 1.22     | --       | 0.53     | --       | 0.43     | 0.53     | 0.83     | 0.81     | 0.05     | --       | 0.7      | 0.62     | 1.4      | 0.67     | 0.1      | 0.88     |
| LRBA_BRARP                                | 1.02     | --       | 0.75     | 0.3      | 0.57     | 0.49     | 0.41     | 1.65     | --       | 0.24     | --       | 0.18     | 0.53     | 0.67     | 0.67     | --       | 0.65     | 0.2      | 0.2      | 0.05     | 0.67     | 0.1      | 0.88     |
| LRBA_CICLE                                | 0.09     | 1.39     | 0.9      | --       | 0.47     | 0.93     | --       | 1.16     | 1.5      | --       | --       | 0.39     | 0.53     | 0.67     | 0.24     | --       | 1.14     | --       | 0.43     | 0.07     | 0.67     | 0.1      | 0.88     |
| LRBA_POPTR                                | 0.59     | 1.25     | 1.17     | --       | --       | --       | --       | 1.23     | 1.51     | 0.18     | 0.14     | 0.39     | 0.54     | --       | 0.36     | --       | 0.66     | --       | 0.43     | 0.07     | 0.67     | 0.1      | 0.88     |
| LRBB_POPTR                                | 0.4      | 1.09     | 1.24     | --       | 0.35     | --       | --       | 1.13     | 1.21     | --       | --       | 0.39     | 0.54     | 0.79     | 0.39     | --       | 0.66     | --       | 0.43     | 0.07     | 0.67     | 0.1      | 0.88     |
| LRBA_PRUPE                                | 0.12     | 1.7      | 0.44     | 1.7      | 0.25     | 0.41     | --       | 0.74     | 1.63     | 0.14     | --       | 0.39     | 0.53     | 0.67     | 0.37     | --       | --       | --       | 0.39     | 0.05     | 0.67     | 0.1      | 0.88     |
| LRBA_RICCO                                | 0.94     | 0.01     | 1.03     | 0.32     | --       | --       | --       | 1.24     | --       | --       | --       | 0.39     | 0.54     | 0.9      | 0.3      | --       | 0.65     | --       | 0.36     | 0.07     | 0.67     | 0.1      | 0.88     |
| LRBA_CARUB                                | 1.03     | --       | 0.98     | 0.51     | 0.75     | 0.52     | 0.41     | 1.66     | 0.14     | 0.52     | --       | 0.43     | 0.53     | 0.9      | 0.3      | --       | 0.62     | 0.2      | 0.07     | --       | 0.67     | 0.1      | 0.88     |
| LRBB_CARUB                                | 0.4      | 0.99     | 0.93     | 0.53     | 0.48     | 1.01     | 1.43     | 1.08     | 0.47     | --       | --       | 0.43     | 0.54     | 0.83     | 0.81     | 0.05     | --       | --       | --       | 0.07     | 0.67     | 0.1      | 0.88     |
| LRBB_GLYMA                                | 1.12     | 1.32     | 0.75     | --       | --       | 0.49     | --       | 1.38     | --       | --       | --       | 0.7      | 0.53     | 0.51     | --       | --       | --       | --       | 0.42     | 0.002    | 0.91     | --       | 0.89     |
| LRBA_ORYSJ                                | --       | 0.79     | --       | --       | --       | 1.39     | 0.38     | 1.06     | --       | --       | --       | --       | --       | --       | 0.43     | --       | 0.12     | 0.67     | 0.84     | 0.45     | 0.11     | 0.2      | 0.61     |
| LRBA_MAIZE                                | --       | --       | --       | --       | --       | 0.41     | 1.32     | 0.87     | 0.44     | 0.88     | --       | --       | --       | --       | 0.39     | --       | --       | 0.67     | 0.84     | 0.45     | 0.11     | 0.2      | 0.61     |
| LRBB_MAIZE                                | --       | --       | --       | --       | --       | 0.41     | 1.32     | 0.87     | 0.44     | 0.88     | --       | --       | --       | --       | 0.39     | --       | --       | 0.67     | 0.84     | 0.45     | 0.11     | 0.2      | 0.61     |
| <b>Phosphorylation Site Conservation:</b> | <b>N</b> | <b>N</b> | <b>N</b> | <b>N</b> | <b>N</b> | <b>N</b> | <b>N</b> | <b>Y</b> | <b>N</b> | <b>N</b> | <b>N</b> | <b>N</b> | <b>N</b> | <b>N</b> | <b>A</b> | <b>N</b> | <b>N</b> | <b>N</b> | <b>A</b> | <b>N</b> | <b>Y</b> | <b>A</b> | <b>Y</b> |

The given phosphorylation values for each LRB protein as marked in the MSA from **Supplemental Figure 6**. Phosphorylation values greater than 1 indicate an almost certainty of phosphorylation. The overall conservation of a specific site is listed below each of the phosphorylation sites, with **N** corresponding with not being conserved, **Y** corresponding with a conserved residue, and **A** indicating a site that is almost completely conserved.

## VIII. REFERENCES

1. Leivar, P., Monte, E., Cohn, M. M. & Quail, P. H. Phytochrome Signaling in Green Arabidopsis Seedlings: Impact Assessment of a Mutually Negative phyB–PIF Feedback Loop. *Mol. Plant* **5**, 734–749 (2012).
2. Christians, M. J., Gingerich, D. J., Hua, Z., Lauer, T. D. & Vierstra, R. D. The Light-Response BTB1 and BTB2 Proteins Assemble Nuclear Ubiquitin Ligases That Modify Phytochrome B and D Signaling in Arabidopsis. *Plant Physiol.* **160**, 118–134 (2012).
3. Franklin, K. A. & Quail, P. H. Phytochrome functions in Arabidopsis development. *J. Exp. Bot.* **61**, 11–24 (2010).
4. Chen, M., Chory, J. & Fankhauser, C. Light Signal Transduction in Higher Plants. *Annu. Rev. Genet.* **38**, 87–117 (2004).
5. Noack, S., Michael, N., Rosen, R. & Lamparter, T. Protein Conformational Changes of Agrobacterium Phytochrome Agp1 during Chromophore Assembly and Photoconversion†. *Biochemistry (Mosc.)* **46**, 4164–4176 (2007).
6. Mata, N. L., Radu, R. A., Clemmons, R. S. & Travis, G. H. Isomerization and Oxidation of Vitamin A in Cone-Dominant Retinas: A Novel Pathway for Visual-Pigment Regeneration in Daylight. *Neuron* **36**, 69–80 (2002).
7. Josse, E.-M. & Halliday, K. J. Skotomorphogenesis: The Dark Side of Light Signalling. *Curr. Biol.* **18**, R1144–R1146 (2008).
8. Burgie, E. S., Bussell, A. N., Walker, J. M., Dubiel, K. & Vierstra, R. D. Crystal structure of the photosensing module from a red/far-red light-absorbing plant phytochrome. *Proc. Natl. Acad. Sci. U. S. A.* **111**, 10179–10184 (2014).
9. Quail, P. H. Phytochrome photosensory signalling networks. *Nat. Rev. Mol. Cell Biol.* **3**, 85–93 (2002).
10. Jeong, J. & Choi, G. Phytochrome-Interacting Factors Have Both Shared and Distinct Biological Roles. *Mol. Cells* **35**, 371–380 (2013).
11. Ni, W. *et al.* Multisite Light-Induced Phosphorylation of the Transcription Factor PIF3 Is Necessary for Both Its Rapid Degradation and Concomitant Negative Feedback Modulation of Photoreceptor phyB Levels in Arabidopsis. *Plant Cell Online* **25**, 2679–2698 (2013).
12. Park, E. *et al.* Phytochrome B inhibits binding of phytochrome-interacting factors to their target promoters: *PhyB disrupts DNA binding of PIFs*. *Plant J.* **72**, 537–546 (2012).
13. Kim, J. Functional Characterization of Phytochrome Interacting Factor 3 in Phytochrome-Mediated Light Signal Transduction. *PLANT CELL ONLINE* **15**, 2399–2407 (2003).
14. Yeh, K.-C. & Lagarias, J. C. Eukaryotic phytochromes: Light-regulated serine/threonine protein kinases with histidine kinase ancestry. *Proc. Natl. Acad. Sci. U. S. A.* **95**, 13976 (1998).
15. Shen, Y. *et al.* Phytochrome A Mediates Rapid Red Light-Induced Phosphorylation of Arabidopsis FAR-RED ELONGATED HYPOCOTYL1 in a Low Fluence Response. *PLANT CELL ONLINE* **21**, 494–506 (2009).
16. Ni, W. *et al.* A mutually assured destruction mechanism attenuates light signaling in Arabidopsis. *Science* **344**, 1160–1164 (2014).

17. Vierstra, R. D. The Expanding Universe of Ubiquitin and Ubiquitin-Like Modifiers. *Plant Physiol.* **160**, 2–14 (2012).
18. Moon, J., Parry, G. & Estelle, M. The Ubiquitin-Proteasome Pathway and Plant Development. *Plant Cell Online* **16**, 3181–3195 (2004).
19. Braun, S. & Madhani, H. D. Shaping the landscape: mechanistic consequences of ubiquitin modification of chromatin. *EMBO Rep.* **13**, 619–630 (2012).
20. Vierstra, R. D. The ubiquitin/26S proteasome pathway, the complex last chapter in the life of many plant proteins. *Trends Plant Sci.* **8**, 135–142 (2003).
21. Jun, J. H., Ha, C. M. & Fletcher, J. C. BLADE-ON-PETIOLE1 coordinates organ determinacy and axial polarity in arabidopsis by directly activating ASYMMETRIC LEAVES2. *Plant Cell* **22**, 62–76 (2010).
22. Schöning, J. C., Streitner, C., Meyer, I. M., Gao, Y. & Staiger, D. Reciprocal regulation of glycine-rich RNA-binding proteins via an interlocked feedback loop coupling alternative splicing to nonsense-mediated decay in Arabidopsis. *Nucleic Acids Res.* **36**, 6977–6987 (2008).
23. Hartmann, T., Pan, Z.-Q. & Sarikas, A. The cullin protein family. *Genome Biol. Online Ed.* **12**, 220 (2011).
24. Hua, Z. & Vierstra, R. D. The Cullin-RING Ubiquitin-Protein Ligases. *Annu. Rev. Plant Biol.* **62**, 299–334 (2011).
25. Hee Jin Park, H. C. P. Ubiquitin and Ubiquitin-like Modifiers in Plants. *J. Plant Biol.* **54**, 275–285 (2011).
26. Zheng, N. *et al.* Structure of the Cul1-Rbx1-Skp1-F boxSkp2 SCF ubiquitin ligase complex. *Nature* **416**, 703–709 (2002).
27. Choo, Y. Y. & Hagen, T. Mechanism of Cullin3 E3 Ubiquitin Ligase Dimerization. *PLoS ONE* **7**, e41350 (2012).
28. Pintard, L., Willems, A. & Peter, M. Cullin-based ubiquitin ligases: Cul3–BTB complexes join the family. *EMBO J.* **23**, 1681–1687 (2004).
29. Scott, D. C. *et al.* Structure of a RING E3 Trapped in Action Reveals Ligation Mechanism for the Ubiquitin-like Protein NEDD8. *Cell* **157**, 1671–1684 (2014).
30. Angers, S. *et al.* Molecular architecture and assembly of the DDB1–CUL4A ubiquitin ligase machinery. *Nature* **443**, 590–593 (2006).
31. Wang, K. L.-C., Yoshida, H., Lurin, C. & Ecker, J. R. Regulation of ethylene gas biosynthesis by the Arabidopsis ETO1 protein. *Nature* **428**, 945–950 (2004).
32. Robert, H. S., Quint, A., Brand, D., Vivian-Smith, A. & Offringa, R. BTB and TAZ domain scaffold proteins perform a crucial function in Arabidopsis development. *Plant J.* **58**, 109–121 (2009).
33. Cheng, Y., Qin, G., Dai, X. & Zhao, Y. NPY1, a BTB-NPH3-like protein, plays a critical role in auxin-regulated organogenesis in Arabidopsis. *Proc. Natl. Acad. Sci.* **104**, 18825–18829 (2007).
34. Stogios, P. J., Downs, G. S., Jauhal, J. J. S., Nandra, S. K. & Privé, G. G. Sequence and structural analysis of BTB domain proteins. *Genome Biol.* **6**, R82 (2005).
35. Canning, P. *et al.* Structural Basis for Cul3 Protein Assembly with the BTB-Kelch Family of E3 Ubiquitin Ligases. *J. Biol. Chem.* **288**, 7803–7814 (2013).

36. Ahmad, K. F., Engel, C. K. & Privé, G. G. Crystal structure of the BTB domain from PLZF. *Proc. Natl. Acad. Sci. U. S. A.* **95**, 12123–12128 (1998).
37. Stogios, P. J. & Privé, G. G. The BACK domain in BTB-kelch proteins. *Trends Biochem. Sci.* **29**, 634–637 (2004).
38. Letunic, I., Doerks, T. & Bork, P. SMART: recent updates, new developments and status in 2015. *Nucleic Acids Res.* **43**, D257–D260 (2015).
39. Mitchell, A. *et al.* The InterPro protein families database: the classification resource after 15 years. *Nucleic Acids Res.* **43**, D213–D221 (2015).
40. Polekhina, G. *et al.* Siah ubiquitin ligase is structurally related to TRAF and modulates TNF- $\alpha$  signaling. *Nat. Struct. Mol. Biol.* **9**, 68–75 (2002).
41. Humphrey, W., Dalke, A. & Schulten, K. VMD: Visual molecular dynamics. *J. Mol. Graph.* **14**, 33–38 (1996).
42. Zhuang, M. *et al.* Structures of SPOP-Substrate Complexes: Insights into Molecular Architectures of BTB-Cul3 Ubiquitin Ligases. *Mol. Cell* **36**, 39–50 (2009).
43. Whitby, F. G., Xia, G., Pickart, C. M. & Hill, C. P. Crystal Structure of the Human Ubiquitin-like Protein NEDD8 and Interactions with Ubiquitin Pathway Enzymes. *J. Biol. Chem.* **273**, 34983–34991 (1998).
44. Merlet, J., Burger, J., Gomes, J. –. & Pintard, L. Regulation of cullin-RING E3 ubiquitin-ligases by neddylation and dimerization. *Cell. Mol. Life Sci.* **66**, 1924–38 (2009).
45. Rabut, G. & Peter, M. Function and regulation of protein neddylation. ‘Protein modifications: beyond the usual suspects’ review series. *EMBO Rep.* **9**, 969–976 (2008).
46. Xirodimas, D. P., Saville, M. K., Bourdon, J.-C., Hay, R. T. & Lane, D. P. Mdm2-mediated NEDD8 conjugation of p53 inhibits its transcriptional activity. *Cell* **118**, 83–97 (2004).
47. Hu, X. *et al.* Proteasome-Mediated Degradation of FRIGIDA Modulates Flowering Time in Arabidopsis during Vernalization. *Plant Cell Online* tpc.114.132738 (2014). doi:10.1105/tpc.114.132738
48. Li, W. *et al.* The EMBL-EBI bioinformatics web and programmatic tools framework. *Nucleic Acids Res.* (2015). doi:10.1093/nar/gkv279
49. Amasino, R. Vernalization, Competence, and the Epigenetic Memory of Winter. *Plant Cell* **16**, 2553–2559 (2004).
50. Choi, K. *et al.* The FRIGIDA Complex Activates Transcription of FLC, a Strong Flowering Repressor in Arabidopsis, by Recruiting Chromatin Modification Factors. *Plant Cell* **23**, 289–303 (2011).
51. Chang-Ro Lee, Y.-H. P. Phosphorylation-Dependent Mobility Shift of Proteins on SDS-PAGE is Due to Decreased Binding of SDS. *Bull. Korean Chem. Soc.* **34**, (2013).
52. Hakenjos, J. P. *et al.* MLN4924 Is an Efficient Inhibitor of NEDD8 Conjugation in Plants. *Plant Physiol.* **156**, 527–536 (2011).
53. Michaels, S. D., Bezerra, I. C. & Amasino, R. M. FRIGIDA-related genes are required for the winter-annual habit in Arabidopsis. *Proc. Natl. Acad. Sci. U. S. A.* **101**, 3281–3285 (2004).
54. Consortium, T. U. UniProt: a hub for protein information. *Nucleic Acids Res.* **43**, D204–D212 (2015).
55. The UniProt Consortium. Activities at the Universal Protein Resource (UniProt). *Nucleic Acids Res.* **42**, D191–D198 (2014).



56. Notredame, C., Higgins, D. G. & Heringa, J. T-coffee: a novel method for fast and accurate multiple sequence alignment. *J. Mol. Biol.* **302**, 205–217 (2000).
57. Armougom, F. *et al.* Espresso: automatic incorporation of structural information in multiple sequence alignments using 3D-Coffee. *Nucleic Acids Res.* **34**, W604–608 (2006).
58. Dereeper, A. *et al.* Phylogeny.fr: robust phylogenetic analysis for the non-specialist. *Nucleic Acids Res.* **36**, W465–W469 (2008).
59. Ashkenazi, S., Snir, R. & Ofra, Y. Assessing the relationship between conservation of function and conservation of sequence using photosynthetic proteins. *Bioinformatics* **28**, 3203–3210 (2012).
60. Lamesch, P. *et al.* The Arabidopsis Information Resource (TAIR): improved gene annotation and new tools. *Nucleic Acids Res.* **40**, D1202–D1210 (2012).
61. Bailey, T. L., Williams, N., Misleh, C. & Li, W. W. MEME: discovering and analyzing DNA and protein sequence motifs. *Nucleic Acids Res.* **34**, W369–W373 (2006).
62. Valdar, W. S. J. Scoring residue conservation. *Proteins Struct. Funct. Bioinforma.* **48**, 227–241 (2002).
63. Baker, D. & Sali, A. Protein Structure Prediction and Structural Genomics. *Science* **294**, 93–96 (2001).
64. Berman, H. M. *et al.* The Protein Data Bank. *Nucleic Acids Res.* **28**, 235–242 (2000).
65. Kelley, L. A. & Sternberg, M. J. E. Protein structure prediction on the Web: a case study using the Phyre server. *Nat. Protoc.* **4**, 363–71 (2009).
66. Söding, J., Biegert, A. & Lupas, A. N. The HHpred interactive server for protein homology detection and structure prediction. *Nucleic Acids Res.* **33**, W244–W248 (2005).
67. Zhang, Y. I-TASSER: Fully automated protein structure prediction in CASP8. *Proteins Struct. Funct. Bioinforma.* **77**, 100–113 (2009).
68. Kiefer, F., Arnold, K., Kunzli, M., Bordoli, L. & Schwede, T. The SWISS-MODEL Repository and associated resources. *Nucleic Acids Res.* **37**, D387–D392 (2009).
69. Nema, V. & Pal, S. K. Exploration of freely available web-interfaces for comparative homology modelling of microbial proteins. *Bioinformatics* **9**, 796–801 (2013).
70. Söding, J. Protein homology detection by HMM–HMM comparison. *Bioinformatics* **21**, 951–960 (2005).
71. Jefferys, B. R., Kelley, L. A. & Sternberg, M. J. E. Protein Folding Requires Crowd Control in a Simulated Cell. *J. Mol. Biol.* **397**, 1329–1338 (2010).
72. Kelley, L. A., Mezulis, S., Yates, C. M., Wass, M. N. & Sternberg, M. J. E. The Phyre2 web portal for protein modeling, prediction and analysis. *Nat. Protoc.* **10**, 845–858 (2015).
73. Benkert, P., Künzli, M. & Schwede, T. QMEAN server for protein model quality estimation. *Nucleic Acids Res.* **37**, W510–514 (2009).
74. Benkert, P., Tosatto, S. C. E. & Schomburg, D. QMEAN: A comprehensive scoring function for model quality assessment. *Proteins* **71**, 261–277 (2008).
75. Benkert, P., Biasini, M. & Schwede, T. Toward the estimation of the absolute quality of individual protein structure models. *Bioinforma. Oxf. Engl.* **27**, 343–350 (2011).
76. Porollo, A. & Meller, J. Versatile annotation and publication quality visualization of protein complexes using POLYVIEW-3D. *BMC Bioinformatics* **8**, 316 (2007).
77. Celniker, G. *et al.* ConSurf: Using Evolutionary Data to Raise Testable Hypotheses about Protein Function. *Isr. J. Chem.* **53**, 199–206 (2013).

78. Durek, P. *et al.* PhosPhAt: the Arabidopsis thaliana phosphorylation site database. An update. *Nucleic Acids Res.* **38**, D828–834 (2010).
79. Zulawski, M., Braginets, R. & Schulze, W. X. PhosPhAt goes kinases--searchable protein kinase target information in the plant phosphorylation site database PhosPhAt. *Nucleic Acids Res.* **41**, D1176–1184 (2013).
80. Peck, S. C. Analysis of protein phosphorylation: methods and strategies for studying kinases and substrates. *Plant J. Cell Mol. Biol.* **45**, 512–522 (2006).
81. Kinoshita, E., Kinoshita-Kikuta, E., Takiyama, K. & Koike, T. Phosphate-binding tag, a new tool to visualize phosphorylated proteins. *Mol. Cell. Proteomics MCP* **5**, 749–757 (2006).
82. WesternAndMPX\_SfwGuide\_15158.pdf - File Shared from Box. at <https://licor.app.boxenterprise.net/s/ui03xwikn5rkuyjvjk17iiseagxxeng>
83. Kandala, S., Kim, I. & Su, H. Neddylation and deneddylation in cardiac biology. *Am. J. Cardiovasc. Dis.* **4**, 140–158 (2014).
84. De Lucia, F., Crevillen, P., Jones, A. M. E., Greb, T. & Dean, C. A PHD-Polycomb Repressive Complex 2 triggers the epigenetic silencing of FLC during vernalization. *Proc. Natl. Acad. Sci. U. S. A.* **105**, 16831–16836 (2008).
85. Goujon, M. *et al.* A new bioinformatics analysis tools framework at EMBL-EBI. *Nucleic Acids Res.* **38**, W695–W699 (2010).
86. McWilliam, H. *et al.* Analysis Tool Web Services from the EMBL-EBI. *Nucleic Acids Res.* **41**, W597–W600 (2013).
87. Sánchez, R. & Šali, A. Evaluation of comparative protein structure modeling by MODELLER-3. *Proteins Struct. Funct. Bioinforma.* **29**, 50–58 (1997).
88. Roberts, E., Eargle, J., Wright, D. & Luthey-Schulten, Z. MultiSeq: unifying sequence and structure data for evolutionary analysis. *BMC Bioinformatics* **7**, 382 (2006).
89. Benkert, P., Schwede, T. & Tosatto, S. C. QMEANclust: estimation of protein model quality by combining a composite scoring function with structural density information. *BMC Struct. Biol.* **9**, 35 (2009).
90. Buchan, D. W. A., Minnici, F., Nugent, T. C. O., Bryson, K. & Jones, D. T. Scalable web services for the PSIPRED Protein Analysis Workbench. *Nucleic Acids Res.* **41**, W349–W357 (2013).
91. Touw, W. G. *et al.* A series of PDB-related databanks for everyday needs. *Nucleic Acids Res.* **43**, D364–D368 (2015).
92. Pollastri, G., Baldi, P., Fariselli, P. & Casadio, R. Prediction of coordination number and relative solvent accessibility in proteins. *Proteins Struct. Funct. Bioinforma.* **47**, 142–153 (2002).

*This page intentionally left blank.*